UNIVERSITEIT VAN PRETORIA
UNIVERSITY OF PRETORIA
YUNIBESITHI YA PRETORIA

Seasonal Maize Yield Simulations for South Africa using a Multi-Model Ensemble System

by

Noelien le Roux

Submitted in partial fulfillment of the requirements

for the degree of

MASTER OF SCIENCE

in the

Faculty of Natural and Agricultural Sciences

University of Pretoria

April 2009

UNIVERSITEIT VAN PRETORIA
UNIVERSITY OF PRETORIA
YUNIBESITHI YA PRETORIA

Seasonal Maize Yield Simulations for South Africa using a Multi-Model Ensemble System

Noelien le Roux

Supervisor:	Prof. W.A. Landman
Co-supervisor:	Dr. F.A. Engelbrecht
Department:	Department of Geography, Geoinformatics and Meteorology
Faculty:	Faculty of Natural and Agricultural Sciences
University:	University of Pretoria
Degree:	Master of Science

ABSTRACT

Agricultural production is highly sensitive to climate and weather perturbations. Maize is the main crop cultivated in South Africa and production is predominantly rain-fed. South Africa's climate, especially rainfall, is extremely variable which influences the water available for agriculture and makes rain-fed cropping very risky. In the aim to reduce the uncertainty in the climate of the forthcoming season, this study investigates whether seasonal climate forecasts can be used to predict maize yields for South Africa with a usable level of skill. Maize yield, under rain-fed conditions, is simulated for each of the magisterial districts in the primary maize producing region of South Africa for the period from 1979 to 1999. The ability of the CERES-Maize model to simulate South African maize yields is established by forcing the CERES-Maize model with observed weather data. The simulated maize yields obtained by forcing the CERES-Maize model with observed weather data set the target skill level for the simulation systems that incorporate Global Circulation Models (GCMs). Two GCMs produced the simulated fields for this study, they are the Conformal Cubic Atmospheric Model (CCAM) and the ECHAM4.5 model. CCAM ran a 5 and ECHAM4.5 a 6-member ensemble of simulations on horizontal grids of 2.1° x 2.1° and 2.8° x 2.8° respectively. Both models were forced with observed sea-surface temperatures for the period 1979 to 2003. The CERES-Maize model is forced with each ensemble member of the CCAM-simulated fields and with each ensemble member of the ECHAM4.5-simulated fields. The CERES-CCAM simulated maize yields and CERES-ECHAM4.5 simulated maize yields are combined to form a Multi-Model maize yield ensemble system. The simulated yields are verified against actual maize yields. The CERES-Maize model shows significant skill in simulating South Africa maize yields. CERES-Maize model simulations using the CCAM-simulated fields produced skill levels comparable to the target skill, while the CERES-ECHAM4.5 simulation system illustrated poor skill. The Multi-Model system presented here could therefore not outscore the skill of the best single-model simulation system (CERES-CCAM). Notwithstanding, the CERES-Maize model has the potential to be used in an operational environment to predict South African maize yields, provided that the GCM forecast fields used to force the model are adequately skilful. Such a yield prediction system does not currently exist in South Africa.

I declare that the thesis that I hereby submit for the degree ..... at the University of Pretoria is my own work and has not previously been submitted by me for degree purposes at any other university or institution.

_____ _____

SIGNATURE DATE

PREFACE

Agricultural production is highly sensitive to climate and weather perturbations (Podesta *et al.*, 1999; Chimeli *et al.*, 2002; Cantelaube and Terres, 2005; Sivakumar, 2006). Rainfall as such, can be considered as the atmospheric variable with the largest limiting effect on crop growth and development (Taljaard, 1986; DoA, 2007), which makes rain-fed agriculture particularly vulnerable to extreme weather events that significantly influences water availability. In South Africa, crop production is predominantly rain-fed, with only about 1% of the total cultivated area being irrigated (Chenje and Johnson, 1994). Due to the extreme variability of South Africa's climate, crop production is exceptionally risky. Therefore, the climate can be seen as one of the main factors responsible for year-to-year variations in South African crop yields.

Agriculture represents one of the main pillars of the economy of South Africa as a developing country, not only in terms of crop production and the main source of food, but also in terms of employment (Oram, 1989; Sivakumar, 2006; DoA, 2007). In a country like South Africa, where rain-fed agriculture dominates, a good rainy season normally results in good crop production, whereas a season with insufficient rain or the occurrence of a natural disaster (drought or flood) can result in crop failure (Arndt *et al.*, 2002; Sivakumar, 2006). This vulnerability of crop production to fluctuations in the climate, which consequently leads to variable yields, can cause the economy of the entire country to suffer (Cantelaube and Terres, 2005; Sivakumar, 2006). Southern Africa is a region subject to climate extremes (Tyson, 1986; Reason *et al.*, 2006a) and as a result often faces threats of food shortages (Devereux, 2000). The world's population is expected to exceed 8 billion by the year 2020, which places even more pressure on the agricultural sector in terms of food security (Sivakumar, 2006).

To ensure food security, excellent crop management is of utmost importance. This is a complicated practice, as weather is the primary source of uncertainty in crop management (Vossen, 1995). From the start of the season and right through, farmers have to make critical land and water management decisions which are primarily based on climatic conditions (Sivakumar, 2006). These decisions are often made weeks to months in advance of a specific weather event, like for instance the onset of the rainfall. Since unexpected climatic extremes can have detrimental effects on the yield, there is a need to investigate ways by which the uncertainty in the expected climate regime of the forthcoming season can be reduced. Seasonal climate forecasts provide insight into the expected mean

weather conditions of the approaching season, but farmers can benefit more from information when it is presented in terms of production outcomes.

In this study a maize yield forecast system is constructed using a crop model and two Global Circulation Models (GCMs) that aims to produce useable maize yield predictions for South Africa which will allow farmers to take advantage of probable good seasons and reduce unwanted impacts in probable poor seasons.

The hypotheses that will be tested are:

1. that the crop model has skill in simulating South African maize yields when forced with observed weather data;

2. that crop model-GCM based maize yield simulation systems can produce skill levels comparable to the target skill level set by forcing the crop model with observed weather data;

3. that the skill of a simple Multi-Model maize yield ensemble system outscores that of the best crop model-GCM based maize yield simulation system.

The steps required to test these hypotheses are to:

1. run the crop model for each of the magisterial districts in the primary maize producing area of South Africa for the period 1979/80 to 1998/99 with observed weather data;

2. quantify the skill of the crop model by comparing the simulated maize yields to actual maize yields and so that a target skill level can be set;

3. use the GCM-simulated fields as forcing in the crop model and perform the same crop model runs as done with the observed weather data;

4. combine the simulated maize yields from the two crop model-GCM based simulation systems to form a simple Multi-Model maize yield ensemble system;

5. verify the simulated maize yields obtained from the crop model-GCM based systems and from the Multi-Model maize yield ensemble system against actual maize yields and against the target skill level.

This dissertation consists of four chapters. Chapter 1 describes the growth stages of the maize plant, the factors influencing South Africa's climate, the seasonal predictability of South African rainfall, seasonal climate forecasting, ensemble and multi-model forecasting as well as an overview of crop yield forecasting worldwide. The data and models used and set up of the maize yield simulation experiments are detailed in Chapter 2. The methods used to verify the simulated maize yields are also described in this chapter. Chapter 3 discusses the maize yield simulation results. The simulated maize yields are verified spatially, inter-seasonally and probabilistically. The results are summarized and conclusions are made in Chapter 4.

ACKNOWLEDGEMENTS

Many thanks and appreciation to:

- First and most importantly the Lord, who gave me the strength and ability to complete this study.
- Prof. W.A. Landman (Chief Scientist, Seasonal Forecasting, South African Weather Service) for his enthusiasm, advice and support during the course of the study.
- Dr. F.A. Engelbrecht (University of Pretoria) for supplying the CCAM-simulated fields, assistance (especially related to the programming involved in this study), valuable inputs and willingness to help.
- Mr. Asmerom Beraki (SAWS) for supplying ECHAM4.5-simulated fields, for his hard work in getting the data into the correct format and for some of the skill calculations.
- Dr. J.F. Eloff, Mr. T. Dohse, Dr. D. Beukes, Dr. D. Turner and Mrs. M. van der Walt from the Agricultural Research Council, Institute for Soil, Climate and Water for their assistance in the soil component of this study.
- Matthew Jones from SASRI and Wiltrud Du Rand from the Agricultural Research Council – Grain Crops Institute who assisted me with DSSAT problems.
- Talita Germishuyse (ARC-ISCW) for assistance with actual maize yield figures.
- Rejaene van Dyk, the Librarian of ARC-ISCW for helping with the quest to find articles, sometimes in a rush.
- Christien Engelbrecht (ARC-ISCW) for the patching of weather station data.
- Philip Beukes (ARC-ISCW) for assistance with many GIS problems.
- The ARC-ISCW who funded this MSc. Thank you for the opportunity.
- My family and friends who supported me, encouraged me and prayed for me throughout the study.
- Brendan, vir jou geduld, ondersteuning, woorde van moed en gebede! Baie, baie dankie!

TABLE OF CONTENTS

LIST OF FIGURES

LIST OF TABLES

CHAPTER 1

INTRODUCTION

1.1 AGRICULTURE IN SOUTH AFRICA

The main crops cultivated in South Africa include maize, barley, wheat, sunflower, potatoes, sugarcane, soybeans and sorghum. Figure 1.1 shows the area that was harvested in 2008 for each of these crops (BFAP, 2008). It can be seen from Figure 1.1 that maize is the primary crop grown in South Africa, with 2.8 million hectares of land harvested. The second largest cultivated crop is barley (746 000 ha) and the third largest cultivated crop is wheat (718 000 ha). As maize is the main crop cultivated in South Africa and significantly contributes to the country's economy, this study focuses on maize.

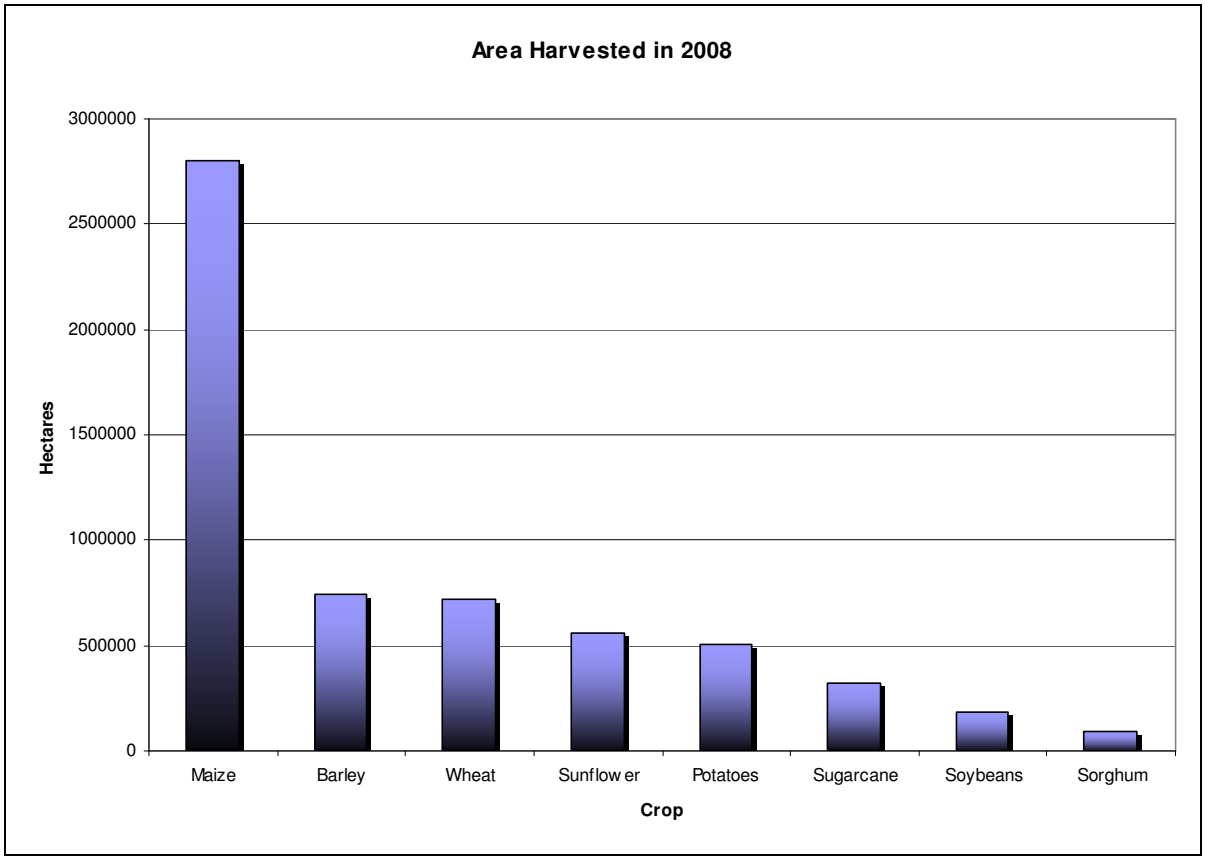

Figure 1.1: The area harvested in 2008 for each of the main crops cultivated in South Africa (BFAP, 2008).

1.2 THE GROWTH AND DEVELOPMENT OF THE MAIZE PLANT

The maize plant flourishes under warm conditions, and is only grown in areas where the average daily temperature is greater than 19℃ or where the average temperature of summer is greater than 23℃ (Du Toit, 1997). However, a minimum temperature of 10℃ is needed for germination. The critical temperature that can negatively influence the yield is approximately 32℃, and water availability normally limits maize yields. To obtain a yield of 3.2 t/ha a minimum rainfall of 350 mm is required per annum. Approximately 10 kg to 16 kg of grain are produced per hectare for every millimetre of water used. In the absence of moisture stress a total of 250 ℓ of water would have been used by each maize plant by the time it reaches maturity.

To understand the vulnerability of maize to climate variability, in particular related to rainfall, it is necessary to know the development stages of the maize plant and how each of these stages are influenced by unfavourable climatic conditions. High maize yields can only be obtained when the soil and climatic conditions are favourable during all the development stages of the plant (Sun *et al.*, 2007). The ten development stages of the maize plant, as stipulated by Hanway (1966) and Du Toit (1997), are described in the following subsections.

1.2.1 Stage 0 – From planting to seed emergence

When maize production takes place under rain-fed conditions, farmers need to wait for the first rains before planting can take place as the seed requires sufficient moisture to germinate. Under optimal warm and moist conditions the seedlings will emerge within 6 to 10 days, while unfavourable cold and dry conditions can lead to the seedlings only emerging after 2 weeks. The optimal temperatures for germination is between 20℃ and 30℃ and the plant available water in the soil should optimally be 60% of the capacity of the soil.

1.2.2 Stage 1 – Four leaves completely unfolded

The maximum number of leaves and lateral shoots are by now already determined, and approximately every 3rd day a new leave unfolds. The parts of the plant at this stage visible above the soil surface are limited to the leaf sheaths and blades. Tasseling is also initiated during this stage. The rate of development of the primary root system decreases rapidly until almost no further development takes place. If the nodes of the plant below the soil surface experience extremely dry or wet conditions, the adventitious roots will not develop

which makes the plant solely dependant on the primary root system for nutrient and water uptake. Dry climatic conditions can also lead to the roots shooting deeper. Unfavourable climatic conditions in the early development stages of the maize plant can limit the size of the leaves (Sun *et al.,* 2007).

1.2.3 Stage 2 – Eight leaves completely unfolded

During this stage the leave area of the plant increases 5 to 10 times and the mass of the stem increases 50 to 100 times. Thus, the size of the leaves and thickness of the stem are determined. The 9th, 10th and 11th leaves have reached their final size. The development of ears also commence during this stage.

1.2.4 Stage 3 – Twelve leaves completely unfolded

The leaves have now reached their final size. The stem is thickening and the lowest four leaves are dying off. The tassel in the growth point is now starting to develop rapidly. Lateral shoots bearing ears are developing from nodes 6 to 8 above the soil surface and the potential number of seed buds of the ear is genetically predetermined. During this stage plant nutrients are absorbed at a very fast rate. Prop roots are now also developing out of the first few nodes above the soil surface. At this stage the root system can extend up to 0.8 m in the horizontal and 1.2 m in the vertical.

1.2.5 Stage 4 – Sixteen leaves completely unfolded

The stem is lengthening rapidly and the tassel is almost completely developed. The tassel is pushed up higher in the plant and starts to emerge at the top. Silks begin to develop and lengthen from the base of the upper ear. Prop roots also develop out of the 7th node above the soil surface.

1.2.6 Stage 5 – Silk appearance and pollen shedding

All the leaves are completely unfolded and the tassel has been visible for 2 to 3 days. Pollen starts shedding. By now the plant has also reached its maximum height. The environment plays an important role in the determination of the height of the plant. Under unfavourable conditions, shorter plants may occur. The lateral shoot bearing the main ear have almost reached maturity. The seed buds are enlarging, while the silks are still

lengthening in the preparation for pollination. At this point leaf loss, high temperatures and too much rain can reduce the number of silks produced, cause poor pollination, and limit the size or number of kernels which will have detrimental effects on the yield (Ritchie *et al.*, 1993; Frost, 2006). The demand for water and nutrients are very high during this stage.

1.2.7 Stage 6 – Green maize stage

Pollination has now taken place. The ear and lateral shoots are now fully developed and starch begins to accumulate in the endosperm. The kernels are growing in size and rapidly increasing in mass. The kernels are filled with a milky fluid which contains a high concentration of sugar.

1.2.8 Stage 7 – Soft dough stage

The kernels are still relatively soft, and can be broken easily (Frost, 2006). The mass of the kernels are still increasing rapidly and the sugar is being converted into starch. Moisture stress can negatively influence the mass of the kernels at this stage.

1.2.9 Stage 8 – Hard dough stage

The sugar in the kernels is disappearing quickly. Starch accumulates in the crown of the kernels and extends downward. Moisture stress can also influence the mass of the kernels at this stage.

1.2.10 Stage 9 – Physiological maturity

The kernels have reached their maximum dry mass and a layer of black cells have developed at the base of the kernels. The kernels are now physiologically mature, but the moisture content still needs to be reduced. As soon as 90% to 95% of the kernels at the base of the ear appear black, the moisture content of the kernels should be in the 35% to 40% range.

1.2.11 Stage 10 – Biological maturity

Even though the kernels are physiologically mature, they have to dry out before reaching biological maturity. The drying of the kernels depends on the climatic conditions. Under

favourable conditions drying takes place at a rate of 5% per week until it reaches 20% where after the drying goes much slower.

The yield obtained at any give point is a direct product of the soil conditions and climate that prevailed during that specific season (Du Toit, 1997). Although, non-climatic factors such as crop genetic and management technique improvements also influence maize yields over time (Podesta *et al.*, 1999; Sun *et al.*, 2007). An upward trend has been found in South African maize production between 1951 and 1981, where after a downward trend followed (Du Toit *et al.*, 2001). The use of high yielding cultivars, improved fertilizer strategies, the availability of chemical weed control and improved management practices all contributed to the upward trend, while a combination of extreme weather events, rising input costs and the unstable maize price may have led to the downward trend (Du Toit *et al.*, 2001).

1.3 SOUTH AFRICAN CLIMATE

South Africa (situated at the southern tip of Africa) lies in the subtropical high pressure belt, an atmospheric zone dominated by dry descending air (Preston-Whyte and Tyson, 1993). The country has a hot and dry climate, with an average annual rainfall less than 500 mm (DoA, 2007). The distribution of rainfall is uneven, with only 35% of the country receiving more than 500 mm of rainfall per annum (DoA, 2007). The eastern parts of the country experience humid, subtropical conditions, while the western parts of the country experience dry, desert like conditions (DoA, 2007). Thus, the summer is characterized by a decrease in rainfall from east to west across the country (Preston-Whyte and Tyson, 1993; Schulze and Lynch, 2007). Three distinct regions are evident in South Africa, namely the summer rainfall region, winter rainfall region and region receiving rainfall throughout the year. The winter rainfall region is confined to the Western Cape Province and the western parts of the Northern Cape Province, the coastline of the Eastern Cape Province and parts of the Western Cape Province receives rainfall throughout the year and the remainder of the country receives summer rainfall (Schulze and Maharaj, 2007).

In terms of agriculture, a minimum annual rainfall of 500 mm is required for rain-fed cropping (DoA, 2007). The rainfall of South Africa is highly variable from year to year (Cook *et al.*, 2004) and to some extent insufficient. The country is subject to very high potential evapotranspiration that often exceeds the rainfall (DoA, 2007). The extreme irregularity of South Africa's rainfall largely influences the water resources available for agriculture (Cook *et al.*, 2004).

Maize production in South Africa is predominantly rain-fed (Martin *et al.*, 2000) and largely takes place in the central and northern interior regions of the country. This area receives summer rainfall with seasonal rainfall totals varying between 134 mm and 446 mm in the central interior parts, and between 209 mm and 584 mm in the northern interior parts (Tennant and Hewitson, 2002). Another characteristic of this region is the occurrence of mid-summer droughts, which normally takes place during January (DoA, 2007). These mid-summer droughts often coincide with the tasseling stage of the maize crop (DoA, 2007), a critical stage in its development. Moisture stress during the vital growth stages can have damaging effects on the maize plant, as a result limiting the growth and reducing the yield (Sun *et al.*, 2007).

1.4 OCEAN-ATMOSPHERE INTERACTIONS AND THE VARIABILITY IN SUMMER RAINFALL OVER SOUTH AFRICA

As rainfall is the most important factor essentially regulating maize production in South Africa, it is crucial to understand the range of factors responsible for the variability in South African summer rainfall. During the summer, temperature differences develop between the land surface of South Africa and the neighbouring oceans. This results in low surface pressure over the continent and higher surface pressure over the oceans (Preston-Whyte and Tyson, 1993). These pressure differences regularly initiate the development of subtropical troughs that are normally situated over the west coast of the country (Preston-Whyte and Tyson, 1993). Subtropical troughs, mid-latitude frontal systems and tropical circulation perturbations are the main forces responsible for moisture advection and summer rainfall over southern Africa (Hattle, 1968; Preston-Whyte and Tyson, 1993). Southern Africa can be seen as the section of Africa south of the equator. Early-summer moisture transport is mostly influenced by mid-latitude circulation patterns and mid- to late-summer moisture transport by tropical circulation patterns, causing a change in the synoptic flow during December/January (D'Abreton and Tyson, 1995). An association between wet conditions early in the summer and moisture from the tropical southeast Atlantic and south-west Indian Ocean (SWIO) converging north of South Africa have also been found (D'Abreton and Tyson, 1995). Late summer wet conditions were found to be associated with an anomalous Hadley cell, resulting in an increased flow of moisture from the north, and with the Inter-Tropical Convergence Zone (ITCZ) shifting to the south. Except for the neighbouring oceans, tropical Africa (D'Abreton and Tyson, 1995) and the Agulhas current (Jury *et al.*, 1993) were also investigated as possible sources of moisture, inducing summer rainfall over South Africa (Cook *et al.*, 2004). Furthermore, the heat and moisture fluxes in

the Agulhas retroflection region possibly influence the atmospheric pressure over the continent which may contribute to summer rainfall patterns over southern Africa (Walker, 1990; Crimp *et al.*, 1998).

Thus, many factors influence the inter-annual variability of rainfall over South Africa. A number of studies have demonstrated that some variability is remotely forced by ENSO, a phenomenon in the Equatorial Pacific Ocean (Nicholson and Entekhabi, 1986; Ropelewski and Halpert, 1987; Allan *et al.*, 1996; Mason and Jury, 1997; Reason and Rouault, 2002). ENSO is the most dominant and best defined inter-annual mode in the tropical Southern Hemisphere (Goddard *et al.*, 2001; Cane, 2004), and most previous work on the variability of the climate of southern Africa have focused on ENSO (Reason *et al.*, 2006a). The acronym ENSO originated from its oceanic component El Niño and its atmospheric component the Southern Oscillation (Cane, 2004). The correlation between ENSO and summer rainfall over southern Africa has been found to be strongest for the central continental parts (Lindesay and Vogel, 1990). However, a large amount of spatial variation occurs in ENSO rainfall impacts over southern Africa from one event to another (Reason and Jagadheesha, 2005). For example, one of the strongest El Niño events on record (1997/98) caused less intense dry conditions over southern Africa than the relatively weak 1991/92 and 2002/03 events that caused severe drought over the region (Reason and Jagadheesha, 2005). The high-phase of the atmospheric part of ENSO, the Southern Oscillation, has also been found to correlate with an increase in rainfall and the low-phase with a decrease in rainfall over southern Africa (Van Heerden *et al.*, 1988; Mason and Jury, 1997).

Even though the physical mechanisms related to ENSO are much better understood as those responsible for SST variability in the tropical Atlantic and Indian Oceans (Goddard *et al.*, 2001), several studies have confirmed that the neighbouring Indian and Atlantic Oceans also contribute to the variability in rainfall over South Africa (Walker, 1990; Jury and Pathack, 1991; Mason, 1995; Todd and Washington, 1998; Tennant and Hewitson, 2002; Reason *et al.*, 2006a). During wet events over South Africa, warm SSTs can be expected to the east and cooler SSTs to the west of the country (Tyson, 1986). Warm SSTs in the SWIO and cooler SSTs in the tropical Indian Ocean to the east of Madagascar were demonstrated to result in wet summer conditions over the continental parts of South Africa (Walker, 1990; Reason and Mulenga, 1999). Above-normal rainfall conditions over South Africa frequently relate to warm SSTs in the tropical western Indian Ocean (Landman and Mason, 1999a). SSTs south-east of South Africa also appear to be related to rainfall fluctuations over the country (Rautenbach and Smith, 2001). In addition, increasing

evidence exists that variability in the Atlantic Ocean is important for the climate of southern Africa (Reason *et al.*, 2006a). The influence of the Atlantic Ocean on the climate of southern Africa is largely related to the changing position of the ITCZ and variability in the South Atlantic anticyclone and mid-latitude westerlies (Reason *et al.*, 2006a). The link between the Benguela Niño in the Atlantic Ocean and zonal winds over the Equatorial Atlantic Ocean has also been found to be important in rainfall variability over southern Africa (Shannon *et al.*, 1986; Reason *et al.*, 2006a). Moisture fluxes, cloudband development and rainfall seasonality over some parts of southern Africa are influenced by the cycle in winds and SST anomalies over the southeast Atlantic Ocean (Reason *et al.*, 2006a). El Niño events and anomalies over the southeast Atlantic Ocean seem to be the two main factors responsible for severe drought conditions over southern Africa (Reason *et al.*, 2006a). In has been found that the upper ocean circulation and SST evolution of the South Atlantic responds to ENSO induced changes with a one-season lag (Colberg *et al.*, 2004). The impact of ENSO on the SSTs in the South Atlantic and South Indian Oceans and on the South Atlantic anticyclone have also made it evident that ENSO influences the onset of the summer rainfall season as well as dry spell frequencies within the summer season of southern Africa (Reason *et al.*, 2006a). Although it is clear that both the Indian and Atlantic Oceans potentially influences the climate of southern Africa, and some of these definitely have a relationship with ENSO, it must be kept in mind that the SSTs of the South Indian Ocean are thought to have a greater impact than the SSTs of the South Atlantic Ocean (Nicholson and Entekhabi, 1986; Reason, 2002).

1.5 SOUTH AFRICAN MAIZE YIELDS AND CLIMATE VARIABILITY

Before initiating the development of a maize yield forecast system that will aim to improve agricultural management systems by preparing the farmer for the climatic conditions of the forthcoming season, there should be a confirmed relationship between climate variability and South African maize yields. In many countries the variability in the climate accounts for as much as 80% of the year-to-year variability in crop yields (Petr, 1991; Fageria, 1992; Sivakumar, 2006). To confirm that ENSO-related climate variability largely contributes towards the variability in South African maize yields, historical maize yield figures for South Africa (GrainSA, 2007) are compared to Oceanic Nino Index (ONI) values (http://www.cpc.ncep.noaa.gov/products/analysis_monitoring/ensostuff/ensoyears.shtml) averaged over the growing season (OND, NDJ, DJF, JFM and FMA) (Figure 1.2).

The ONI is a principal measure for monitoring, assessing and predicting the El Niño Southern Oscillation (ENSO) phenomenon. ENSO results from an interaction between the

atmosphere and underlying ocean in the Equatorial Pacific Ocean and is seen as one of the key mechanisms responsible for climate variability in many parts of the world (Podesta *et al.*, 1999). This phenomenon involves two phases, a warm phase also known as an El Niño event and a cold phase also known as a La Niña event. The ONI is based on sea surface temperature (SST) departures from the average in the Nino 3.4 region in the Equatorial Pacific Ocean. If the SST anomaly is greater than or equal to +0.5°C for five consecutive seasons, it indicates an El Niño event, whereas a SST anomaly of less than or equal to -0.5°C for five consecutive seasons indicates a La Niña event.

ENSO is recognized as a phenomenon that significantly impacts the entire southern Africa region (Nicholson and Entekhabi, 1986; Mason and Jury, 1997), with El Niño events normally coinciding with below-normal and La Niña events normally coinciding with above-normal summer rainfall totals over the region (Ropelewski and Halpert, 1987; Mason and Jury, 1997; Reason *et al.*, 2006a). These exact ENSO impacts were observed over the central and western interior of South Africa (Rautenbach and Smith, 2001). The influence of ENSO on southern African rainfall was also found to have significant spatial and inter-event variations (Reason and Jagadheesha, 2005). Many studies have described the relationship between SST anomalies in the Equatorial Pacific Ocean and rainfall over southern Africa (van Heerden *et al.*, 1988; Allan *et al.*, 1996).

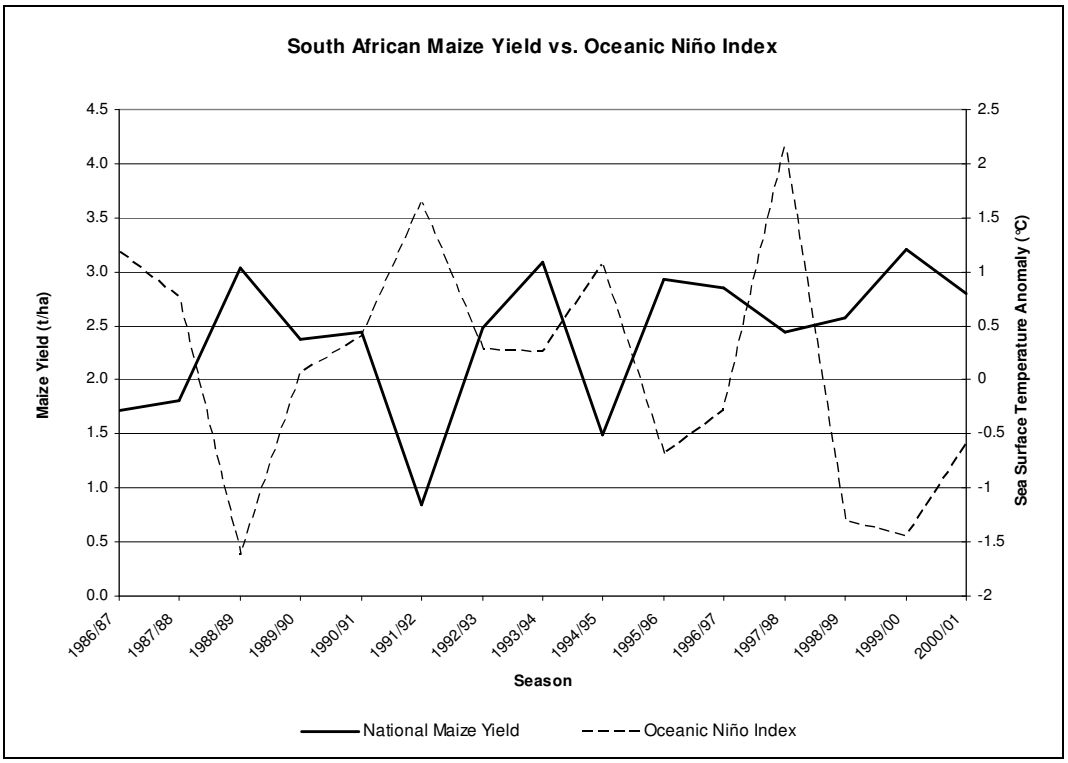

Figure 1.2: Historical maize yield figures for South Africa compared to Oceanic Nino Index values averaged over the growing season (OND, NDJ, DJF, JFM and FMA).

As ENSO directly affects the rainfall of South Africa, it should also have an effect on South African maize yields, seeing that rainfall is the sole source of water for maize production under rain-fed conditions. From Figure 1.2 it can be seen that the maize yield and ONI, are inversely proportional to each other. This means that if the ONI is positive, indicating an El Niño season and more often than not below-normal summer rainfall totals, the maize yield is low, while if the ONI is negative, indicating a La Niña season and more often than not above-normal summer rainfall totals, the maize yield is high. This is evidence that climate variability associated with ENSO contributes significantly towards the variability in South African maize yields.

1.6 THE SEASONAL PREDICTABILITY OF SOUTH AFRICAN RAINFALL

Numerical weather predictions of the exact state of the atmosphere is limited to a lead-time of about 2 weeks (1963, Lorenz). This is a result of the uncertainty associated with describing the initial state of the atmosphere, and the sensitivity of the dynamics of Global Circulation Models (GCMs) to the initial conditions. Lorenz's finding leads to the question; how is a seasonal climate forecast that provides insight into future averaged weather evolution with a lead time of, for example, 3 months then possible? Seasonal climate forecasts are possible due to an increased understanding of air-sea interactions, and in particular the interactions related to ENSO (Barnston *et al.*, 1994; Chen *et al.*, 1995; Neelin *et al.*, 1998; Palmer *et al.*, 2004; Hansen *et al.*, 2006; Vogel and O'Brien, 2006). At seasonal time scales the ocean plays a vital role (Doblas-Reyes *et al.*, 2006). The atmosphere reacts to changes in the SSTs within a few weeks, while the ocean takes 3 months or longer to react to changes in the atmosphere (Sivakumar, 2006). This slow evolution of the ocean offers the opportunity for making seasonal climate forecasts (CSIRO, 1998). Seasonal climate forecasts are far from perfect, but offer some predictability in terms of future temperatures and rainfall amounts (Ziervogel *et al.*, 2005).

Research done over the last few decades has revealed that the seasonal climate of many countries in the world is potentially predictable (Goddard *et al.*, 2001), with seasonal forecasts proving to be skilful for a number of regions particularly important for agricultural production (Challinor *et al.*, 2005). The highly variable nature of southern African rainfall, the key factor in rain-fed maize production, emphasizes the need of accurate and reliable seasonal rainfall forecasts prior to the summer season (Klopper, 1999). Skilful seasonal forecasts will allow farmers to alter management practices in light of expected weather conditions (Hollinger, 1988; Hammer, 1996; Hansen *et al.*, 2006). Even though major improvements have been made in understanding the seasonal predictability of rainfall over

southern Africa (e.g. Landman and Goddard, 2002), the region responds to a large number of factors, and this makes seasonal forecasting a challenging task (Reason *et al.*, 2006a). SST anomalies provide the main source of predictability of atmospheric developments at seasonal time-scales, since changes in the oceans result in changes in the atmosphere (Palmer and Anderson, 1994; Goddard *et al.*, 2001; Gong *et al.*, 2003; Sivakumar, 2006). Many predictability studies as well as projects involving the development of forecast models have focused on establishing relationships between global SSTs and seasonal rainfall anomalies over various regions including South Africa (Rautenbach and Smith, 2001;Tennant and Hewitson, 2002; Landman *et al.*, 2008). Thus, if a relationship is found between SST anomalies and rainfall over southern Africa, skilful seasonal rainfall forecasts will be possible if the SSTs responsible for the rainfall variability over land are predictable (Goddard *et al.*, 2001; Gong *et al.*, 2003). SST forcings account for a major portion of rainfall variability over southern Africa during the austral summer (Landman and Mason, 1999b), the most important season in maize production.

High predictability has been found for the Tropics, but most of southern Africa is situated outside of the Tropics where in general the seasonal predictability is lower (Palmer and Anderson, 1994; Landman and Goddard, 2002). Tropical atmospheric circulation patterns, which result from a direct response to SST changes, were observed to be the main source of seasonal predictability for the southern Africa region (Walker, 1990; Mason, 1995). As the peak summer rainfall period from December to February is dominated by tropical disturbances in the atmosphere (Harrison, 1984), the highest forecast skill has been obtained for this period (Barston *et al.*, 1996; Mason *et al.*, 1996). One of the most predictable tropical disturbances that impact the entire globe is the ENSO phenomenon (Allan, 2000; Goddard *et al.*, 2001). Much of the skill in predicting southern African rainfall is derived from ENSO, but definitely not dominated by it (Mason and Jury, 1997). ENSO events interact with other features in the global oceans and atmosphere which may also influence rainfall variability over southern Africa (Reason *et al.*, 2000). Therefore, the SST anomalies of the oceans surrounding southern Africa should also be taken into account when predicting southern African seasonal rainfall (Walker and Lidesay, 1989). It should also be emphasized that at seasonal time-scales there are no skill in predicting on which day a specific region will receive rainfall, but there is usable skill in predicting seasonal mean rainfall totals and intra-seasonal weather characteristics which forms part of large-scale patterns (Jury, 2002; Sun *et al.*, 2005).

1.6.1 Statistical Forecasting

Over the past few years, the South African Weather Service (SAWS) as well as a number of local universities started to issue operational seasonal rainfall forecasts for the southern Africa region (Mason *et al.*, 1996; Klopper, 1999; Landman and Mason, 1999b). Many of the seasonal forecasts were produced using statistical based techniques that include regression analysis, discriminate analysis, canonical correlation analysis, cluster analysis, time series analysis, period analysis and analogue methods (Landman and Mason, 1999b). The Climatology Research Group at the University of the Witwatersrand used a quadratic discriminant analysis model to produce seasonal rainfall outlooks for South Africa (Mason, 1998). The rainfall forecasts were produced for regions with similar inter-annual rainfall variability by relating the rainfall of each region to principal components of SST anomalies in the Indian, Atlantic and Pacific Oceans. 3-month forecasts and 6-month forecasts were produced. Skill in the 3-month forecasts for the summer rainfall region was limited to late-spring and early-summer, while the 6-month forecasts showed skill for early- to mid-summer. Even though forecast skill of the 6-month forecasts was found to be significantly higher that that of the 3-month forecasts, the 3-month forecasts revealed a high level of skill in predicting 'very dry' and 'very wet' conditions. In general, high forecast skill was obtained for the largest part of the country throughout the year, with the most reliable forecasts evident shortly before or after the start of the summer rainfall season.

Canonical correlation analysis (CCA) has also been used to investigate the variability and predictability of summer rainfall over South Africa (Landman and Mason, 1999b). CCA is a statistical method normally used to identify linear relationships between two highly correlated variables (Landman and Mason, 1999b). South African summer rainfall was the predictand and SST data of the global oceans the predictor. For each of the homogeneous regions over the country a forecast of total precipitation was produced for the October-November-December (OND) and January-February-March (JFM) seasons. The CCA model demonstrated low to moderate skill, with correlations higher than 0.5. Greater rainfall predictability was found for the JFM season than that for the OND season, which makes it extremely difficult to predict the onset of rainfall. OND predictability was restricted to the north-eastern regions and JFM predictability to the central and western regions. In general, predictions with high skill can only be expected for El Niño and La Niña years, as the Equatorial Pacific Ocean is the main source of predictability with weaker signals from the Equatorial Indian and Atlantic Oceans (Landman and Mason, 1999b).

A statistical model has also been used to investigate the climate signals around southern Africa and to predict area-average rainfall (Jury *et al.*, 2004). The investigation was based on the hypothesis that climate signals important in the prediction of southern Africa rainfall originate from slowly varying waves. Sea level pressure (SLP) and SSTs of the Atlantic and Indian Oceans as well as southern Africa rainfall were considered. The multi-variate model demonstrated useful skill in predicting southern Africa rainfall at 1-year lead time and is particularly skilful in predicting extreme events. The strongest SST and SLP signals are evident 6 to 12 months before the rainfall season which indicates potential predictability (Jury *et al.*, 2004).

1.6.2 Multi-tiered Forecasting

Even though most statistical forecast methods make use of linear relationships, many climate processes show strong non-linearities (Landman *et al.*, 2001). This ultimately limits the forecast skill of statistical models (Carson, 1998). However, these non-linearities can possibly be simulated with GCMs (Landman and Mason, 1999a). A GCM represents a simplification of the climate system through the equations of motion but suffer from initial condition and inherent model uncertainties which may lead to model output not reflecting the real system accurately (Holton, 1979; Hollinger, 1988; Doblas-Reyes *et al.*, 2006). Even so, the use of GCMs offers great opportunities for improving the seasonal predictability of summer rainfall over South Africa. The skill of a statistical model and that of a GCM has been compared over a 10-year retro-active period when predicting December-January-February (DJF) summer rainfall for southern Africa (Landman *et al.,* 2001). CCA was used as the statistical model and the GCM used was the Centre for Ocean-Land-Atmosphere Studies (COLA) T30 model with a horizontal resolution of approximately 400 km. The lower boundary conditions used to force the GCM was SSTs predicted with the CCA model. The GCM output was downscaled using the perfect prognosis approach (Wilks, 2006). This combination of statistical and dynamical forecasting techniques is known as a multi-tiered scheme. The results found suggested that the multi-tiered approach produce more skilful forecasts than that produced by the CCA statistical model. Even though skilful 1- and 3-month lead time predictions of Equatorial Pacific and Indian Ocean SSTs anomalies were obtained through CCA (Landman and Mason, 2001), improved SST forecasts can result in the multi-tiered approach increasing the skill of seasonal rainfall forecasts for South Africa. GCMs will most probably form the centre of seasonal forecasting in the years ahead, and no longer statistical models (Landman *et al.,* 2001).

1.6.3 Dynamical Forecasting

The capability of the CSIRO-9 GCM to model the major global SST forcings that contribute to the inter-annual variability in rainfall over South Africa and Namibia has been investigated (Rautenbach and Smith, 2001). The GCM was forced with observed global SST anomalies for the 30-year period from 1961 – 1990, and an ensemble of five simulations was produced, each initialized with different initial conditions. Skilful model results that correlate strongly with the observations were obtained for the dominant austral summer season (October-March). It was also demonstrated that the model simulated rainfall variability during the austral summer season compare well with SST perturbations in the Equatorial Pacific and tropical western Indian Oceans.

The ability of a GCM to simulate the impact of five ENSO events on southern Africa rainfall has been tested (Reason and Jagadheesa, 2005). The GCM used was the UKMO HadAM3 model which was forced in hindcast mode for a period from 1990 to 2003 with observed SSTs. The model was implemented at the University of Cape Town as part of a dynamical seasonal forecasting project. The investigation focused on the OND and JFM seasons. The GCM showed highest skill for the 1997/8 El Niño event, with lower skill for the 1991/2 and 2002/3 El Niño events and 1995/6 and 1999/00 La Niña events. The GCM was found to experience difficulty in capturing changes in the Angola low, a centre of tropical convection often associated with rainfall impacts over southern Africa during ENSO events. Therefore, as the GCM did not represent the Angola low properly, it struggled to simulate the ENSO rainfall impacts over southern Africa. In a study done on wet and dry spells over South Africa, Cook *et al.* (2004) also highlighted the importance of the Angola low in seasonal rainfall over South Africa.

Due to current computational capabilities, the spatial resolution of seasonal forecasts obtained from GCMs is often limited, in the range of 100 km x 100 km (Palmer *et al.*, 2004; Hansen *et al.*, 2006) or even courser. The GCMs focus on large-scale weather systems and are less skilful in representing local weather conditions, especially precipitation (Cantelaube and Terres, 2005). To obtain a higher spatial resolution over a specific area (downscaling) one can make use of a Regional Climate Model (RCM), which is normally nested within the GCM (Kgatuke *et al.*, 2008). A number of RCMs are currently used for seasonal simulations over southern Africa, with the MM5 RCM being used in Ghana, Nigeria, Zambia and Zimbabwe (Tadross *et al.*, 2006). The MM5 RCM has been used to simulate rainfall for a wet DJF season (1988/9) and a dry DJF season (1991/2) over southern Africa, and at the same time also investigated the influence of two different

planetary boundary layer and two different cumulus convection parameterization schemes on the model output (Tadross *et al.*, 2006). The simulated rainfall results were compared to observed precipitation (seasonal and diurnal), number of rain days, diurnal short-wave fluxes and optical depth. All four model configurations simulated the total precipitation for the wet DJF season well, but it was found that the model underestimates the inter-annual change. It was also demonstrated that the biases in the simulated DJF rainfall are largely related to biases in the number of rain days and the diurnal moisture and energy cycles.

From the research described above it appears as if the region and season for which models show skill vary from one model to another. It is also clear that significant progress has been made in seasonal forecasting techniques over the last decade. The majority of seasonal forecasting systems currently in use all make use of GCMs, several in multi-tiered or two-tiered approaches. Even though seasonal forecasts produced by GCMs will never be perfect, GCMs have proved to be skilful in many regions and in particular the Tropics (Hunt *et al.*, 1994; Mason *et al.*, 1999). GCMs are capable of simulating much of the large-scale atmospheric circulation, but often struggle to capture local sub-grid-scale variability (Goddard *et al.*, 2001). Even though GCMs tend to overestimate and spatially distort rainfall over southern Africa (Joubert and Hewitson, 1997), when forced with observed SSTs these models have seem to capture the main austral summer seasonal rainfall variability over the region (Rautenbach and Smith, 2001; Goddard and Mason, 2002; Reason and Jagadheesha, 2005), but skill is limited in non-ENSO years (Landman and Mason, 1999b). Even in ENSO years when the seasonal predictability is relatively high, it must be kept in mind that inter – El Niño differences exist (Hoerling and Kumar, 1997) which influences the confidence in the expected conditions predicted during these years (Mason and Goddard, 2001). The predictability of rainfall over the summer rainfall season of South Africa, from October to March, varies significantly when using SSTs as precursor (Landman and Mason, 1999b). October rainfall was found to be the least predictable when using only SSTs, while November rainfall was predictable using central-south Atlantic SSTs. The Equatorial Pacific Ocean and Arabian Sea were found to be important in predicting December rainfall, but January rainfall related poorly to SSTs. Most predictability for February and March rainfall were found to originate from the central Equatorial Indian Ocean (Pathack *et al.*, 1993).

The GCM fields that are used in this study as input into the crop model are not actual forecasts, but simulation data. Simulation data are obtained by forcing a GCM with simultaneous observed SSTs, while a real-time forecast is obtained by forcing a GCM with predicted SSTs. To recalibrate the circulation patterns generated by a GCM, a model

output statistics (MOS) method has been applied and results presented for the DJF rainfall season over southern Africa (Landman and Goddard, 2002). Two datasets were used, the first dataset was obtained by forcing the GCM with simultaneous observed SSTs for the DJF season (simulation data) and the second dataset was obtained by forcing the GCM with persisted November SSTs through the DJF season (hindcast data). The second dataset in effect has a lead-time of one month and could therefore be associated with a real-time forecast issued early December for the upcoming DJF season. Both the simulation-MOS and hindcast-MOS forecasts agreed significantly with the observations. Thus, similarly skilful seasonal rainfall forecasts could be produced using both the simulation data and hindcast data which correspond to a real-time forecast with a 1-month lead-time. Therefore, it can be assumed that the maize yield simulations produced in this study using the GCM-simulated fields as input into the crop model will yield similar results to maize yield forecasts produced using actual seasonal forecasts with a 1-month lead-time as input into the crop model.

1.7 ENSEMBLE AND MULTI-MODEL FORECASTING

Model ensembles have become an essential part of forecasting over the last few years (Krishnamurti *et al.*, 1999). Due to the atmosphere behaving in a chaotic manner, the initial state of the atmosphere is not certain (Palmer *et al.*, 2004; Sivakumar, 2006). The initial state of the atmosphere is used to initialize a GCM, which then integrates that initial conditions into the future to obtain a forecast. Thus, with an increase in lead time even the most sophisticated forecast model will diverge further and further away from reality. To address this source of uncertainty, the GCM is initialized from a number of possible atmospheric initial states (Sivakumar, 2006). In other words, several forecasts are made by each time introducing slightly different initial conditions into the GCM (Palmer *et al.*, 2004; Doblas-Reyes *et al.*, 2006). This is called an ensemble, with each forecast representing a member of the ensemble. This approach provides a range of possible outcomes (Sivakumar, 2006) and by investigating the ensemble spread the uncertainty in the forecasts associated with the initial conditions can be estimated (Barnston *et al.*, 2003; Palmer *et al.*, 2004; Hansen *et al.*, 2006). From the ensemble of forecasts a probability distribution function can be obtained (Doblas-Reyes *et al.*, 2006; Hansen *et al.*, 2006) by calculating the percentage of ensemble members that fall either within the below-normal, near-normal or above-normal categories (Reason *et al.*, 2006b). When an ensemble of seasonal forecasts is produced, the set of forecasts represent the probability distribution of climate in its response to SST forcings. When two or more skilful but independent forecasts of the same event are combined, the final forecast will be more accurate than any of the

individual forecasts by itself (Leith, 1974). Thus, ensemble forecasting improves the skill of forecasts (Barnston *et al.,* 2003; Palmer *et al.*, 2004).

A number of other factors also contribute to the uncertainty in GCM forecasts. The main factors include the way in which small-scale features are represented within the model (parameterization) (Palmer *et al.*, 2005), the way in which data is introduced into the model (assimilation), assumptions made within the model and model equation errors (Palmer *et al.*, 2005). To account for these uncertainties more than one GCM can be used, as each GCM makes use of different parameterization schemes, data assimilation procedures and assumptions and may even have different inherent model equation inaccuracies. Thus, each GCM will probably perform different due to these differences (Landman and Goddard, 2003). In effect each individual model runs its own ensemble, which can be combined to form a multi-model ensemble or super-ensemble (Barnston *et al.*, 2003; Palmer *et al.*, 2004; Sivakumar, 2006).

A number of studies have shown evidence that a multi-model forecast system provides more skilful forecasts than any individual model. In the PROVOST (Prediction of Climate Variations on Seasonal to Interannual Timescales) project (Palmer *et al.*, 2004) carried out in Europe, a number of GCMs were used to perform 4-month forecasts when forced with SSTs. Each model was initialized 9 times from slightly different atmosphere initial conditions, while the same boundary conditions (SSTs) were used to force all the GCMs. Results from the PROVOST project showed that regardless of identical SSTs, the ensembles from the individual models varied considerably in the seasonal-mean signal from the SSTs. Despite this, the multi-model ensemble system still proved to produce more reliable forecasts than any of the single-model ensembles.

In a more complex and more well know study also done in Europe, the DEMETER (Development of a European Multi-model Ensemble system for seasonal to inTERannual prediction) project (Palmer *et al.*, 2004), 7 coupled ocean-atmosphere global circulation models (CGCMs), each running its own ensemble of 9 simulations from different ocean initial conditions, were used to perform a series of six-month hindcasts. Thus, a multi-model ensemble of 7 x 9 was produced. In CGCMs the atmosphere and oceans can evolve freely and are consequently allowed to influence each other (Goddard *et al.*, 2001). The DEMETER results indicated that the multi-model forecasting technique is feasible to represent model uncertainty on seasonal and inter-annual time-scales. It was also found that on average the multi-model system provides more skilful seasonal forecasts than that

produced by a single-model system. In the USA similar attempts have been made under the Dynamic Seasonal Prediction (DPS) projects (Sivakumar, 2006).

An investigation has been done to assess whether the advantage of the multi-model system over the single-model system is only due to an increase in ensemble size (Hagedorn *et al.,* 2005). A single-model ensemble and a multi-model ensemble of the same size (54-members) were compared. Results indicated that even with the same ensemble size, the overall performance of the multi-model system is better.

Sufficient evidence has been presented that multi-model systems can improve on the skill of both weather and seasonal forecasts produced by a single-model system (Krishnamurti *et al*., 1999; Harrison, 2003; Cantelaube and Terres, 2005; Doblas-Reyes *et al*., 2006). The question arises whether this is also true for South Africa. Multi-model summer rainfall forecasts for southern Africa have shown to be more skilful than single-model forecasts produced for this region (Reason *et al*., 2006b). The skill of a multi-model system in predicting DJF rainfall for southern Africa has been investigated (Klopper and Landman, 2003). The three models used included two statistical models (CCA and quadratic discriminate analysis) and one GCM (ECHAM 3.6). Each model produced forecasts with different levels of skill, which means that a combined forecast will incorporate the strengths of each model. The forecasts were combined through simple unweighted averaging. The results showed that the multi-model forecast improved on the skill of the individual model forecasts, and that on average the combined forecast showed higher skill, at least for the majority of summer rainfall regions over southern Africa.

The skill in predicting DJF rainfall over southern Africa using a multi-model ensemble system has been evaluated (Landman and Goddard, 2003). The analysis used simulation data obtained by forcing five GCMs (CCM3.2, ECHAM4.5, NCEP-MRF9, COLA T63, NASA-NSIPP1) with simultaneous observed SST anomalies. Thus, DJF rainfall was predicted using observed DJF SST anomalies. The simulations performed by each GCM were recalibrated to homogeneous rainfall regions over southern Africa using the statistical method called MOS (Model Output Statistics). The simulations from the individual models were then combined by averaging the downscaled results. Results suggested that the combination of models improve on the performance of the best single-model ensemble (ECHAM4.5 – MOS).

1.8 OPERATIONAL SEASONAL FORECASTING AT SAWS AND UP

Routine seasonal climate forecasts using the Conformal-Cubic Atmospheric model (CCAM) has been produced at the University of Pretoria (UP) since August 2007. The model is also being applied at UP in the fields of climate simulation (Engelbrecht *et al.*, 2009) and short-range weather forecasting (Potgieter, 2007). In operational seasonal forecasting mode, CCAM is initialized using the 0Z analysis fields obtained from the Global Forecasting System (GFS). A three-month seasonal forecast (having 12 ensemble members initialized on 12 consecutive days) is issued on a monthly basis. Lower boundary forcing is prescribed from persisted SSTs, as obtained from the GFS. The model runs globally at C48 (approximately 200 km) horizontal resolution on a quasi-uniform grid. Output for a number of variables is available on a global 1° latitude-longitude grid. The forecasts are performed on the Velocity-cluster at the University of Pretoria and feeds into the multi-model seasonal forecast system of SAWS (Landman *et al.*, 2008). This dissertation reports on the use of CCAM-simulated fields as part of a maize yield forecast system for South Africa.

The latest development at the South African Weather Service (SAWS) is described in Landman *et al.* (2008). Here, the use of multi-model ensembles in operational predictability of seasonal to inter-annual rainfall over South Africa has been investigated. The models that were used include the ECHAM4.5 GCM, the CCAM GCM, the UKMO CGCM and a statistical CCA SST-rainfall model. The ECHAM4.5 model output were obtained from the International Research Institute (IRI), CCAM output data from UP and UKMO CGCM output form the European Centre for Medium-range Weather Forecasts (ECMWF). The ECHAM4.5 model has also been installed on the supercomputer of the SAWS and a 6-member ensemble of multi-decadal simulations, forcing the model with simultaneous observed SSTs, has been performed. Each model ran its own ensemble of simulations. Before combining the ensembles from the individual models, the ensemble mean was obtained for each model and MOS was applied to it for downscaling purposes. It was found that the model combinations did not always outscore the individual models, but the use of longer training periods and by combining only the best models are necessary requirements to improve on forecast skill. Inclusion of the statistical model that only uses antecedent SSTs as predictors in the multi-model systems made the results worse. It also appeared as if seasonal rainfall predictability is limited to mid-summer months which coincide with ENSO events and the highest skill during these seasons occur over the north-east and central-western regions of South Africa. Overall, useful skill was obtained from the multi-model systems for the DJF season. As a result of this project the first operational multi-model forecast, which made use of an 8-member ensemble CCAM forecast and a 24-member

ensemble ECHAM4.5 forecast for the April-May-June season, was issued for South Africa on 31 March 2008.

In the mean time, the multi-model system has been finalized, and operational rainfall and temperature forecasts are currently made routinely for the Southern African Development Community (SADC) region. SAWS has also obtained Global Producing Centre for Long-Range Forecasting status from the World Meteorological Organisation. The ECHAM4.5 GCM, which runs on the NAC SX-8 supercomputer of SAWS, is used for this purpose. ECHAM4.5 forecasts are also used in the operational multi-model forecasts mentioned above. This dissertation reports on the use of ECHAM4.5-simulated fields as part of a maize yield forecast system for South Africa.

1.9 CROP YIELD FORECASTING

Several studies have emphasized the sensitivity of agricultural production to weather (Hollinger, 1988). The vulnerability of field grown crops to fluctuations in the weather on a daily, monthly and seasonal time-scale (Doblas-Reyes *et al.*, 2006) affects the welfare of farmers due to the irregularity in crop yields from one year to another (Sivakumar, 2006). Therefore, many scientists have attempted to reduce the uncertainties associated with the growing season so that famers can make more informed decisions and take advantage of good seasons. The growth, development and yield of a crop are the function of interactions between the plant, weather, soil and management practices (Hansen *et al.*, 2006). The recent advances in the ability to predict fluctuations in the climate several months in advance have increased the opportunities of seasonal forecasts to alter management decisions and reduce the negative impacts of climate variability on crops (Hammer *et al.*, 2001; Mason, 2001; Sivakumar, 2006). However, farmers can benefit more from information when it is presented in terms of production outcomes than from a seasonal climate forecast by itself (Hansen and Indeje, 2004; Hansen *et al.*, 2006). Crop yield forecasts at an early enough lead-time can warn the farmer of a probable poor season and consequently allow the farmer to change the planting date, cultivar type as well as management and planning activities like the necessity of fertilizer and irrigation, in light of the expected conditions (Martin *et al.*, 2000).

Some of the first crop yield forecasting attempts were based on empirical relationships between variables in the environment and crop yield (Isard *et al.*, 1995). An advance in agricultural science took place in the 1970's with the development of the first crop simulation model (Fodor and Kovacs, 2003) and since then several simulation models have

been developed for a range of different crops (Whisler *et al.*, 1986; Ritchie, 1994). These models are by no means perfect, but can assist in understanding how cropping systems function (Bannayan and Court, 1999; Matthews, 2002). The main aim of the development of these crop simulation models was for application in agricultural research (Hoogenboom *et al.*, 1992), in particular the possibility of application in yield forecasting (Bannayan and Court, 1999). A crop simulation model is a mathematical representation of the complex real-world system (Fodor and Kovacs, 2003) and can simulate crop growth and estimate crop yield as a function of weather, soil and crop management conditions (Egli and Bruening, 1992; Boote *et al.*, 1996; Hoogenboom, 2000; Matthews, 2002; Palmer *et al.*, 2004). Numerous crop yield forecasting efforts have made use and are currently using dynamic crop simulation models as a tool to convert weather and climate forecasts into an estimation of the production in response to predicted future conditions (Challinor *et al.*, 2005; Hansen *et al.*, 2006).

Using a crop simulation model to predict crop yield for the forthcoming season or the season in progress requires weather input data for the entire growing season (Bannayan and Court, 1999; Lawless and Semenov, 2005). The key weather input variables are precipitation, temperature and solar radiation (Hoogenboom, 2000; Doblas-Reyes *et al.*, 2006). Thus, a forecast of these weather variables will need to be made weeks or even months prior to the specific season of interest (Doblas-Reyes *et al.*, 2006). The accuracy of the weather input data will influence the yield output produced by the crop simulation model (Nonhebel, 1994). Thus, improved weather forecasts will translate into more accurate yield forecasts (Challinor *et al.*, 2005). Many crop yield forecasting studies have used stochastic weather generators to construct synthetic weather for the growing season. These weather generators require some form of historical data for each weather variable as input in order to generate synthetic weather for a specific site (Bannayan and Court, 1999; Hoogenboom, 2000; Lawless and Semenov, 2005). Other crop yield forecasting studies have used daily GCM output for the growing season as input to a crop simulation model (Hansen *et al.*, 2006). Even though GCMs tend to distort daily variability, particularly precipitation, many of these studies were very successful by either calibrating the simulated yields produced with the raw GCM data, rescaling to GCM mean bias or by correcting the rainfall frequency and intensity of the GCM output (Hansen *et al.*, 2006). The set up of the crop model-GCM based simulation system used in this study is done in such a way to establish the skill of the system without any additional GCM output manipulation, therefore setting a baseline against which newly developed systems can be compared.

1.9.1 Yield Predictions in Europe

A method which uses the SUCROS crop simulation model in combination with the SIMMETEO stochastic weather generator has been tested for real-time winter wheat biomass and yield predictions at four sites in the UK (Bannayan and Court, 1999). Observed monthly mean values were used by SIMMETEO to generate representative weather data for each site. The simulations performed with SUCROS were updated throughout the growing season, by combining generated weather data with observed weather data. SUCROS simulated crop biomass, and yields were calculated by multiplying the simulated biomass with the measured harvest index at each site. The correlation between simulated and observed biomass and yield were found to increase as the growing season progresses, due to model updating. The forecasts showed reasonable skill which would provide an opportunity for the farmer to alter or adapt management before harvest.

In a similar study, the Sirius crop simulation model was used in combination with the LARS-WG weather generator for predicting within-season wheat yields at five sites in Europe and one site in New Zealand (Lawless and Semenov, 2007). The study aimed to assess lead-time for making skilful predictions before crop maturity. LARS-WG produced an ensemble of "artificial" weather datasets for each site. Each of the "artificial" weather ensemble members were combined with observed weather data and used to force the Sirius crop model. The combined datasets contained observed weather data for the initial part of the season and "artificial" weather data for the remainder of the season. As the season progressed, at 10-day increments, the observed data was increased and the "artificial" weather data reduced and new runs performed with the Sirius crop model. The results indicated that the uncertainty in the predictions decreases as the season evolves and that a usable level of skill is reached before crop maturity, but that the lead-time of skilful predictions varies significantly from one location to another.

Another objective of the DEMETER project was to demonstrate the value of seasonal climate forecasts by coupling the multi-model ensemble to application models (Palmer *et al.*, 2004). The WOFOST (WOrld FOod STudies) crop model from the Joint Research Centre (JRC) in Europe was used as the application model in this study. Output from the 7 CGCMs used in the DEMETER project was on a low spatial (1.5° x 1.5°) and temporal (monthly mean values) scale and had to be downscaled in both space and time before the data could be used to force the crop model. Hindcasts for each of the February-July seasons within the period from 1995 to 1998 were downscaled using singular value decomposition, MOS and a weather generator. Thereafter, the downscaled meteorological

data from each individual ensemble member was used to run the crop model for the four year period (1995 - 1998), which resulted in a wheat yield prediction ensemble and could consequently be used to derive a probability distribution function of wheat yield for Europe. The results were verified against actual wheat yield figures as well as yield simulations performed by the operational yield forecasting system of the JRC. The results were found to vary from country to country, with the highest correlation (0.73) between DEMETER-based yield predictions and actual yield figures found for the main wheat producing countries in Europe (France, Germany and the United Kingdom). It was concluded that reliable crop yield predictions is possible with the use of a multi-model ensemble of seasonal climate forecasts.

Crop simulation models have also been used in climate change studies. An investigation on the response of winter wheat production in France to climate change has been done, by forcing the CERES-Wheat model with raw daily output from the HadCM2 GCM (Mavromatis and Jones, 1998). The HadCM2-based yield predictions were found to correlate well with average yields simulated for the past century using observed weather data as input into the crop model. Furthermore, it was also observed from the results that the CERES-Wheat model captured the trend in yield associated with the trend in observed temperature well, but that the model did not capture the inter-annual variability in yield very well.

1.9.2 Yield Predictions in the United States of America

The United States Department of Agriculture uses a statistical model, which relates weather to yield, for their yield predictions (Lawless and Semenov, 2005). Long-term mean weather data are used as input into this statistical model, but this approach has been demonstrated to be inappropriate for yield predictions, due to the non-linear response of crops to their environment (Porter and Semenov, 1999).

The crop simulation model CORN-CROPS has been used to simulate the interactions of management practices and weather on maize yields in east central Illinois (Hollinger, 1988). Five plant dates, three plant populations, three cultivars, each with a different maturity rating, and weather data for a 14 year period (1970 - 1983) were considered for the analysis. The crop model was set up and run for the 14 year period and for all possible combinations of management inputs. The simulated yields were verified against actual yield estimates for Champaign County. Results revealed a strong agreement between the simulated yields and actual yield estimates, which is evidence that the crop model succeeds in representing the real world. It was concluded that CORN-CROPS has the potential to

influence crop management, by proposing different techniques that could lead to increased yields under the given weather conditions.

An examination on the possibility of using monthly weather projections for soybean yield estimates has been done for the Mississippi Delta (Reddy and Pachepsky, 2000). The crop simulation model GLYCIM and weather projections from three GCMs (GFDL R30, UKMO 89 and NCAR) were used. As crop simulation models normally use daily weather data as input, the monthly projections from the three GCMs were downscaled to daily weather data. Two methods were used to simulate soybean yields. The first method used the downscaled GCM data as input into the GLYCIM crop model and the second method employed a group method of data handling (GMDH) network with monthly weather data as input, to relate soybean yields to CO_2 levels, total solar radiation, average maximum and minimum temperature and rainfall for five months of the growing season. It was found that the GMDH network reproduced the GLYCIM simulated yields with a reasonably high level of accuracy and that this method could be used to obtain general relationships between crop yields and combinations of GCM projected temperature, precipitation and CO_2 concentrations.

1.9.3 Yield Predictions in Asia

To investigate the potential effect of climate change of rain-fed and irrigated maize yields in eastern China, three GCMs were coupled to the CERES-Maize model (Jinghua and Erda, 1996). The three GCMs that were used to produce the climate change projections included the Geophysical Fluid Dynamics Laboratory (GFDL) model, the high-resolution United Kingdom Meteorological Office (UKMO) model and the Max Planck Institute (MPI) model. The seasonal mean changes in temperature and precipitation evident from the output of the GCMs were applied to monthly temperature and precipitation of the baseline climate created by the Chinese Weather Generator, and this climate change data was then used to force the CERES-Maize model. Output from the CERES-Maize model under the climate change scenarios was compared to output from the simulations performed with the baseline climate data. Both rain-fed and irrigated maize yields were found to decrease under climate change conditions. This is a realistic result as an increase in temperature shortens maize growth, particularly the grain filling stage, and consequently results in lower yields.

As so many studies have focused on presenting crop yield forecasts deterministically, crop yield predictability using a probabilistic method has also been explored (Challinor *et al.*, 2005). The use of weather ensembles provides an opportunity for examining crop yield predictability probabilistically. A multi-model ensemble and the GLAM (General Large-Area

Model) crop simulation model were used to predict groundnut yields in western India. Daily output from the 7 CGCMs of the DEMETER project, each running their own ensemble of 9 seasonal hindcasts, were used as input into the GLAM crop model. GLAM was forced with the data of each individual ensemble member to produce both ensemble mean and probabilistic groundnut yield forecasts per district. The ensemble mean yield predictions were found to capture the inter-annual variability in yield relatively well, while predictive skill was found in predicting crop failure probabilistically.

1.9.4 Yield Predictions in Australia

One of the first studies for Australia, attempted to forecast crop yields by relating historical crop yields to the Southern Oscillation Index (SOI) (Nicholls, 1985). A number of years later, an investigation was done on the possibility of producing reliable sorghum yield predictions for the shires in Queensland by combining crop simulation and geographical information system technologies (Rosenthal *et al.*, 1998). Spatial rainfall, temperature and solar radiation data were overlaid and utilized in driving the QSORG sorghum simulation model for 300 locations in Queensland for the period from 1977 – 1988. Linear regression was used to find a relationship between the historical yields and simulated yields to obtain calibration equations for each shire. The predicted yields, at shire and state level, were verified against historical yields using regression analysis. The predicted yields were found to correlate exceptionally well with the historical yields at both shire and state level ($r = 0.96$). When comparing maps of predicted yield to maps of historical yield, it was found that this combined technique captures the spatial distribution of the yield among shires. It was concluded that this system can produce reliable sorghum production estimates on both shire and state level and that there exist good prospects for real-time use, especially in terms of the significance of seasonal climate forecasts on decision making at shire scale.

In Queensland the Agricultural Systems Research Unit developed “Whopper Chopper” software to predict production risk faced by farmers (Cox *et al.*, 2004). The software combined seasonal climate forecasts with crop modelling to assist farmers in selecting the management options that would result in the highest yields under the climatic conditions of the upcoming season. This system allowed farmers to investigate the effect of different plant dates, plant populations, nitrogen fertilizer application rates and many other variables on the expected yield.

1.9.5 Yield Predictions in South America

By using the information contained within seasonal climate forecasts, the potential predictability of maize yields in Ceara, Brazil has been investigated (Sun *et al.*, 2007). The predictability was analyzed for a period from 1971 to 2000 through the use of a 10-member ensemble of seasonal hindcasts produced by a RCM (the Regional Spectral model) nested within a GCM (the ECHAM4.5 model). The RCM integrations were for the main rainy season February-March-April-May. Two variables were considered to estimate the maize yield by means of linear regression in a cross-validated mode. The variables included seasonal mean rainfall and a weather index. In the maize yield simulations performed with the RCM data, the weather index showed superiority over the seasonal mean rainfall. When simulating maize yield with observed weather index values, it was found that the weather index accounts for almost 50% of the variance in maize yield in Ceara. It was concluded that the hindcasts correlate well with the observations and that the nested RCM is skilful in simulating seasonal mean rainfall and within-season weather statistics over the Ceara region.

1.9.6 Yield Predictions in Southern Africa

In the past, research mainly focused on relating crop yields to predictors such as rainfall. Numerous seasonal crop yield predictions for southern Africa have been derived from rainfall forecasts alone, but these forecasts do not account for the response of yields to other climatic variables like temperature, radiation, humidity and wind (Martin *et al.*, 2000).

A method for assessing the impact of drought on maize production in South Africa has been developed, by predicting the response of maize to drought that might occur during the course of the growing season (Du Pisani, 1987). The proposed method was tested for five locations, and historical climate records were used. For each of the variables in the historical climate records, median values were calculated for each month over the entire record. Thus, 12 median values were calculated (January to December) per variable and per location. Thereafter, the months in the historical records that yielded median values closest to the median values calculated over the entire record were used to construct a “median year” for each location (i.e. rainfall for location 1 can be made up of January 1939, February 1969, March 1981, April 1970 etc.). It was investigated whether it is possible to predict climatic impact at the end of December, January and February, by replacing the current season’s weather data with the median year’s data for the remainder of the growing season (January to May, February to May and March to May) and then forcing the CERES-

Maize model with these combined sets of genuine and "median year" data. The yield predictions based on the combined set of genuine and "median year" data were found to correlate well with the yield predictions based on a full set of genuine data. It was concluded that with the use of this method the impact of drought on maize yield should be predictable with a usable level of skill up to four months prior to harvest.

The impact of the ENSO phenomenon on rainfall variability over Zimbabwe and the potential for using ENSO predictions for maize management at site level were investigated (Phillips *et al*., 1998). A period from 1951 to 1991 was selected for the study. The mean NDJ SST anomaly in the Nino-3 region in the Equatorial Pacific Ocean were calculated for each of the 40 seasons and then used to group them into El Niño, La Niña and neutral years. Daily weather data, for the period under investigation, for four sites in Zimbabwe were used to drive the CERES-Maize model. The CERES-Maize model ran with different management strategies (2 nitrogen fertilizer treatments and 3 plant dates) to test for differences in yields between ENSO phases. The simulated yields were compared to observed yields and used as indicator of the potential usefulness of ENSO predictions. High variability in rainfall and high variability in the standard deviation of the simulated yields at each of the sites were found during all the ENSO phases. Thus, it was concluded that although ENSO is one of the most dominant sources of inter-annual climate variability at the four sites under investigation in this study, forecasts based on ENSO categories alone will probably not provide information with a level of skill high enough to be used in maize production decision making. In a similar and very successful study the Nino-3 index was used as the predictor to forecast both rainfall and maize yield for Zimbabwe (Cane *et al*., 1994). The results of this study indicated a stronger relationship between Zimbabwean maize yields and SSTs in the Nino-3 region than between rainfall over Zimbabwe and the SSTs in the Nino-3 region.

Seasonal maize water-stress forecasts for the primary maize-growing regions of South Africa and Zimbabwe have been prepared using a crop water-balance model (Martin *et al*., 2000). Historical gridded climate data for the period from 1961 to 1994 were used to force the simulations with the crop water-balance model. The model calculates water stress on a 0.5° x 0.5° grid from gridded rainfall, temperature, soil water holding capacity, plant date, monthly average wind speed, monthly average sunshine hours, cloud cover, and vapour pressure. Linear regression was then used to relate the output from the model (water-stress) to ENSO indices (SOI and Nino-3) with a 4-month lead-time to harvest. It was found that water-stress forecasts relate more strongly to ENSO than seasonal rainfall alone, but that the water-stress forecasts may provide a useful indication of climate fluctuations.

Exceptionally good results were found when forecasting water-stress for the main maize-growing regions in South Africa using the SOI.

In a more recent study, it was attempted to forecast maize yield for the Highveld region of South Africa using a weather analogue program (WAP) (Du Toit *et al.*, 2001). WAP identifies historical seasons with similar weather characteristics as the current season by considering the up-to-date weather conditions of the current season. Weather data of the five best-fitting seasons were used to force the CERES-Maize model to obtain a maize yield forecast. The impacts of climate variability on the economy of South Africa have also been examined (Jury, 2002). As maize production largely contributes to South Africa's gross domestic product (GDP), one of the objectives was to investigate the impact of rainfall variability on maize yields. July-August-September and September-October-November were identified as the two key seasons. The statistical method used intended to predict fluctuations in the maize yields at a lead-time of 3 to 6 months. A total of 18 predictors were considered. The predictors were selected based on principal component analysis of the maize yield and by correlation and composite mapping with respect to summer rainfall. An adjusted fit of 38% was found for the maize simulations when outgoing long-wave radiation in the central Indian Ocean and the stratospheric quasi-biennial oscillation were used as predictors. It was concluded that more that one-third of the variability in maize yields can be predicted at a lead-time of 6 months (a maize yield forecast issued in November for April).

1.10 AIMS AND APPROACH OF RESEARCH

The principal aim of this dissertation is to investigate the possibility of producing usable maize yield predictions for South Africa by using seasonal climate forecasts from a multi-model ensemble system as input into a crop model, thus simulating the response of the maize to potential climatic conditions.

The skill of the crop model is tested by firstly forcing it with observed weather data. These crop model integrations are performed for each of the magisterial districts in the main maize producing area of South Africa for the period 1979/80 to 1998/99. This simulation system sets the target skill level for the other simulation systems. The simulated maize yields are compared to actual maize yields.

Two crop model-GCM based maize yield simulation systems are described, in which GCM-simulated fields are used to force the crop model for each of the magisterial districts in the main maize producing area of South Africa. The skill of the two crop model-GCM based

simulation systems are tested over the same period used in the target simulations, by comparing the simulated maize yields to actual maize yields.

By combining the simulated maize yields produced by the two crop model-GCM based simulation systems, it can be tested whether the skill of a multi-model system outscores that of the best crop model-GCM based simulation system.

1.11 SUMMARY

To understand the effect of weather on maize yields, the growth stages of the maize plant have been described. The climate of South Africa and factors influencing South Africa's climate and the seasonal predictability of South African rainfall has also been discussed. The status of crop yield forecasting, globally as well as locally, has been summarized. Finally, the chapter concluded with the aim and approach of the research of this dissertation. In the next chapter the data, methods and models used to conduct the research are described in detail.

CHAPTER 2

DESIGN OF THE YIELD SIMULATIONS OVER SOUTH AFRICA

2.1 INTRODUCTION

In this chapter the research methodology applied and data used to obtain the maize yield simulations for South Africa are described in detail. This chapter is divided into five sections. In the first section the area of interest is depicted. The second section discusses the different weather datasets that are used in this study. The crop model that is used to simulate maize growth and development and to estimate the yield is described in section 3 and in section 4 all other data, other than weather data, required by the crop model in order to successfully simulate maize yield as well as the set up of the experiments, are described. The last section discusses the actual maize yields that are used as verification data in this study and the methods used to verify the simulated maize yields produced by the crop model.

2.2 AREA OF INTEREST

Maize is the primary grain crop grown in South Africa (Du Plessis, 2003). Approximately 8 million tons of maize grain is produced annually (Du Toit, 1997). Although maize production takes place across the country under various terrain, soil and climatic conditions (Du Plessis, 2003), the Free State and North-West Province constitute 65% of the total area under maize production in South Africa and 58% of the national maize yield are obtained from these two provinces (Du Toit, 1997). Based on their enormous contribution towards the national maize yield, the Free State and North-West Province are consequently selected as the combined area of interest for this study. Each magisterial district in the Free State and North-West Province are considered in this study, but unfortunately a number of districts are excluded from the investigation due to the lack of actual maize yields.

Three maize production regions are evident within the two provinces under investigation (ARC-GCI, 2008). These regions are based on spatial rainfall, temperature and heat unit differences and are known as the dry/warm western region, temperate eastern region and wet/cool eastern region (Figure 2.1). Different management practices are applied in each of the three regions in order to adapt to the climatic conditions (Du Toit *et al.*, 2000).

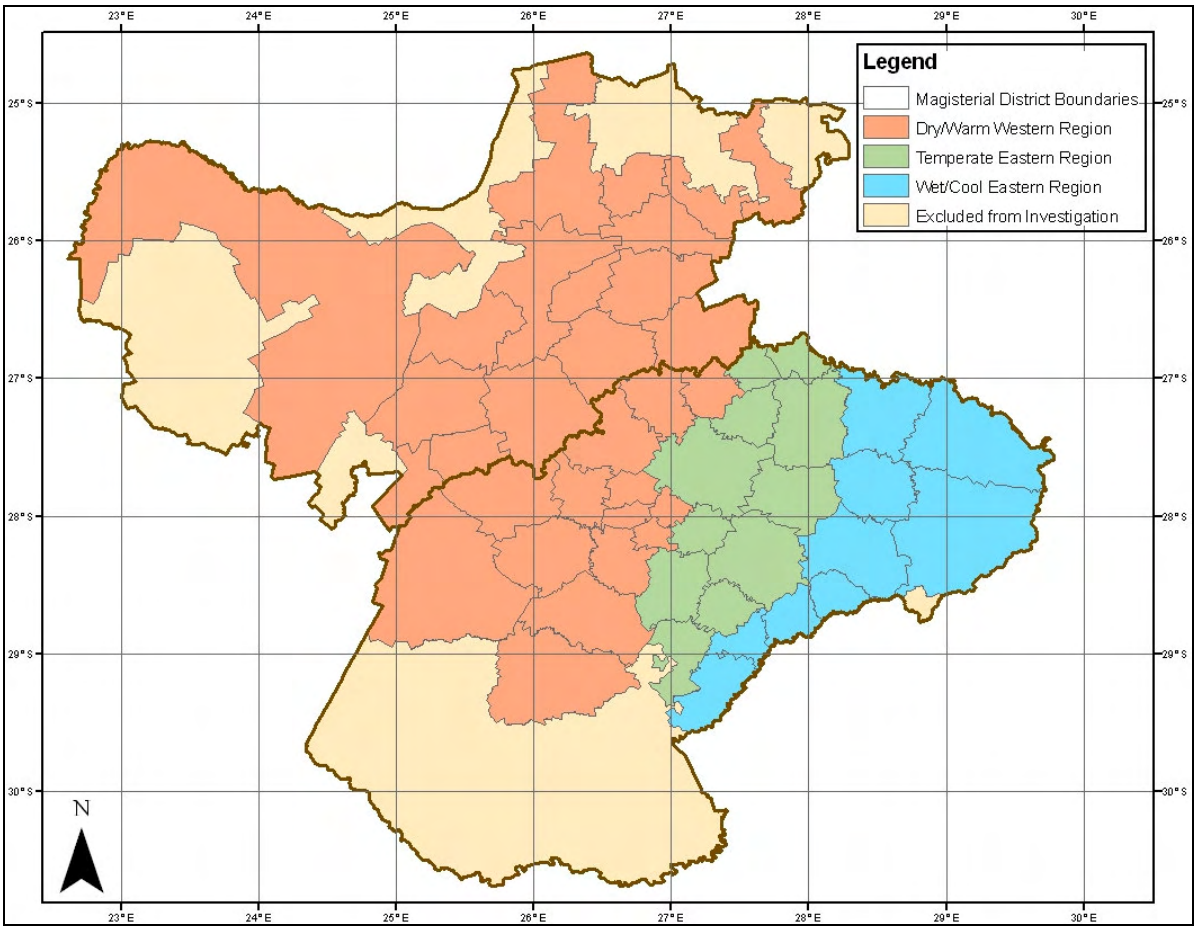

Figure 2.1: The study area and the three maize production regions.

2.3 WEATHER DATASETS

2.3.1 Observed Data

In order to simulate maize yield, daily rainfall, maximum temperature, minimum temperature and solar radiation data are required. Initially, weather station data was selected as the observed weather data in this study, but only 22 weather stations, both Agricultural Research Council and South African Weather Service stations, were identified within the study area that recorded the required variables for the entire period under investigation (1979 to 1999). From the uneven spatial distribution of the identified weather stations over the study area it was clear that the weather station data is not representative of the entire study area and therefore it was decided to use the weather data contained within the Southern African Quaternary Catchment Database (Schulze *et al.,* 2005) as an alternative.

This database comprises of a dense rain gauge network and originated out of a Water Research Commission project that was intended to be used for research purposes (Schulze

et al., 2005). The database contains daily hydroclimatic data for each quaternary catchment in South Africa and for a 50-year period from 1950 to 1999. The hydroclimatic variables that are included in this database are rainfall, maximum temperature, minimum temperature, vapour pressure deficit, minimum relative humidity, maximum relative humidity, solar radiation, Penman-Monteith reference evapotranspiration, soil water content in the A-horizon of the soil, soil water content in the B-horizon of the soil, soil moisture deficit in the A-horizon of the soil, soil moisture deficit in the B-horizon of the soil, saturated drainage from the A-horizon of the soil to the B-horizon of the soil and saturated drainage from the B-horizon of the soil to the groundwater zone.

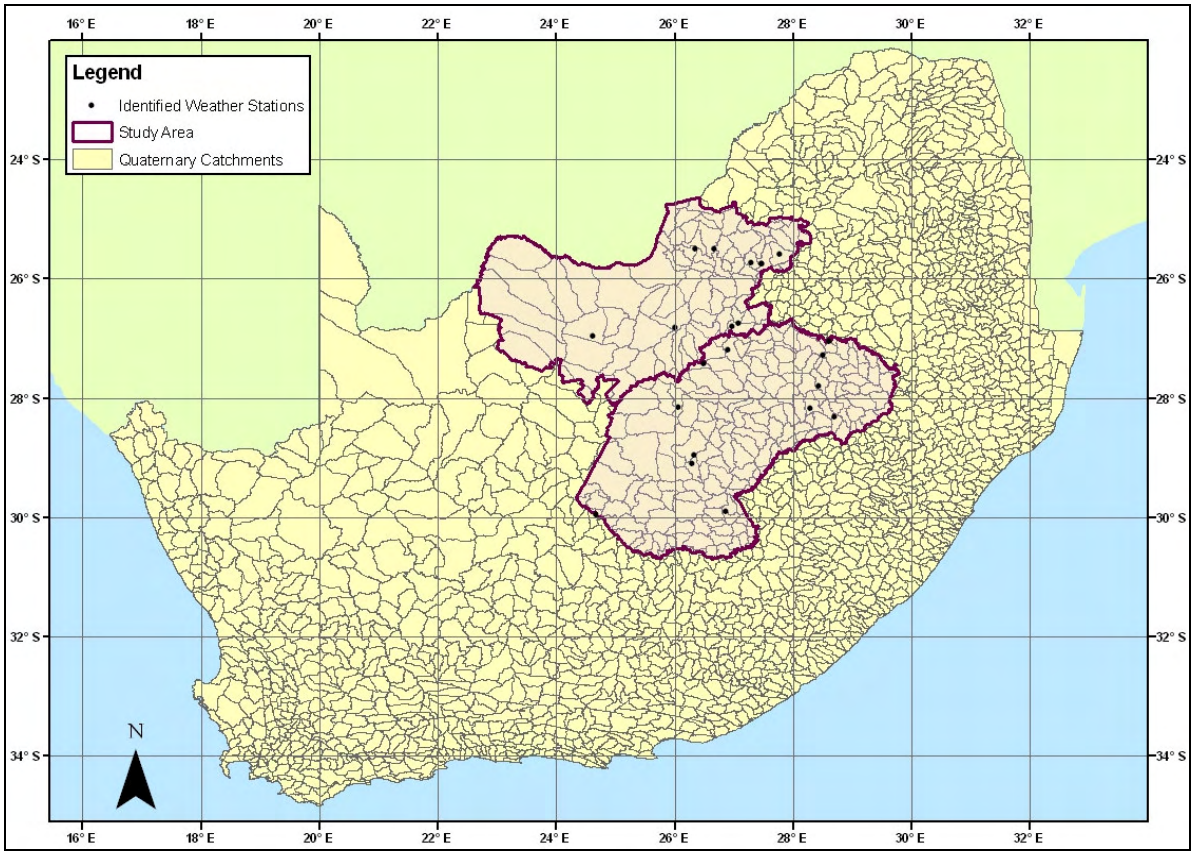

Figure 2.2: The distribution of the identified weather stations (black dots) within the study area compared to the distribution of quaternary catchments within the study area.

Figure 2.2 shows the quaternary catchments for the entire country as well as the positions of the 22 originally identified weather stations in the study area. From this figure it is evident that the quaternary catchment weather data is a much better geographical representation of the study area than the weather station data. Another advantage of the quaternary catchment database is that the data contained within the database closely fit the specific needs of this study. In other words, daily rainfall, temperature and solar radiation data are

available for each quaternary catchment in the study area for the entire period under investigation (1979 to 1999).

2.3.2 Simulated Fields

The numerically simulated fields that are used in this study were produced by two Global Circulation Models (GCMs). They are the Conformal-Cubic Atmospheric Model (CCAM) (McGregor and Dix, 2001) and the ECHAM4.5 model (Roeckner *et al.*, 1996). In order to account for the uncertainty in the initial state of the atmosphere, each model produced an ensemble of simulations from varying initial conditions. These two GCMs form a multi-model system by statistically combining the ensembles from the individual models.

2.3.2.1 CCAM

2.3.2.1.1 Model Description

CCAM is a GCM developed by the CSIRO Marine and Atmospheric Research in Australia (McGregor, 2005a). The model may be integrated in variable-resolution mode with high resolution over an area of interest using the Schmidt stretching factor, thereby allowing it to function as a regional climate model (Engelbrecht *et al.*, 2009). CCAM replaced the limited-area nested climate model DARLAM that was used for regional climate modelling applications (McGregor and Nguyen, 1999; Engelbrecht *et al.*, 2002). Variable-resolution global modelling offers vast flexibility for dynamic downscaling from other GCMs or reanalysis data, effectively requiring only sea surface temperatures (SSTs) and, optionally, far-field winds from the global model in which it is nudged (McGregor and Dix, 2001; Wang *et al.*, 2004).

The model uses a quasi-uniform grid, which is obtained by projecting the six panels of a cube onto the spherical surface of the earth (McGregor and Nguyen, 1999). Since the grid has a fairly uniform resolution over the globe it avoids problems associated with normal latitude-longitude grid projections that require filtering in the vicinity of the poles due to the clustering of grid points (McGregor, 2005a).

CCAM employs a two-time-level, semi-implicit discretization of the hydrostatic primitive equations (McGregor, 1996; McGregor, 2005a). The model also makes use of a semi-Lagrangian scheme for horizontal advection, which in combination with the semi-implicit procedure ensures numerical stability when using large time steps (McGregor, 2005a).

Total-variation-diminishing vertical advection is employed. An unstaggered grid is used, with winds transformed to/from C-staggered locations before/after gravity wave calculations (McGregor, 2005b). More details on the geometrical aspects and dynamic formulation of CCAM can be found in McGregor (2005a).

Furthermore, CCAM comprises of a comprehensive set of physical parameterization schemes. These include the CSIRO mass-flux cumulus convection scheme that takes downdrafts and the evaporation of rainfall into account, the long and shortwave radiation scheme of GFDL (Schwarzkopf and Fels, 1991) with interactive diagnosed cloud distributions (Rotstayn, 1997), a gravity wave drag scheme, a stability-dependent boundary layer scheme with non-local vertical mixing and a soil and canopy scheme describing six soil layers of temperature and moisture as well as three layers for snow (Gordon *et al.*, 2002).

2.3.2.1.2 Design of Simulations

CCAM performed five 25-year (1979 to 2003) integrations for the entire globe on a horizontal grid of approximately 2.1° x 2.1° degrees, with 18 σ-levels in the vertical. The simulations were initialised using a lagged average forecast approach (Hoffman and Kalnay, 1983). Each simulation was forced with observed monthly sea surface temperatures (SSTs), obtained from the Atmospheric Model Intercomparison Project (AMIP) dataset, at its lower boundary. Model output is available for a number of variables on a 1° latitude-longitude grid, at daily time intervals starting on 1 January 1979 and ending on 31 December 2003. These simulations were performed on the Velocity-cluster at the University of Pretoria.

2.3.2.2 ECHAM4.5

2.3.2.2.1 Model Description

The ECHAM4.5 GCM is a primitive equation model that was developed by the Max Planck Institute for Meteorology in Hamburg, Germany (Roeckner *et al.*, 1996). Many features of this model were adopted from the spectral weather prediction model of the European Centre for Medium Range Forecasts (ECMWF). However, a different set of parameterization schemes were employed for ECHAM4.5 than for the ECMWF model.

ECHAM4.5 uses a Gaussian transform grid on which the nonlinear terms and most of the parameterized physics is calculated. Furthermore, a semi-implicit time stepping scheme and weak time filter are used. This avoids the decoupling of the solutions at the two time levels in the time stepping scheme. The model employs a 19 – level hybrid sigma-pressure coordinate system which extends up to 10 hPa in the vertical.

The model occupies a semi-Lagrangian scheme to calculate the transport of water vapour, cloud water and trace constituents (Williams and Rasch, 1994). Land surface data that are supplied to the model include orography, albedo, roughness length, vegetation type, leaf area index, soil water holding capacity, soil heat capacity and soil thermal conductivity.

The physical parameterizations that are incorporated in the model includes a horizontal diffusion scheme which uses a high-order for diffusion in the troposphere, a surface flux and vertical diffusion scheme using the Monin-Obukhov theory to calculate turbulent fluxes at the surface, a land surface processes scheme which comprises of water and heat in the soil, snow pack over land, the heat budget of land ice, interception of rainfall and evapotranspiration, a gravity wave drag scheme using the McFarlane (1987) and Palmer *et al.* (1986) method, a cumulus convection scheme based on the bulk mass flux concept, a stratiform clouds scheme and a radiation scheme (Roeckner *et al.,* 1996).

2.3.2.2.2 Design of Simulations

A 6-member ensemble of simulations was produced by ECHAM4.5 for the period 1979 to 2003. The model ran globally at a horizontal resolution of approximately 2.8° x 2.8° with 19 levels in the vertical. The model was forced at its lower boundary using AMIP SSTs, equivalent to the lower boundary forcing applied in the CCAM simulations. Lagged Average Forecasting was likewise used to initialize the different ECHAM4.5 ensemble members. Model output, in daily time steps, is available on the 2.8° latitude-longitude grid and for a number of variables. These model runs were performed at the South African Weather Service (SAWS).

2.4 CROP GROWTH SIMULATION MODEL

The CERES-Maize model that forms part of the Decision Support System for Agrotechnology Transfer (DSSAT) is used in this study to simulate maize growth and estimate maize yield. A total of 25 model configurations are built into DSSAT for a number

of different crops such as cereals, legumes, root crops, oil crops, vegetables, forages and fruits. The DSSAT cropping system model was selected for this study based on it being an internationally recognized model which is used by researchers worldwide (Jones *et al.*, 2003) including researchers in South Africa (e.g. Du Toit, 1997; Du Toit *et al.*, 2000). In southern Africa the CERES-Maize model has been used to asses the impact of drought on maize production in South Africa (Du Pisani, 1987), to investigate the potential of ENSO predictions for maize management in Zimbabwe (Phillips *et al.*, 1998) and to forecast the maize yield of the Highveld region of South Africa (Du Toit *et al.*, 2001).

2.4.1 Model Description

DSSAT was developed through the collaboration of a number of researchers across the globe (Jones *et al.*, 2003). The development of this cropping system model formed part of the International Benchmark Sites Network for Agrotechnology Transfer (IBSNAT) project (Tsuji, 1998). The main drive behind the development of the DSSAT system was the need to make better decisions about transferring production technology from one site to another, where completely different soil and climate conditions prevail (Uehara and Tsuji, 1998).

In DSSAT a group of independent programs are joined together in order to predict the behaviour of a certain crop under specified conditions (Jones *et al.*, 2003). In other words, the growth, development and yield of a crop is simulated based on prescribed climatic conditions, soil conditions, cultivar specific genetic inputs and management information. The system allows the user to investigate the effect of different management practices on a particular crop in a specified environment (Du Toit *et al.*, 1994).

The CERES-Maize model within DSSAT was designed to simulate maize growth with a minimum set of data (Du Toit *et al.*, 2002). CERES-Maize is a daily time step model and therefore requires daily weather data that includes rainfall, maximum air temperature, minimum air temperature and solar radiation. The model uses the weather data supplied to compute the rate at which the plant progresses from one growth stage to another, daily plant growth, dry matter production, water stress and temperature stress (Jones *et al.*, 2003). A detailed description of the soil, in the form of a one dimensional profile, is also required by the model. Soil input data are used to compute daily changes in soil water content due to the infiltration of rainfall and irrigation, vertical drainage, unsaturated flow, soil evaporation, plant transpiration as well as root water uptake (Jones *et al.*, 2003). Another input required by the model is cultivar specific genetic coefficients (Table 2.1) which describes the phenology of each maize cultivar. Lastly, the CERES-Maize model requires

information on the management practices applied to the specific maize cultivar cultivated under the prescribed climatic and soil conditions. The management information includes data on planting, irrigation, fertilizer, organic amendments, chemical application, tillage and harvest.

Variable	Description
P1	Thermal time from seedling emergence to end of juvenile phase, during which the plant is not responsive to changes in photoperiod
P2	Extent to which development is delayed for each hour increase in photoperiod above the longest photoperiod at which development proceeds at a maximum rate.
P5	Thermal time from silking to physiological maturity
G2	Maximum possible number of kernels per plant.
G3	Kernel filling rate during the linear grain filling stage and under optimum conditions
PHINT	Interval in thermal time between excessive leaf tip appearances

Table 2.1: Genetic coefficients for maize as required by the CERES-Maize model (Jones *et al.*, 2003).

2.4.2 Agricultural Inputs

CERES-Maize model simulations are performed for each magisterial districts in the study area. Consequently, it is necessary to obtain the agricultural inputs required by the model to perform successful simulations for each magisterial district under investigation.

2.4.2.1 Soil Inputs

To simulate maize yield, the CERES-Maize model needs a detailed description of the soil in each magisterial district. The Soil Profile Information System of the Agricultural Research Council, Institute for Soil, Climate and Water contains descriptions and analyses data of soil profiles taken at numerous points all over South Africa. The data of all the soil profiles taken within the study area are extracted from this database. The number of soil profiles in each magisterial district varies. Six magisterial districts are eliminated from the study, as no soil profile data are available for them. These districts include Parys, Odendaalsrus, Fouriesburg, Clocolan, Frankfort and Ventersburg. Figure 2.3 shows the eliminated magisterial districts (light purple colour).

A number of different soils can occur in a single magisterial district, but it is unknown on which of these soils maize is cultivated. To take this uncertainty into account a range of

soils are selected for each magisterial district. The soils are categorized into four classes; high agricultural potential soils, medium agricultural potential soils, low agricultural potential soils and soils not suitable for agriculture. This categorization is based purely on the characteristics (soil depth and texture) of each soil. Out of the several soils that occur within a given magisterial district, a soil in each of the classes is selected for use in this study. Thus, three soils are selected per magisterial district, one with high potential, one with medium potential and one with low potential. Not all of the magisterial districts have a soil in each of the classes. This results in several districts with only two selected soils as well as districts with only one selected soil. Table 2.2 shows the soils that are selected for each of the magisterial districts as well as the soil profile data which the CERES-Maize model requires.

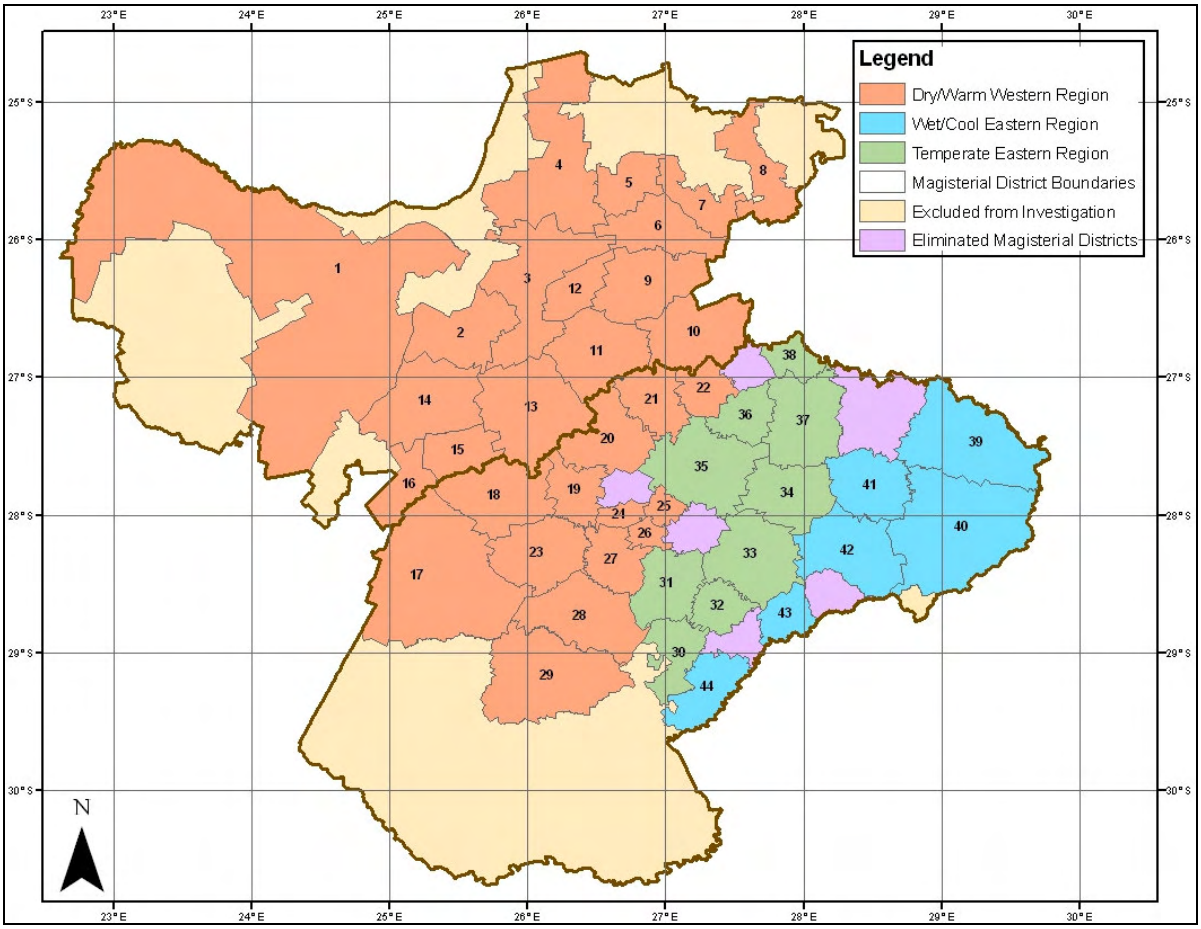

Figure 2.3: The magisterial districts eliminated from the study due to the lack of soil data (light purple colour).

Except for the information in Table 2.2, the CERES-Maize model also requires the colour, drainage, runoff potential, percentage stones, total nitrogen percentage of each soil as well as the slope of the site where the soil profile was taken. The colour of the soils is

determined from Macvicar *et al.* (1977) and Soil Classification Working Group (1991). Drainage are obtained from Schoeman *et al.* (2000) and runoff potential from Schulze (1985). The percentage stones in each of the selected soils are assumed to be zero based on information in the Land Types of South Africa, Soil Inventory Database (Land Type Survey Staff, 1972 – 2008). As the total nitrogen percentage of 500 soil profiles all range between 0.05% and 0.1% (Soil Survey Staff, 2008) an average value of 0.075% is assumed for each of the selected soils in Table 2.2. The slope of the sites are assumed to be perfectly flat (slope = 0%). It is important to keep these assumptions in mind when evaluating the model's performance.

Apart from the soil profile data entered into the CERES-Maize model the model also calculates a number of variables which include the lower limit (LL), drained upper limit (DUL), saturation, bulk density, saturated hydraulic conduct and root growth factor of each soil. These model calculated values can be edited. The LL and DUL is the water holding properties of the soil (Botha and Eisenberg, 1992). The LL can be interpreted as the soil water content at which the development and growth of a plant stops and the DUL as the soil-water content at which drainage from a pre-wetted soil comes to an end (Gebregiorgis and Savage, 2006). Thus, the LL and DUL of the soil plays an important role in crop growth in terms of the amount of water available to the plant. Therefore it was decided to replace the model calculated LL and DUL values (Rawls *et al.,* 1982) with values calculated using the methods described in Botha and Eisenberg (1992). These methods use clay content and cation exchange capacity to calculate soil water retention. It was tested for South Africa for a range of matric potentials, and excellent results were obtained when comparing the calculated water content values with observed values. The Botha and Eisenberg (1992) methods that are used to calculate the new LL and DUL values are as follows:

Lower limit (LL): $LL = 0.393 + 0.2556 * clay\% + 0.04043 * CEC$

Drained Upper Limit (DUL): $DUL = 2.315 + 0.2796 * clay\% + 0.07383 * CEC$

where CEC is the Cation Exchange Capacity in me kg^{-1} and LL and DUL is in %.

Number	Magisterial District	Classification	Soil Name	Master Horizon	Depth bottom (cm)	Clay (%)	Silt (%)	Organic Carbon (%)	pH in Water	Cation Exchange Capacity (cmol/kg)
1	Vryburg	High potential	Clovelly Setlagole (Cv3100)	A	30	9.6	1.4	0.2	6.8	5.0
				B	120	13.8	2.0	0.2	6.1	7.5
		Medium potential	Clovelly Annandale (Cv33)	A1	35	16.7	0.9	0.2	6.1	3.9
				B21	70	11.8	1.3	0.2	5.8	3
		Low potential	Hutton Mangano (Hu33)	A1	25	5.7	0.1	0.1	6.9	2.3
				B2	54	11.9	2.7	0.2	6.3	4.9
2	Delaryville	High potential	Avalon Soetmelk (Av36)	A1	20	11.3	2.2	0.5	5.8	3.2
				B21	90	20.2	3.0	0.2	6.2	4.0
				B22	140	26.4	3.7	0.2	6.2	4.5
		Medium potential	Avalon Mafikeng (Av3200)	A	30	12.1	1.6	0.3	7.0	5.8
				B1	75	27.8	2.5	0.3	7.2	10.3
		Low potential	Glencoe Beatrix (Gc33)	A1	27	10.8	2.0	0.3	6.3	7.4
				B21	60	12.9	1.9	0.1	7.6	3.3
3	Lichtenburg	High potential	Hutton Ventersdorp (Hu3200)	A	35	10.4	2.8	0.5	6.6	6.0
				B	120	19.9	1.8	0.3	6.7	7.2
		Medium potential	Avalon Mafikeng (Av3200)	A	30	11.9	1.7	0.4	7.0	7.3
				B1	90	24.4	2.1	0.3	7.1	13.6
		Low potential	Preiska Hougham (Pr1110)	A	20	19.8	3.9	0.8	7.8	7.5
				B	60	22.8	3.4	0.5	7.7	9.4

4	Marico	High potential	Hutton Msinga (Hu26)	A1	18	13.3	13.2	0.5	5.8	3.8
				B21	62	19.0	9.1	0.4	5.9	4.5
				B22	120	23.7	10.2	0.2	5.9	3.5
		Medium otential	Shortlands Glendale (Sd21)	A1	35	27.9	11.5	0.6	5.9	10.4
				B21	85	42.9	14.1	0.5	6.3	13.6
		Low potential	Hutton Roodepoort (Hu30)	A1	34	5.7	53.1	0.5	5.7	3.5
				B21	80	5.6	3.2	0.3	6.0	3.1
5	Swartruggens	High potential	Hutton Clansthal (Hu24)	A1	23	11.6	3.3	0.4	5.9	2.7
				B2	120	12.7	3.0	0.1	5.8	2.0
6	Koster	High potential	Shortlands Glendale (Sd21)	A1	32	25.0	20.5	0.8	6.7	9.5
				B21	120	37.6	26.4	0.4	6.5	11.1
		Medium potential	Hutton Suurbekom (Hu2200)	A	20	32.5	9.9	1.4	5.8	9.0
				B1	80	40.9	11.9	0.6	6.2	7.5
		Low potential	Clovelly Southwold (Cv26)	A1	27	15.7	4.9	0.6	5.5	3.5
				B2	50	20.0	5.2	0.4	5.3	3.3
7	Rustenburg	High potential	Hutton Doveton (Hu27)	Ap	32	10.2	3.1	0.4	7.2	4.5
				B21	83	38.4	5.8	0.3	7.2	7.3
				B22	120	28.2	2.4	0.3	7.1	6.8
		Medium potential	Hutton Hayfield (Hu2100)	A	30	30.4	5.1	1.3	6.0	6.7
				B	120	34.9	5.6	0.8	5.8	5.4
		Low potential	Westleigh Mareetsane (We2000)	A	25	6.9	4.2	0.5	5.8	1.2
				B1	50	21.8	5.8	0.3	5.5	5.0

8	Brits	High potential	Hutton Ventersdorp (Hu3200)	A	30	15.9	7.8	0.8	7.1	6.2
				B	120	22.8	6.9	0.4	7.9	7.0
		Medium potential	Bloemdal Roodeplaat (Bd3200)	A	30	14.7	6.1	0.7	7.9	5.8
				B1	80	23.6	7.0	0.4	8.0	5.8
		Low potential	Kroonstad Morgendal (Kd1000)	A	20	7.8	8.1	0.8	6.8	5.4
				G	70	9.2	11.9	0.3	7.5	5.4
9	Ventersdorp	Medium potential	Hutton Msinga (Hu26)	A1	20	23.4	7.4	0.7	5.6	6.8
				B2	70	26.6	7.3	0.3	5.9	5.1
		Low potential	Hutton Suurbekom (Hu2200)	A	20	14.6	3.6	0.5	5.1	4.3
				B1	60	23.7	5.3	0.4	6.2	5.7
10	Potchefstroom	High potential	Hutton Shorrocks (Hu36)	A1	58	21.5	15.8	0.6	6.7	7.8
				B2	110	18.1	19.1	0.2	6.9	5.0
11	Klerksdorp	High potential	Hutton Suurbekom (Hu2200)	A	30	14.9	5.5	0.6	5.9	4.8
				B	120	20.0	5.3	0.3	6.3	7.3
		Medium potential	Bainsvlei Amalia (Bv3200)	A	30	15.2	4.1	0.6	6.2	6.0
				B1	90	25.8	4.1	0.3	6.5	8.2
		Low potential	Hutton Stella (Hu3100)	A	25	9.3	2.8	0.3	6.7	3.7
				B	60	13.4	3.3	0.3	6.6	3.4
12	Coligny	High potential	Hutton Shorrocks (Hu36)	A1	20	24.9	8.0	0.6	6.3	6.5
				B21	56	33.5	13.4	0.6	6.2	8.4
				B22	100	32.7	19.2	0.4	6.0	8.0
		Medium potential	Avalon Mafikeng (Av3200)	A	30	18.4	5.0	0.5	6.2	6.8
				B1	90	31.5	5.4	0.6	6.1	11.9
		Low potential	Bloemdal Vrede (Bd3100)	A	30	6.9	2.7	0.3	7.9	3.1
				B1	70	11.5	3.3	0.2	6.8	3.5

13	Wolmaransstad	High potential	Avalon Mafikeng (Av3200)	A	30	13.5	2.9	0.4	5.2	5.5
				B1	100	21.2	2.6	0.3	6.8	6.7
		Medium potential	Hutton Shorrocks (Hu36)	A1	20	10.3	5.3	0.4	6.2	5.0
				B2	80	17.2	4.7	0.3	6.4	5.4
		Low potential	Westleigh Mareetsane (We2000)	A	30	9.5	1.5	0.3	7.1	6.0
				B2	80	25.9	1.5	0.3	6.5	12.2
14	Schweizer Reneke	High potential	Hutton Portsmouth (Hu35)	A1	24	10.9	2.4	0.2	6.3	5.7
				B2	130	6.9	3.1	0.2	6.2	3.8
		Medium potential	Hutton Ventersdorp (Hu3200)	A	20	14.1	3.3	0.3	6.1	6.9
				B	70	26.2	3.2	0.3	6.7	10.7
		Low potential	Glencoe Vlakput (Gc3200)	A	30	8.3	1.9	0.3	6.8	6.1
				B1	80	16.1	3.1	0.3	6.8	12.2
15	Bloemhof	Medium potential	Hutton Shorrocks (Hu36)	A1	20	14.9	5.4	0.3	6.1	6.6
				B2	80	25.6	5.3	0.3	6.3	8.6
16	Christiana	Low potential	Hutton Shorrocks (Hu36)	A1	25	11.4	1.3	0.4	7.8	6.6
				B2	55	24.5	1.6	0.4	7.2	12.3
17	Boshof	High potential	Hutton Mangona (Hu33)	A1	35	7.4	1.4	0.3	7.6	3.2
				B21	75	11.2	0.8	0.2	7.3	3.2
				B22	120	14.5	0.6	0.1	6.8	4.3
		Medium potential	Shortlands Kinross (Sd20)	A1	32	17.8	5.4	0.6	6.8	8.1
				B21	95	28.4	4.7	0.4	7.1	13.9
		Low potential	Sterkspruit Bakklysdrif (Ss13)	A1	12	12.5	2.0	0.3	8.1	6.2
				B21	40	28.2	4.8	0.7	7.9	15.3

18	Hoopstad	High potential	Clovelly Makuya (Cv34)	A1	40	8.0	0.2	0.2	8.5	4.7
				B2	120	10.6	1.3	0.2	8.4	5.7
		Medium potential	Oaklea Limpopo (Oa46)	B2	90	23.3	6.0	0.2	8.8	8.4
				C	130	22.5	36.5	0.1	9.0	7.6
19	Wesselsbron	High potential	Hutton Mangano (Hu33)	A1	56	8.4	2.5	0.2	8.5	2.9
				B21	92	12.6	2.4	0.2	6.5	3.6
				B22	130	18.7	2.2	0.2	6.4	5.5
		Low potential	Sterkspruit Stanfort (Ss23)	A1	18	8.3	2.4	0.4	7.4	3.6
				B2	36	25.6	4.5	0.6	9.1	13.7
20	Bothaville	High potential	Avalon Heidelberg (Av34)	A1	35	5.9	4.9	0.2	7.0	2.8
				B21	100	15.0	4.2	0.2	6.7	4.0
				B22	240	18.2	1.5	0.2	7.6	6.3
		Medium potential	Hutton Shorrocks (Hu36)	A1	25	24.7	3.1	0.3	6.7	9.1
				B2	75	25.4	3.8	0.2	6.8	9.1
		Low potential	Bonhein Weenen (Bo40)	A1	31	17.5	3.9	0.6	8.7	11.0
				B2	70	25.6	4.2	0.2	7.9	13.0
21	Viljoenskroon	Medium potential	Glencoe Weltevrede (Gc14)	A1	55	5.7	0.6	0.3	5.1	1.7
				B21	100	8.8	4.8	0.2	4.8	2.3
				B22	110	9.0	3.3	0.2	5.8	3.0
		Low potential	Westleigh Sibasa (We13)	A11	20	11.6	1.4	0.2	6.2	3.7
				A12	30	21.7	2.3	0.3	5.7	6.5
				B2	60	36.8	4.4	0.3	6.1	11.8
22	Vredefort	High potential	Hutton Msinga (Hu26)	A1	35	20.7	5.7	0.5	6.1	4.6
				B2	87	30.2	8.5	0.3	6.0	5.1
				B3	115	23.3	9.7	0.2	5.7	5.1

23	Bultfontein	High potential	Clovelly Annandale (Cv33)	A1	34	6.2	1.2	0.3	7.1	2.7
				B21	67	8.5	1.1	0.2	7.4	2.4
				B22	115	16.7	1.0	0.1	7.2	3.8
		Low potential	Hutton Shorrocks (Hu36)	A1	20	12.6	4.9	0.5	6.5	6.6
				B2	60	26.1	4.6	0.4	6.1	11.4
24	Welkom	High potential	Avalon Soetmelk (Av36)	A1	40	33.6	2.8	0.4	7.5	3.8
				B21	80	23.3	4.4	0.4	7.2	6.2
				B22	120	25.7	2.4	0.2	7.2	5.3
25	Henneman	Medium potential	Hutton Shorrocks (Hu36)	A1	28	17.8	1.5	0.6	7.2	7.3
				B2	72	28.2	2.4	0.5	6.9	12.6
26	Virginia	Medium potential	Clovelly Blinkklip (Cv36)	A1	35	11.3	1.2	0.4	7.7	3.5
				B21	95	22.7	1.2	0.3	7.3	6.6
27	Theunissen	High potential	Clovelly Blinkklip (Cv36)	A1	35	12.5	1.9	0.3	6.9	3.2
				B21	120	25.0	2.2	0.3	6.9	5.8
		Low potential	Valsrivier Waterval (Va11)	A1	25	13.8	3.1	0.4	6.7	5.1
				B21	65	43.0	3.7	0.4	7.1	11.3
28	Brandfort	High potential	Oaklea Limpopo (Oa46)	Ap	20	20.0	9.4	0.5	7.9	10.7
				B21	50	26.3	10.1	0.2	8.8	13.9
				B22	120	27.0	17.0	0.2	9.6	14.0
		Medium potential	Shortlands Glendale (Sd21)	A1	28	19.9	3.8	0.6	6.9	5.8
				B21	68	40.7	2.6	0.3	7.0	12.8

29	Bloemfontein	High potential	Hutton Shorrocks (Hu36)	A1	30	12.9	1.4	0.4	8.2	5.4
				B21	65	24.8	0.6	0.4	7.3	9.5
				B22	120	31.8	1.9	0.3	7.1	11.5
		Medium potential	Bainsvlei Bainsvlei (Bv36)	A1	30	10.8	2.1	0.3	7.6	3.9
				B21	65	27.1	1.8	0.3	6.9	6.9
		Low potential	Valsrivier Waterval (Va11)	A1	33	9.1	2.4	0.4	6.9	4.5
				B21	65	37.9	0.6	0.5	6.6	11.6
				B22	90	33.3	1.7	0.3	6.9	12.0
30	Excelsior	Medium potential	Westleigh Rietvlei (We12)	A1	35	16.4	9.2	0.5	5.7	5.7
				B21	60	33.1	10.7	0.4	6.3	8.4
				B22	90	70.5	6.1	0.1	6.5	18.1
		Low potential	Valsrivier Arniston (Va31)	A1	30	12.3	8.1	0.7	6.0	5.1
				B2	60	47.6	6.7	0.7	6.9	16.6
31	Winburg	Medium potential	Westleigh Sibasa (We13)	A1	40	18.1	3.5	0.4	7.8	5.3
				B21	85	33.6	2.8	0.4	6.8	8.4
		Low potential	Valsrivier Arniston (Va31)	A1	30	14.6	11.5	0.4	5.7	4.9
				B21	55	45.7	10.7	0.6	7.1	14.0
32	Marquard	Medium potential	Oaklea Leeufontain (Oa16)	A1	28	14.3	7.6	0.6	5.9	5.3
				B2	60	24.3	8.3	0.3	6.4	6.9
		Low potential	Westleigh Sibasa (We13)	A1	34	11.2	9.9	0.3	6.5	3.6
				B2	60	53.2	7.2	0.6	6.3	13.1
33	Senekal	Medium potential	Westleigh Sibasa (We13)	A1	58	12.8	2.3	0.3	6.2	5.0
				B2	84	55.5	4.0	0.3	6.2	11.7
		Low potential	Valsrivier Sheppardvale (Va42)	A1	23	22.1	8.0	0.7	6.8	7.3
				B2	54	55.2	16.1	0.7	7.6	18.6

34	Lindley	Medium potential	Hutton Msinga (Hu26)	A1	55	11.5	3.8	0.5	5.9	3.5
				B2	90	15.9	4.9	0.4	5.6	3.6
35	Kroonstad	High potential	Avalon Soetmelk (Av36)	A1	32	17.2	3.9	0.4	5.9	4.6
				B21	63	31.5	5.1	0.4	5.8	7.0
				B22	115	39.8	6.3	0.2	6.0	8.3
		Medium potential	Bainsvlei Bainsvlei (Bv36)	A1	30	12.7	2.2	0.3	6.4	3.7
				B21	60	20.7	2.7	0.3	6.4	5.3
				B22	100	23.0	4.6	0.3	6.6	8.2
36	Koppies	High potential	Hutton Schorrocks (Hu36)	A1	49	9.7	2.1	0.2	6.3	4.1
				B21	86	16.0	2.3	0.2	5.8	5.7
				B22	120	18.5	2.3	0.1	6.1	5.1
37	Heilbron	Medium potential	Clovelly Southwold (Cv26)	A1	33	23.9	10.4	0.7	6.0	6.5
				B2	67	30.4	10.1	0.5	5.8	6.9
38	Sasolburg	High potential	Avalon Mooiveld (Av31)	A1	40	3.3	1.3	0.3	5.1	1.5
				B21	110	3.1	0.6	0.1	4.9	1.0
				B22	120	9.5	0.8	0.1	5.1	1.7
39	Vrede	High potential	Avalon Bezuidenhout (Av37)	A1	60	22.9	4.8	0.9	6.3	6.1
				B21	92	36.0	5.0	0.6	5.8	9.2
				B22	110	43.8	8.2	0.2	6.3	9.9
		Medium potential	Clovelly Clovelly (Cv17)	A1	28	34.1	16.7	1.1	5.2	7.3
				B2	70	35.2	17.4	0.6	5.1	5.5
		Low potential	Clovelly Southwold (Cv26)	A1	40	16.3	4.2	0.7	5.6	4.2
				B2	65	18.1	1.8	0.5	5.3	3.8

40	Harrismith	High potential	Avalon Bezuidenhout (Av37)	A1	45	30.5	9.3	1.2	6.0	10.3
				B21	90	45.9	11.7	0.6	6.6	13.5
				B22	120	55.1	13.7	0.5	6.8	19.3
		Medium potential	Oaklea Jozini (Oa36)	A1	40	25.8	13.1	1.1	5.7	10.0
				B2	85	28.7	14.8	0.5	5.8	9.5
		Low potential	Longlands Waaisand (Lo11)	A1	35	17.5	10.7	0.7	5.9	5.3
				E	55	11.8	10.3	0.2	6.9	2.4
				B2	70	21.8	11.7	0.1	7.4	6.2
41	Reitz	High potential	Avalon Bleeksand (Av33)	A1	50	8.0	3.0	0.9	5.8	4.1
				B21	95	8.0	2.0	0.2	5.5	2.4
				B22	140	7.0	3.0	0.1	6.2	1.5
		Medium potential	Clovelly Blinkklip (Cv36)	A1	30	19.4	9.0	1.3	6.3	7.9
				B21	60	16.6	5.7	0.7	6.4	4.7
				B22	92	23.5	5.5	0.8	6.7	5.9
		Low potential	Longlands Waaisand (Lo11)	A1	35	17.5	10.7	0.7	5.9	5.3
				E	55	11.8	10.3	0.2	6.9	2.4
				B2	70	21.8	11.7	0.1	7.4	6.2
42	Bethlehem	High potential	Avalon Bezuidenhout (Av37)	A1	28	21.4	3.0	1.0	5.8	7.3
				B21	52	35.2	3.2	0.5	5.9	7.8
				B22	80	43.2	4.7	0.2	5.2	11.7
				B23	106	39.9	5.7	0.2	5.5	14.3
		Medium potential	Oaklea Jozini (Oa36)	A1	40	11.0	3.0	0.6	6.9	8.2
				B2	87	17.3	8.2	0.9	7.8	9.4
		Low potential	Sterkspruit Sterkspruit (Ss26)	A1	22	27.8	10.7	0.7	7.5	9.1
				B2	44	60.2	10.5	0.6	7.7	22.5

43	Ficksburg	High potential	Avalon Avalon (Av26)	A1	60	13.3	4.8	0.5	6.0	4.3
				B21	110	19.5	5.3	0.2	6.3	4.4
				B22	140	45.5	6.6	0.2	6.0	8.7
44	Ladybrand	Medium potential	Avalon Soetmelk (Av36)	A1	58	12.4	0.2	0.4	5.9	4.0
				B21	90	17.9	5.9	0.3	6.2	5.1
				B22	130	43.8	6.8	0.3	6.0	9.6
		Low potential	Estcourt Dohne (Es13)	A1	34	11.8	11.7	0.4	6.2	4.0
				E	56	9.8	13.1	0.2	6.5	2.3
				B2	90	31.2	13.4	0.3	7.0	7.8

Table 2.2: The soils selected for each magisterial district and the corresponding soil profile data (Soil Survey Staff, 2008) as used as input for the CERES-Maize model.

2.4.2.2 Cultivar Inputs

It is unknown which maize cultivars were planted in each of the magisterial districts over the period under investigation (1979 to 1999). Due to the different climatic conditions, the maize cultivars planted in each of the production regions in the study area (Figure 2.1) differ. Cultivar coefficients for a number of maize cultivars that were planted in each of the regions are obtained from the Agricultural Research Council, Grain Crops Institute. In terms of the number of days from planting to maturity, three types of maize cultivars can generally be distinguished. They are short season maize (60 - 75 days to flowering), medium season maize (65 - 80 days to flowering) and long season maize (70 - 85 days to flowering). It was decided to select three cultivars, a short season maize cultivar, a medium season maize cultivar and a long season maize cultivar, for each of the production regions in the study area. The three cultivars selected for each of the respective production regions, are used in the CERES-Maize model simulations performed for the magisterial districts that fall within each region. Table 2.3 shows the cultivar coefficients, as needed by the CERES-Maize model (Table 2.1), for the three cultivars that are selected for each of the production regions. Thus, as the selected cultivars remain the same over the entire period under investigation, it must be kept in mind that this study does not account for the change in hardiness of maize cultivars over time.

Production Region	Growing season length	Cultivar Name	P1	P2	P5	G2	G3	PHINT
Dry/Warm Western Region (Magisterial districts 1 – 29)	Short	DK618	198.7	0.659	871.0	945.8	14.13	82.34
	Medium	CRN4526	218.0	0.660	999.9	618.0	7.11	75.00
	Long	SR52	281.0	1.000	999.9	422.1	7.78	75.00
Temperate Eastern Region (Magisterial districts 30 – 38)	Short	DK61_24	283.2	0.957	979.0	999.0	18.28	99.00
	Medium	RO411	271.0	0.999	999.9	505.0	7.28	75.00
	Long	PAN6528	241.0	0.660	999.9	734.0	6.80	75.00
Wet/Cool Eastern Region (Magisterial districts 39 – 44)	Short	KK8202	211.0	0.659	999.0	839.9	14.71	82.34
	Medium	PAN6552	221.0	0.660	999.9	546.5	7.55	75.00
	Long	Tx24	220.0	0.990	999.0	592.0	7.40	75.00

Table 2.3: Cultivar coefficients for the selected cultivars used in the CERES-Maize model simulations performed for the magisterial districts under investigation.

2.4.2.3 Management Inputs

Different management practices are applied in each of the three production regions in the study area. Thus, the following management inputs, described per production region, are used in the CERES-Maize model simulations performed for the magisterial districts that fall within each of the respective regions.

2.4.2.3.1 Plant Dates

Broad optimal maize plant dates for the three respective production regions can be summarized as follows; the dry/warm western region from the second week in November to middle December, the temperate eastern region from the last week in October to middle November and the wet/cool eastern region from the beginning of October to the first week in November (Du Toit, 1997). As sufficient soil water is needed before planting can take place (Walter, 1967), these optimal plant dates for maize are probably based on the onset of the first rains. The inter-annual variability of the onset of the maize growing season over South Africa has been investigated (Tadross *et al.*, 2003). From the data used to analyse the mean onset, it could be seen that the eastern parts of the country receive earlier rains than the western parts of the country. In a study which investigated the rainfall seasonality over South Africa, the exact same results were found (Schulze and Maharaj, 2007).

Production Region	Growing season length	Plant date 1	Plant date 2	Plant date 3
Dry/Warm Western Region (2nd week in Nov. – middle Dec.)	Short	30-Nov	05-Dec	10-Dec
	Medium	20-Nov	25-Nov	30-Nov
	Long	10-Nov	15-Nov	20-Nov
Temperate Eastern Region (last week in Oct. – middle Nov.)	Short	10-Nov	15-Nov	20-Nov
	Medium	30-Oct	05-Nov	10-Nov
	Long	20-Oct	25-Oct	30-Oct
Wet/Cool eastern Region (beginning of Oct. – 1st week in Nov.)	Short	25-Oct	30-Oct	05-Nov
	Medium	15-Oct	20-Oct	25-Oct
	Long	05-Oct	10-Oct	15-Oct

Table 2.4: The range of possible plant dates selected for the cultivars in Table 2.3.

Maize cultivars with different growing season lengths are planted on different plant dates. As it is unknown which of the growing season length cultivars (short, medium or long) were planted and on which plant dates, a range of possible plant dates (within the optimal

planting period for each of the production regions) are selected for each of the cultivars in Table 2.3. Table 2.4 shows the plant dates that are selected, based on the fact that the days to flowering only increase with a maximum of 10 days between a short and medium season maize cultivar and 10 days between a medium and long season maize cultivar (ARC-GCI, 2008).

2.4.2.3.2 Planting Depth

The CERES-Maize model also requires the depth at which the dry maize seed are planted. Planting depths for maize normally range between 5 cm and 10 cm depending on the plant date and depth of the soil (Du Toit, 1997). Early plantings can be planted shallower (Du Toit, 1997). Only the plant dates are considered to obtain planting depths for this study. Table 2.5 shows the planting depths selected based on the plant dates in Table 2.4. The long season maize cultivars are planted early in the season and therefore planted shallower than the other cultivars, while the short season maize cultivars are planted later in the season and therefore planted deeper than the other cultivars.

Production Region	Growing season length	Planting depth on Plant date 1	Planting depth on Plant date 2	Planting depth on Plant date 3
Dry/Warm Western Region	Short	10 cm	10 cm	10 cm
	Medium	7.5 cm	7.5 cm	7.5 cm
	Long	5 cm	5 cm	5 cm
Temperate Eastern Region	Short	10 cm	10 cm	10 cm
	Medium	7.5 cm	7.5 cm	7.5 cm
	Long	5 cm	5 cm	5 cm
Wet/Cool eastern Region	Short	10 cm	10 cm	10 cm
	Medium	7.5 cm	7.5 cm	7.5 cm
	Long	5 cm	5 cm	5 cm

Table 2.5: The planting depths selected for each of the selected cultivars in Table 2.3.

2.4.2.3.3 Row Spacing & Plant Population

In South Africa wide rows (150 cm – 210 cm) are used in low to medium rainfall areas, whereas narrow rows (90 cm – 100 cm) are used in medium to high rainfall areas (Du Toit, 1997). The wider rows in the drier areas are normally accompanied by low plant populations. This production method eliminates competition between the plants by ensuring

that each plant has access to soil water (Du Toit *et al.*, 2000). Narrower rows and more dense plant populations are allowed in the wetter parts, as production are not as water-limited as in the drier parts (Du Toit *et al.*, 2000).

As the dry/warm western production region (see Figure 2.1) receives low to medium rainfall, it is assumed that wide rows and low plant populations are used. The temperate and wet/cool eastern production regions receive medium to high rainfall and are therefore assumed to utilize narrow rows and more dense plant populations.

Since it is unknown where in the dry/warm western production region 150 cm and where 210 cm rows are used, a middle value of 180 cm is chosen for the entire region. A row spacing of 90 cm is selected for the wet/cool eastern production region and 100 cm for the temperate eastern production region.

To acquire a maize yield of 3 t/ha in each of the production regions in the study area, different plant populations needs to be used. A plant population of 14 000 plants/ha are assumed for the dry/warm western region, 16 000 plants/ha for the temperate eastern region and 19 000 plants/ha for the wet/cool eastern region (Du Toit, 1997).

2.4.2.3.4 Irrigation

As this study focuses on rain-fed maize, no irrigation is applied to the experiments done for each of the magisterial districts under investigation.

2.4.2.3.5 Fertilizer

The CERES-Maize model simulations for each of the magisterial districts are nitrogen non-limited. Thus, the plants do not experience any N-stress. The CERES-Maize model supplies the plant with Nitrogen as needed.

2.4.2.3.6 Harvest

The CERES-Maize model harvests the maize at maturity.

2.4.2.3.7 Other Assumptions

Furthermore it is assumed that weeds, pests and diseases are controlled and that nutrients are not limited. Over the period modelled in this study technology is kept constant. These assumptions may all contribute to an overestimation in simulated yields (Rosenzweig and Iglesias, 1994).

2.4.3 Incorporating the Weather Data into the CERES-Maize Model

2.4.3.1 Observed Data

Daily rainfall, maximum temperature, minimum temperature and solar radiation data for the period 1979 to 1999 are extracted from the Southern African Quaternary Catchment Database (Schulze *et al.,* 2005) for each of the quaternary catchments in the study area. By superimposing the magisterial district boundaries over the quaternary catchment boundaries in the study area, the quaternary catchments that fall either completely or partially within each magisterial district are identified. Table 2.6 lists the quaternary catchments included in each magisterial district. The daily data of the quaternary catchments in a given magisterial district are then averaged in order to obtain a single weather dataset per magisterial district. These average daily values per district are then used as input for the CERES-Maize model to perform the observed weather data simulations.

Number	Magisterial District	Quaternary Catchments
1	Vryburg	C32A, C32B, C32D, C33A, D41B, D41C, D41D, D41E, D41F, D41H
2	Delaryville	C31B, C31D, C31E, C32C, C41B
3	Lichtenburg	C31A, C31B, C31C, D41A
4	Marico	A10C, A31A, A31B, A31C, A31E, A31F, A31J, A32C, A32D, D41A
5	Swartruggens	A22A, A22D, A22E, A31B, A31G
6	Koster	A22A, A22B, A22C, A22G, C23F, C24C
7	Rustenburg	A21K, A22C, A22D, A22F, A22G, A22H
8	Brits	A21H, A21J, A21K, A21L, A22J, A23L, A23A
9	Ventersdorp	C23F, C23G, C24C, C24D, C24E
10	Potchefstroom	C23C, C23G, C23H, C23J, C23K, C23L
11	Klerksdorp	C24A, C24G, C24H, C24J
12	Coligny	C24F
13	Wolmaransstad	C25A, C25C, C25D, C25E
14	Schweizer Reneke	C31F, C31E, C32C, C32D, C91A
15	Bloemhof	C25F, C91A

16	Christiana	C91B
17	Boshof	C52H, C52K, C91B, C91C, C91D
18	Hoopstad	C25F, C43C, C43D, C91A, C91B
19	Wesselsbron	C25B, C25F, C43B
20	Bothaville	C24J, C25B, C25C, C60J
21	Viljoenskroon	C24B, C24J, C70J, C70K
22	Vredefort	C23C, C23L, C70E, C70F, C70J
23	Bultfontein	C43A, C43C, C43D, C52H, C91C
24	Welkom	C42J, C43B
25	Henneman	C42J, C60H
26	Virginia	C42H, C42J, C42K
27	Theunissen	C41G, C41J, C42K, C42L
28	Brandfort	C41F, C41H, C52C, C52E, C52G, C52H
29	Bloemfontein	C51D, C51E, C52B, C52C, C52D, C52E, C52F, C52G, C52H, C52J
30	Excelsior	C41C, C41D, D23C
31	Winburg	C41A, C41B, C41D, C41E, C42E, C42G, C42K
32	Marquard	C41A, C41B, C42E
33	Senekal	C42A, C42B, C42C, C42D, C42E, C42F, C60E, D22A
34	Lindley	C60A, C60B, C60C, C70A, C83F
35	Kroonstad	C60C, C60D, C60F, C60G, C60H, C70D, C70G, C70H
36	Koppies	C70C, C70D, C70E, C70F, C70G
37	Heilbron	C22G, C23A, C70A, C70B, C70C, C83K, C83L, C83M
38	Sasolburg	C22F, C22G, C22K
39	Vrede	C12A, C12B, C12C, C12D, C13C, C13E, C13F, C13G, C13H, C82E, C82F, C82H
40	Harrismith	C13C, C81A, C81B, C81C, C81D, C81E, C81F, C81G, C81H, C81J, C81K, C81L, C81M, C82A, C82B, C82C, C82E
41	Reitz	C82D, C82G, C83E, C83F, C83G, C83H
42	Bethlehem	C42A, C60A, C81G, C83A, C83B, C83C, C83D, D21D
43	Ficksburg	D21H, D22A, D22B, D22D
44	Ladybrand	D22G, D22H, D22L, D23A, D23C, D23D, D23E

Table 2.6: The quaternary catchments either completely or partially within the magisterial districts under investigation.

2.4.3.2 Simulated Fields

2.4.3.2.1 CCAM

CCAM simulated daily rainfall, maximum temperature and minimum temperature are available on a 1° x 1° grid for each of the five ensemble members. The daily weather information at the CCAM grid point closest to the centre of a magisterial district is

objectively selected to represent the CCAM-simulated weather for that district (nearest neighbour approach). This is then used in the CERES-Maize model simulations performed for each district. Solar radiation was not available from the CCAM output, but is needed by the CERES-Maize model to simulate maize yield. To overcome this limitation, a daily solar radiation climatology is calculated for each of the magisterial districts using the observed weather data. This solar radiation data then makes up the complete dataset needed by the CERES-Maize model to simulate the yield.

2.4.3.2.2 ECHAM4.5

ECHAM4.5 simulated data are extracted for the domain 16°E to 34°E and 22°S to 35°S. Daily simulated rainfall, maximum temperature and minimum temperature data are available for each of the six ensemble members. The daily weather information at the ECHAM4.5 grid point closest to the centre of a magisterial district is objectively selected to represent the ECHAM4.5-simulated weather for that district (nearest neighbour approach). The simulated data of that specific ECHAM4.5 point are then used to run the CERES-Maize model for the corresponding magisterial district. As no ECHAM4.5 simulated solar radiation data are available, the same daily solar radiation climatology used in the CERES-Maize model runs performed with the CCAM-simulated fields are also used in the CERES-Maize model runs performed with the ECHAM4.5-simualted fields.

2.4.4 Set up of CERES-Maize Model Experiments

Due to the uncertainty in the soil on which maize was planted, the cultivar that was planted and when the maize was planted, a number of options are considered for each of these inputs (Table 2.2, 2.3 and 2.4). To investigate each soil option, with each cultivar option and with each plant date option, a number of scenarios resulted. A total of 27 scenarios can be set up for magisterial districts with three selected soils, 18 scenarios for districts with two selected soils and 9 scenarios for districts with only one selected soil. Table 2.7 shows all the possible scenarios that can be set up, while keeping the other management inputs (planting depth, plant population and row spacing) and weather inputs constant.

Scenario	Description
1	Short season maize planted on plant date 1 and on a high potential soil
2	Short season maize planted on plant date 1 and on a medium potential soil
3	Short season maize planted on plant date 1 and on a low potential soil
4	Short season maize planted on plant date 2 and on a high potential soil

5	Short season maize planted on plant date 2 and on a medium potential soil
6	Short season maize planted on plant date 2 and on a low potential soil
7	Short season maize planted on plant date 3 and on a high potential soil
8	Short season maize planted on plant date 3 and on a medium potential soil
9	Short season maize planted on plant date 3 and on a low potential soil
10	Medium season maize planted on plant date 1 and on a high potential soil
11	Medium season maize planted on plant date 1 and on a medium potential soil
12	Medium season maize planted on plant date 1 and on a low potential soil
13	Medium season maize planted on plant date 2 and on a high potential soil
14	Medium season maize planted on plant date 2 and on a medium potential soil
15	Medium season maize planted on plant date 2 and on a low potential soil
16	Medium season maize planted on plant date 3 and on a high potential soil
17	Medium season maize planted on plant date 3 and on a medium potential soil
18	Medium season maize planted on plant date 3 and on a low potential soil
19	Long season maize planted on plant date 1 and on a high potential soil
20	Long season maize planted on plant date 1 and on a medium potential soil
21	Long season maize planted on plant date 1 and on a low potential soil
22	Long season maize planted on plant date 2 and on a high potential soil
23	Long season maize planted on plant date 2 and on a medium potential soil
24	Long season maize planted on plant date 2 and on a low potential soil
25	Long season maize planted on plant date 3 and on a high potential soil
26	Long season maize planted on plant date 3 and on a medium potential soil
27	Long season maize planted on plant date 3 and on a low potential soil

Table 2.7: The range of possible scenarios resulting from different combinations of input data.

After setting up the scenarios for each of the magisterial districts, three different sets of maize yield simulations are performed by the CERES-Maize model. Firstly, the CERES-Maize model is forced with observed weather data (Figure 2.4), secondly with CCAM-simulated fields (Figure 2.5) and thirdly with ECHAM4.5-simulated fields (Figure 2.6). One observed weather data run, five CCAM-simulated field runs (one for each ensemble member) and six ECHAM4.5-simulated field runs (one for each ensemble member) are performed by the CERES-Maize model for each magisterial district. Thus, maize yield is simulated for each scenario under observed, CCAM-simulated and ECHAM4.5-simulated weather conditions. A total of 10 044 simulations are performed with the CERES-Maize model. The Multi-Model system is obtained by combining the ensemble of CERES-CCAM simulated maize yields and the ensemble of CERES-ECHAM4.5 simulated maize yields through a simple un-weighted averaging approach. This is good first approach to follow, as other combination methods struggle to beat the high standard of the simple averaging method (Mason, 2008).

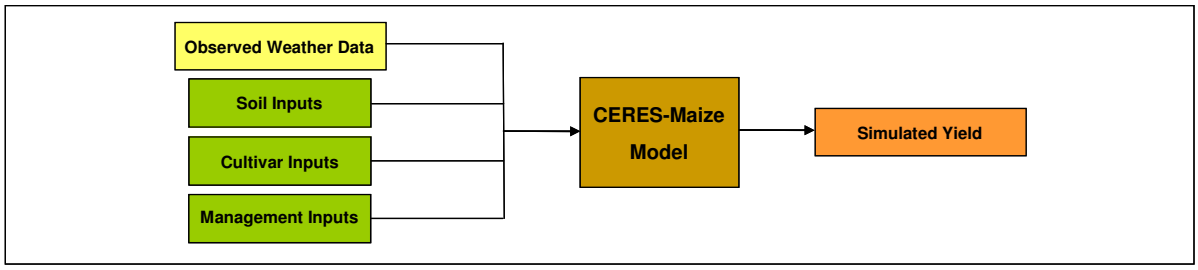

Figure 2.4: Flow diagram of the simulations performed with the CERES-Maize model.

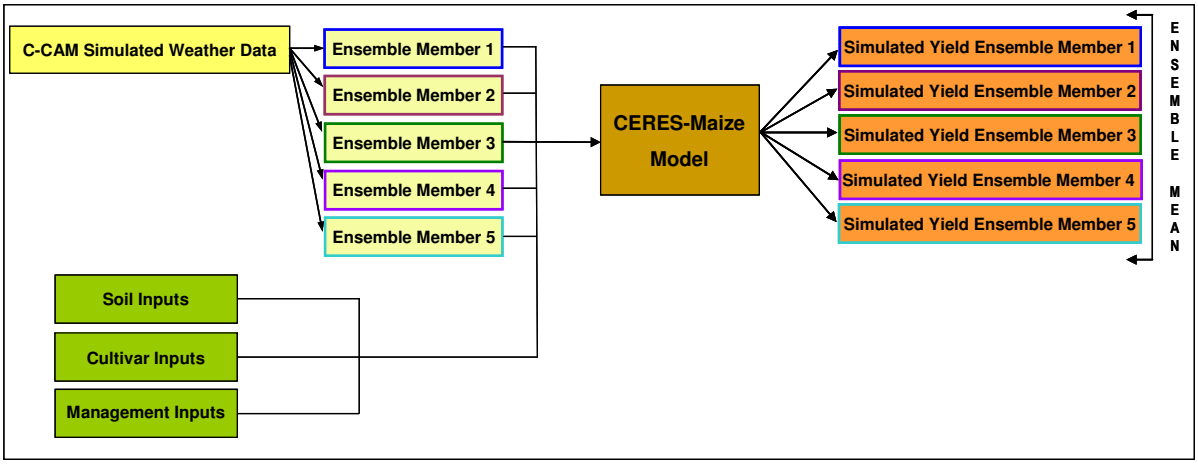

Figure 2.5: Flow diagram of the simulations performed with the CERES-Maize model when forced with each of the 5 ensemble members of the CCAM-simulated fields.

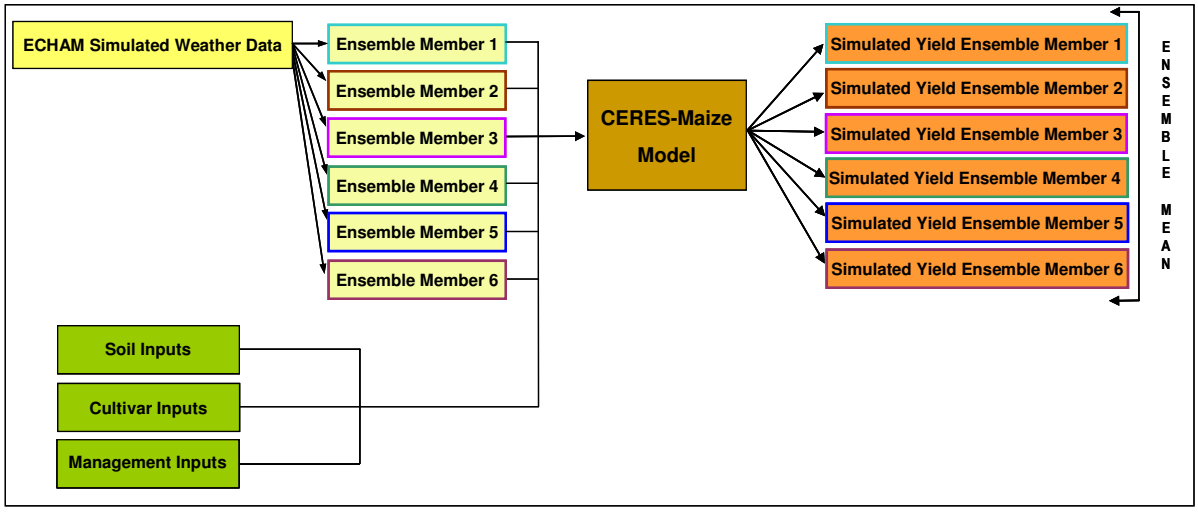

Figure 2.6: Flow diagram of the simulations performed with the CERES-Maize model when forced with each of the 6 ensemble members of the ECHAM4.5-simulated fields.

2.5 VERIFICATION OF THE SIMULATED MAIZE YIELDS

2.5.1 Verification Data

A number of maize yield datasets are available for South Africa. GrainSA is the custodian of a maize yield dataset that contains provincial maize yield figures for a period from 1980 to 2008. This dataset is compiled from information gathered from the silos in each province with regards to maize intake at the end of the season. Except for the fact that farmers often retain some maize for feed, the transportation process from the farm to the silo also results in some maize loss. Thus, a discrepancy may be evident between the maize yield figures in this dataset and the maize yield that was present on the land at the end of the season.

Another provincial maize yield dataset can be obtained from the Crop Estimate Committee of South Africa. This Committee meets once a month, starting at the beginning of the growing season, and uses a number of inputs to estimate the expected maize yield for that season. Thus, the yield estimates in this dataset are revised on a monthly basis until the final estimate is released. This data is available for a period from 1980 to 2008.

A subjective yield survey dataset that contains maize yield figures for 2000 random points over South Africa is also available from 2001. These figures are based on a questionnaire completed at each point before the start of the growing season. In these questionnaires the farmers state the plant density and area that is going to be planted and then also estimate the maize yield for that season.

For the objective yield survey dataset 200 out of the 2000 points in the subjective yield survey dataset are visited three times during the growing season. During these visitations the plant population is determined, number of cobs per plant is counted, the cobs are weighed and a maize yield is estimated accordingly. This dataset contains the three maize yield estimates for each of the 200 points for a period from 2001 to 2008.

The fifth maize yield dataset that is available for South Africa is the Co-operators yield dataset. This dataset contains maize yield figures per magisterial district for seasons 1980/1981 to 2007/2008. On a monthly basis from the start of the season, the Department of Agriculture sends questionnaires to the co-operating farmers in each magisterial district in which the expected maize yield for that season is stated. At the end of the season, after harvest, the co-operating farmers complete a final questionnaire in which the maize yield that was obtained is specified and this information then makes up the Co-operators yield dataset. The number of co-operating farmers in each magisterial district differs and

therefore these figures are not necessarily representative. The data in this dataset is confidential, but historical data were made available for research purposes.

In this study the CERES-Maize model simulates maize yield for 20 seasons in the period 1979 to 1999. In terms of verification the ideal would be to compare the CERES-Maize model results of maize yield to actual maize yield figures for the exact same period. From the five maize yield datasets described above, the Co-operators yield dataset is the only dataset suitable to be used as verification data in this study, because the data contained in the Co-operators yield dataset are for 19 out of the 20 seasons under investigation and on a higher spatial resolution (per magisterial district) than the other datasets that also have data for these seasons. Thus, CERES-Maize model output per magisterial district for the seasons 1980/1981 to 1998/1999 are verified against the Co-operators yield.

2.5.2 Verification Methods

Even though CERES-Maize model runs are performed for each of the 5 ensemble members of the CCAM-simulated fields and each of the 6 ensemble members of the ECHAM4.5-simulated fields, only the ensemble mean maize yield results of the CERES-CCAM runs, the ensemble mean maize yield results of the CERES-ECHAM4.5 runs and the ensemble mean maize yields results of the Multi-Model system are discussed. Although, the full ensemble of each simulation system is considered in the estimation of the skill when the maize yield simulations are expressed probabilistically.

From here onwards the maize yield results obtained from the CERES-Maize model runs performed with the observed weather data will be referred to as the CERES-Observed weather yield, the ensemble mean of the maize yield results obtained from the CERES-Maize model runs performed with the CCAM-simulated fields will be referred to as the CERES-CCAM ensemble mean yield, the ensemble mean of the maize yield results obtained from the CERES-Maize model runs performed with the ECHAM4.5-simulated fields will be referred to as the CERES-ECHAM4.5 ensemble mean yield and the combination between the CERES-CCAM and CERES-ECHAM4.5 maize yield results will be referred to as the Multi-Model ensemble mean yield.

Due to the limitation in the availability of soil data the number of soils that are selected for each magisterial district range between 1 and 3 (see Table 2.2). As the scenarios for which the CERES-Maize model is run for each magisterial district results from all the possible combinations of input data, 3 soils in combination with the other input data make up 27

scenarios, 2 soils make up 18 scenarios and 1 soil make up 9 scenarios. Thus, in the case of 3 selected soils, one scenario is duplicated for 3 soils and in the case of 2 selected soils, one scenario is duplicated for 2 soils. To simplify the verification process and obtain uniformity between the results obtained for the magisterial districts, the maize yield results of the duplicated scenarios are averaged across the different soils. Consequently each magisterial district ends up with maize yield results for only 9 scenarios (Table 2.8) and these results are presented in this study.

Scenario	Description
1	Short season maize planted on plant date 1
2	Short season maize planted on plant date 2
3	Short season maize planted on plant date 3
4	Medium season maize planted on plant date 1
5	Medium season maize planted on plant date 2
6	Medium season maize planted on plant date 3
7	Long season maize planted on plant date 1
8	Long season maize planted on plant date 2
9	Long season maize planted on plant date 3

Table 2.8: The 9 scenarios for which results are discussed.

2.5.2.1 Spatial Verification

The distribution of the simulated maize yields among magisterial districts is investigated through spatial verification. The aim is to determine whether the different simulation systems (CERES-Maize model integrations performed with observed weather data, performed with CCAM-simulated fields, performed with ECHAM4.5-simulated fields as well as the Multi-Model system) are able to capture the spatial distribution in maize yield across the study area.

To compare the simulated maize yields obtained from each of the different simulation systems to the actual maize yields, each of the simulated maize yield datasets and the actual maize yield dataset are normalized to a standard deviation of one and a mean of zero. Each dataset (simulated and actual) is normalized independently as follows:

$$NormalizedValue = \frac{x - \bar{x}}{\sigma} \tag{2.1}$$

where x represents the yield in t/ha of a specific magisterial district for a specific season, $\bar{x}$ represents the average yield in t/ha calculated for that specific season across all the magisterial districts in the study area and σ represents the standard deviation in t/ha calculated for that specific season across all the magisterial districts in the study area. Note that these normalized values are unit-less and consequently expressed as an index. The standard deviation is calculated as follows (Steyn *et al.*, 1998):

$$\sigma = \sqrt{\frac{\sum (x - \bar{x})^2}{N - 1}} \tag{2.2}$$

where x is the yield in t/ha of a specific magisterial district for a specific season, $\bar{x}$ the average yield in t/ha calculated for that specific season across all the magisterial districts in the study area and N the number of magisterial districts in the study area.

From each of these normalized datasets an average is calculated for each magisterial district across the 19 seasons, to obtain a single index value per district. Spatial maps of these average maize yield index values are displayed for the actual and simulated maize yields for each of the 9 scenarios in Table 2.8. The actual maize yield index map indicates which magisterial districts normally produce higher yields and which districts normally produce lower yields with respect to the entire study area. The maize yield index maps for each of the different simulation systems are visually compared to the actual maize yield index map in section 3.2.

2.5.2.2 Inter-Seasonal Variability Verification

This verification procedure examines the season-to-season variability in the simulated maize yields over the 19 seasons from 1980/81 to 1998/99. The aim is to determine whether each of the different maize yield simulation systems are able to capture the inter-seasonal variability in maize yield.

2.5.2.2.1 Subjective Validation

Once again the simulated maize yields obtained from each of the different simulation systems and the actual maize yields are normalized before any verification is done. The normalization is done similar to what is done for the spatial verification, although here the $\bar{x}$

in equation 2.1 and equation 2.2 represents the average yield in t/ha calculated for a specific magisterial district across the 19 seasons, σ in equation 2.1 represents the standard deviation in t/ha calculated for that specific magisterial district across the 19 seasons and N in equation 2.2 represents the number of seasons. It must be kept in mind that these normalized values are unit-less and therefore expressed as an index.

Figure 2.3 shows the magisterial districts that fall in each of the three production regions in the study area. The inter-seasonal verification is done per production region and therefore averages are calculated across the normalized values of the magisterial districts that fall in one production region to obtain one index value per season for each of the production regions. Thus, the normalized values of magisterial districts 1 to 29 are averaged for the Dry/Warm Western Region, 30 to 38 for the Temperate Eastern Region and 39 to 44 for the Wet/Cool Eastern Region. This is done for the simulated maize yield datasets of each of the different simulation systems as well as the actual maize yield dataset.

Time series graphs which depicts these average maize yield index values for the actual yield and simulated yields for each of the 9 scenarios in Table 2.8 are displayed for each of the 3 production regions. The actual maize yield index time series indicates which seasons had the highest maize yields and which seasons had the lowest maize yields with respect to the entire 20 year period under investigation. The maize yield index time series of the different simulation systems are visually compared to the actual maize yield index time series in section 3.3.

2.5.2.2.2 Objective Validation

Spearman's Rank Correlation Coefficient

Robust and resistant alternatives to the Pearson product-moment correlation are available. The first of these is known as the Spearman rank correlation. The normalized values previously calculated for each magisterial district are also used here. Spearman rank correlations are calculated between the actual maize yield index and each of the simulated maize yield indices of the different simulation systems for each magisterial district in the study area. Before calculating the correlations between the actual maize yield index and one of the simulated maize yield indices, the datasets are ranked, independently from each other, from the highest to the lowest value. The correlations are then calculated as follows (Steyn *et al.*, 1998):

$$R_S = 1 - \frac{6\sum_{i=1}^{n} D_i^2}{n^3 - n} \tag{2.3}$$

where D_i is the difference between the ranks of the actual maize yield index for a specific season and the simulated maize yield index for that corresponding season and n is the number of seasons. R_S values range between -1 and 1, where -1 is a perfect negative correlation, 0 is no correlation and 1 is a perfect positive correlation (Steyn *et al.*, 1998).

These Spearman rank correlations which indicate the direction and strength of the relationship between the actual maize yield index and each of the simulated maize yield indices over the 19 seasons are displayed spatially and discussed in section 3.3.

Significance Testing

Here, it is tested if the number of magisterial districts with statistically significant local Spearman rank correlations between each of the simulated maize yield datasets and the actual maize yield dataset is significantly high (Wilks, 2006). A Monte Carlo test is performed to establish local significance at the 95% level. Since the magisterial districts are correlated spatially, re-randomization of each magisterial district's data are done by re-sampling random seasons, i.e., if the third season (1982/83) is the first season selected, then the first data vector of the re-randomized data will be the third season for all magisterial districts.

The re-randomized datasets for each magisterial district are then correlated with the actual maize yields, where after the re-randomization process is repeated for a large number of times (e.g., 1000 times). The subsequent Spearman rank correlations for each magisterial district are sorted and the 95th percentile identified. Thus, a set of Spearman rank correlations which represent the critical Spearman rank correlations at the 95% confidence level is available. From the unsorted Spearman rank correlations associated with each magisterial district, for each of the 1000 iterations, it is determined if the correlations are greater than or equal to its corresponding 95% confidence level. The number of times the 95% level is exceeded is counted. This is done for each magisterial district and for each of the 1000 iterations. Thus, in the end there is a 1000 counts ranging between and including

0 and the number of magisterial districts (44). This whole procedure is done for the data obtained from each of the different simulation systems.

If from the actual maize yield data it is established that 21 out of the 44 magisterial districts have significant local Spearman rank correlations, the number of the times the counts from the above explained procedure are greater than 21, are counted. This number then gives an indication of the probability of getting the actual maize yield results or better by chance. The magisterial districts with local significance at the 95% confidence level are described together with the Spearman rank correlations in section 3.3.

2.5.2.3 Probability Distributions

In this study the use of weather ensembles provides the opportunity to examine the predictability of maize yield probabilistically. The simulated maize yields, of those simulation systems that use weather ensembles, can be expressed probabilistically by calculating the percentage of the simulated maize yield ensemble members that fall in the below-normal, near-normal and above-normal categories. The aim is to determine the operational potential of this maize yield forecast system, as operational maize yield forecasts will most likely be expressed in terms of probabilities.

2.5.2.3.1 Subjective Validation

As the three production regions divide the study area into zones with similar climate and zones in which similar maize production methods are used, it would make sense to issue operational maize yield forecasts for each of these three production regions. Therefore, this analysis is performed for each of the three production regions. It is possible to calculate probabilities for the CERES-CCAM maize yield integrations (which has 5 ensemble members), for the CERES-ECHAM4.5 maize yield integrations (which has 6 ensemble members) and for the Multi-Model system (which is a combination between the CERES-CCAM and CERES-ECHAM4.5 simulations and consequently has 11 ensemble members), while the actual maize yields and the CERES-Observed weather yields are expressed deterministically.

Averages are calculated across the magisterial districts to obtain maize yield values per production region. This is done for the actual maize yields, the CERES-Observed weather maize yields as well as for each of the CERES-CCAM maize yield ensemble members and

each of the CERES-ECHAM4.5 maize yield ensemble members. These average maize yield values (actual and simulated) for each production region are then normalized to a standard deviation of one and a mean of zero, where $\bar{x}$ in equation 2.1 and equation 2.2 represents the average yield in t/ha calculated for a specific production region across the 19 seasons, σ in equation 2.1 represents the standard deviation in t/ha calculated for that specific production region across the 19 seasons and N in equation 2.2 represents the number of seasons. Once again, these normalized maize yield values are unit-less and therefore referred to as a maize yield index.

Before organising the maize yield index values into the below-normal, near-normal and above-normal categories, it is necessary to establish what 'near-normal' refers to. In this study, 'near-normal' refers to a range of values. The 19 maize yield index values of all 5 ensemble members of the CERES-CCAM simulations are combined (95 maize yield index values), sorted ascending and the third of the values in the middle of the arranged dataset are used as the 'near-normal' range. This exact procedure is followed to obtain the 'near-normal' range of the CERES-ECHAM4.5 simulated maize yields, but this time for 6 ensemble members (114 maize yield index values). From this the CERES-CCAM yield probabilities and the CERES-ECHAM4.5 yield probabilities are calculated for each of the 19 seasons. The yield probabilities of the Multi-Model system on the other hand are calculated by averaging the CERES-CCAM probabilities obtained for a specific season and the CERES-ECHAM4.5 probabilities for that same season. To obtain the 'near-normal' range of the actual maize yields, the 19 maize yield index values are sorted ascending and the values in the middle of the arranged dataset are used. Based on this, it is determined whether the actual maize yield of each of the 19 seasons was below-normal, near-normal or above-normal. This is repeated for the CERES-Observed weather yields. This whole procedure is done for each of the production regions.

Time series graphs of these probabilities are displayed for each of the three production regions and for 3 scenarios per region. Graphs were prepared for all 9 scenarios in Table 2.8, but as the changes in the probabilities from the one plant date to the next were insignificant, it was decided to average across the plant dates to obtain only 3 scenarios (Table 2.9). The CERES-CCAM yield probabilities, CERES-ECHAM4.5 yield probabilities and the Multi-Model yield probabilities are compared to the actual maize yields and CERES-Observed weather yields in section 3.4.

Scenario	Description
1	Short season maize
2	Medium season maize
3	Long season maize

Table 2.9: The resultant 3 scenarios obtained when averaging over the different plant dates.

2.5.2.3.2 Objective Validation

In probabilistic forecasts, the probability of occurrence of a certain event is estimated (Stefanova and Krishnamurti, 2001). Probabilistic forecasts are verified through the combined distribution of forecasts and observations (Stefanova and Krishnamurti, 2001). The relative operating characteristic (ROC) is one of the most commonly used methods to assess the skill of a forecasting system, by comparing the hit rate and the false-alarm rate (Mason, 1982). ROC scores are used to evaluate the value of probabilistic forecasts (Stanski *et al.*, 1989; Mason and Graham, 1999).

The probabilities displayed in the time series graphs of the subjective validation are also used here. ROC curves are constructed for each of the three equiprobable categories (below-normal, near-normal and above-normal) of the CERES-CCAM maize yield probabilities, CERES-ECHAM4.5 maize yield probabilities and the Multi-Model maize yield probabilities. The ROC curves are obtained by plotting the hit rates (HRs) and false alarm rates (FARs) against each other. HR and FAR are calculated as follows (Kharin and Zwiers, 2003):

$$HR(P_{cr}) = \frac{1}{\Pr(E=1)} \int_{\Omega_\beta} f_\beta(\beta) f(E=1 \mid \beta) d\beta \tag{2.4}$$

$$FAR(P_{cr}) = \frac{1}{\Pr(E=0)} \int_{\Omega_\beta} f_\beta(\beta) f(E=0 \mid \beta) d\beta \tag{2.5}$$

where P_{cr} is a critical threshold probability, $\Pr(E=1)$ denote a predictand when the event occurs and $\Pr(E=0)$ when the event does not occur and Ω_β is all the values of β (a potential predictable signal) for which $P > P_{cr}$. The HRs and FARs of a forecasting system with no skill are equal. The HR of a perfect forecast is 1 and the FAR is 0 (Kharin and Zwiers, 2003). The area under the ROC curve can be defined as the ROC score.

Forecasts with no skill have ROC scores of 0.5 and perfect forecasts have ROC scores of 1 (Kharin and Zwiers, 2003).

The ROC curves and ROC scores which give and indication of the skill of the different simulation systems and the value of the simulated maize yield probabilities are displayed and discussed in section 3.4 for each of the three production regions and each of the three scenarios in Table 2.9.

2.6 SUMMARY

The data, models and methods that are used to construct the different maize yield simulation systems have been described. The properties of the crop model and two GCMs used have been highlighted. The relevant input data required by the crop model and the set up of the experiments have been detailed. Finally, the data and methods used to verify the simulated maize yields have been discussed. In the next chapter the maize yield results obtained from each of the simulation systems for the main maize producing region of South Africa are discussed.

CHAPTER 3

VERIFICATION OF THE YIELD SIMULATIONS OVER SOUTH AFRICA

3.1 INTRODUCTION

This chapter describes the results of the yield simulations that are performed with the CERES-Maize model for each of the magisterial districts in the main maize producing area of South Africa (see Figure 2.1). The aim of this Chapter is to quantify the skill of the CERES-Maize model, evaluate the accuracy of the simulated maize yields obtained from each of the different simulation systems, assess the ability of each of the different simulation systems in estimating maize yield and determine the operational potential of this maize yield forecast system. Verification is done by comparing the simulated maize yields to actual maize yields. Firstly, the simulated maize yields are verified spatially over the entire study area, secondly, the inter-seasonal variability in the simulated maize yields are verified for each of the three production regions in the study area and thirdly, the simulated maize yields for each of the three production regions are expressed probabilistically and then verified against actual maize yields.

3.2 SPATIAL VERIFICATION RESULTS

In Figures 3.1 to 3.9 the actual maize yield index and each of the simulated maize yield indices obtained from the different simulation systems are displayed spatially for each of the 9 scenarios in Table 2.8. These spatial maps represent the maize yield index values obtained from averaging over the 19 seasons from 1980/81 to 1998/99. In each of these figures the actual maize yield index is displayed as map (a). The actual maize yield index map provides a view of the distribution of maize yield across the study area and gives an indication of which magisterial districts normally produce higher and which districts normally produce lower maize yields with respect to the entire study area. From the actual maize yield index map a decrease in maize yield can be observed from east to west across the study area. Thus, the study area is characterised by high maize yields in the eastern parts and lower maize yields in the western parts. This gradient in maize yield can most likely be attributed to the fact that the average annual rainfall of the eastern parts of South Africa is higher than that of the western parts of the country (Schulze and Lynch, 2007). Apart from this gradient, a small region with higher maize yields than its surroundings is evident in the Free State, directly next to the border separating the Free State and North West Province

from each other (magisterial districts Wesselsbron (19), Bothaville (20) and Viljoenskroon (21)). Furthermore it can be seen that magisterial districts Wesselsbron (19), Viljoenskroon (21), Harrismith (40) and Bethlehem (42) normally produce the highest maize yields and magisterial districts Vryburg (1) and Brandfort (28) the lowest maize yields.

In Figures 3.1 to 3.9 map (b) represents the CERES-Observed weather yield index for each of the 9 scenarios. By comparing the CERES-Observed weather yield index to the actual maize yield index, the ability of the CERES-Maize model can be quantified, as this gives an indication of how realistically the model can simulate maize yield when the weather conditions are perfectly known. In operational maize yield forecasting, the weather conditions will be forecast. Thus, if the CERES-Maize model is unable to produce realistic maize yields under known weather conditions, it will certainly not be able to produce skilful maize yield forecasts under predicted weather conditions. Therefore, the quantification of the CERES-Maize model's ability in simulating South African maize yields is of great importance. The CERES-Observed weather yield index maps of all 9 scenarios show that the CERES-Maize model successfully simulates the east-west decrease in maize yield across the study area. Although, for the long season maize scenarios (Figures 3.7 to 3.9) the CERES-Maize model extends the high maize yields in the east to a much larger and more prominent area than that observed in the actual maize yield index map and for the short season maize scenarios (Figures 3.1 to 3.3) the CERES-Maize model simulates the maize yield of magisterial district 37 (Heilbron) to be unusually low. Furthermore, the CERES-Maize model is unable to capture the high yields of the small region in the Free State described above. The many uncertainties in the soil, cultivar and management input data may have contributed to these misrepresentations. The CERES-Observed weather yield index maps of the medium season maize scenarios (Figures 3.4 to 3.6) seem to show the best agreement with the actual maize yield index map, both in terms of the spatial distribution of the yields as well as the relative magnitude of the yields. Very small differences are distinguishable in the CERES-Observed weather yield index maps for each of the three cultivars (short, medium and long season maize) from the one plant date to the next.

The CERES-CCAM ensemble mean yield index for each of the 9 scenarios is displayed as map (c) in Figures 3.1 to 3.9. All 9 scenarios show that the characteristic pattern of high maize yields in the eastern parts and lower maize yields in the western parts of the study area is captured when the CERES-Maize model is forced with CCAM-simulated fields. The short season maize scenarios (Figures 3.1 to 3.3) show an increase in maize yield in the western parts of the Free State, from plant date 1 to plant date 3, the medium season maize

scenarios (Figures 3.4 to 3.6) show higher yields in the Free State than in the North-West Province and the long season maize scenarios (Figures 3.7 to 3.9) show a similar pattern to that evident in the CERES-Observed weather yield index maps, a much larger and more prominent high maize yield area in the east than that observed from the actual maize yield index map.

Map (d) in Figures 3.1 to 3.9 shows the CERES-ECHAM4.5 ensemble mean yield index for each of the 9 scenarios. Once again all 9 scenarios show higher maize yields in the east and lower maize yields in the west. Thus, the CERES-Maize model forced with ECHAM4.5-simulated fields is able to capture the gradient in maize yield across the study area. Although, for the short and medium season maize scenarios (Figures 3.1 to 3.6) the CERES-Maize model simulates the maize yield of the western parts of the North-West province to be slightly higher in comparison to the actual maize yield index map. However, this simulation system performs exceptionally well in capturing the distribution in maize yield in the eastern part of the Free State (except for magisterial district 39 (Vrede)) in two of the short season maize scenarios (plant dates 2 and 3). The CERES-ECHAM4.5 ensemble mean yield index maps of the long season maize scenarios (Figures 3.6 to 3.9) appear almost identical to the CERES-CCAM ensemble mean yield index maps and the CERES-Observed weather yield index maps.

The Multi-Model ensemble mean yield index for each of the 9 scenarios is shown in Figures 3.1 to 3.9 as map (e). From these figures it can be seen that the Multi-Model system also succeeds in capturing the maize yield gradient from east to west across the study area. Once again, two of the short season maize scenarios (Figures 3.2 and 3.3) represent the distribution of maize yield in the eastern parts of the Free State exceptionally well. As this Multi-Model system is a combination between the CERES-CCAM integrations and the CERES-ECHAM4.5 integrations, the slightly higher maize yields evident in the western parts of the North-West Province in the CERES-ECHAM4.5 ensemble mean yield index maps for the short and medium season scenarios are somewhat balanced out by the CERES-CCAM integrations. The long season maize scenarios (Figures 3.7 to 3.8) of the Multi-Model ensemble mean yield index maps are very similar to that of the CERES-CCAM ensemble mean yield index maps and the CERES-ECHAM4.5 ensemble mean yield index maps. Thus, in terms of the spatial distribution of the simulated maize yields, the four different maize yield simulation systems successfully simulate the east-west gradient in maize yield across the study area.

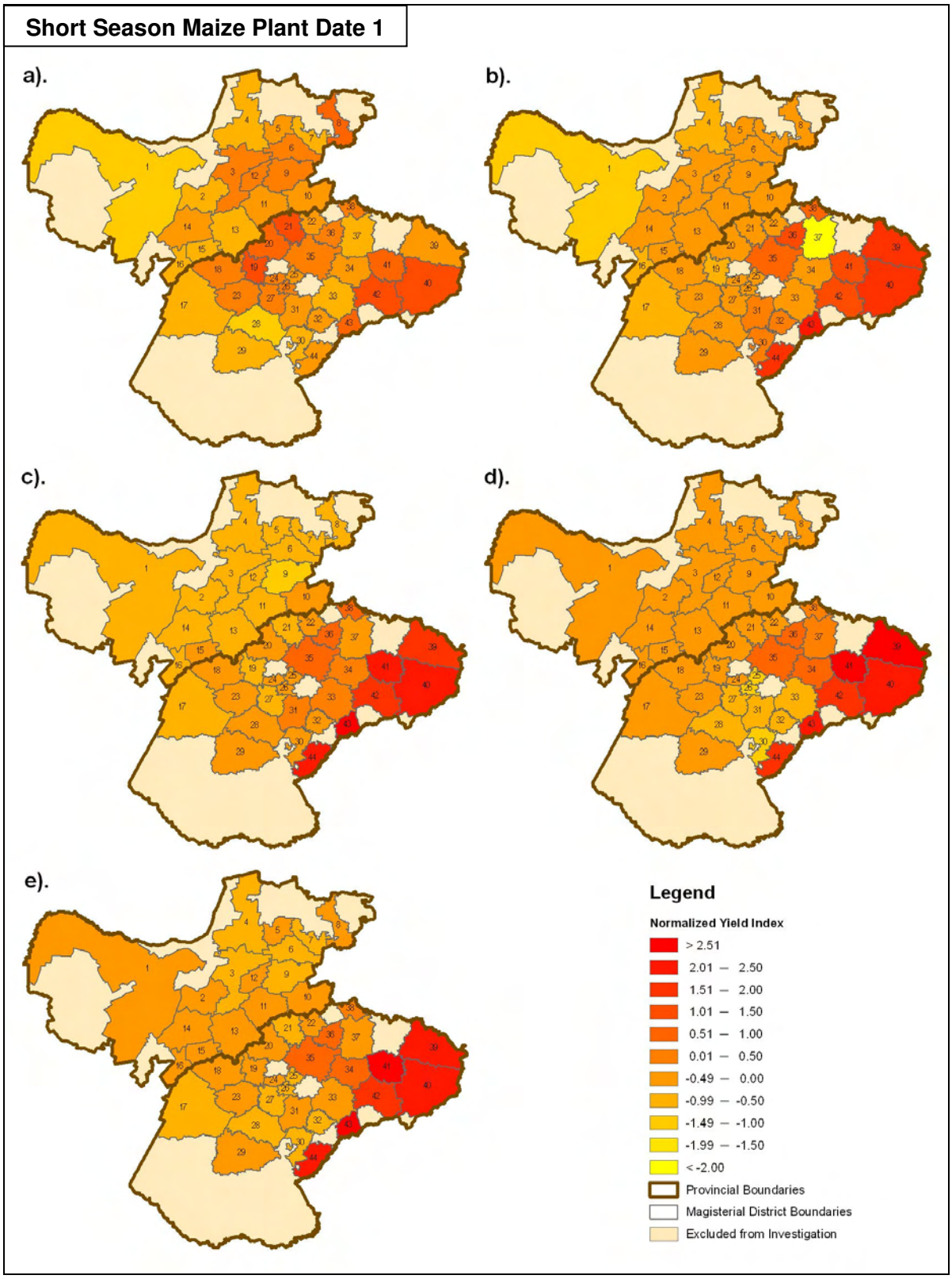

Figure 3.1: Actual maize yield index and simulated maize yield indices for scenario 1 (short season maize planted on plant date 1) averaged over the 19 seasons from 1980/81 to 1998/99. (a) Actual maize yield index, (b) CERES-Observed weather yield index, (c) CERES-CCAM ensemble mean yield index, (d) CERES-ECHAM4.5 ensemble mean yield index and (e) Multi-Model ensemble mean yield index.

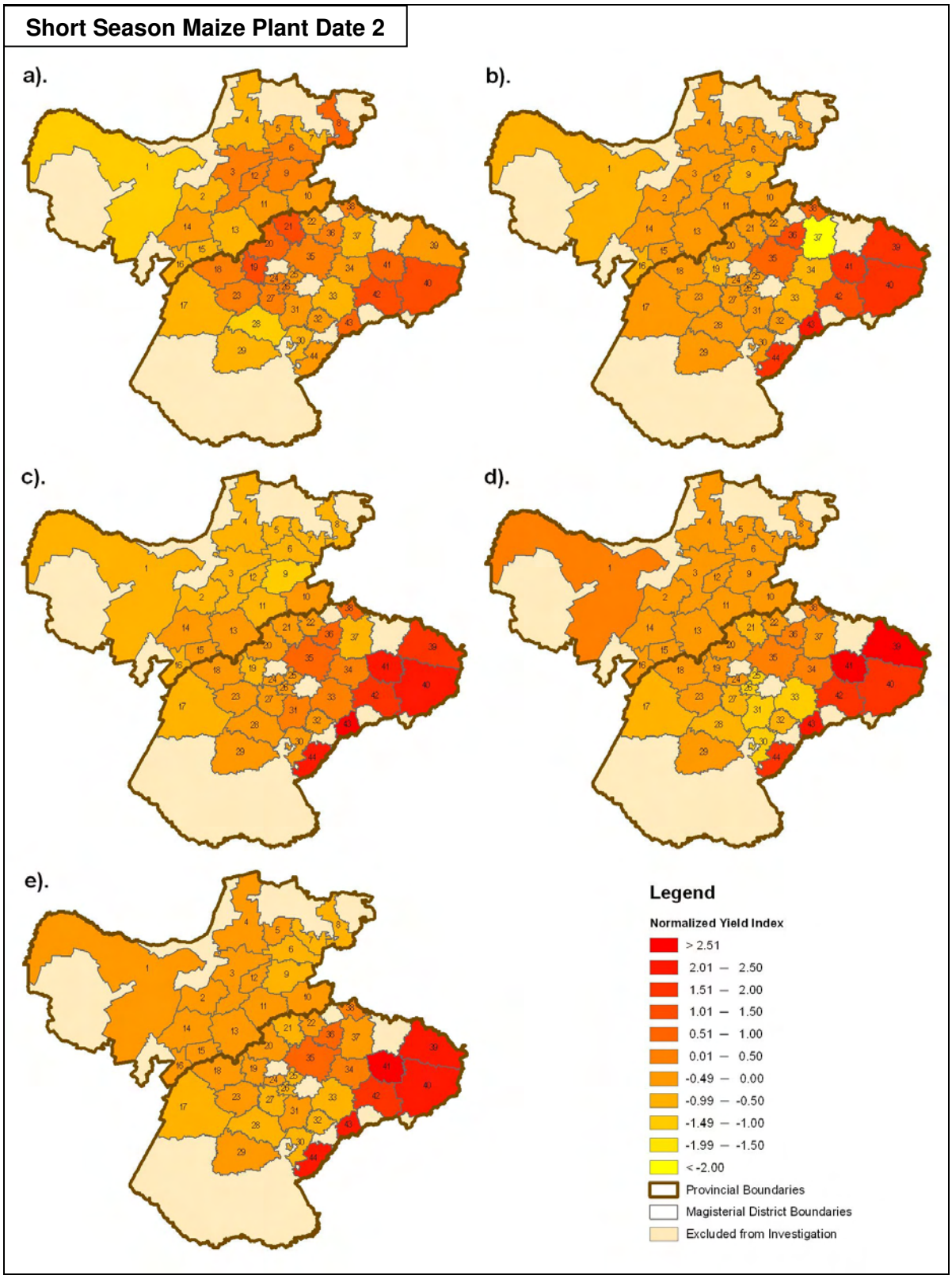

Figure 3.2: Actual maize yield index and simulated maize yield indices for scenario 2 (short season maize planted on plant date 2) averaged over the 19 seasons from 1980/81 to 1998/99. (a) Actual maize yield index, (b) CERES-Observed weather yield index, (c) CERES-CCAM ensemble mean yield index, (d) CERES-ECHAM4.5 ensemble mean yield index and (e) Multi-Model ensemble mean yield index.

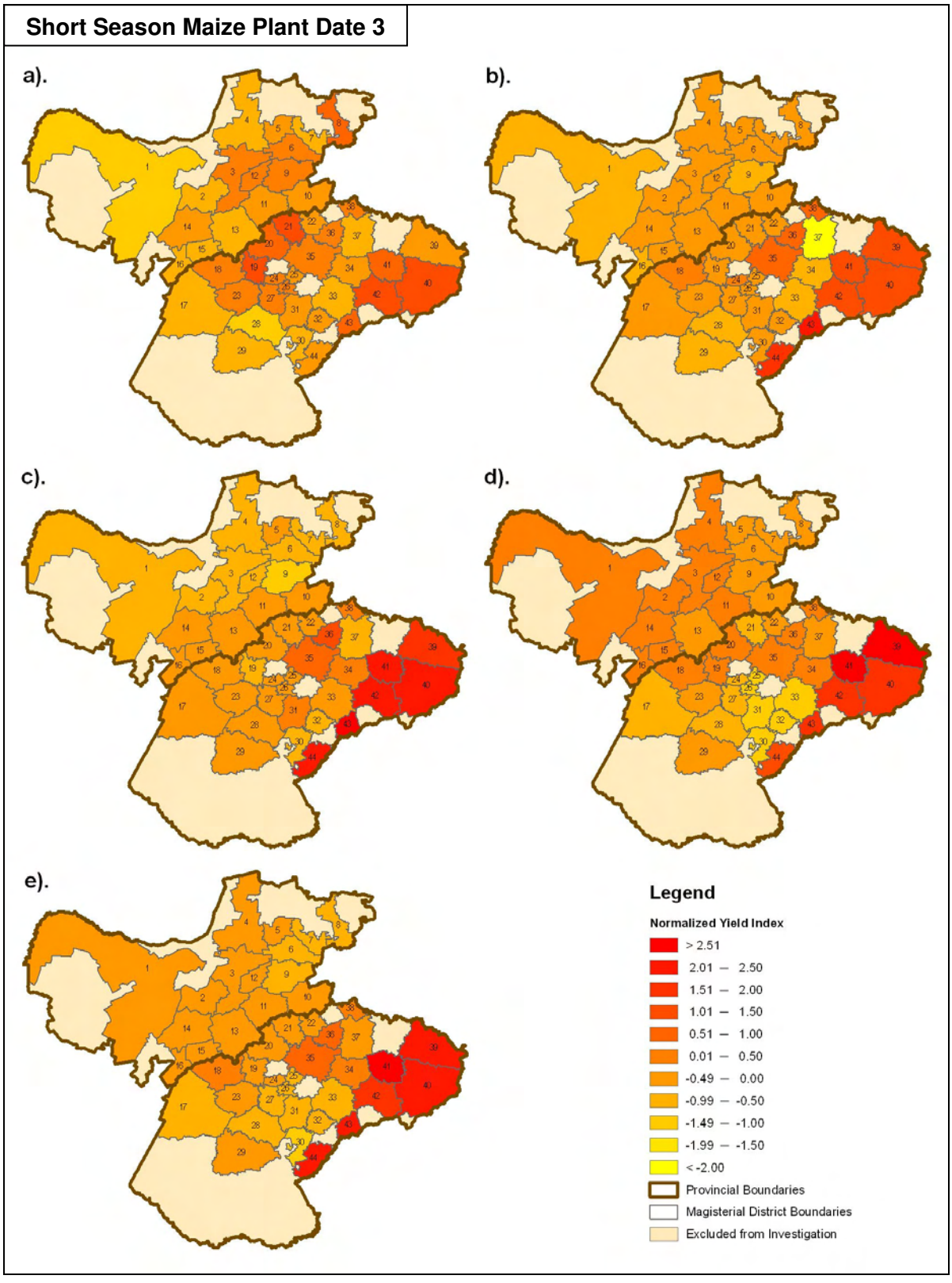

Figure 3.3: Actual maize yield index and simulated maize yield indices for scenario 3 (short season maize planted on plant date 3) averaged over the 19 seasons from 1980/81 to 1998/99. (a) Actual maize yield index, (b) CERES-Observed weather yield index, (c) CERES-CCAM ensemble mean yield index, (d) CERES-ECHAM4.5 ensemble mean yield index and (e) Multi-Model ensemble mean yield index.

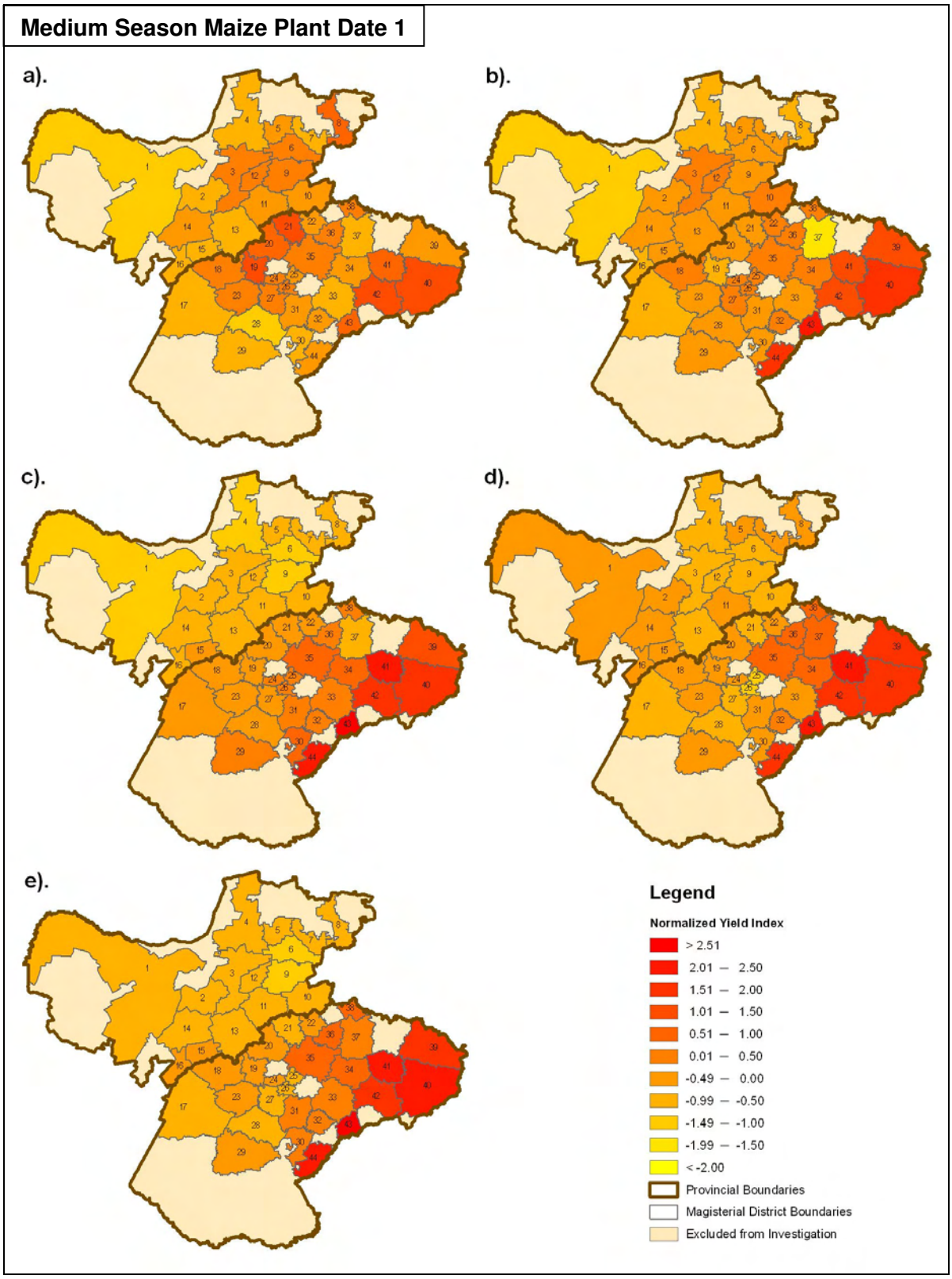

Figure 3.4: Actual maize yield index and simulated maize yield indices for scenario 4 (medium season maize planted on plant date 1) averaged over the 19 seasons from 1980/81 to 1998/99. (a) Actual maize yield index, (b) CERES-Observed weather yield index, (c) CERES-CCAM ensemble mean yield index, (d) CERES-ECHAM4.5 ensemble mean yield index and (e) Multi-Model ensemble mean yield index.

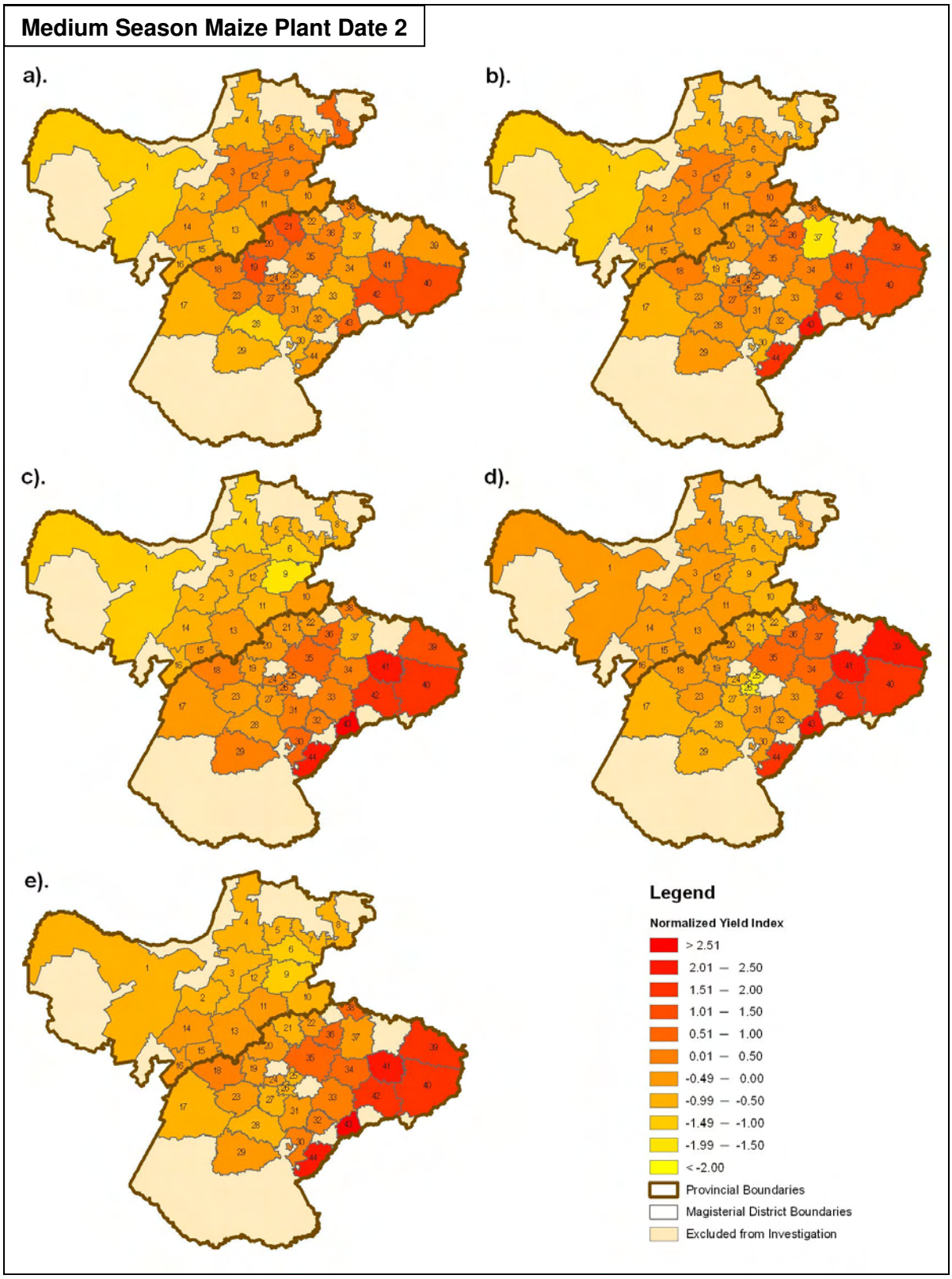

Figure 3.5: Actual maize yield index and simulated maize yield indices for scenario 5 (medium season maize planted on plant date 2) averaged over the 19 seasons from 1980/81 to 1998/99. (a) Actual maize yield index, (b) CERES-Observed weather yield index, (c) CERES-CCAM ensemble mean yield index, (d) CERES-ECHAM4.5 ensemble mean yield index and (e) Multi-Model ensemble mean yield index.

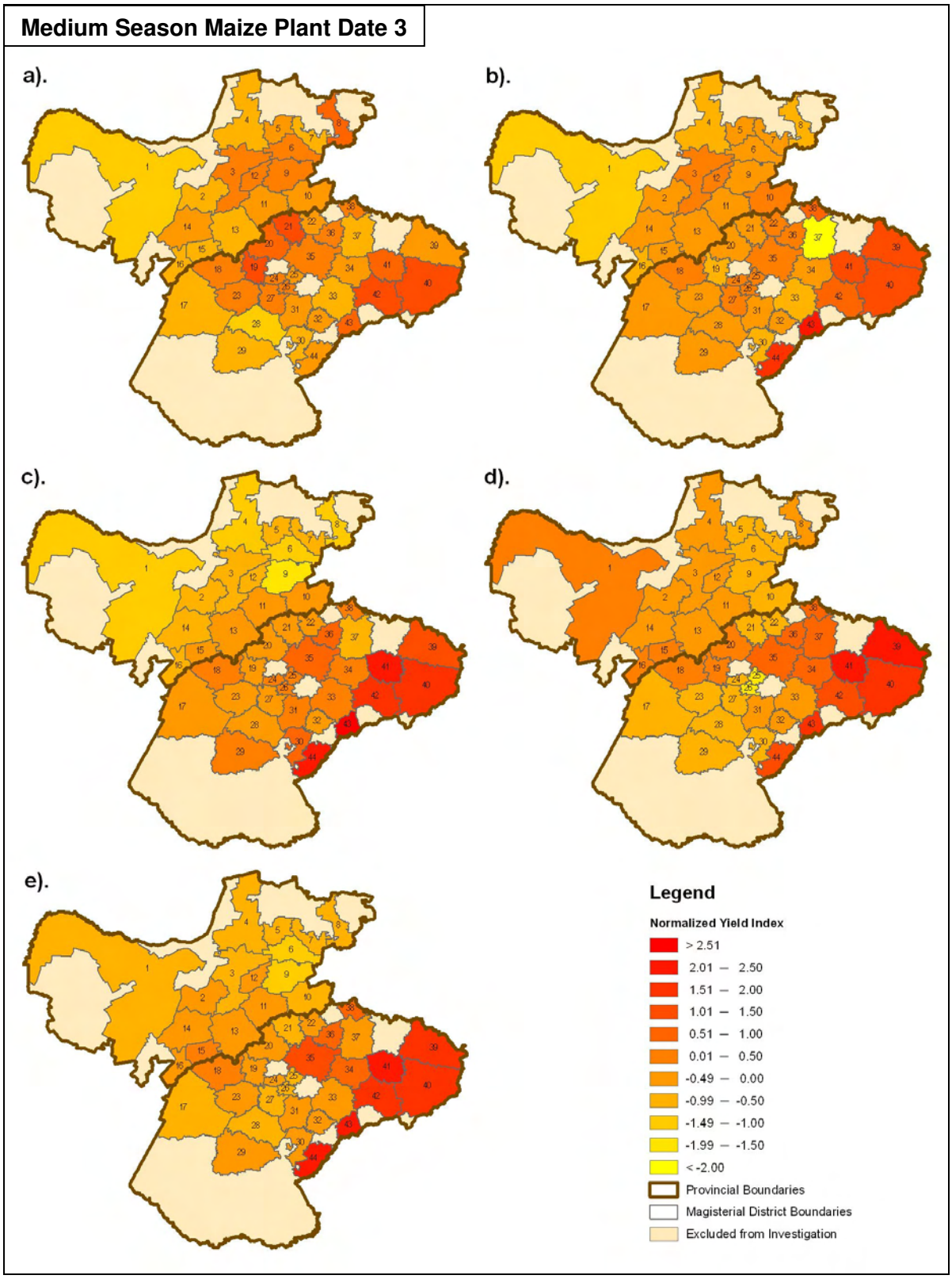

Figure 3.6: Actual maize yield index and simulated maize yield indices for scenario 6 (medium season maize planted on plant date 3) averaged over the 19 seasons from 1980/81 to 1998/99. (a) Actual maize yield index, (b) CERES-Observed weather yield index, (c) CERES-CCAM ensemble mean yield index, (d) CERES-ECHAM4.5 ensemble mean yield index and (e) Multi-Model ensemble mean yield index.

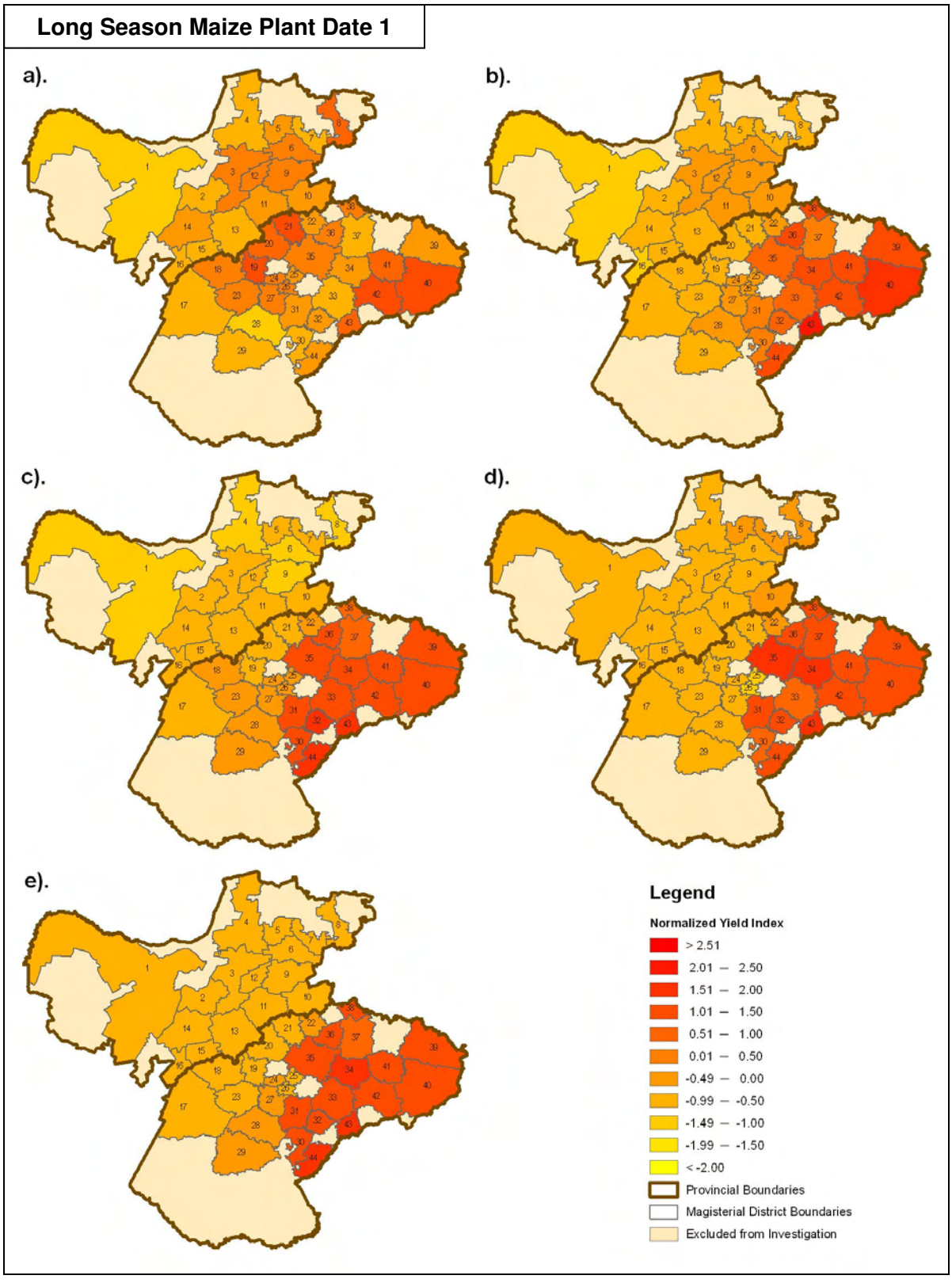

Figure 3.7: Actual maize yield index and simulated maize yield indices for scenario 7 (long season maize planted on plant date 1) averaged over the 19 seasons from 1980/81 to 1998/99. (a) Actual maize yield index, (b) CERES-Observed weather yield index, (c) CERES-CCAM ensemble mean yield index, (d) CERES-ECHAM4.5 ensemble mean yield index and (e) Multi-Model ensemble mean yield index.

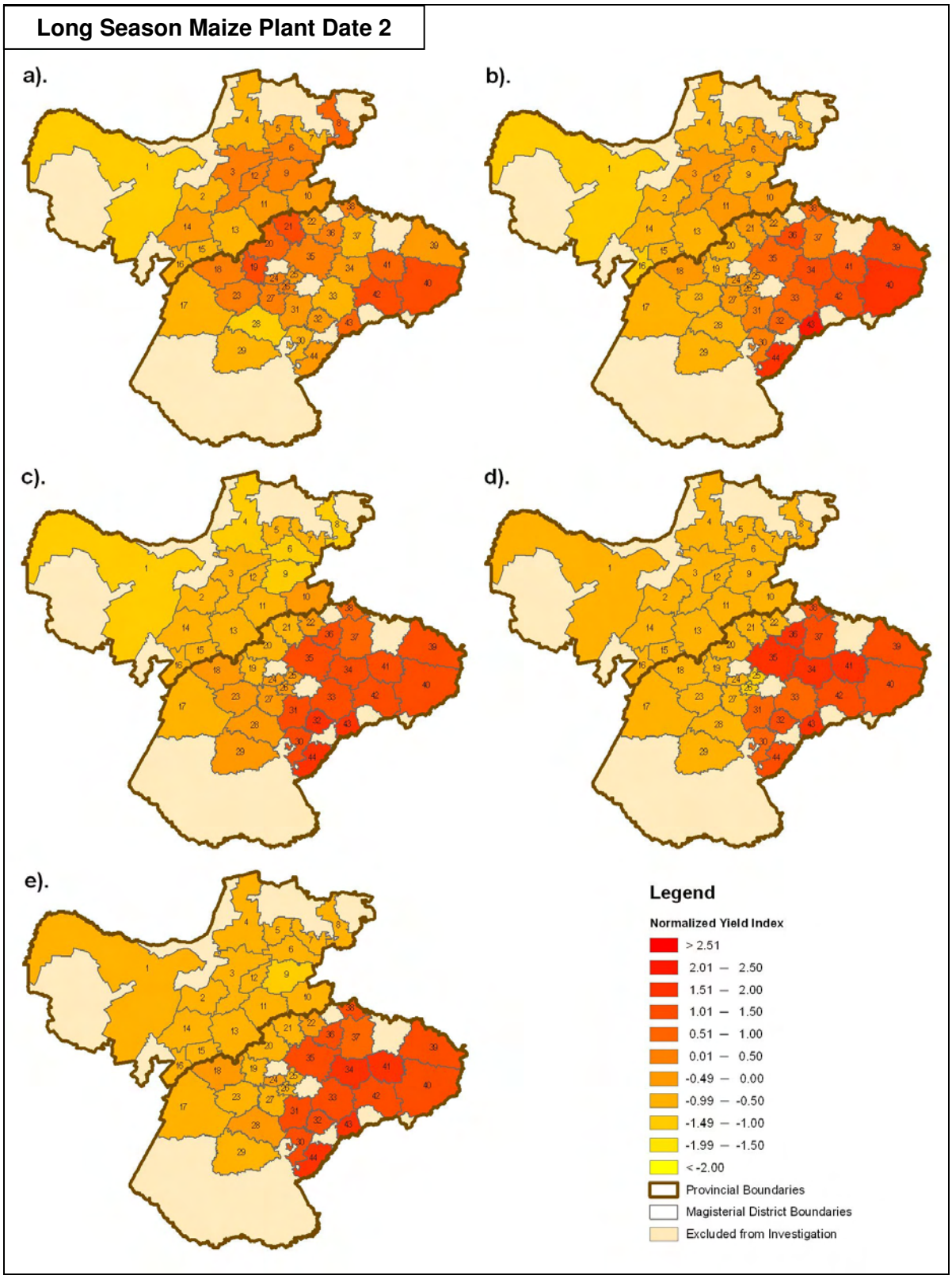

Figure 3.8: Actual maize yield index and simulated maize yield indices for scenario 8 (long season maize planted on plant date 2) averaged over the 19 seasons from 1980/81 to 1998/99. (a) Actual maize yield index, (b) CERES-Observed weather yield index, (c) CERES-CCAM ensemble mean yield index, (d) CERES-ECHAM4.5 ensemble mean yield index and (e) Multi-Model ensemble mean yield index.

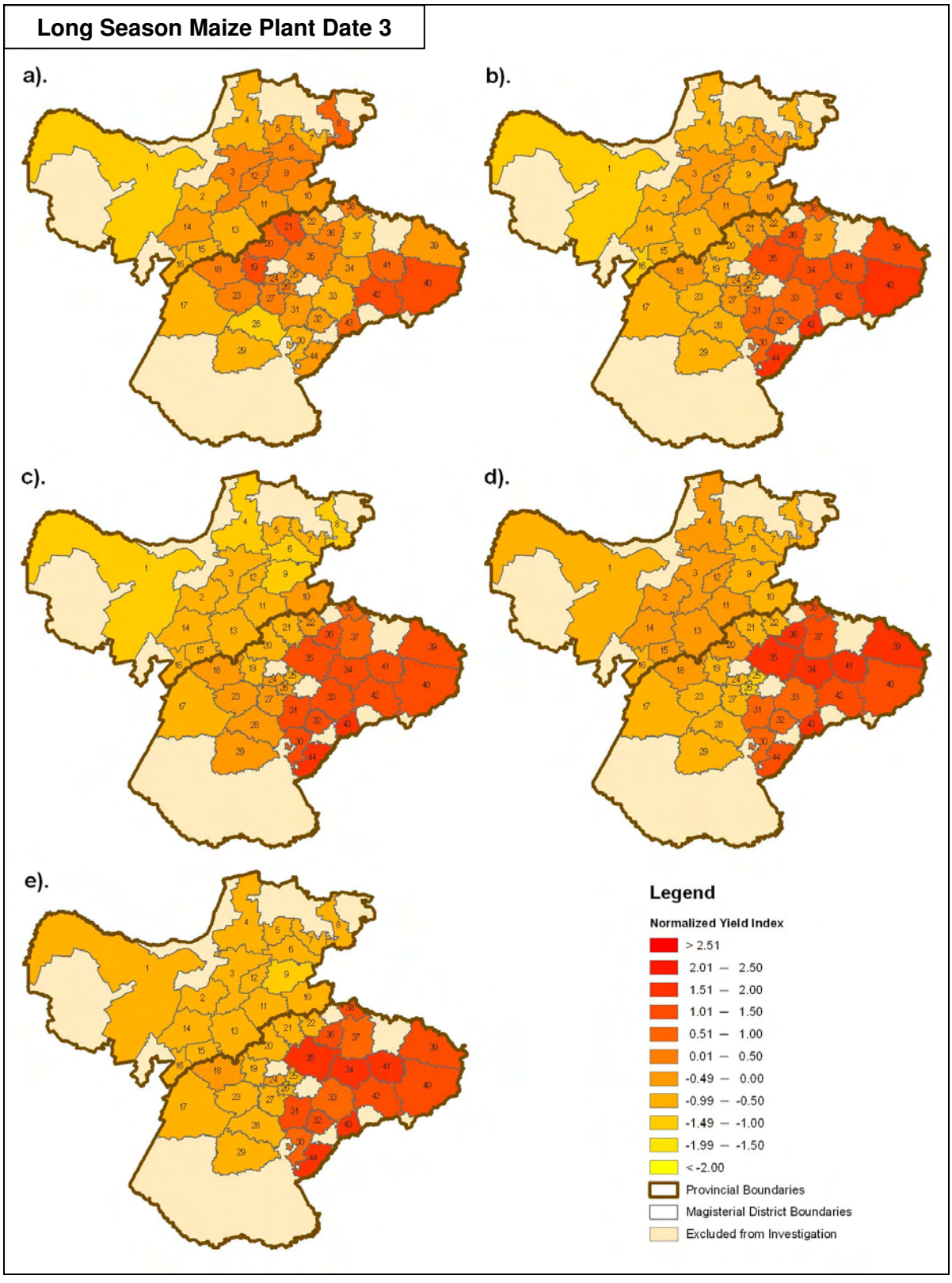

Figure 3.9: Actual maize yield index and simulated maize yield indices for scenario 9 (long season maize planted on plant date 3) averaged over the 19 seasons from 1980/81 to 1998/99. (a) Actual maize yield index, (b) CERES-Observed weather yield index, (c) CERES-CCAM ensemble mean yield index, (d) CERES-ECHAM4.5 ensemble mean yield index and (e) Multi-Model ensemble mean yield index.

3.3 INTER-SEASONAL VARIABILITY VERIFICATION RESULTS

3.3.1 Subjective Validation

3.3.1.1 Dry/Warm Western Region

The time series of the actual maize yield index and simulated maize yield indices, obtained from each of the different simulation systems, are shown for the dry/warm western production region in Figures 3.10 (scenario 1 to 4), 3.11 (scenario 5 to 8) and 3.12 (scenario 9). From the actual yield index time series (AYI - red) it can be observed that over the 20 year period investigated in this study the 1980's (1981/82 – 1987/88) was characterised by much lower maize yields than the late 1990's (1995/96 – 1998/99). This phenomenon can possibly be explained by the advances that took place in technology over this 20 years with respect to improvements in the climatic tolerance of cultivars and improved crop management strategies (Du Toit *et al.*, 2001). Furthermore, it can also be seen that over this 20 year period, the 1995/96 season rendered the highest maize yield and the 1991/92 season the lowest maize yield. A La Niña event (cold ENSO phase) was present during the 1995/96 season and an El Niño event (warm ENSO phase) during the 1991/92 season. La Niña events often coincide with below-normal and El Niño events with above-normal summer rainfall totals over the central and western parts of South Africa (Ropelewski and Halpert, 1987, Rautenbach and Smith, 2001). Even though the 1995/96 La Niña event was relatively weak, this event was associated with significantly wet anomalies over the south-eastern parts of southern Africa (Reason and Jagadheesa, 2005). This could possibly explain the high maize yield obtained for that season. In comparison to the very strong El Niño that occurred during the 1997/98 season, the 1991/92 El Niño event was fairly weak but led to much more severe summer drought conditions over large parts of southern Africa (Reason and Jagadheesa, 2005). These severe summer drought conditions likely led to the low maize yield obtained for the 1995/96 season.

3.3.1.1.1 Short Season Maize

In Figure 3.10, (a), (b) and (c) represent short season maize planted on plant date 1, 2 and 3 respectively. Table 2.4 shows the exact month and day plant date 1, 2 and 3 refers to. By examining the CERES-Observed weather yield index time series (COYI – green) and comparing it to the actual maize yield index time series (AYI – red), it is possible to get an idea of the ability of the CERES-Maize model in simulating the inter-seasonal variability in maize yield in the dry/warm western production region. For all three short season maize scenarios the CERES-Maize model is able to successfully simulate the low maize yield of

the 1991/92 season, the season with the lowest maize yield out of the 19 seasons under investigation. It can also be observed that the CERES-Maize model correctly indicates the sign of the anomaly of the yield (above or below normal) of many seasons, especially those seasons with an actual maize yield index value (AYI – red) less than -1 and more than 1. Another prominent feature in all three short season maize scenarios is that the CERES-Maize model struggles to simulate the maize yield of the three seasons from 1984/85 to 1986/87, a La Niña season followed by an ENSO-neutral season followed by an El Niño season. The ability of the CERES-Maize model seems to decrease from plant date 1 to plant date 3, as the number of seasons for which the model successfully simulates the sign of the anomaly of the yield decreases from 15 to 11.

The CERES-CCAM ensemble mean yield index time series (CCYI – blue) for the three short season maize scenarios show that when forced with CCAM-simulated fields the CERES-Maize model is unable to capture the low maize yield of the 1991/92 El Niño season, but instead makes the maize yields of the 1987/88 and 1994/95 El Niño seasons much lower. This also appears for the 1994/95 La Niña season, the CERES-CCAM ensemble mean yield index shows much higher maize yields for the 1988/89 and 1998/99 La Niña seasons than for the 1994/95 season which in reality produced the highest maize yield out of the 19 seasons considered in this study. Furthermore, it also appear as if the CERES-CCAM ensemble mean yield index shows greater variability between seasons than that observed from the actual yield index.

From the CERES-ECHAM4.5 ensemble mean yield index time series (CEYI – orange) for the three short season maize scenarios it can be seen that the CERES-Maize model fails to capture the sign of the anomaly of the yield of almost three quarters of the seasons when it is forced with ECHAM4.5-simulated fields. Another interesting observation that can be made is the fact that the seasons for which the CERES-Maize model forced with ECHAM4.5-simulated fields actually succeeds in capturing the sign of the anomaly of the yield, are primarily ENSO-neutral seasons (1980/81, 1981/82, 1990/91 and 1992/93). The Multi-model system (MMYI – purple) on the other hand performs better in simulating the change in the sign of the anomaly of the yield from one season to another than that of the CERES-ECHAM4.5 maize yield simulation system, but does not perform better than the CERES-CCAM maize yield simulation system.

3.3.1.1.2 Medium Season Maize

The time series of the maize yield indices (actual and simulated) for medium season maize planted on plant date 1, 2 and 3 are shown in Figure 3.10 (d) and Figure 3.11 (e) and (f) respectively. From the CERES-Observed weather yield index time series (COYI – green) it can be seen that the CERES-Maize model successfully simulates the low maize yield of the 1991/92 El Niño season. In all three scenarios the CERES-Maize model performs very well in simulating the relative magnitude of the yields of the 1980/81 and 1983/84 ENSO-neutral seasons. Furthermore, the ability of the CERES-Maize model in simulating the yield appears to improve from plant date 1 to plant date 3, as the number of seasons for which the model correctly indicates the sign of the anomaly of the yield increases from 10 to 15. Similar to the short season maize scenarios, the CERES-Maize model once again struggles to simulate the maize yield of the 4 seasons from 1984/85 to 1987/88.

From the CERES-CCAM ensemble mean yield index time series (CCYI – blue) for the three medium season maize scenarios it can be observed that the medium season maize planted on plant date 2 scenario (Figure 3.11 (e)) shows the best agreement with the actual yield index time-series, both in terms of the sign of the anomaly of the yield and the relative magnitude of the yield. For this scenario the CERES-Maize model is able to correctly simulate the sign of the anomaly of the yield for 15 out of the 19 seasons. Also evident from these three time series graphs is that when forced with CCAM-simulated fields the CERES-Maize model seems to perform the best for seasons with actual maize yield index values (AYI – red) less than -1 and more than 1. This is particularly true for the seasons in the 1980's. As with the short season maize scenarios, the maize yield results of the medium season maize scenarios also show that the CERES-Maize model forced with CCAM-simulated fields fails to capture the low maize yield of the 1991/92 season and the high maize yield of the 1995/96 season, but instead simulates the impact of other El Niño and La Niña events on the maize yield in the dry/warm western production region to be much more severe.

The CERES-ECHAM4.5 ensemble mean yield index time series (CEYI – orange) for the three medium season maize scenarios show that the CERES-Maize model does not perform well in simulating the maize yield of the dry/warm western production region when it is forced with ECHAM4.5-simulated fields. This simulation system can only indicate the sign of the anomaly of the yield for 5 out of the 19 seasons correctly.

The Multi-Model ensemble mean yield index time series (MMYI – purple) for the medium season maize scenarios show little variation from plant date 1 to plant date 3. As this simulation system is a combination between the CERES-CCAM integrations and the CERES-ECHAM4.5 integrations, it performs better than the CERES-ECHAM4.5 simulation system, but does not perform as good as the CERES-CCAM simulation system. Besides this, the Multi-Model ensemble mean yield index captures the relative magnitude of the 1980/81 and 1982/83 yields exceptionally well.

3.3.1.1.3 Long Season Maize

Figure 3.11 (g) and (h) and Figure 3.12 shows the maize yield indices (actual and simulated) for each of the 19 seasons considered in this study for long season maize planted on plant date 1, 2 and 3 respectively. When the CERES-Observed weather yield index time series (COYI – green) of each of the three long season maize scenarios are examined, it can be seen that the CERES-Maize model performs well in simulating both the sign of the anomaly and relative magnitude of the maize yields. The feature that stands out from the CERES-Observed weather yield index time series is the fact that the CERES-Maize model is able to capture both the high maize yield of the 1995/96 La Niña season as well as the low maize yield of the 1991/92 El Niño season. In addition, the CERES-Maize model also represents the relative magnitude of the maize yields of the 1980/81, 1982/83, 1983/84, 1986/87, 1988/89, 1996/97 and 1997/98 seasons exceptionally well. In terms of getting the sign of the anomaly of the yield correct, the CERES-Maize model performs the best for the first plant date (Figure 3.11 (g)), in which the sign of the anomaly of the yield for 15 out the 19 seasons are simulated successfully.

The CERES-CCAM ensemble mean yield index time series (CCYI – blue) shows that the CERES-Maize model forced with CCAM-simulated fields is once again, as in the short and medium season maize scenarios, unable to simulate the high maize yield of the 1995/96 La Niña season and the low maize yield of the 1991/92 El Niño season. In these long season maize scenarios the CERES-Maize model makes the maize yield of the 1998/99 La Niña season the highest and the maize yield of the 1987/88 El Niño the lowest out of the 19 seasons investigated in this study. Those seasons for which the CERES-Maize model forced with CCAM-simulated fields produce realistic yields in comparison to both the actual yield index (AYI – red) and the CERES-Observed weather yield index (COYI – green) include the 1983/84 (see in particular Figure 3.12), 1986/87 (see in particular Figure 3.11 (g)) and 1988/89 (see in particular Figure 3.11 (h)) seasons. In all three scenarios the sign

of the anomaly of the yield for 13 out of the 19 seasons are indicated correctly by the CERES-Maize model.

The CERES-ECHAM4.5 ensemble mean yield index time series (CEYI – orange) and Multi-Model ensemble mean yield index time series (MMYI – purple) for the long season maize scenarios show similar results to that found for the short and medium season maize scenarios. When forced with ECHAM4.5-simulated fields the CERES-Maize model does not perform well in simulating the maize yields. This simulation system fails to capture the sign of the anomaly of the yield for 13 out of the 19 seasons. The Multi-Model simulation system on the other hand shows somewhat better results than the CERES-ECHAM4.5 simulation system, with the best results found for the long season maize planted on plant date 1 scenario (Figure 3.11 (g)).

In general, the ability of the different simulation systems in simulating the season-to-season change in maize yield seems to be the lowest for the short season maize scenarios and the highest for the long season maize scenarios. The CERES-Observed weather yield index performs the best in simulating the maize yields of the long season maize planted on plant date 1 scenario.

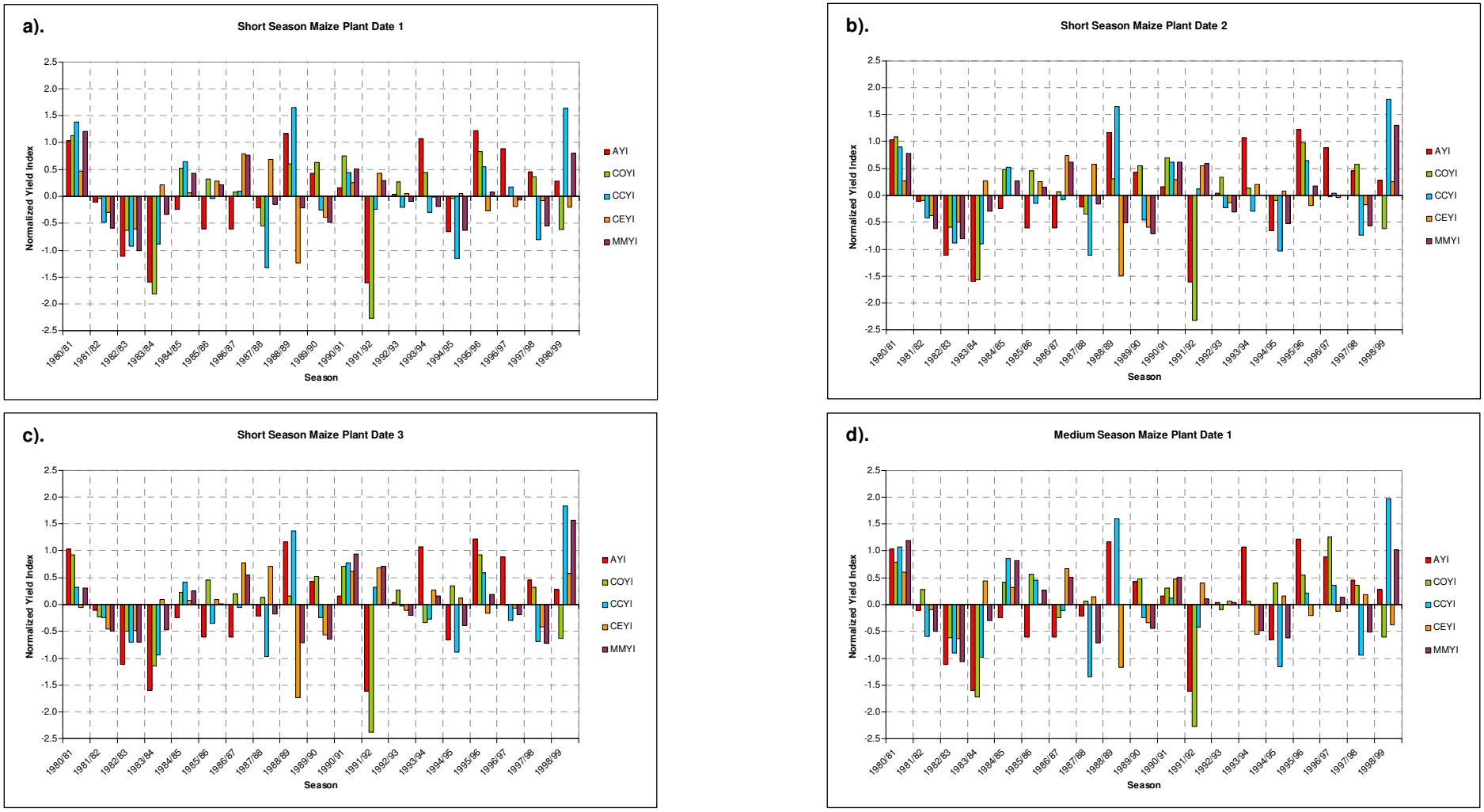

Figure 3.10: Maize yield index time-series (1980/81 – 1998/99) for the Dry/Warm Western Region. Actual maize yield index (AYI), CERES-Observed weather yield index (COYI), CERES-CCAM ensemble mean yield index (CCYI), CERES-ECHAM4.5 ensemble mean yield index (CEYI) and Multi-Model ensemble mean yield index (MMYI). Graphs (a) to (d) represent scenarios 1 to 4, as described in Table 2.8.

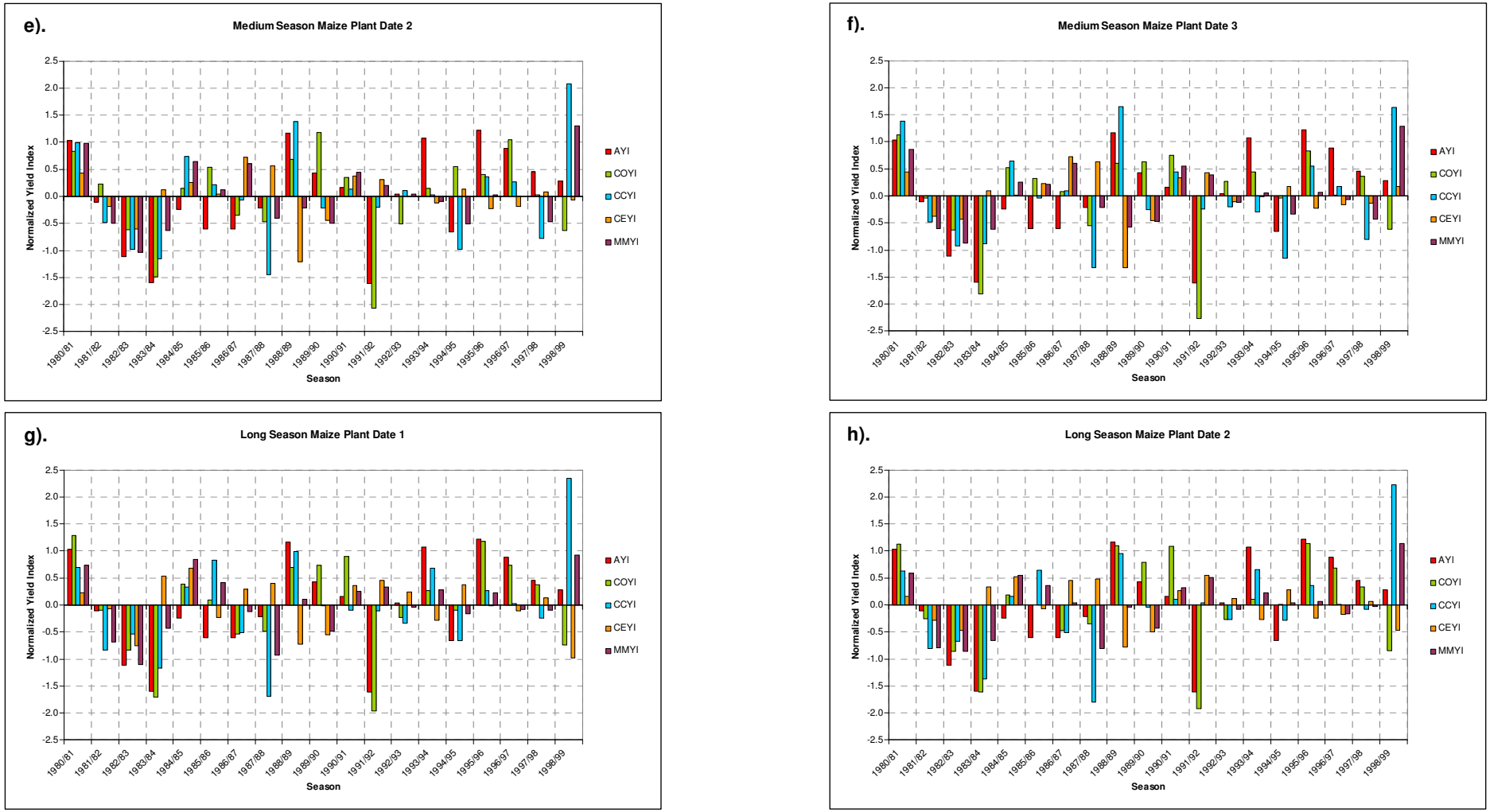

Figure 3.11: Maize yield index time-series (1980/81 – 1998/99) for the Dry/Warm Western Region. Actual maize yield index (AYI), CERES-Observed weather yield index (COYI), CERES-CCAM ensemble mean yield index (CCYI), CERES-ECHAM4.5 ensemble mean yield index (CEYI) and Multi-Model ensemble mean yield index (MMYI). Graphs (e) to (h) represent scenarios 5 to 8, as described in Table 2.8.

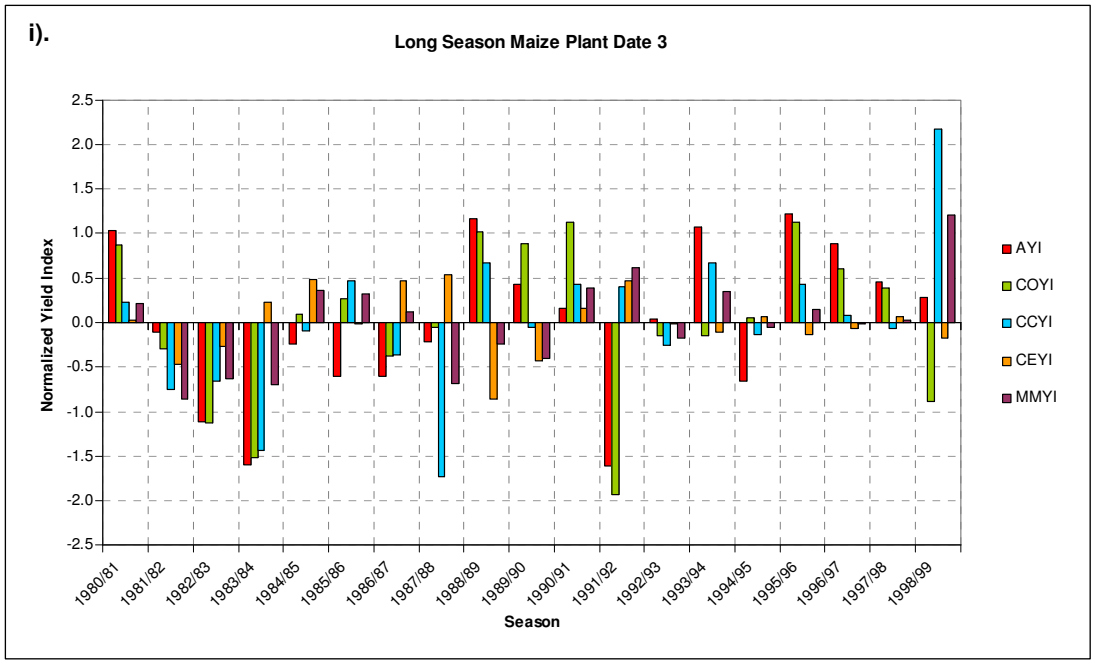

Figure 3.12: Maize yield index time-series (1980/81 – 1998/99) for the Dry/Warm Western Region. Actual maize yield index (AYI), CERES-Observed weather yield index (COYI), CERES-CCAM ensemble mean yield index (CCYI), CERES-ECHAM4.5 ensemble mean yield index (CEYI) and Multi-Model ensemble mean yield index (MMYI). This graph represents scenario 9, as described in Table 2.8.

3.3.1.2 Temperate Eastern Region

The time series of the actual maize yield index and simulated maize yield indices, obtained from each of the different simulation systems, are shown for the temperate eastern production region in Figures 3.13 (scenario 1 to 4), 3.14 (scenario 5 to 8) and 3.15 (scenario 9). From the actual yield index time series (AYI - red) it can be observed that the maize yields of the 1980's were generally much lower than the maize yields of the 1990's, except for the 1991/92 and 1994/95 seasons. Two interesting features evident from the actual yield index time series include the increasing trend in the maize yield from the 1982/83 season to the 1988/89 season and the decreasing trend in the maize yield from the 1993/94 season to the 1998/99 season. The decrease in maize yield in the late 1990's could have been due to climatic conditions, rising input costs and the unstable maize price which all added to the fact that maize production with the use of the production systems available at that stage were no longer economically viable (Du Toit *et al.*, 2001). Furthermore, it can also be seen that over this 20 year period, the 1993/94 ENSO-neutral season rendered the highest maize yield and the 1991/92 El Niño season, the same as for the dry/warm western production region, the lowest maize yield. Reasonable variation has been found in the

rainfall impacts of ENSO over southern Africa (Reason and Jagadheesa, 2005). Weak El Niño (La Niña) events can lead to more widespread and more severe rainfall impacts over southern Africa than strong El Niño (La Niña) events (Reason and Jagadheesa, 2005). This may explain the fact that in the temperate eastern production region an ENSO-neutral season resulted in the highest maize yield over the 19 seasons, while in the dry/warm western production region a La Niña season produced the highest maize yield.

3.3.1.2.1 Short Season Maize

Figure 3.13, (a), (b) and (c) represent short season maize planted on plant date 1, 2 and 3 respectively. To quantify the ability of the CERES-Maize model in simulating the inter-seasonal variability in maize yield of the temperate eastern production region it is necessary to investigate the CERES-Observed weather yield index time series (COYI – green) and compare it to the actual maize yield index time series (AYI – red). For all three short season maize scenarios the CERES-Maize model is able to successfully simulate the low maize yield of the 1991/92 El Niño season, but unable to simulate the high maize yield of the 1993/94 ENSO-neutral season. The CERES-Maize model performs well in capturing the increase in maize yield from the 1982/83 season to the 1988/89 season, but it is simulated in much more prominent steps than that observed in reality (AYI - red). Furthermore, the CERES-Maize model is able to correctly indicate the sign of the anomaly of the yield for 11 out of the 19 seasons and additionally simulates the relative magnitude of the yield of the 1981/82, 1983/84 and 1992/93 seasons remarkably well.

The CERES-CCAM ensemble mean yield index time series (CCYI – blue) for the three short season maize scenarios show that when forced with CCAM-simulated fields the CERES-Maize model is unable to capture the extremely low maize yield of the 1991/92 season and the high maize yield of the 1993/94 season. It can also be observed that for short season maize this simulation system does not perform well in simulating the relative magnitude of the yields. Furthermore, the ability of the CERES-CCAM simulation system in simulating the maize yield seems to decrease from plant date 1 to plant date 3, as the number of seasons for which the sign of the anomaly of the yield is successfully simulated decreases from 8 to 6.

From the CERES-ECHAM4.5 ensemble mean yield index time series (CEYI – orange) for the three short season maize scenarios it can be seen that for approximately 80% of the seasons the inter-seasonal variability in terms of the sign of the anomaly of the yield follows the same pattern as the CERES-CCAM ensemble mean yield index (CCYI – blue), which

results in the Multi-Model ensemble mean yield index (MMYI – purple) also following the same pattern. Similar to the results obtained for the CERES-CCAM simulation system, the CERES-ECHAM4.5 and Multi-Model simulation systems also do not perform well in simulating the relative magnitude of the yields. The 1981/82 season stands out, as for this season the CERES-ECHAM4.5 and Multi-Model simulation systems perform much better in simulating the yield than the CERES-CCAM simulation system.

3.3.1.2.2 Medium Season Maize

The time series of the maize yield indices (actual and simulated) for medium season maize planted on plant date 1, 2 and 3 are shown in Figure 3.13 (d) and Figure 3.14 (e) and (f) respectively. The first observation that can be made from the CERES-Observed weather yield index time series (COYI – green) for the three medium season maize scenarios, is that both the sign of the anomaly and relative magnitude of the yields are best represented by the CERES-Maize model in the medium season maize planted on plant date 1 and 2 scenarios. The sign of the anomaly of the yield for 16 out of the 19 seasons are simulated successfully by the CERES-Maize model in the medium season maize planted on plant date 1 and 2 scenarios. For the medium season maize planted on plant date 3 scenario, the CERES-Maize model struggles to simulate the relative magnitude of the maize yields of the 1995/1996, 1996/97 and 1997/98 seasons, while the CERES-Maize performs well in capturing the relative magnitude of the yields of these seasons in the other two medium season maize scenarios. In all three scenarios the CERES-Maize model produces the most realistic maize yields for the 1980/81, 1982/83, 1983/84, 1991/92 and 1992/93 seasons.

When the CERES-CCAM ensemble mean yield index time series (CCYI – blue) for each of the three medium season maize scenarios are examined, it can be seen that the CERES-Maize model forced with CCAM-simulated fields fails to simulate the high maize yield of the 1993/94 ENSO-neutral season and the low maize yield of the 1991/92 El Niño season. A prominent feature that can be observed from the CERES-CCAM ensemble mean yield index time series is the extremely high maize yield of the 1998/99 La Niña season. The CERES-CCAM ensemble mean yield index appears to show greater variability between seasons than that observed from the actual yield index. Similar to the CERES-Observed weather yield index, the CERES-CCAM simulation system also performs better in simulating the sign of the anomaly of the yields of the medium season maize planted on plant date 1 and 2 scenarios than the medium season maize planted on plant date 3 scenario.

The CERES-ECHAM4.5 ensemble mean yield index time series (CEYI – orange) for the three medium season maize scenarios show a decrease in performance from plant date 1 to plant date 3. When forced with ECHAM4.5-simulated fields the CERES-Maize model does not capture the low maize yield of the 1991/92 season, but instead simulates the maize yield of the 1988/89 La Niña season to be unusually low. From the Multi-Model ensemble mean yield index time series (MMYI – purple) for the three medium season maize scenarios it can be seen that for several seasons the Multi-Model simulation system provides better yield estimates than the CERES-CCAM or CERES-ECHAM4.5 simulation systems on their own. These seasons include 1981/82 (see Figure 3.13 (d)), 1983/84 (see Figure 3.14 (f)), 1984/85 (see Figure 3.13 (d)) and 1996/97 (see Figure 3.13 (d)).

3.3.1.2.3 Long Season Maize

Figure 3.14 (g) and (h) and Figure 3.15 shows the maize yield indices (actual and simulated) for the 19 seasons considered in this study for long season maize planted on plant date 1, 2 and 3 respectively. By examining the CERES-Observed weather yield index time series (COYI – green) it can be seen that the CERES-Maize model correctly indicates the sign of the anomaly of the yield of almost all the seasons. The CERES-Observed weather yield index shows little variation between the three scenarios. In all three scenarios the CERES-Maize model performs very well in simulating the relative magnitude of the yields of those seasons with actual yield index values less that -1, as can be seen for the 1982/83, 1983/84 and 1991/92 seasons.

The CERES-CCAM ensemble mean yield index time series (CCYI – blue) for the three long season maize scenarios show that for 12 out of the 19 seasons considered here the CERES-CCAM simulation system is able to correctly indicate the sign of the anomaly of the yield. It can also be noted that the CERES-Maize model largely overestimates the maize yields of the 1988/89 and 1998/99 La Niña seasons. In all three scenarios the CERES-Maize model forced with CCAM-simulated fields performs exceptionally well in capturing the relative magnitude of the yield of the 1994/95 El Niño season.

The time series of the CERES-ECHAM4.5 ensemble mean yield index (CEYI – orange) for long season maize planted on plant date 1, 2 and 3 show that even though the CERES-Maize model forced with ECHAM4.5-simulated fields is unable to capture the sign of the anomaly of the yield of almost half of the seasons considered in this study, for several seasons the relative magnitude of the yield is estimated extremely well. In all three

scenarios this simulation system captures the relative magnitude of the yield of the 1985/86, 1990/91 and 1997/98 seasons better than any of the other simulation systems.

The combination between the CERES-CCAM and CERES-ECHAM4.5 integrations for the long season maize scenarios is expressed as the Multi-Model ensemble mean yield index (MMYI – purple) in Figure 3.14 (g) and (h) and Figure 3.15. In all three scenarios the Multi-Model simulation system succeeds in simulating the sign of the anomaly of the yield of 10 seasons. This system also performs relatively well in estimating the relative magnitude of the yields of the 1980/81, 1982/83 and 1996/97 seasons. Even though the yield estimates for these seasons are not necessarily an improvement from the CERES-CCAM ensemble mean yield index (CCYI – blue) or CERES-ECHAM4.5 ensemble mean yield index (CEYI – orange), these estimates are still fairly good.

In general, all four simulation systems show a decrease in performance from plant date 1 to plant date 3 in the short season maize scenarios, better performance for plant dates 1 and 2 in the medium season maize scenarios than for plant date 3 and the best performance for the long season maize scenarios. The best results are once again found for the long season maize planted on plant date 1 scenario. For this scenario the CERES-Observed weather simulation system correctly indicates the sign of the anomaly of the yield of almost all 19 seasons.

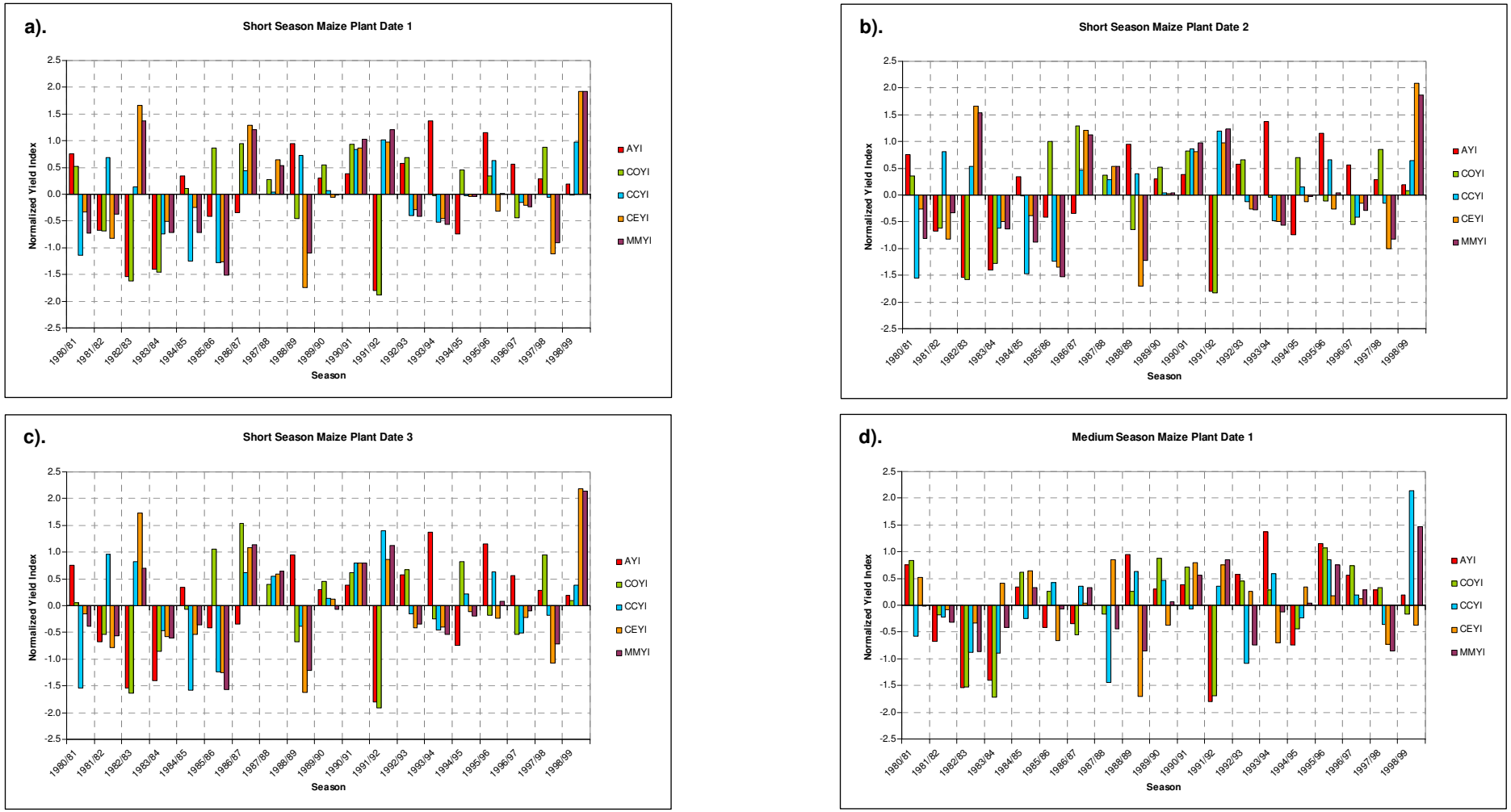

Figure 3.13: Maize yield index time-series (1980/81 – 1998/99) for the Temperate Eastern Region. Actual maize yield index (AYI), CERES-Observed weather yield index (COYI), CERES-CCAM ensemble mean yield index (CCYI), CERES-ECHAM4.5 ensemble mean yield index (CEYI) and Multi-Model ensemble mean yield index (MMYI). Graphs (a) to (d) represent scenarios 1 to 4, as described in Table 2.8.

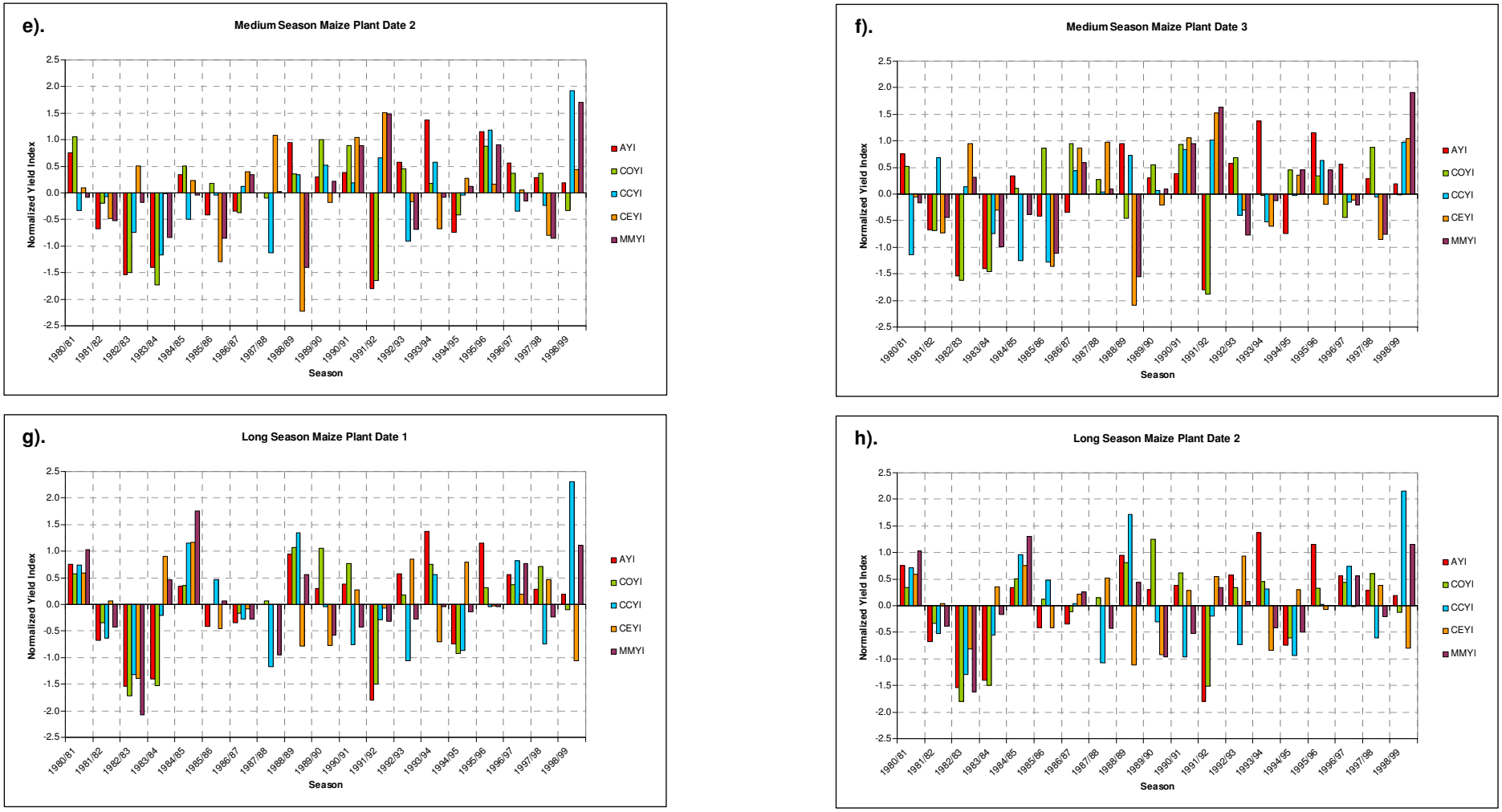

Figure 3.14: Maize yield index time-series (1980/81 – 1998/99) for the Temperate Eastern Region. Actual maize yield index (AYI), CERES-Observed weather yield index (COYI), CERES-CCAM ensemble mean yield index (CCYI), CERES-ECHAM4.5 ensemble mean yield index (CEYI) and Multi-Model ensemble mean yield index (MMYI). Graphs (e) to (h) represent scenarios 5 to 8, as described in Table 2.8.

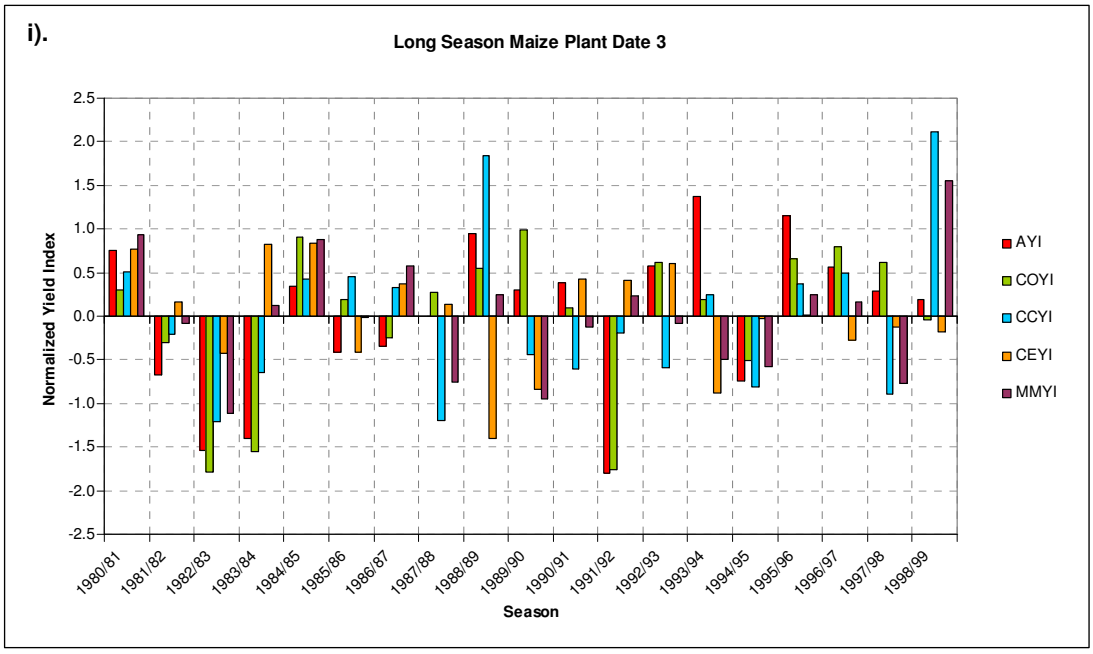

Figure 3.15: Maize yield index time-series (1980/81 – 1998/99) for the Temperate Eastern Region. Actual maize yield index (AYI), CERES-Observed weather yield index (COYI), CERES-CCAM ensemble mean yield index (CCYI), CERES-ECHAM4.5 ensemble mean yield index (CEYI) and Multi-Model ensemble mean yield index (MMYI). This graph represents scenario 9, as described in Table 2.8.

3.3.1.3 Wet/Cool Eastern Region

The time series of the actual maize yield index and simulated maize yield indices, obtained from each of the different simulation systems, are shown for the wet/cool eastern production region in Figures 3.16 (scenario 1 to 4), 3.17 (scenario 5 to 8) and 3.18 (scenario 9). From the actual yield index time series (AYI - red) it can be observed that maize production in the 1980's in the wet/cool eastern production region was characterised by relatively low maize yields from the 1981/82 season to the 1983/84 season, followed by a period of slightly higher (at least above normal) yields from the 1984/85 season to the 1990/91 season, with the exception of the 1986/87 season. The 1990's on the other hand commenced with the lowest maize yield of the entire 20 year period (1991/92), followed shortly by the highest maize yield of the entire 20 year period (1993/94) where after a decrease in maize yield took place from the 1995/96 season to the 1997/98 season. As mentioned for the dry/warm western and temperate eastern production regions, an El Niño event occurred during the 1991/92 season, while 1993/94 was an ENSO-neutral season.

3.3.1.3.1 Short Season Maize

Figure 3.16 (a), (b) and (c) shows the yield indices (actual and simulated) for short season maize planted on plant date 1, 2 and 3 respectively. It is essential to quantify the ability of the CERES-Maize model in simulating the yield of the wet/cool eastern production region. This is done by examining the CERES-Observed weather yield index time series (COYI – green). From the three graphs it can be seen that the ability of the CERES-Maize model in simulating the sign of the anomaly of the yield decreases from plant date 1 to plant date 3. Even though the relative magnitude of the yields are not simulated that well, in the short season maize planted on plant date 1 scenario (Figure 3.16 (a)) the CERES-Maize model is able to capture the increase in maize yield from 1982/83 to 1985/86. Furthermore it is also evident that when forced with observed weather data the CERES-Maize model fails to simulate the anomalously low maize yield of the 1991/92 El Niño season and the anomalously high maize yield of the 1993/94 ENSO-neutral season. In all three short season maize scenarios the relative magnitude of the yields of the 1980/81, 1983/84 and 1984/85 seasons are simulated very well.

The time series of the CERES-CCAM ensemble mean yield index (CCYI – blue) for short season maize shows that this simulation system struggles to simulate the maize yields of the late 1980's to early 1990's (1985/86 – 1990/91), except for the 1988/89 season. Thus, the CERES-Maize model forced with CCAM-simulated fields performs a great deal better in simulating the maize yields of the early 1980's and late 1990's than it performs for the period in between. In all three short season maize scenarios this simulation system simulates the relative magnitude of the yields of the 1982/83, 1988/89, 1994/95 and 1996/97 seasons extremely well. Another interesting feature is the fact that the CERES-CCAM ensemble mean yield index shows a large overestimation of the yield of the 1998/99 La Niña season

When the CERES-ECHAM4.5 ensemble mean yield index time series (CEYI – orange) of each of the three short season maize scenarios are examined, it can be seen that this simulation system largely underestimates the yield of the 1988/89 La Niña season, but performs better than the CERES-CCAM simulation system in estimating the yield of the 1987/88 El Niño season. Furthermore, the CERES-ECHAM4.5 ensemble mean yield index reveals a realistic maize yield for the 1998/99 season (see in particular Figure 3.16 (b) and (c)).

From the Multi-Model ensemble mean yield index time series (MMYI – purple) it can be seen that this simulation system also severely overestimates the maize yield of the 1998/99 La Niña season, as is the case with the CERES-CCAM simulation system. Another observation that can be made is the fact that the Multi-Model simulation system does not perform well in capturing the sign of the anomaly of the yield of the five seasons from 1989/90 to 1993/94. Furthermore, over the three short season maize scenarios this simulation system is able to correctly indicate the sign of the anomaly of the yield of an average for 9 seasons out of the 19 under investigation.

3.3.1.3.2 Medium Season Maize

Time series of the maize yield indices (actual and simulated) for medium season maize planted on plant date 1, 2 and 3 are shown in Figure 3.16 (d) and Figure 3.17 (e) and (f) respectively. From the CERES-Observed weather yield index times series (COYI – green) for these three scenarios it can be seen that the CERES-Maize model performs well in capturing the sign of the anomaly of the yield, but fails to simulate the relative magnitude of the yields. Furthermore, it also appears as if the relative magnitude of the simulated yields vary considerably between the three scenarios, which makes it difficult to determine for which medium season maize scenario the CERES-Maize model performs the best.

When the CERES-CCAM ensemble mean yield index time series (CCYI – blue) for each of the three medium season maize scenarios are examined, the first observation that can be made is the large overestimation of the yield of the 1998/99 La Niña season. This simulation system performs relatively well in capturing the relative magnitude of the maize yields.

The CERES-ECHAM4.5 ensemble mean yield index time series (CEYI – orange) for the three medium season maize scenarios show that this simulation system succeeds in simulating the sign of the anomaly of the yield for 9 out of the 19 seasons considered in this study. It can also be seen that the CERES-Maize model forced with ECHAM4.5-simulated fields performs the best in simulating the relative magnitude of the maize yields of the medium season maize planted on plant date 2 scenario, as can be seen, for example, for the 1980/81, 1982,83, 1996/97 and 1997/98 seasons.

From the Multi-Model ensemble mean yield index time series (MMYI – purple) for the three medium season maize scenarios it can be seen that even though this simulation system captures the sign of the anomaly of the yield of several seasons, it often fails to simulate the

relative magnitude of the maize yields. Although, it can be seen that the relative magnitude of the yields of a number of seasons (1980/81, 1983/84 and 1996/97) are captured the best for the medium season maize planted on plant date 3 scenario.

3.3.1.3.3 Long Season Maize

In Figure 3.17 (g) and (h) and Figure 3.18 the maize yield indices (actual and simulated) for long season maize planted on plant date 1, 2 and 3 can be seen. The CERES-Observed weather yield index time series (COYI – green) for these three long season maize scenarios show that the CERES-Maize model performs well in simulating the sign of the anomaly of the maize yields of the wet/cool eastern production region. In the long season maize planted on plant date 1 scenario (Figure 3.17 (g)) the CERES-Maize model is able to correctly indicate the sign of the anomaly of the yield for 17 out of the 19 season. The high maize yield of the 1993/94 ENSO-neutral season is underestimated by the model and the low maize yield of the 1991/92 El Niño season is overestimated.

The CERES-CCAM ensemble mean yield index time series (CCYI – blue) for the long season maize scenarios show that when forced with CCAM-simulated fields the CERES-Maize model performs well in simulating the relative magnitude of the yields of many seasons. This can primarily be seen for the seasons in the 80's and include 1980/81, 1982/83, 1985/86, 1986/87 and 1988/89. An overestimation of the yield of the 1998/99 La Niña season can once again be seen. This simulation system is able to capture the sign of the anomaly of the yield for 14 out of the 19 seasons under investigation in this study.

From the CERES-ECHAM4.5 ensemble mean yield index time series (CEYI – orange) for the three long season maize scenarios it can be seen that when the CERES-Maize model is forced with ECHAM4.5-simulated fields, the ability to simulate the sign of the anomaly of the yield decreases from plant date 1 to plant date 3, as the number of season for which the model correctly indicates the sign of the anomaly of the yield decreases from 11 to 8. In general, this simulation system struggles to simulate the maize yields of the four seasons from 1986/87 to 1989/90. Furthermore it is also evident that for a number of seasons this simulation system produces more realistic maize yields than the CERES-CCAM simulation system, as can be seen for the 1991/92, 1996/97, and 1997/98 seasons.

From the Multi-Model ensemble mean yield index time series (MMYI – purple) for the long season maize scenarios it can be seen that the Multi-model simulation system performs better in simulating the sign of the anomaly of the yield than the CERES-ECHAM4.5 maize

yield simulation system, but does not perform as good as the CERES-CCAM maize yield simulation system. For some seasons the Multi-Model ensemble mean yield index time series show better results in terms of the relative magnitude of the yield than both the CERES-CCAM and CERES-ECHAM4.5 simulation systems, as can be seen, for example, for the 1998/99 season.

In general, all four simulation systems show a decrease in performance from plant date 1 to plant date 3 in the short season maize scenarios, similar results for all three plant dates in the medium season maize scenarios and a decrease in performance from plant date 1 to plant date 3 in the long season maize scenarios. Thus, out of the 9 scenarios investigated, the simulation systems show the best results for the long season maize planted on plant date 1 scenario.

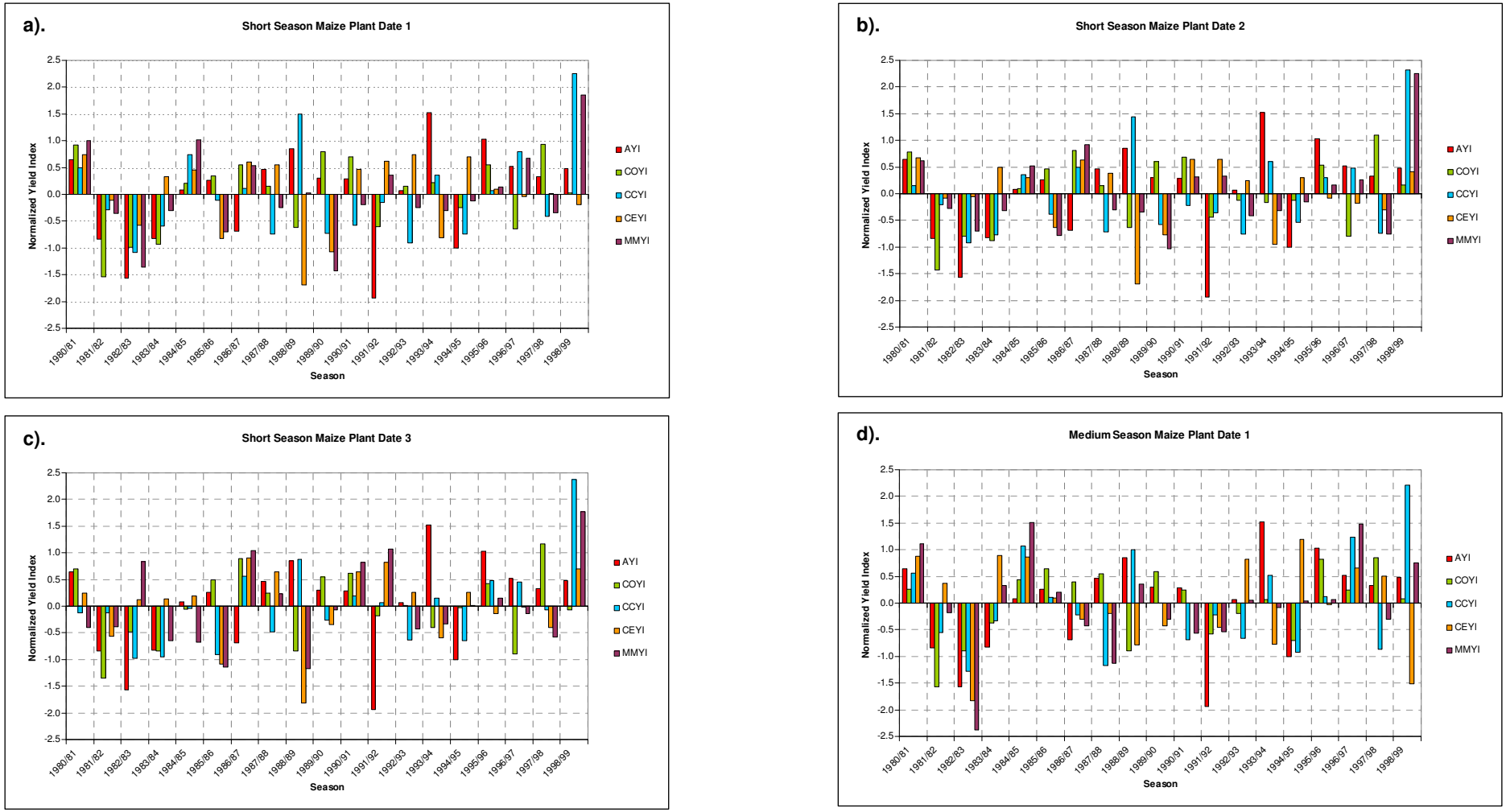

Figure 3.16: Maize yield index time-series (1980/81 – 1998/99) for the Wet/Cool Eastern Region. Actual maize yield index (AYI), CERES-Observed weather yield index (COYI), CERES-CCAM ensemble mean yield index (CCYI), CERES-ECHAM4.5 ensemble mean yield index (CEYI) and Multi-Model ensemble mean yield index (MMYI). Graphs (a) to (d) represent scenarios 1 to 4, as described in Table 2.8.

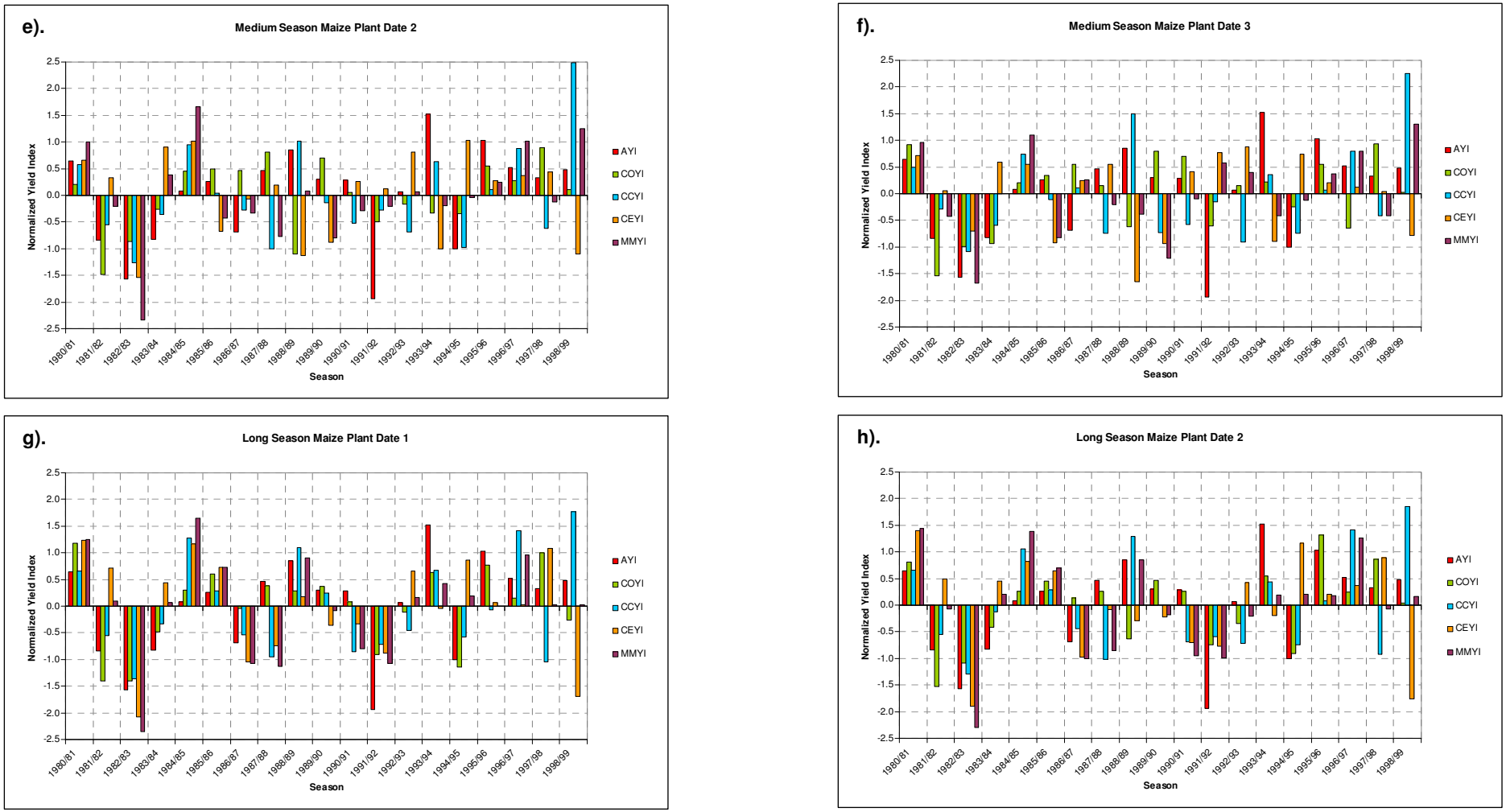

Figure 3.17: Maize yield index time-series (1980/81 – 1998/99) for the Wet/Cool Eastern Region. Actual maize yield index (AYI), CERES-Observed weather yield index (COYI), CERES-CCAM ensemble mean yield index (CCYI), CERES-ECHAM4.5 ensemble mean yield index (CEYI) and Multi-Model ensemble mean yield index (MMYI). Graphs (e) to (h) represent scenarios 5 to 8, as described in Table 2.8.

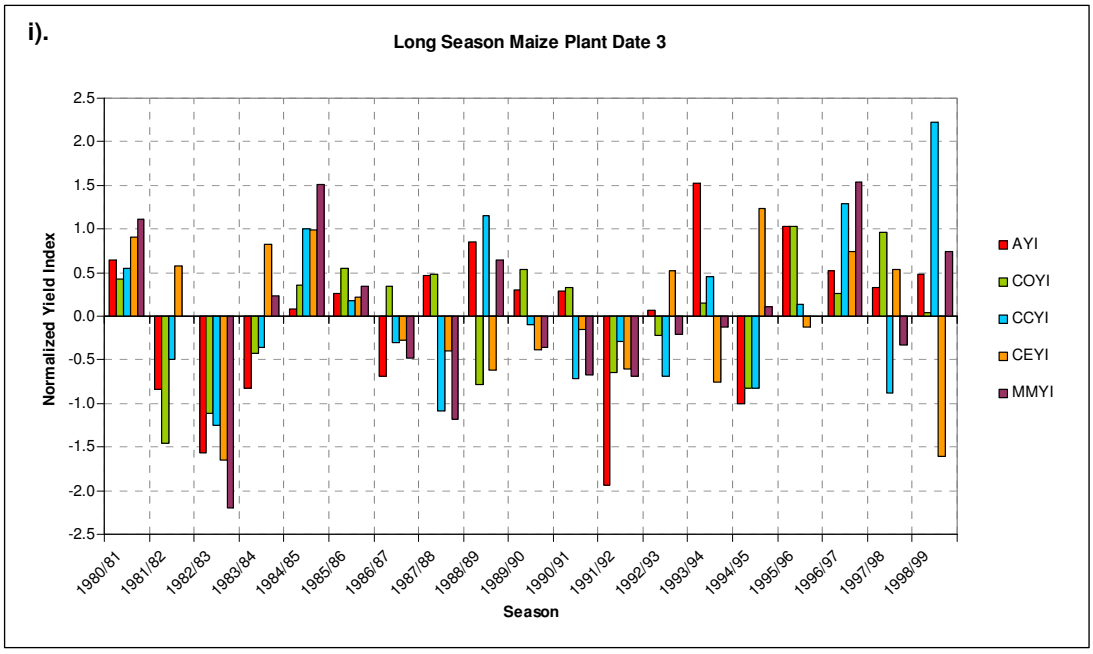

Figure 3.18: Maize yield index time-series (1980/81 – 1998/99) for the Wet/Cool Eastern Region. Actual maize yield index (AYI), CERES-Observed weather yield index (COYI), CERES-CCAM ensemble mean yield index (CCYI), CERES-ECHAM4.5 ensemble mean yield index (CEYI) and Multi-Model ensemble mean yield index (MMYI). This graph represents scenario 9, as described in Table 2.8.

3.3.2 Objective Validation

3.3.2.1 Actual Maize Yield vs. CERES-Observed Weather Maize Yield

Figure 3.19 (a) to (i) shows the Spearman rank correlations between the actual maize yields and CERES-Observed weather maize yields for each of the 9 scenarios in Table 2.8. The magisterial districts with statistically significant correlations are indicated in bold. Strong correlations indicate areas where the association between the actual maize yield and CERES-Observed weather maize yield is greatest, and weak correlations indicate the areas where the association is poor. The threshold correlation for local significance at the 95% level of confidence is approximately 0.46.

The three short season maize scenarios (Figure 3.19 (a), (b) and (c)) show higher correlations for the North-West Province than for the Free State, and also reveal an increase in the correlations from east to west across the study area, with much lower correlations in the east than in the west. In all three short season maize scenarios, the western part of the North-West Province shows the highest correlations. It can also be seen that the skill of the CERES-Maize model decreases from plant date 1 to plant date 3,

as 25 magisterial districts (significant at the 95% level, see section 2.5.2.2.2) have statistically significant correlations for plant date 1 (Figure 3.19 (a)), but only 21 (significant at 95% level) for plant date 2 (Figure 3.19 (b)) and 14 (significant at 95% level) for plant date 3 (Figure 3.19 (c)). The short season maize planted on plant date 3 scenario shows that most of the magisterial districts in the Free State do not have statistically significant correlations.

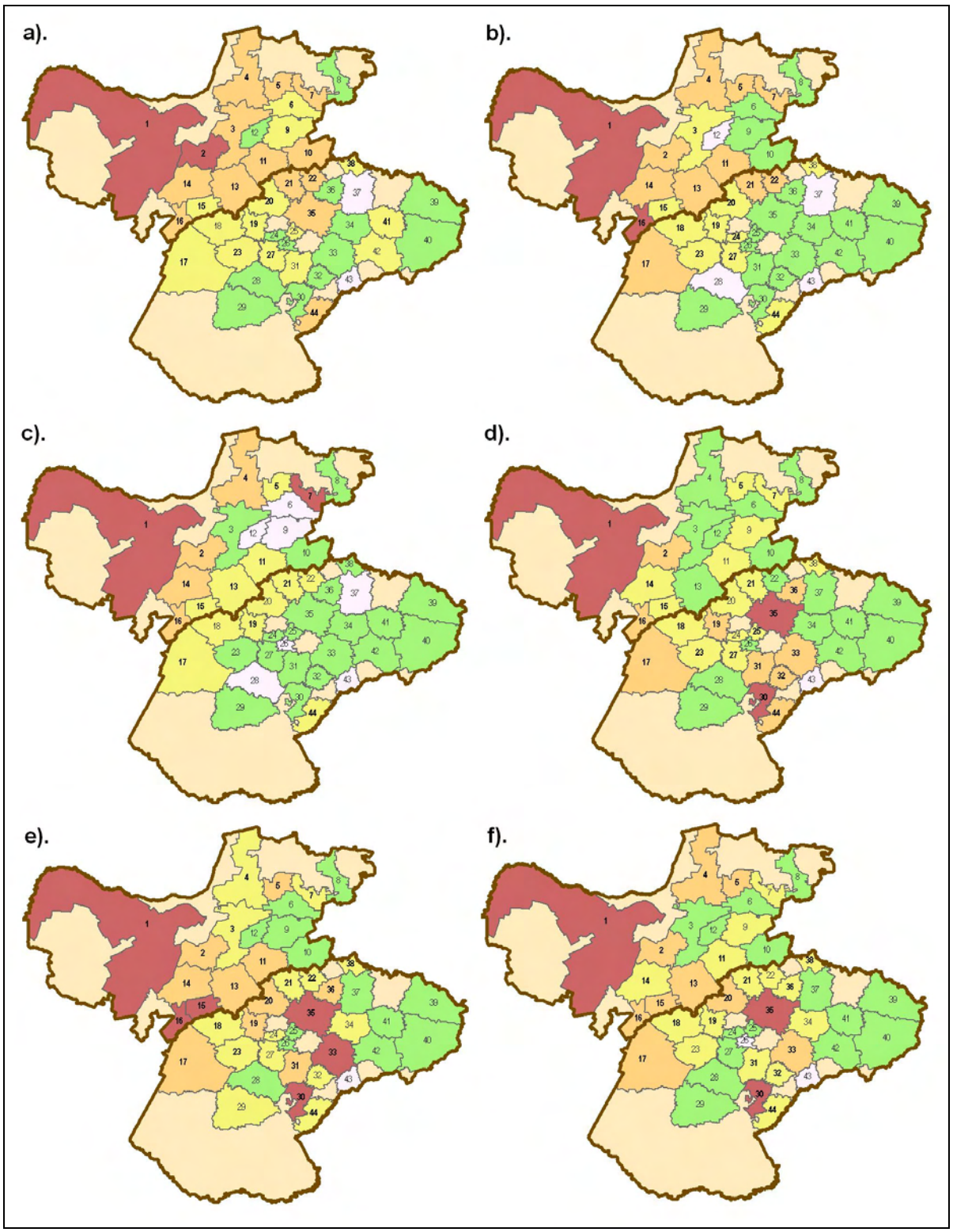

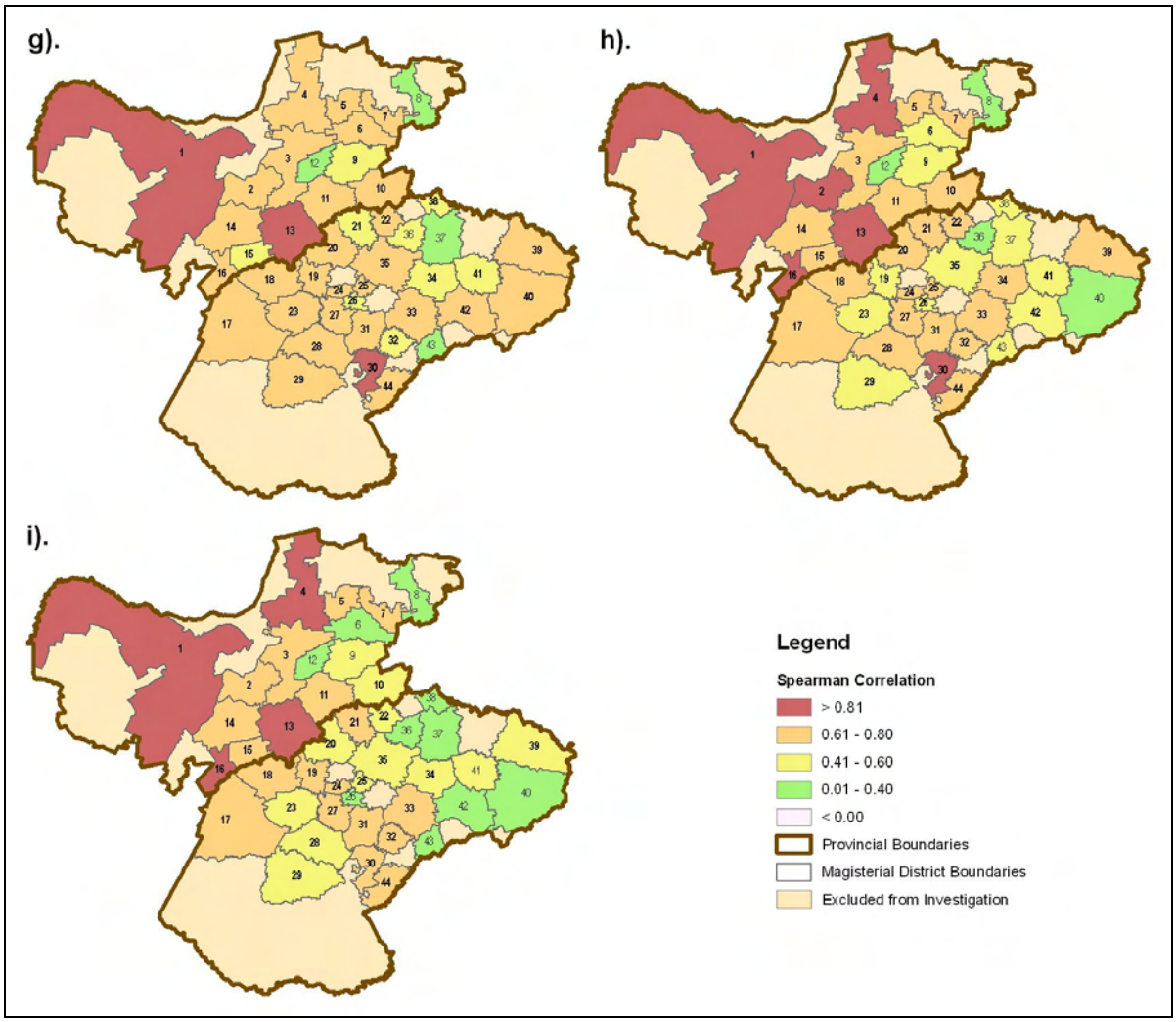

Figure 3.19: Spearman rank correlations calculated between the actual maize yields and CERES-Observed weather maize yields over the 20 year period from 1980 to 1999. (a) Short season maize plant date 1, (b) Short season maize plant date 2, (c) Short season maize plant date 3, (d) Medium season maize plant date 1, (e) Medium season maize plant date 2, (f) Medium season maize plant date 3, (g) Long season maize plant date 1, (h) Long season maize plant date 2 and (i) Long season maize plant date 3. Magisterial districts with statistically significant correlations at the 95% confidence level are indicated in bold.

The three medium season maize scenarios (Figure 3.19 (d), (e) and (f)) also show higher correlations in the western parts of the study area than in the eastern parts of the study area, with the highest correlations (> 0.81) found for the western part of the North-West Province and central part of the Free State. The medium season maize planted on plant date 2 scenario (Figure 3.19 (e)) shows 25 magisterial districts (significant at 95% level) with statistically significant correlations, with only 21 (significant at 95% level) for the medium season maize planted on plant date 1 scenario (Figure 3.19 (d)) and 22 (significant

at 95% level) for the medium season maize planted on plant date 3 scenario (Figure 3.19 (f)). All three scenarios reveal that the CERES-Maize model has poor skill in simulating the maize yield of magisterial district Ficksburg (43).

In the three long season maize scenarios (Figure 3.19 (g), (h) and (i)) the highest correlations, greater than 0.81, are evident for the western and central parts of the North-West Province. Once again, as with the short season maize scenarios, the skill of the CERES-Maize model appears to decrease from plant date 1 to plant date 3. Statistically significant correlations can be seen for 39 (significant at 95% level) out of the 44 magisterial districts in the long season maize planted on plant date 1 scenario (Figure 3.19 (g)). The other two scenarios show slightly lower correlations in the east than in the west, with 37 magisterial districts (significant at 95% level) with statistically significant correlations in the long season maize planted on plant date 2 scenario (Figure 3.19 (h)) and 32 (significant at 95% level) in the long season maize planted on plant date 3 scenario (Figure 3.19 (i)).

Thus, in all 9 scenarios the strongest correlations are typically found for the western part of the North-West Province, with correlations frequently exceeding 0.81. Furthermore, all 9 scenarios reveal a stronger association between the CERES-Observed weather maize yields and actual maize yields in the western parts of the study area than in the eastern parts. In general, the skill of the CERES-Maize model increases from the short season maize scenarios to the long season maize scenarios, with the overall highest correlations found for long season maize planted on plant date 1 (Figure 3.19 (g)). This is in agreement with the results found in the subjective validation.

3.3.2.2 Actual Maize Yield vs. CERES-CCAM Ensemble Mean Maize Yield

Figure 3.20 (a) to (i) shows the Spearman rank correlations between the actual maize yields and CERES-CCAM ensemble mean maize yields for each of the 9 scenarios in Table 2.8. The skill of the CERES-CCAM simulation system is evaluated in terms of the association between the simulated and actual maize yields. The magisterial districts with statistically significant correlations are indicated in bold. The threshold correlation for local significance at the 95% level of confidence is approximately 0.46.

The first feature that can be observed from the three short season maize scenarios (Figure 3.20 (a), (b) and (c)) is that the highest correlations occur in the western part of the Free State. The correlations of the magisterial districts in the North-West Province are primarily

not statistically significant and negative correlations are found for the temperate eastern production region. Thus, the CERES-CCAM simulation system shows poor skill in simulating the maize yields of this production region. It can also be seen that when forced with CCAM-simulated fields the skill of the CERES-Maize model decreases rather drastically from plant date 1 to plant date 3, as 21 magisterial districts (significant at 95% level) have statistically significant correlations for plant date 1 (Figure 3.20 (a)), but only 13 (significant at 95% level) for plant date 2 (Figure 3.20 (b)) and 11 (significant at 95% level) for plant date 3 (Figure 3.20 (c)).

In general, the three medium season maize scenarios (Figure 3.20 (d), (e) and (f)) show more magisterial districts with statistically significant correlations than the short season maize scenarios (Figure 3.20 (a), (b) and (c)). The medium season maize planted on plant date 1 scenario (Figure 4.23 (d)) shows 22 magisterial districts (significant at 95% level) with statistically significant correlations, with 21 (significant at 95% level) for the medium season maize planted on plant date 2 scenario (Figure 3.20 (e)) and 20 (significant at 95% level) for the medium season maize planted on plant date 3 scenario (Figure 3.20 (f)). Thus, the skill of the CERES-CCAM simulation system decreases slightly from plant date 1 to plant date 3. The medium season maize planted on plant date 3 scenario also shows negative correlations for the temperate eastern production region as can be seen in the three short season maize scenarios. The highest correlations occur adjacent to the border separating the Free State from the North-West Province, and in the western part of the Free State.

In the three long season maize scenarios (Figure 3.20 (g), (h) and (i)) the highest correlations (0.61 – 0.8) occur once again in the western part of the Free State and to some extent also in the western part of the North-West Province (see Figure 3.20 (g) and (h)). Similar to the short and medium season maize scenarios, for the long season maize scenarios the skill of the CERES-CCAM simulation system also decreases from plant date 1 to plant date 3. Statistically significant correlations can be seen for 21 (significant at 95% level) out of the 44 magisterial districts in the long season maize planted on plant date 1 scenario (Figure 3.20 (g)), 17 (significant at 95% level) out of the 44 magisterial districts in the long season maize planted on plant date 2 scenario (Figure 3.20 (h)) and 10 (significant at 95% level) out of the 44 magisterial districts for the long season maize planted on plant date 3 scenario (Figure 3.20 (i)). It can also be seen that this simulation system does not perform well in simulating the maize yields of the magisterial districts in the eastern parts of both the Free State and North-West Province.

Thus, in all 9 scenarios the strongest correlations are typically found for the western part of the Free State, with correlations ranging between 0.61 and 0.8. Furthermore, it is evident in all 9 scenarios that the CERES-CCAM simulation system does not perform well in simulating the maize yields of a large part of the temperate eastern production region, with

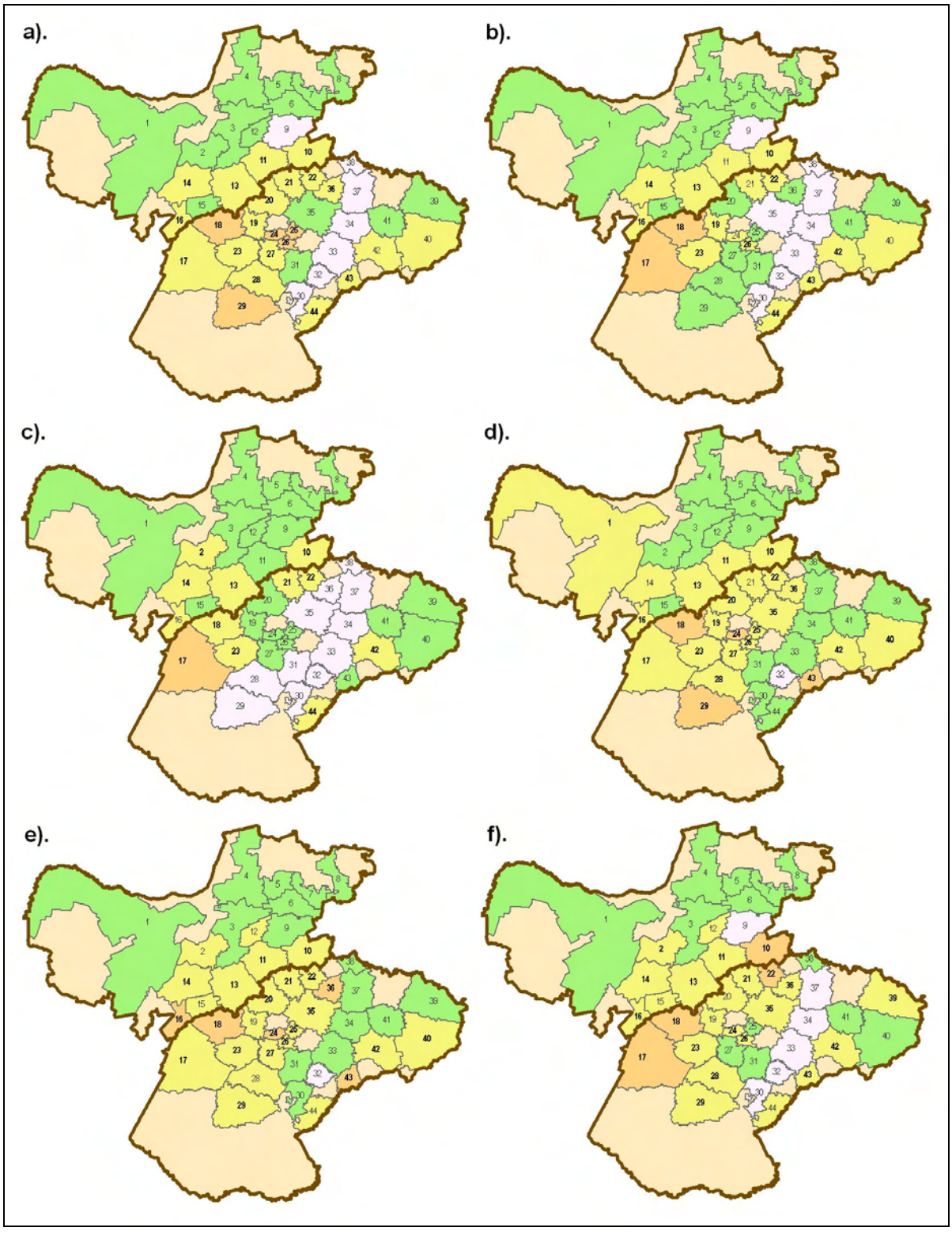

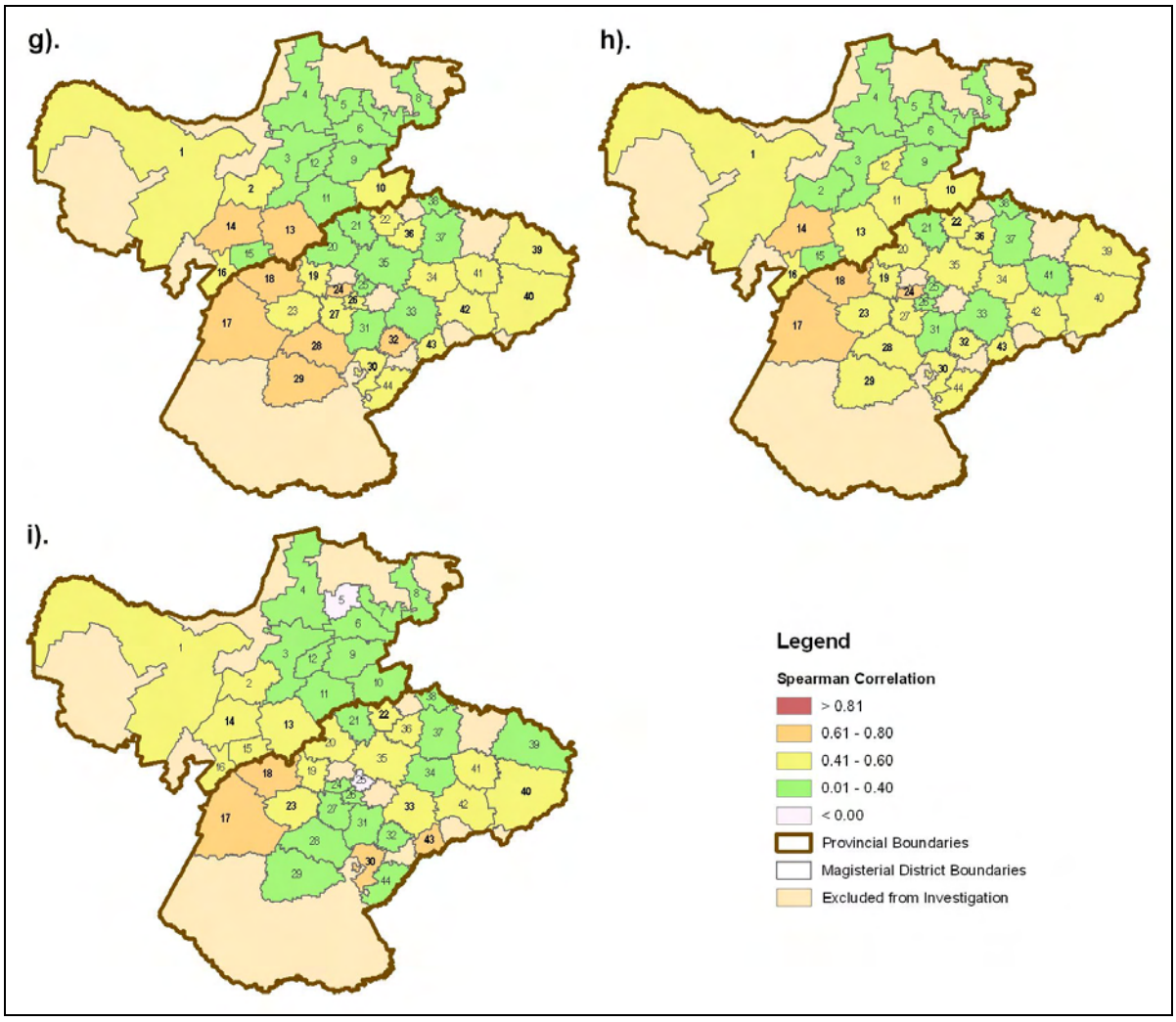

Figure 3.20: Spearman rank correlations calculated between the actual maize yields and CERES-CCAM ensemble mean maize yields over the 20 year period from 1980 to 1999. (a) Short season maize plant date 1, (b) Short season maize plant date 2, (c) Short season maize plant date 3, (d) Medium season maize plant date 1, (e) Medium season maize plant date 2, (f) Medium season maize plant date 3, (g) Long season maize plant date 1, (h) Long season maize plant date 2 and (i) Long season maize plant date 3. Magisterial districts with statistically significant correlations at the 95% confidence level are indicated in bold.

correlations either being negative or not significant. In general, the CERES-Maize model forced with CCAM-simulated fields reveals the highest skill in simulating the maize yields of the first plant dates, thus short season maize planted on plant date 1, medium season maize planted on plant date 1 and long season maize planted on plant date 1 (Figure 3.20 (a), (d) and (g). An increase in skill from the short season maize scenarios to the long season maize scenarios are also revealed, with the highest correlations found for long season maize planted on plant date 1 (figure 3.20 (g)). This phenomenon can also be seen

in the CERES-CCAM simulated maize yields discussed in the subjective validation section (3.3.1).

3.3.2.3 Actual Maize Yield vs. CERES-ECHAM4.5 Ensemble Mean Maize Yield

The Spearman rank correlations between the actual maize yields and CERES-ECHAM4.5 ensemble mean maize yields are not shown, since the skill of this simulation system is poor. A number of factors could have contributed to this result. The ECHAM4.5-simulated fields are on a course grid of approximately 2.8° x 2.8°. Raw output from ECHAM4.5 is used as input into the CERES-Maize model. The same is done for the CERES-CCAM simulation system. Raw output from CCAM is used as input into the CERES-Maize model, but the simulated fields produced by CCAM are written out on a 1° x 1° grid. Due to the higher spatial resolution of the CCAM-simulated fields, the CERES-CCAM simulation system has an advantage over the CERES-ECHAM4.5 simulation system. As a result of the low spatial resolution of the ECHAM4.5-simualted fields it is possible that the ECHAM4.5 GCM is not skilful in providing a good representation of sub-grid scale features like precipitation. GCMs tend to overestimate rainfall over southern Africa, and often also distort the spatial pattern of the rainfall (Joubert and Hewitson, 1997). It may be possible to improve on the spatial resolution of the ECHAM4.5-simulated fields by nesting a Regional Climate Model (RCM) within the ECHAM4.5 GCM. In this study from the gridded GCM output a nearest neighbour approach is used to obtain representative GCM-simulated weather-type data for each magisterial district (see section 2.4.3.2). Thus, the use of a different interpolation routine may also improve the reliability of the GCM-simulated fields.

By investigating the seasonal long-term mean simulated fields of both ECHAM4.5 and CCAM, it is found that ECHAM4.5 has lower skill than CCAM in simulating mid-summer rainfall over the study area. So, it is not too surprising that CCAM produced more reliable weather-type data than ECHAM4.5. Mid-summer is a critical period in the development of the maize plant and therefore any misrepresentations in the rainfall in this season could have led to discrepancies in the maize yields simulated by the CERES-ECHAM4.5 simulation system.

3.3.2.4 Actual Maize Yield vs. Multi-Model Ensemble Mean Maize Yield

Figure 3.21 (a) to (i) shows the Spearman rank correlations between the actual maize yields and Multi-Model ensemble mean maize yields for each of the 9 scenarios in Table 2.8. The

magisterial districts with statistically significant correlations are indicated in bold. Strong correlations indicate high skill and weak correlations indicate poor skill. The threshold correlation for local significance at the 95% level of confidence is approximately 0.46.

The three short season maize scenarios (Figure 3.21 (a), (b) and (c)) show higher correlations for the North-West Province than for the Free State. It can also be seen that in all three scenarios only a few magisterial districts have statistically significant correlations. The highest correlations primarily occur in the western parts of the study area.

From the three medium season maize scenarios (Figure 3.21 (d), (e) and (f)) it can be seen that the highest correlations are either found in the eastern part of the Free State or in the western part of the North-West Province or adjacent to the border separating the Free State from the North-West Province. It also appears as if the Multi-Model simulation system performs better in simulating the maize yields of the western parts of the study area than the eastern parts of the study area. The medium season maize planted on plant date 1 and plant date 3 scenarios (Figure 3.21 (d) and (f)) both show 4 magisterial districts (not significant at 95% level) with statistically significant correlations, while only 3 (not significant at 95% level) is evident for the medium season maize planted on plant date 2 scenario (Figure 3.21 (d)).

Similar to the medium season maize scenarios the long season maize scenarios (Figure 3.21 (g), (h) and (i)) also show the highest correlations either in the eastern part of the Free State or adjacent to the border separating the Free State from the North-West Province. In all three scenarios negative correlations are found for the eastern part of the North-West Province. Statistically significant correlations can be seen for 6 (not significant at 95% level) out of the 44 magisterial districts in the long season maize planted on plant date 1 scenario (Figure 3.21 (g)), 4 (not significant at 95% level) out of the 44 magisterial districts in the long season maize planted on plant date 2 scenario (Figure 3.21 (h)) and 3 (not significant at 95% level) out of the 44 magisterial districts for the long season maize planted in plant date 3 scenario (Figure 3.21 (i)). Thus, the skill of the Multi-Model simulation system in simulating the maize yields decreases from plant date 1 to plant date 3.

Thus, all 9 scenarios illustrate relatively poor skill. This can be explained by the fact that the Multi-Model simulation system is a combination between the CERES-CCAM simulation system and the CERES-ECHAM4.5 simulation system. Therefore, even though good skill is obtained for the maize yields produced by the CERES-CCAM simulation system, the low skill of the CERES-ECHAM4.5 simulation system negatively affects the skill of the Multi-

Model simulation system. In the construction of the Multi-Model simulation system used in this study, equal weights are given to both the CERES-GCM based simulation systems regardless of the skill of each individual simulation system. By giving the simulation systems weights proportional to their skill may perhaps improve the skill of the multi-model simulation system, but this should be investigated.

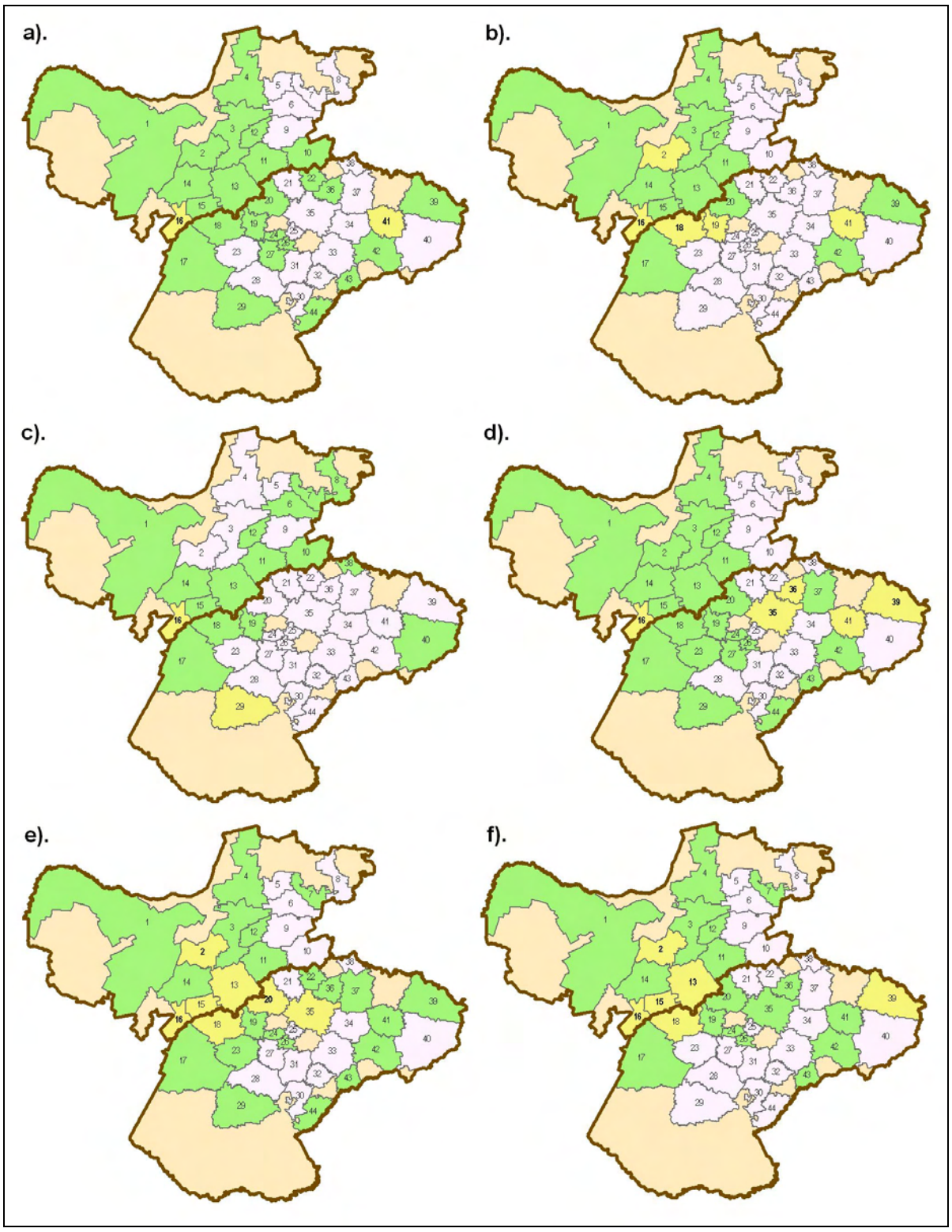

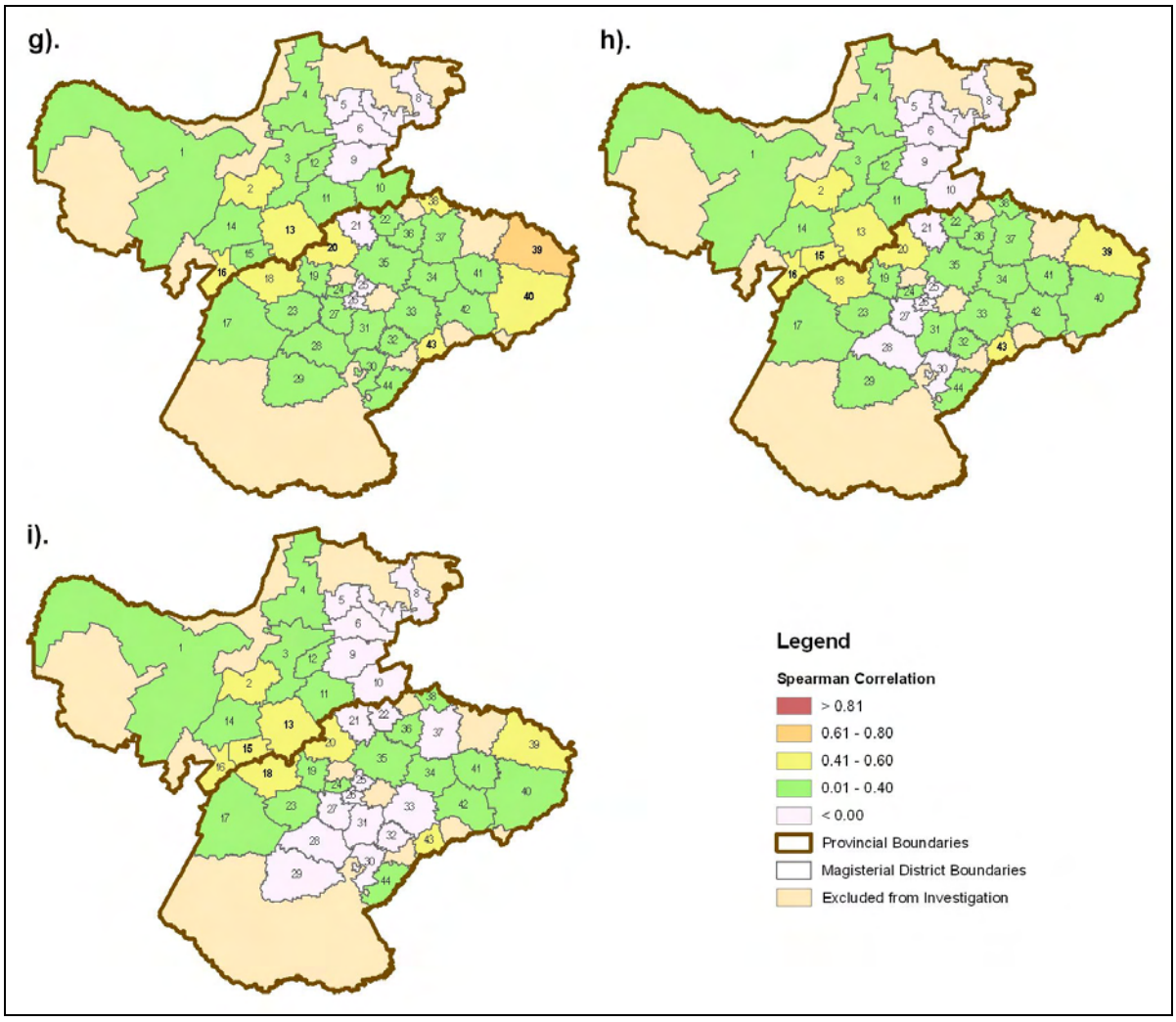

Figure 3.21: Spearman rank correlations calculated between the actual maize yields and Multi-Model ensemble mean maize yields over the 20 year period from 1980 to 1999. (a) Short season maize plant date 1, (b) Short season maize plant date 2, (c) Short season maize plant date 3, (d) Medium season maize plant date 1, (e) Medium season maize plant date 2, (f) Medium season maize plant date 3, (g) Long season maize plant date 1, (h) Long season maize plant date 2 and (i) Long season maize plant date 3. Magisterial districts with statistically significant correlations at the 95% confidence level are indicated in bold.

Once again the skill of the Multi-Model simulation system increases from the short season maize scenarios to the long season maize scenarios, with the highest correlations found for the long season maize planted on plant date 1 scenario. This result can be confirmed by the results found in the subjective validation.

3.4 PROBABILITY DISTRIBUTION RESULTS

3.4.1 Subjective Validation

3.4.1.1 Dry/Warm Western Region

3.4.1.1.1 Short Season Maize

In Figure 3.22 the simulated short season maize yields are expressed probabilistically. The actual maize yields and CERES-Observed weather maize yields are displayed deterministically at the top op the graph. When the CERES-Observed weather maize yields are compared to the actual maize yields it can be seen that the CERES-Maize model is able to correctly indicate the category of the yield (above-normal, near-normal or below-normal) for 8 out of the 19 seasons considered in this study, of which 4 seasons are ENSO-neutral seasons, 3 are El Niño seasons and 1 is a La Niña season. Another interesting feature that can be observed for the other 11 seasons is the fact that the CERES-Observed weather maize yields are always within one category of the actual maize yields and never two categories away from the actual maize yields, as can be seen, for example, for the 1981/82 season in which the actual maize yield is near-normal and the CERES-Observed weather maize yield is below-normal.

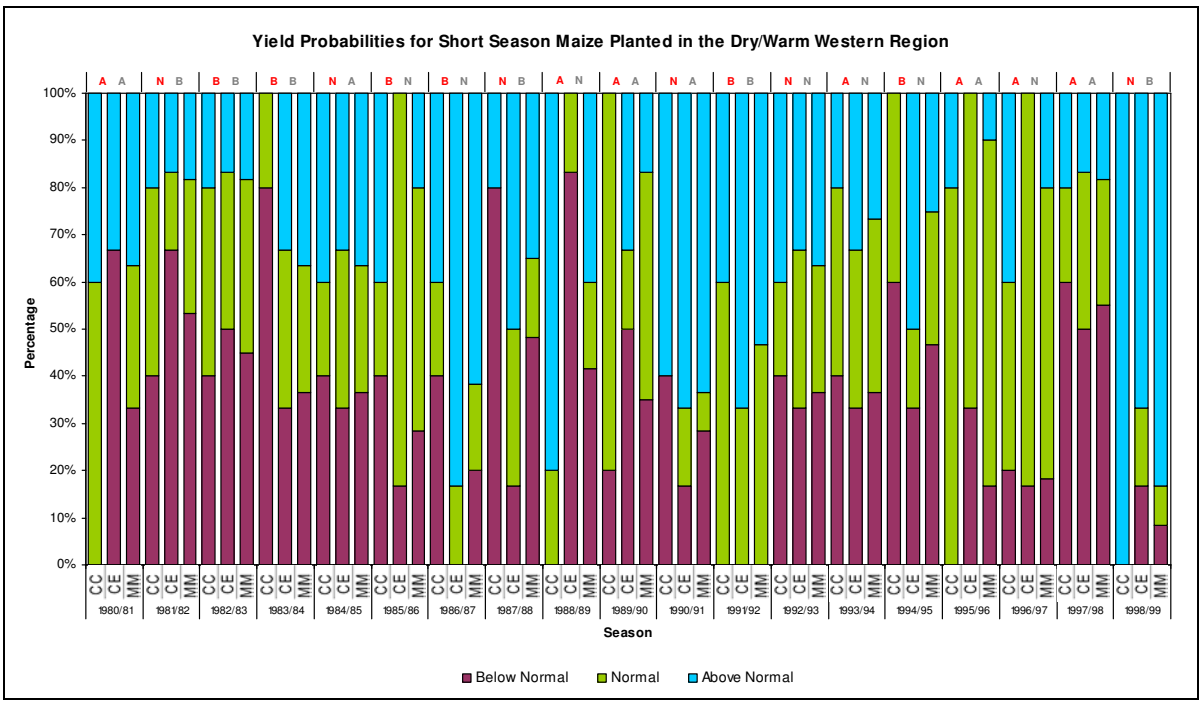

Figure 3.22: Simulated short season maize yield probabilities. CERES-CCAM yield (CC), CERES-ECHAM4.5 yield (CE) and Multi-Model yield (MM). The actual maize yield (red) and CERES-Observed weather yield (grey) are denoted as A (above-normal), N (near-normal) or B (below-normal) at the top of the graph.

When the probabilistic short season maize yields, obtained from the different simulation systems, are compared to the actual maize yields, the 1980/81 ENSO-neutral season stands out, as for this season the Multi-Model simulation system performs better than the single model simulation systems (CERES-CCAM and CERES-ECHAM4.5), although the level of confidence in the probability for above-normal maize yields is not very high (37%). The probability distributions for the 1982/83, 1983/84 and 1994/95 seasons show that one of the single model simulation systems (CERES-CCAM or CERES-ECHAM4.5) and the Multi-Model simulation system correctly indicates the category of the yield (above-normal, near-normal or below-normal), while the probabilities of the other single model system are less reliable. Another interesting season is the 1988/89 season for which the CERES-CCAM simulation system correctly simulates the maize yield to be above-normal with a high level of confidence (80%).

3.4.1.1.2 Medium Season Maize

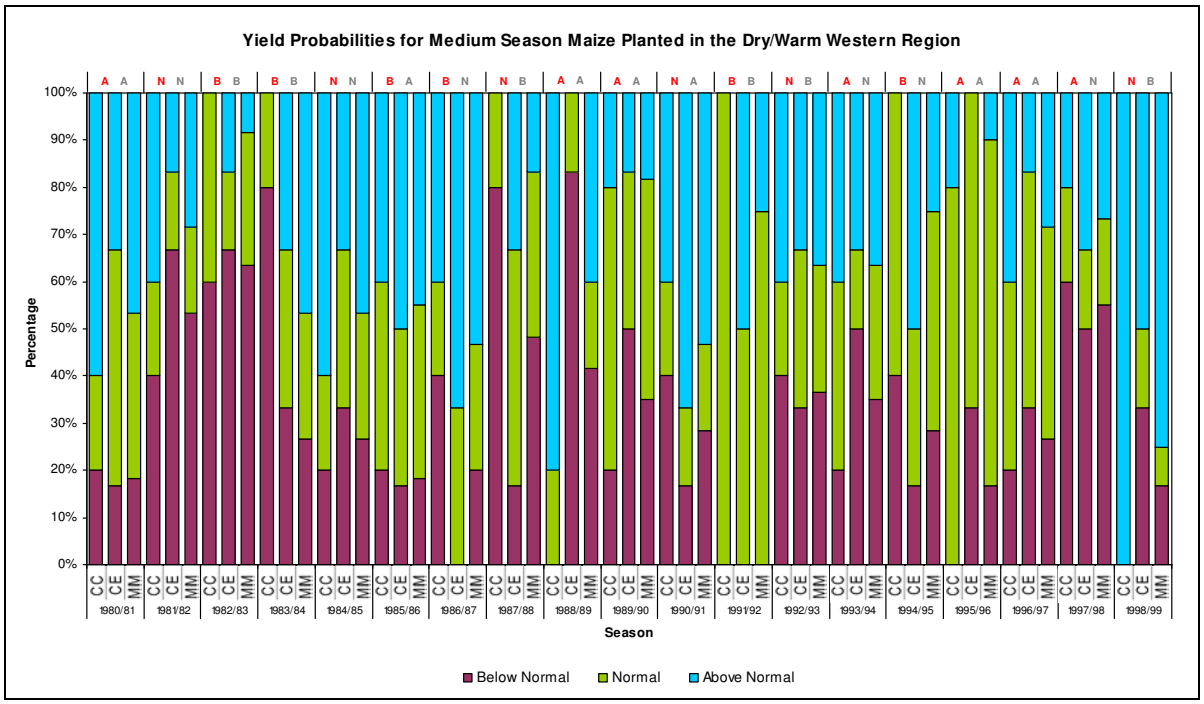

Figure 3.23: Simulated medium season maize yield probabilities. CERES-CCAM yield (CC), CERES-ECHAM4.5 yield (CE) and Multi-Model yield (MM). The actual maize yield (red) and CERES-Observed weather yield (grey) are denoted as A (above-normal), N (near-normal) or B (below-normal) at the top of the graph.

The probability distributions for medium season maize, as simulated by each of the different simulation systems, are shown in Figure 3.23. In comparison to the actual maize yields the

CERES-Observed weather maize yields reveal that the CERES-Maize model is able to correctly simulate the category of the yield (above-normal, near-normal or below-normal) for 10 out of the 19 seasons considered in this study. From the actual maize yields it can be seen than 7 out of the 19 seasons are above-normal maize yield seasons. The CERES-Maize model correctly indicates the category for 5 out of the 7 above-normal maize yield seasons. Thus, the CERES-Maize model appears to perform the best in simulating the maize yields of the above-normal maize yield seasons. Furthermore, the CERES-Maize model performs exceptionally well in capturing the category of the maize yields of the early 1980's (1980/81 – 1984/85). For one season, 1985/86, the CERES-Observed weather maize yield is two categories away from the category of the actual maize yield, which shows that the CERES-Maize model failed in this season.

When the probabilities of the simulated medium season maize yields are assessed, the 1982/83 El Niño season stands out, as for this season all three simulation systems (CERES-CCAM, CERES-ECHAM4.5 and Multi-Model) successfully simulates the category of the maize yield with relatively high probabilities of 60% and higher. For the 1993/94 season, the Multi-Model simulation system performs better than the single model simulation systems (CERES-CCAM and CERES-ECHAM4.5), but once again the level of confidence in the above-normal category is relatively low (37%). The probability distributions for the 1980/81 and 1983/84 seasons show that both the CERES-CCAM and Multi-Model simulation systems are reliable, while the CERES-ECHAM4.5 simulation system is unable to represent the correct outcome (above-normal, near-normal or below-normal maize yields). The CERES-CCAM simulation system once again simulates the category of the maize yield of the 1988/89 season correctly, with a high probability of 80%. The 1991/92 season was one of the driest seasons on record. The CERES-CCAM, CERES-ECHAM4.5 and Multi-Model simulation systems simulates a 0% probability for below-normal maize yield for this season, while the CERES-Observed weather simulation system correctly indicated the below-normal category. This is a result of the fact that GCMs did not anticipate the excessively dry conditions of the 1991/92 season. From this it can be seen that the CERES-Maize model is highly dependant on the weather input data with which it is forced.

3.4.1.1.3 Long Season Maize

Figure 3.24 shows the simulated long season maize probabilities. From the actual maize yields and CERES-Observed weather maize yields displayed deterministically at the top op the graph, it can be seen that the CERES-Maize model is able to correctly indicate the

category of the yield (above-normal, near-normal or below-normal) for 13 out of the 19 seasons investigated in this study. Here, the category of 6 out of the 7 above-normal maize yield season are simulated correctly by the CERES-Maize model which once again points to the fact that the CERES-Maize performs better in capturing above-normal maize yield seasons than near-normal and below-normal maize yields seasons. Moreover, for the other seasons the CERES-Observed weather maize yields are always within one category of the actual maize yields and never two categories away from the actual maize yields.

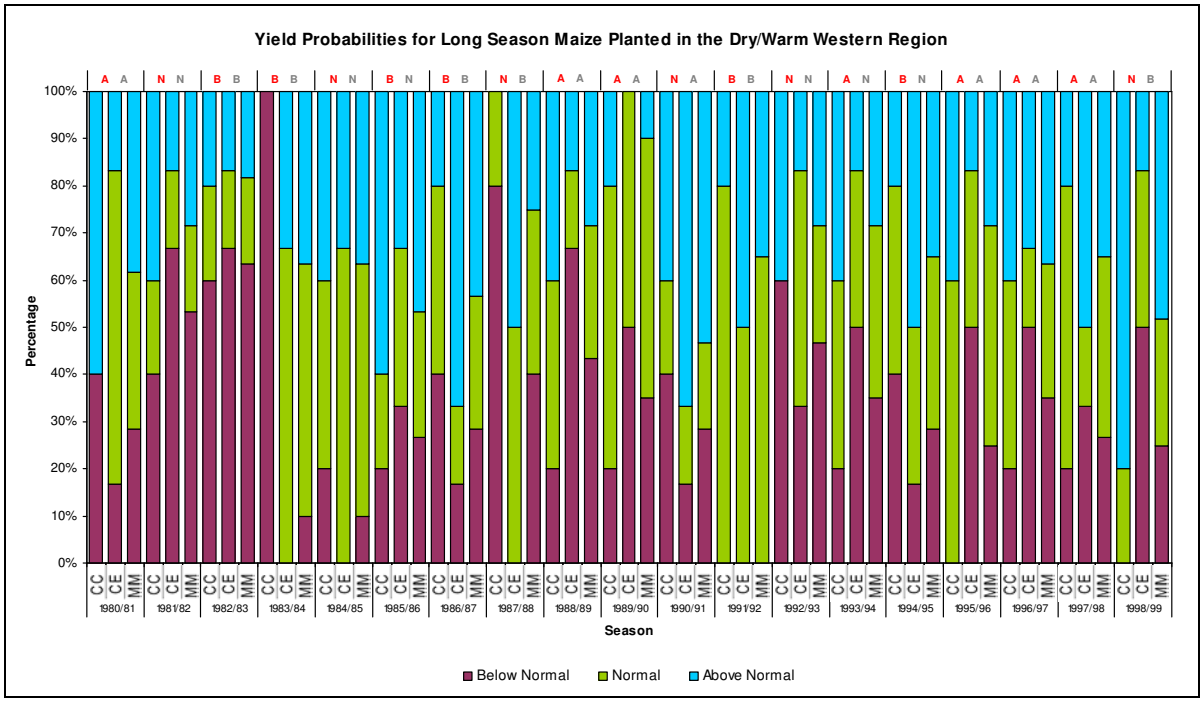

Figure 3.24: Simulated long season maize yield probabilities. CERES-CCAM yield (CC), CERES-ECHAM4.5 yield (CE) and Multi-Model yield (MM). The actual maize yield (red) and CERES-Observed weather yield (grey) are denoted as A (above-normal), N (near-normal) or B (below-normal) at the top of the graph.

When the long season maize yield probabilities, obtained from the different simulation systems, are examined, it can be seen that the maize yield of the 1982/83 El Niño season is once again successfully simulated by all three simulation systems (CERES-CCAM, CERES-ECHAM4.5 and Multi-Model) with relatively high probabilities of 60% and higher. For the 1996/97 season, the Multi-Model simulation system performs better than the single model simulation systems (CERES-CCAM and CERES-ECHAM4.5), but the level of confidence in the above-normal category is relatively low (37%). The probability distributions for the 1980/81, 1983/84 and 1984/85 seasons show that one of the single model simulation systems (CERES-CCAM or CERES-ECHAM4.5) and the Multi-Model simulation system correctly indicates the category of the yield (above-normal, near-normal or below-normal),

while the probabilities of the other single model system is less reliable. The 1992/93 and 1996/97 seasons are very interesting as for these two seasons the CERES-ECHAM4.5 simulation system is the only system able to correctly simulate the category of the maize yields.

In general, it can be seen that the ability of the CERES-Observed weather simulation system in simulating the category of the maize yield increases from the short season maize scenario to the long season maize scenario, with the best performance in capturing above-normal maize yield seasons. The CERES-CCAM simulation system performs relatively well in all three scenarios, while the CERES-ECHAM4.5 simulation system does not perform well. The Multi-Model simulation system performs the best in simulating below-normal maize yields.

3.4.1.2 Temperate Eastern Region

3.4.1.2.1 Short Season Maize

The probability distributions of the simulated short season maize yields are shown in Figure 3.25. The actual maize yields and CERES-Observed weather maize yields are displayed deterministically at the top op the graph. When the CERES-Observed weather maize yields are compared to the actual maize yields it can be seen that the CERES-Maize model is able to correctly indicate the category of the yield (above-normal, near-normal or below-normal) for 9 out of the 19 seasons investigated in this study, of which 4 seasons are ENSO-neutral seasons, 3 are El Niño seasons and 2 are La Niña seasons. From the actual maize yields it can be seen that 6 out of the 19 seasons are below-normal maize yield seasons, and the CERES-Maize model is able to correctly simulate the category for 4 out of the 6 below-normal seasons. Thus, the CERES-Maize model performs better in simulating the maize yields of below-normal maize yield seasons than above-normal and near-normal maize yield seasons. Another notable feature is the fact that for four seasons the CERES-Observed weather maize yields are two categories away from the actual maize yields, as seen for example for the 1985/86 (1988/89) season in which the actual maize yield is below-normal (above-normal) and the CERES-Observed weather maize yield is above-normal (below-normal).

In comparison to the actual maize yields, the simulated short season maize yield probabilities show that for the 1985/86, 1987/88 and 1989/90 seasons all three simulation systems (CERES-CCAM, CERES-ECHAM4.5 and Multi-Model) successfully simulate the

maize yields with reasonably high probabilities ranging between 50% and 83%. The probability distributions for the 1983/84 and 1991/92 seasons show that one of the single model simulation systems (CERES-CCAM or CERES-ECHAM4.5) and the Multi-Model simulation system correctly indicates the category of the yield (above-normal, near-normal or below-normal), while the probabilities of the other single model system is either over or under confident and consequently gives a different category the highest probability. Other interesting seasons include the 1986/87, 1995/96 and 1998/99 seasons for which the CERES-CCAM simulation system correctly simulates the category of the maize yields with probabilities of 60% and higher, and the 1981/82 season for which the CERES-ECHAM4.5 simulation system correctly indicates the category of the maize yield with a probability of 67%.

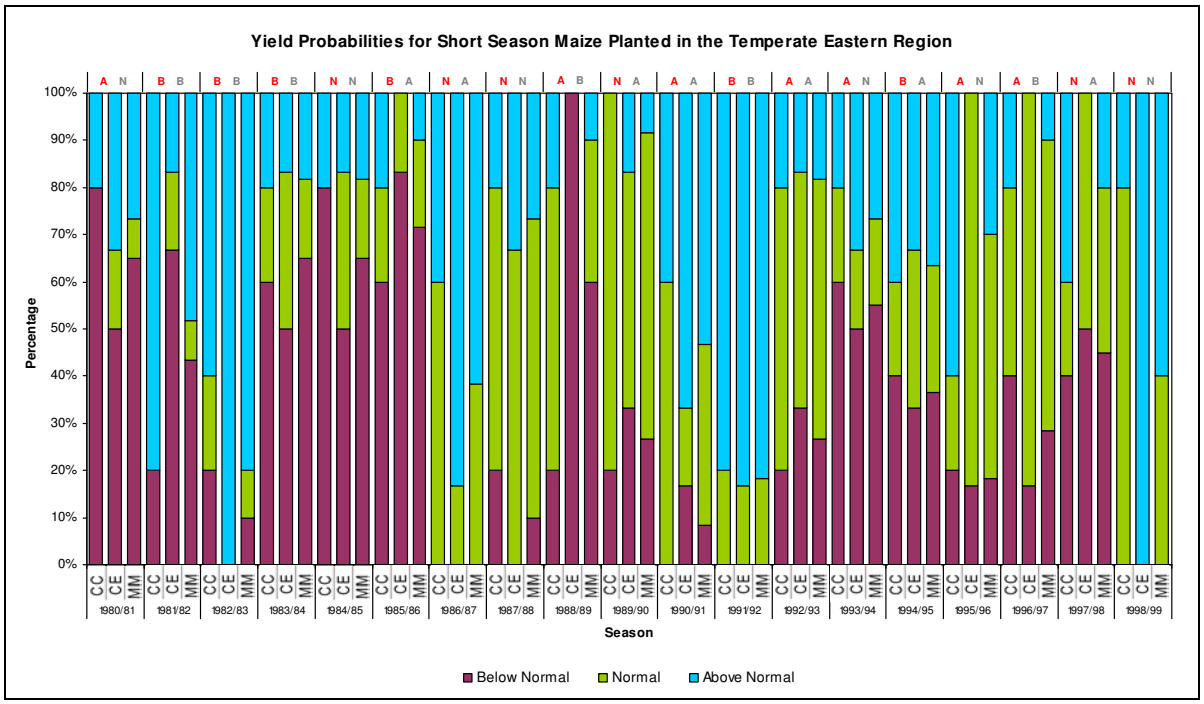

Figure 3.25: Simulated short season maize yield probabilities. CERES-CCAM yield (CC), CERES-ECHAM4.5 yield (CE) and Multi-Model yield (MM). The actual maize yield (red) and CERES-Observed weather yield (grey) are denoted as A (above-normal), N (near-normal) or B (below-normal) at the top of the graph.

3.4.1.2.2 Medium Season Maize

The simulated medium season maize yield probabilities are shown in Figure 3.26. In comparison to the actual maize yields the CERES-Observed weather maize yields reveal that the CERES-Maize model is able to correctly simulate the category of the yield (above-normal, near-normal or below-normal) for 13 out of the 19 seasons considered in this study.

The CERES-Maize model once again appears to perform the best in capturing the maize yields of the below-normal maize yield seasons, with the category for 5 out of the 6 seasons indicated correctly. Furthermore, it can also be seen that the maize yields of the 1980's (1980/81 – 1983/84) and late 1990's (1994/95 – 1998/99) are simulated exceptionally well by the CERES-Maize model.

From the probability distributions of the simulated medium season maize yields it can be seen that for the 1981/82, 1985/86, 1989/90, 1990/91 and 1993/94 seasons one of the single model simulation systems (CERES-CCAM or CERES-ECHAM4.5) and the Multi-Model simulation system correctly indicates the category of the yield (above-normal, near-normal or below-normal), while the other single model simulation system is unable to represent the correct category. For the 1983/84 and 1995/96 seasons the CERES-CCAM simulation system successfully simulates the maize yields with probabilities of 60% and for the 1980/81 season the CERES-ECHAM4.5 simulation system correctly indicates the maize yield with a somewhat lower probability of 50%.

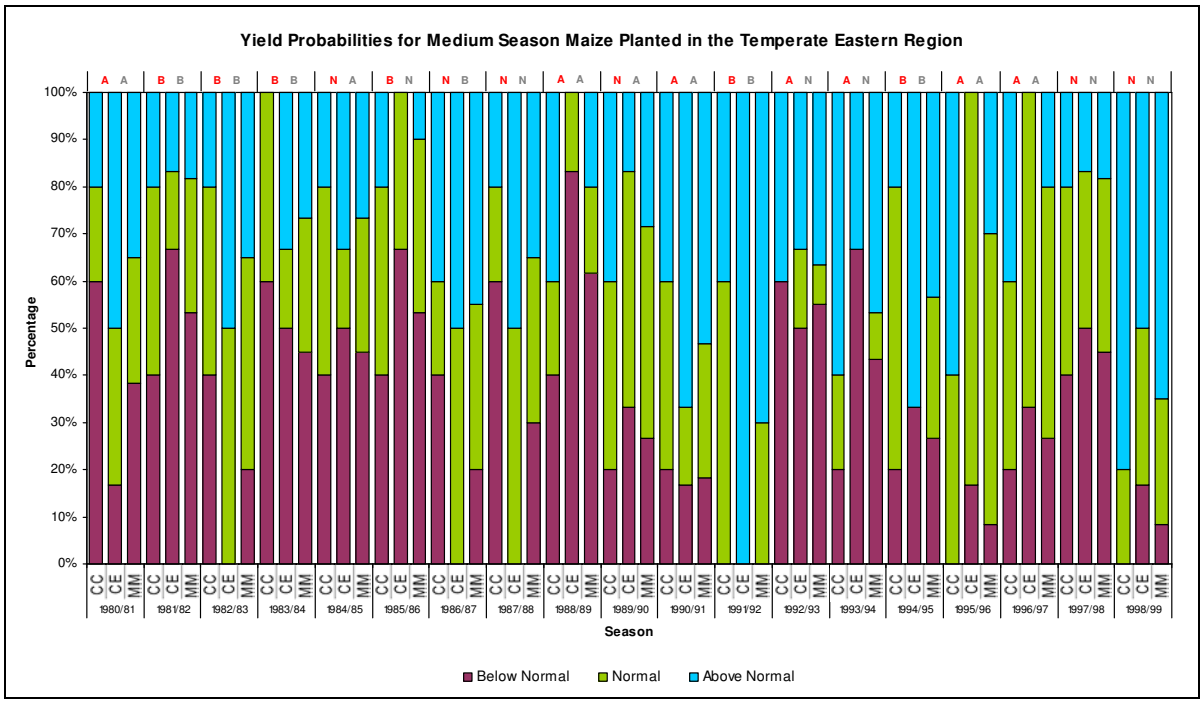

Figure 3.26: Simulated medium season maize yield probabilities. CERES-CCAM yield (CC), CERES-ECHAM4.5 yield (CE) and Multi-Model yield (MM). The actual maize yield (red) and CERES-Observed weather yield (grey) are denoted as A (above-normal), N (near-normal) or B (below-normal) at the top of the graph.

3.4.1.2.3 Long Season Maize

In Figure 3.27 the simulated long season maize yields are expressed probabilistically. The actual maize yields and CERES-Observed weather maize yields are displayed deterministically at the top op the graph and shows that the CERES-Maize model is able to correctly indicate the category of the yield (above-normal, near-normal or below-normal) for 11 out of the 19 seasons considered in this study. Here the CERES-Maize model also appears to perform the best in simulating the maize yields of below-normal maize yield seasons, with the category of 5 out of the 6 below-normal seasons indicated correctly. For the remainder of the seasons, it can be seen that the CERES-Observed weather maize yields are always within one category of the actual maize yields, as seen for the 1984/85 season in which the actual maize yield is near-normal and the CERES-Observed weather maize yield is above-normal.

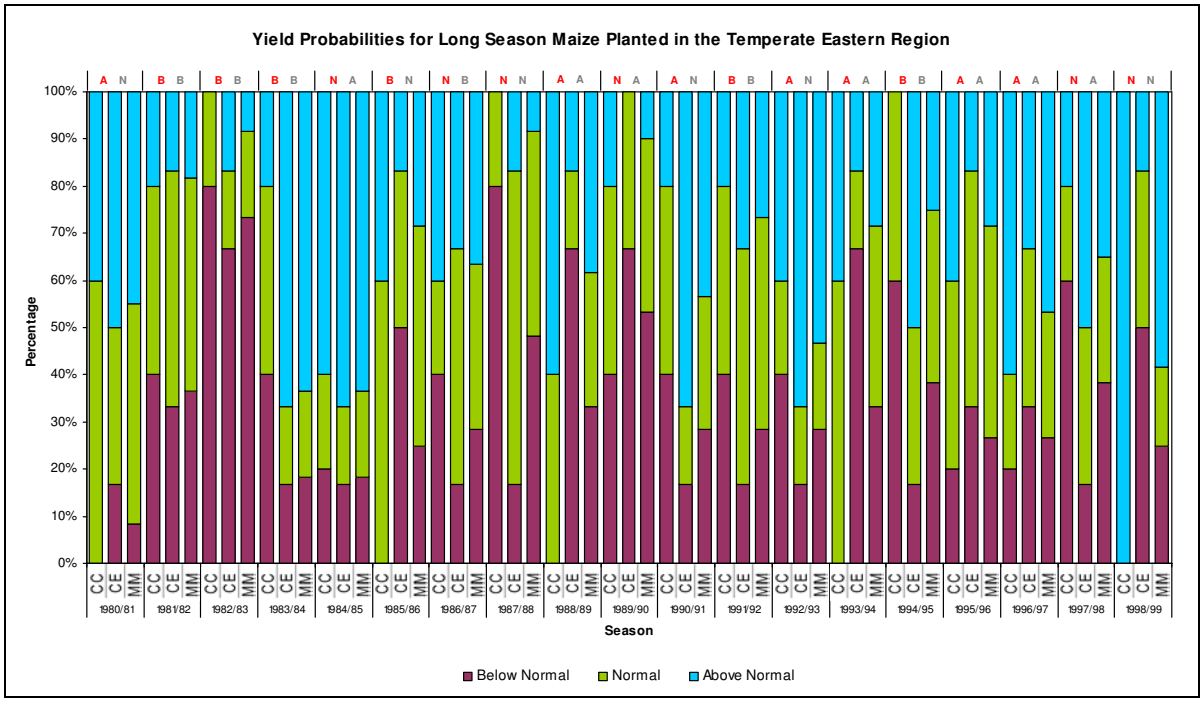

Figure 3.27: Simulated long season maize yield probabilities. CERES-CCAM yield (CC), CERES-ECHAM4.5 yield (CE) and Multi-Model yield (MM). The actual maize yield (red) and CERES-Observed weather yield (grey) are denoted as A (above-normal), N (near-normal) or B (below-normal) at the top of the graph.

When the probabilities of the simulated long season maize yields are compared to the actual maize yields, the 1982/83 El Niño season stands out, as for this season all three simulation systems (CERES-CCAM, CERES-ECHAM4.5 and Multi-Model) successfully simulate the maize yield to be below-normal with reasonably high probabilities ranging

between 67% and 80%. The probability distributions of the 1988/89, 1990/91, 1992/93, 1994/95 and 1996/97 seasons show that one of the single model simulation systems (CERES-CCAM or CERES-ECHAM4.5) and the Multi-Model simulation system are able to correctly indicate the category of the yield (above-normal, near-normal or below-normal). Furthermore, the 1980/81, 1985/86, 1986/87 and 1987/88 seasons are also interesting as for these seasons the CERES-ECHAM4.5 simulation system is the only system that successfully simulates the outcome of the maize yields.

In general, it can be seen that the performance of the CERES-Observed weather simulation system in simulating the category of the maize yield is the best for the medium season maize scenario. This simulation system performs very well in simulating below-normal maize yields. The CERES-CCAM simulation system performs better in simulating above-normal maize yields that below-normal and near-normal maize yields, while the CERES-ECHAM4.5 simulation system shows the best performance for near-normal maize yield seasons.

3.4.1.3 Wet/Cool Eastern Region

3.4.1.3.1 Short Season Maize

The probability distributions of the simulated short season maize yields are shown in Figure 3.28. The actual maize yields and CERES-Observed weather maize yields displayed at the top of the graph show that the CERES-Maize model correctly indicates the category of the yield (above-normal, near-normal or below-normal) for 8 out of the 19 seasons, of which 4 seasons are ENSO-neutral seasons, 2 are El Niño seasons and 2 are La Niña seasons. As for the remainder of the seasons, the CERES-Observed weather maize yields are mostly within one category of the actual maize yields, although for three seasons (1986/87, 1988/89 and 1996/97) the CERES-Observed weather maize yields are two categories away from the actual maize yields, but this is in the minority of cases.

When the probabilistic short season maize yields, obtained from the different simulation systems, are compared to the actual maize yields, it can be seen that all three simulation systems (CERES-CCAM, CERES-ECHAM4.5 and Multi-Model) are able to successfully simulate the above-normal maize yield of the 1998/99 La Niña season, with probabilities ranging between 50% and 100%. The 1993/94 season is also a prominent season, since the Multi-Model simulation system correctly indicates the above-normal maize yield of this season, while the single model systems (CERES-CCAM and CERES-ECHAM4.5) do not.

The probabilities of the CERES-CCAM and Multi-Model simulation systems both correctly indicates the category of the maize yields (above-normal, near-normal or below-normal) of the 1982/83, 1983/84, 1989/90, 1992/93, 1996/97 and 1997/98 seasons, while the probabilities of the CERES-ECHAM4.5 simulation system is less reliable. Four of these seasons are ENSO-neutral seasons and the other two are El Niño seasons. Moreover, the CERES-CCAM simulation system is the only system able to correctly simulate the below-normal maize yield of 1981/82 season and the above-normal maize yield of the 1988/89 season with probabilities of 50% and higher.

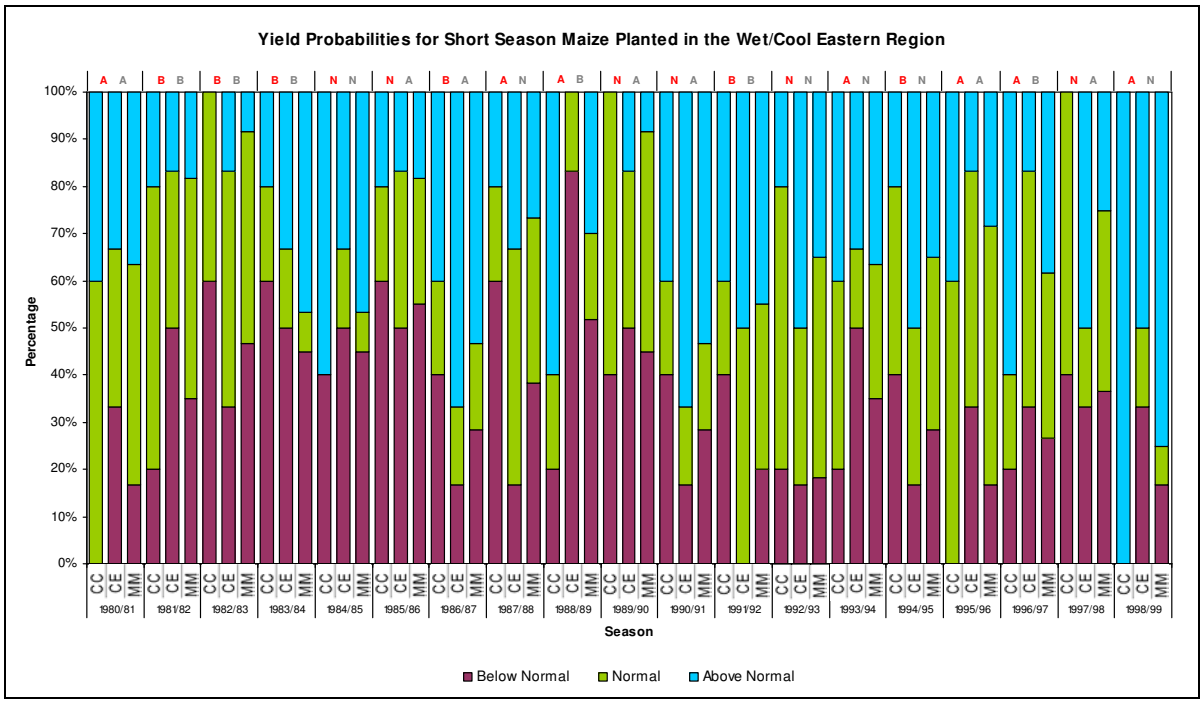

Figure 3.28: Simulated short season maize yield probabilities. CERES-CCAM yield (CC), CERES-ECHAM45 yield (CE) and Multi-Model yield (MM). The actual maize yield (red) and CERES-Observed weather yield (grey) are denoted as A (above-normal), N (near-normal) or B (below-normal) at the top of the graph.

3.4.1.3.2 Medium Season Maize

The simulated medium season maize yield probabilities are shown in Figure 3.29. In comparison to the actual maize yields the CERES-Observed weather maize yields reveal that the CERES-Maize model is able to correctly simulate the category of the yield (above-normal, near-normal or below-normal) for 9 out of the 19 seasons considered in this study. Furthermore it appears as if the CERES-Maize model performs the best in capturing the maize yields of the below-normal maize yield seasons, with the category of 5 out of the 6

seasons indicated correctly. The 1986/87 and 1988/89 seasons are the only two seasons in which the CERES-Observed weather maize yields are two categories away from that of the actual maize yields.

In comparison to the actual maize yields, the simulated medium season maize yield probabilities show that for the 1982/83 and 1996/97 seasons all three simulation systems (CERES-CCAM, CERES-ECHAM4.5 and Multi-Model) successfully simulates the maize yields with relatively high probabilities ranging between 50% and 80%. The probability distributions of the 1986/87, 1988/89, 1990/91 and 1998/99 seasons show that one of the single model simulation systems (CERES-CCAM or CERES-ECHAM4.5) as well as the Multi-Model simulation system correctly indicates the category of the maize yields (above-normal, near-normal or below-normal), while the other single model system is either over or under confident and therefore simulates a different category to have the highest probability. For the 1991/92 season the Multi-Model simulation system shows an improvement from the two single model systems (CERES-CCAM and CERES-ECHAM4.5), while for the 1994/95 season the CERES-CCAM simulation system is the only system able to correctly indicate the below-normal maize yield.

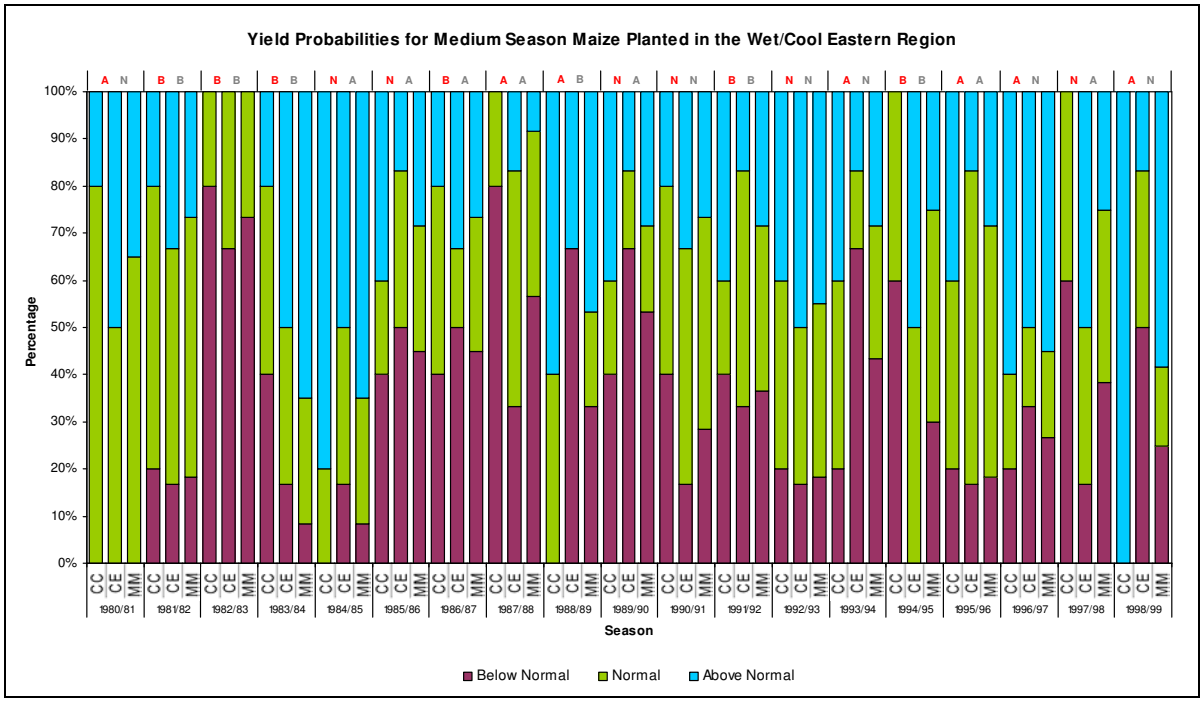

Figure 3.29: Simulated medium season maize yield probabilities. CERES-CCAM yield (CC), CERES-ECHAM4.5 yield (CE) and Multi-Model yield (MM). The actual maize yield (red) and CERES-Observed weather yield (grey) are denoted as A (above-normal), N (near-normal) or B (below-normal) at the top of the graph.

3.4.1.3.3 Long Season Maize

Figure 3.30 shows the simulated long season maize probabilities. The actual maize yields and CERES-Observed weather maize yields are displayed deterministically at the top op the graph. When the CERES-Observed weather maize yields are compared to the actual maize yields it can be seen that the CERES-Maize model is able to correctly indicate the category of the yield (above-normal, near-normal or below-normal) for 11 out of the 19 seasons investigated in this study. From the actual maize yields it can be seen that 6 out of the 19 seasons are below-normal maize yield seasons, and the CERES-Maize model is able to correctly indicate the category of 5 out of the 6 below-normal seasons. Thus, the CERES-Maize model performs better in simulating the maize yields of below-normal maize yield seasons than above-normal and near-normal maize yield seasons. Furthermore, the CERES-Maize model performs well in capturing the category of the maize yields of the early 1980's (1980/81 – 1984/85).

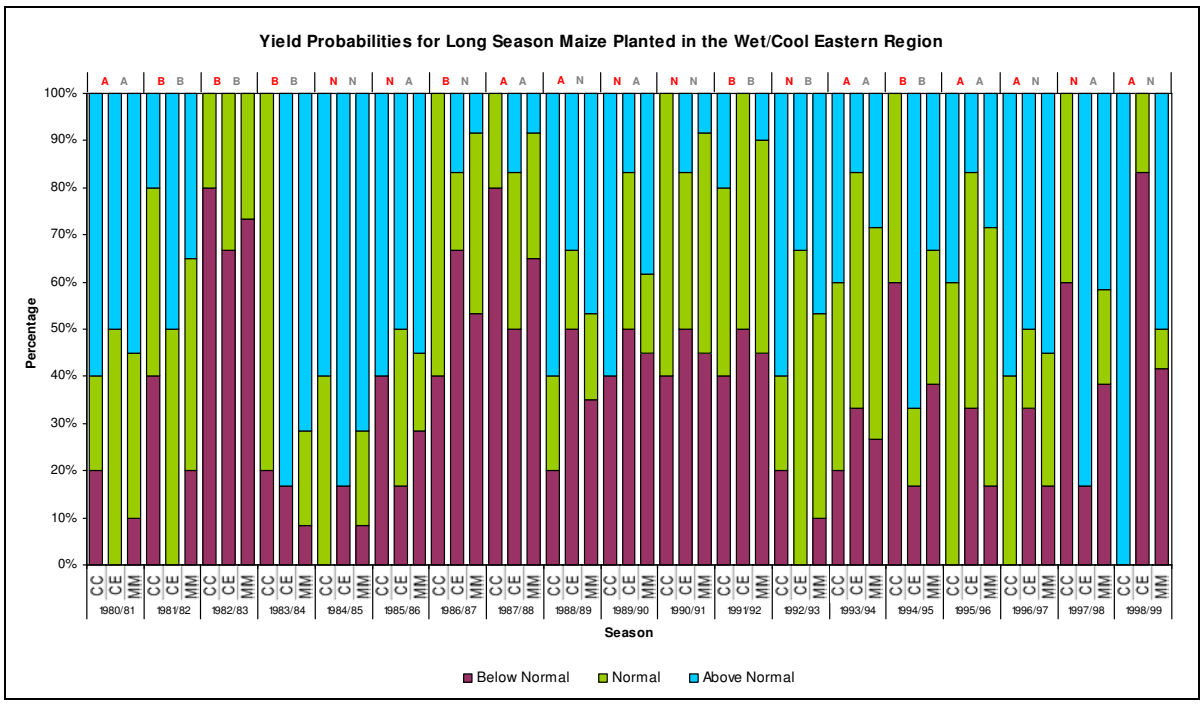

Figure 3.30: Simulated long season maize yield probabilities. CERES-CCAM yield (CC), CERES-ECHAM4.5 yield (CE) and Multi-Model yield (MM). The actual maize yield (red) and CERES-Observed weather yield (grey) are denoted as A (above-normal), N (near-normal) or B (below-normal) at the top of the graph.

From the probability distributions of the simulated long season maize yields it can be seen that for the 1982/83 El Niño season and 1996/97 ENSO-neutral season all three simulation systems (CERES-CCAM, CERES-ECHAM4.5 and Multi-Model) successfully simulate the

below-normal (1982/83) and above-normal (1996/97) maize yields for these two seasons. The probability distributions for the 1980/81, 1988/89, 1990/91, 1994/95 and 1998/99 seasons show that the CERES-CCAM simulation system and Multi-Model simulation system correctly indicates the category of the maize yields (above-normal, near-normal or below-normal), while the CERES-ECHAM4.5 simulation system fails to get the category correct. The 1992/93 season is also interesting as for this season the CERES-CCAM simulation system is the only system able to correctly simulate the category of the maize yield with a high probability of 67%. Furthermore, for many season all three simulation systems simulates the same incorrect category to have the highest probability, as can be seen, for example, for the 1984/85 season in which all three simulation systems gives the highest probability to the near-normal category.

In general, it can be seen that the performance of the CERES-Observed weather simulation system in simulating the category of the maize yield increases from the short season maize scenario to the long season maize scenario, with the best performance evident for below-normal maize yields. The CERES-CCAM and Multi-Model simulation systems seem to perform the best for above-normal maize yield seasons, while the CERES-ECHAM4.5 simulation system does not perform well.

3.4.2 Objective Validation

3.4.2.1 Dry/Warm Western Region

3.4.2.1.1 Short Season Maize

Figure 3.31 shows the short season maize ROC curves for each of the maize yield simulation systems. The CERES-CCAM simulation system (a) shows the best skill in simulating below-normal maize yields for the dry/warm western production region. The ROC curves of the CERES-ECHAM4.5 simulation system (b) falls beneath the no-skill diagonal, which indicates that this simulation system does not have skill in simulating any of the probability categories. Similar to the CERES-CCAM simulation system the Multi-Model simulation system (c) also reveals the highest skill in simulating below-normal maize yields with considerably less skill for the other two categories (near-normal and above-normal). Table 3.1, which shows the ROC scores, confirms these results. All the ROC scores are either equal to or less that 0.5 except for the below-normal category of the CERES-CCAM and Multi-Model simulation systems which are 0.65 and 0.62 respectively.

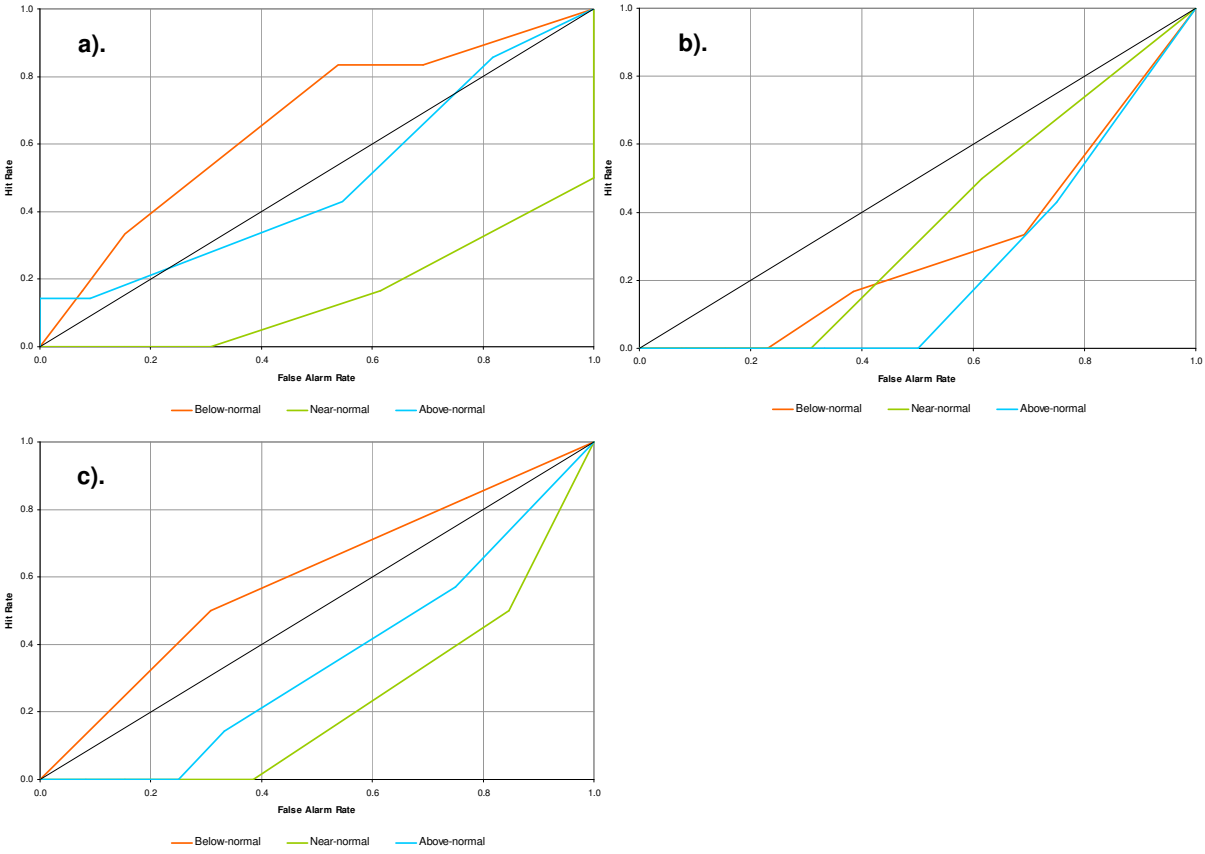

Figure 3.31: ROC curves for above-normal, near-normal and below-normal simulated short season maize yields. (a) CERES-CCAM maize yield simulation system, (b) CERES-ECHAM4.5 maize yield simulation system and (c) Multi-Model maize yield simulation system.

Simulation system	Below-normal	Near-normal	Above-normal
CERES-CCAM	0.65	0.08	0.51
CERES-ECHAM4.5	0.31	0.41	0.26
Multi-Model	0.62	0.20	0.35

Table 3.1: ROC scores for the simulated short season maize yield probabilities.

3.4.2.1.2 Medium Season Maize

The ROC curves for medium season maize can be seen in Figure 3.32. The maize yield simulations performed by the CERES-CCAM simulation system (a) show somewhat higher skill for the above-normal category than for the below-normal category and substantially less skill for the near-normal category. This is not a surprising result, as the skill of GCMs in capturing the main summer seasonal rainfall variability over southern Africa tends to be higher in ENSO years (Landman and Mason, 1999b). Thus, GCMs are more skilful in El Niño and La Niña years than in ENSO-neutral years. El Niño years greatly enhances the

probabilities for below-normal maize yields and La Niña years greatly enhances the probabilities for above-normal maize yields. The ROC curves of the CERES-ECHAM4.5 simulation system (b) are once again beneath the no-skill diagonal with ROC scores ranging between 0.17 and 0.43 (see Table 3.2). The Multi-Model simulation system shows poor skill in simulating any of the probability categories.

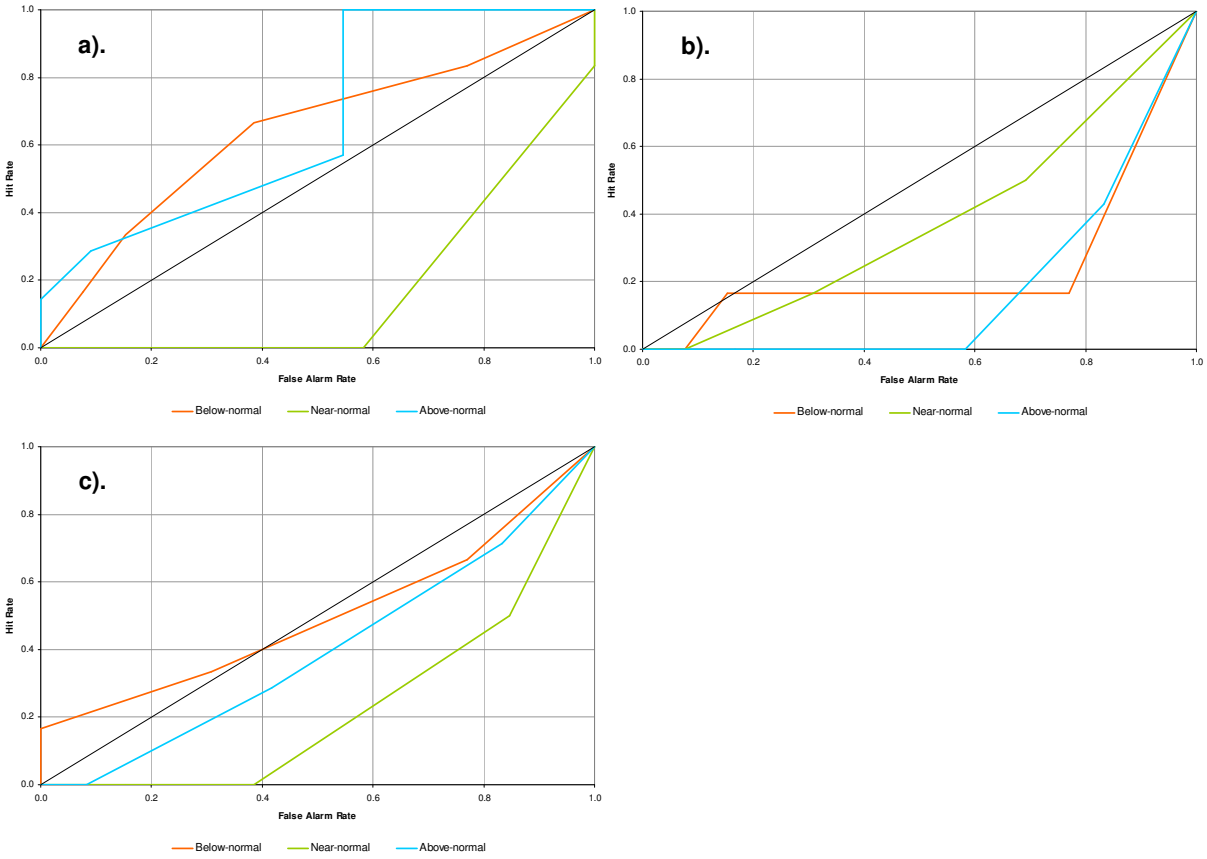

Figure 3.32: ROC curves for above-normal, near-normal and below-normal simulated medium season maize yields. (a) CERES-CCAM maize yield simulation system, (b) CERES-ECHAM4.5 maize yield simulation system and (c) Multi-Model maize yield simulation system.

Simulation system	Below-normal	Near-normal	Above-normal
CERES-CCAM	0.63	0.18	0.74
CERES-ECHAM4.5	0.33	0.38	0.18
Multi-Model	0.47	0.20	0.39

Table 3.2: ROC scores for the simulated medium season maize yield probabilities.

4.6.2.1.3 Long Season Maize

In Figure 3.33 the long season maize ROC curves are shown for each of the maize yield simulation systems. From the ROC curves for the CERES-CCAM simulation system (a) it can be observed that the highest skill occurs for above-normal maize yields, with slightly

lower skill for below-normal maize yields and much reduced skill for near-normal maize yields. The CERES-ECHAM4.5 simulation system (b) shows relatively high skill for the near-normal category, but with the curves of the below-normal and above-normal categories falling beneath the no-skill diagonal. The Multi-Model simulation system (c) on the other hand shows low skill for all three probability categories. Table 3.3 shows the ROC scores for each of the simulation systems and for each of the equiprobable categories. The highest ROC scores are evident for the above-normal category of the CERES-CCAM simulation system (0.62) and the near-normal category of the CERES-ECHAM4.5 simulation system (0.62).

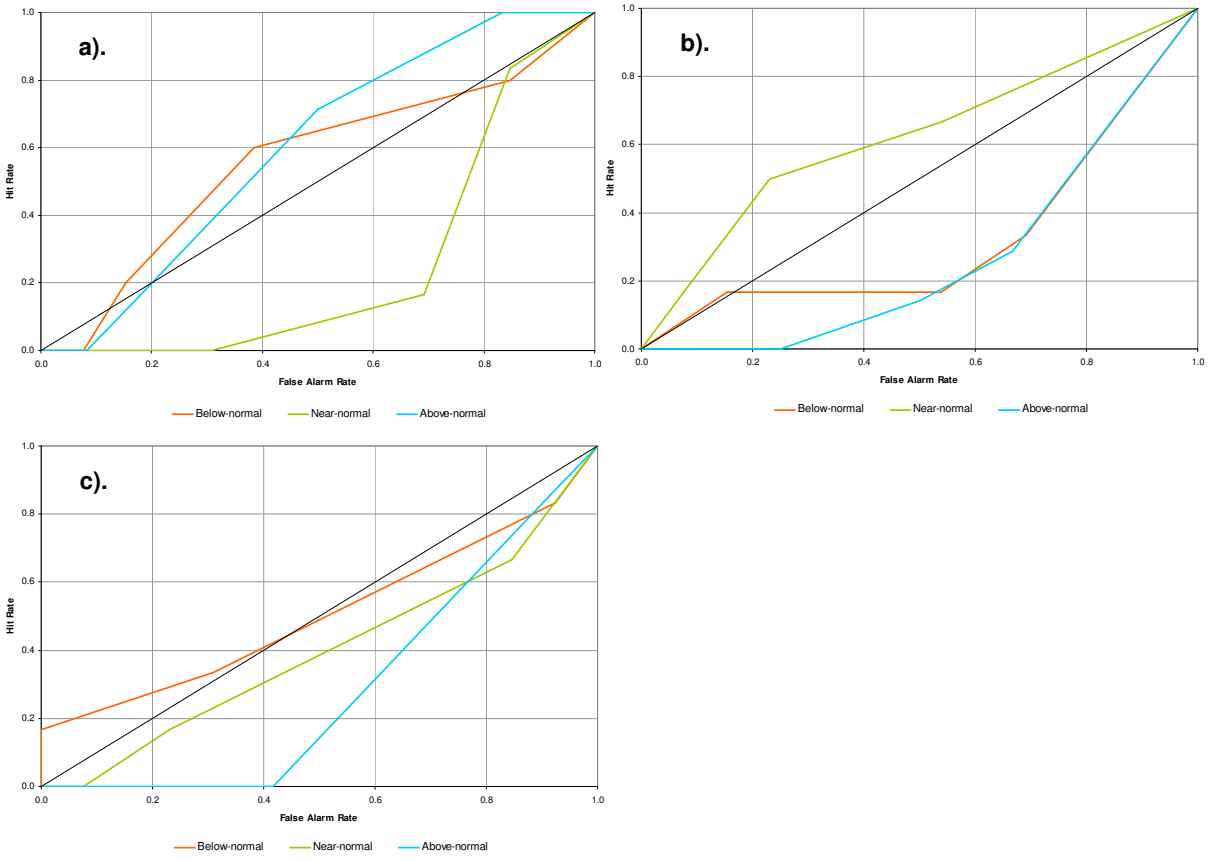

Figure 3.33: ROC curves for above-normal, near-normal and below-normal simulated long season maize yields. (a) CERES-CCAM maize yield simulation system, (b) CERES-ECHAM4.5 maize yield simulation system and (c) Multi-Model maize yield simulation system.

Simulation system	Below-normal	Near-normal	Above-normal
CERES-CCAM	0.56	0.24	0.62
CERES-ECHAM4.5	0.35	0.62	0.26
Multi-Model	0.47	0.40	0.36

Table 3.3: ROC scores for the simulated long season maize yield probabilities.

In general, the ROC scores seem to increase from the short season maize scenario to the long season maize scenario. Although, the highest ROC score (0.74) is evident for the medium season maize scenario (Table 3.2).

3.4.2.2 Temperate Eastern Region

3.4.2.2.1 Short Season Maize

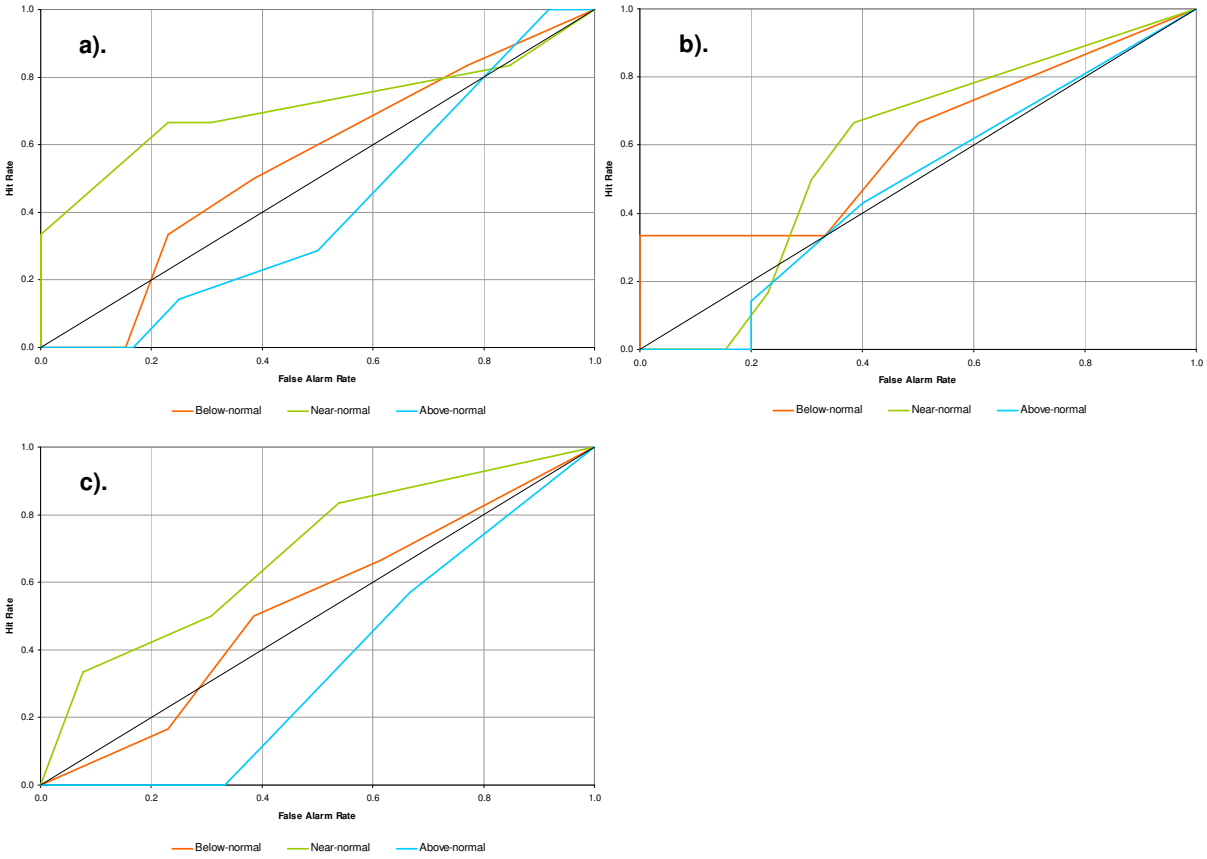

Figure 3.34: ROC curves for above-normal, near-normal and below-normal simulated short season maize yields. (a) CERES-CCAM maize yield simulation system, (b) CERES-ECHAM4.5 maize yield simulation system and (c) Multi-Model maize yield simulation system.

Simulation system	Below-normal	Near-normal	Above-normal
CERES-CCAM	0.58	0.72	0.45
CERES-ECHAM4.5	0.55	0.58	0.47
Multi-Model	0.51	0.70	0.35

Table 3.4: ROC scores for the simulated short season maize yield probabilities.

The ROC curves for short season maize can be seen in Figure 3.34. The CERES-CCAM simulation system (a) shows that for the near-normal category the hit rate largely outscores

the false alarm rate. Thus, the below-normal and above-normal categories are somewhat less skilful than the near-normal category. The ROC curves of the CERES-ECHAM4.5 simulation system (b) shows that the near-normal curve deviates furthest away from the no-skill diagonal, which implies that this simulation approach has highest skill in simulating near-normal maize yield seasons. The Multi-Model simulation system (c) also indicates highest skill for the near-normal category; with a ROC score of 0.70 (see Table 3.4).

3.4.2.2.2 Medium Season Maize

Figure 3.35 shows the medium season maize ROC curves for each of the maize yield simulation systems. The CERES-CCAM simulation system (a) shows the best skill in simulating above-normal maize yields for the temperate eastern production region. The ROC curves of the CERES-ECHAM4.5 simulation system (b) shows best skill for the near-normal category, with much lower skill for the above-normal and below-normal categories.

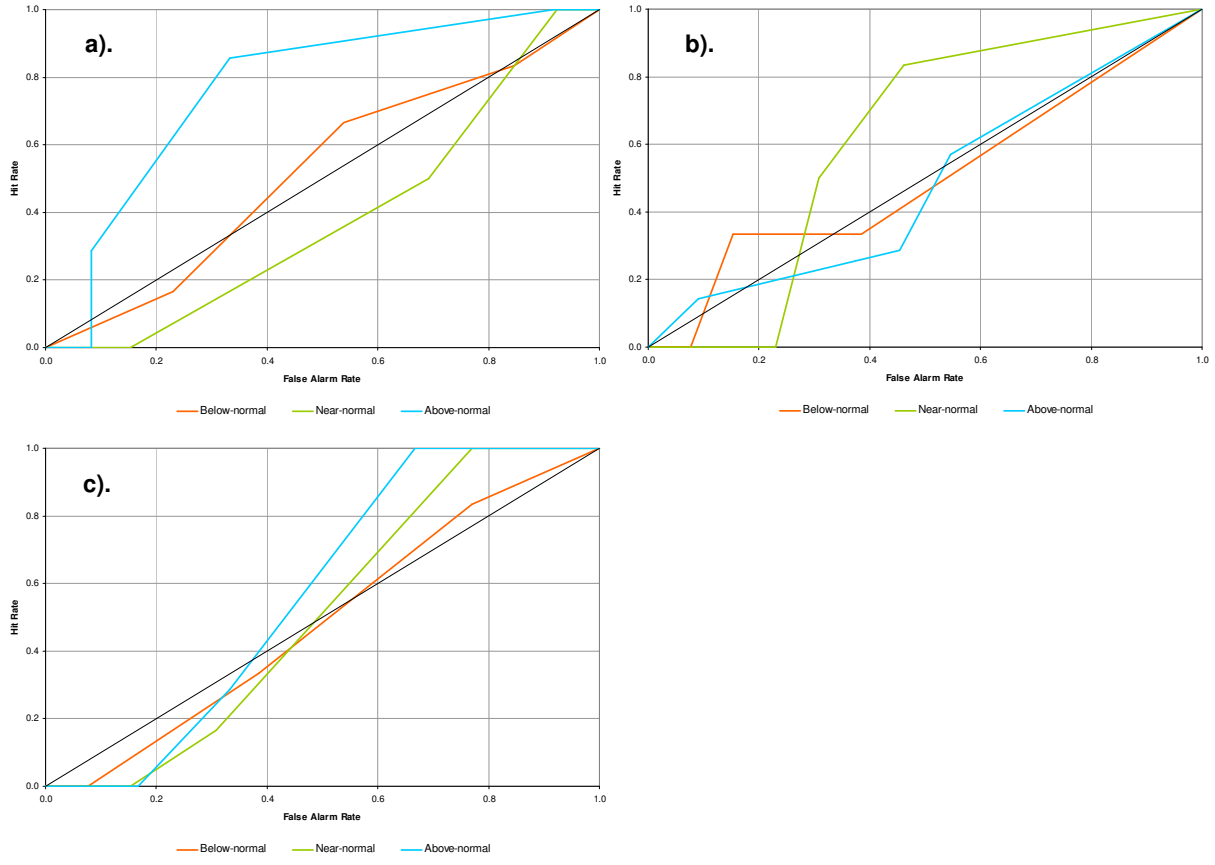

Figure 3.35: ROC curves for above-normal, near-normal and below-normal simulated medium season maize yields. (a) CERES-CCAM maize yield simulation system, (b) CERES-ECHAM4.5 maize yield simulation system and (c) Multi-Model maize yield simulation system.

The ROC curves of the Multi-Model simulation system (see Table 3.5) shows that this simulation system performs the best in simulating above-normal maize yields, with ROC scores of 0.65 for above-normal, 0.55 for near-normal and 0.5 for below-normal.

Simulation system	Below-normal	Near-normal	Above-normal
CERES-CCAM	0.50	0.41	0.79
CERES-ECHAM4.5	0.53	0.70	0.49
Multi-Model	0.50	0.55	0.65

Table 3.5: ROC scores for the simulated medium season maize yield probabilities.

3.4.2.2.3 Long Season Maize

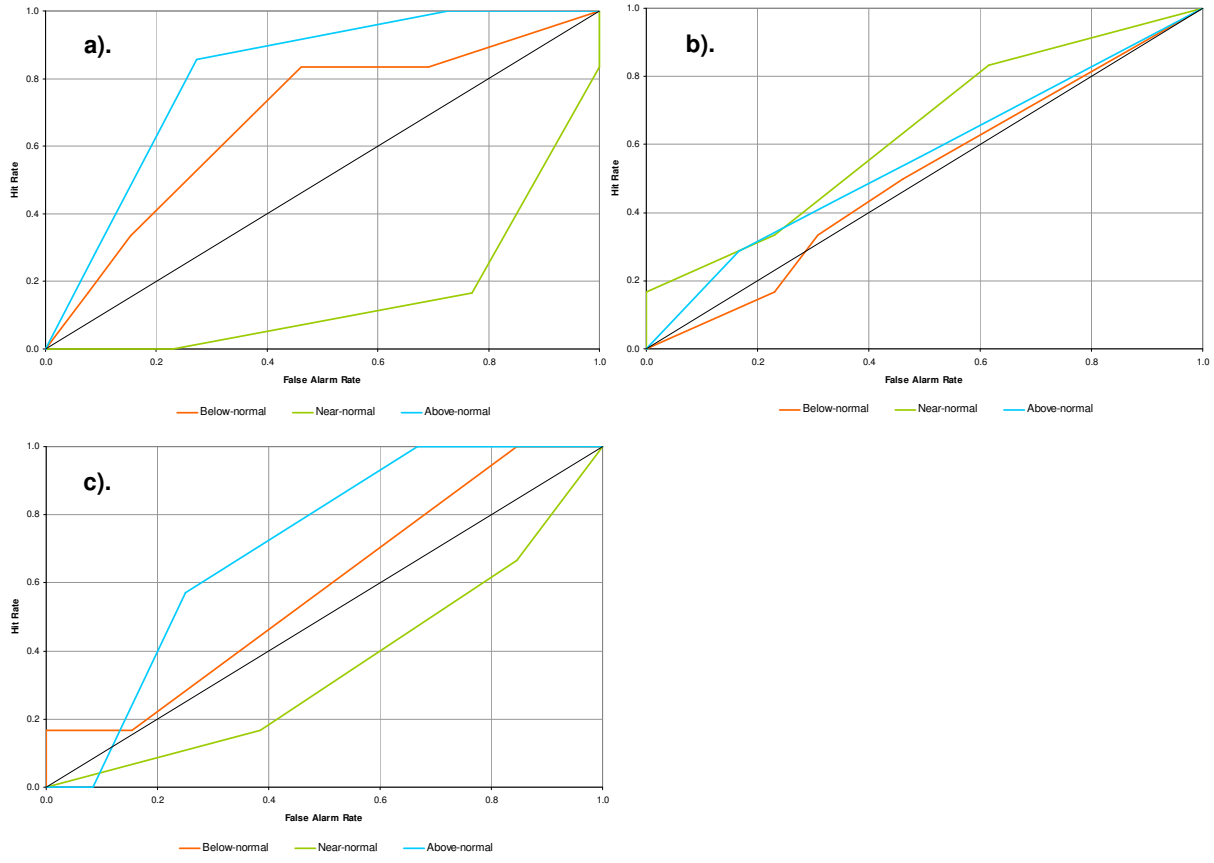

Figure 3.36: ROC curves for above-normal, near-normal and below-normal simulated long season maize yields. (a) CERES-CCAM maize yield simulation system, (b) CERES-ECHAM4.5 maize yield simulation system and (c) Multi-Model maize yield simulation system.

In Figure 3.36 the long season maize ROC curves are shown for each of the maize yield simulation systems. From the ROC curves for the CERES-CCAM simulation system (a) it can be observed that both the above-normal and below-normal categories show high skill, with ROC scores of 0.83 and 0.66 respectively (see Table 3.6). The CERES-ECHAM4.5

simulation system (b) reveals once again best skill for the near-normal category. The ROC curves of the Multi-Model simulation system show that the above-normal simulations produced by this simulation system are most reliable.

Simulation system	Below-normal	Near-normal	Above-normal
CERES-CCAM	0.66	0.08	0.83
CERES-ECHAM4.5	0.49	0.62	0.57
Multi-Model	0.64	0.33	0.85

Table 3.6: ROC scores for the simulated long season maize yield probabilities.

In general, in the short season maize scenario the highest ROC scores occur for the near-normal category, while in the medium season maize scenario and long season maize scenario the highest ROC scores occur for the above-normal category. The highest ROC score of 0.85 is evident for the long season maize scenario (Table 3.6).

3.4.2.3 Wet/Cool Eastern Region

3.4.2.3.1 Short Season Maize

Figure 3.37 shows the short season maize ROC curves for each of the different simulation systems. From the ROC curves for the CERES-CCAM simulation system (a) it can be observed that all three curves are almost completely above the no-skill diagonal line with ROC scores of 0.83 for above-normal, 0.77 for below-normal and 0.57 for near-normal (see Table 3.7). Thus, this simulation system performs best in simulating above-normal maize yields. The CERES-ECHAM4.5 simulation system (b) shows that all three curves fall beneath the no-skill diagonal line, which means that this simulation system does not have skill in simulating any of the equiprobable categories. The Multi-Model simulation system (c) on the other hand shows some skill for the below-normal and above-normal categories.

Simulation system	Below-normal	Near-normal	Above-normal
CERES-CCAM	0.77	0.57	0.83
CERES-ECHAM4.5	0.28	0.35	0.32
Multi-Model	0.57	0.48	0.54

Table 3.7: ROC scores for the simulated short season maize yield probabilities.

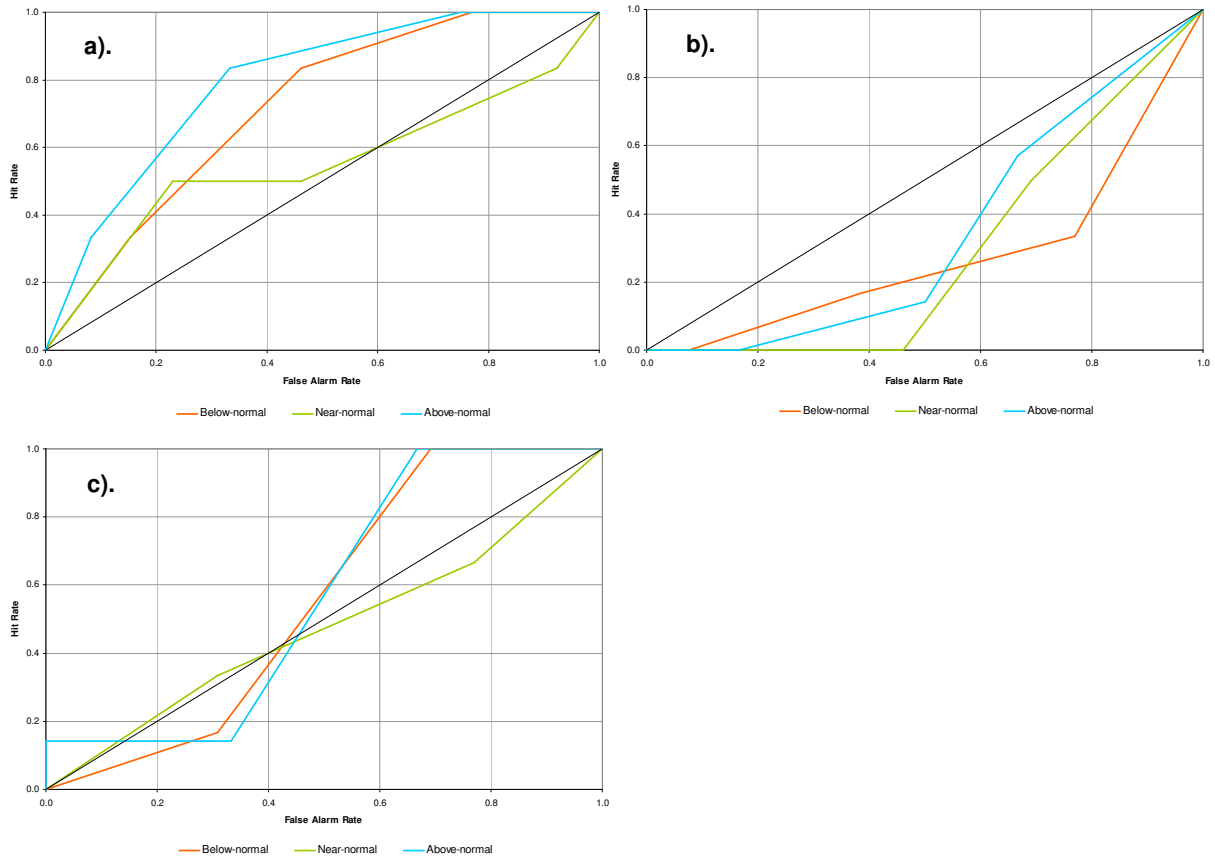

Figure 3.37: ROC curves for above-normal, near-normal and below-normal simulated short season maize yields. (a) CERES-CCAM maize yield simulation system, (b) CERES-ECHAM4.5 maize yield simulation system and (c) Multi-Model maize yield simulation system.

3.4.2.3.2 Medium Season Maize

Simulation system	Below-normal	Near-normal	Above-normal
CERES-CCAM	0.74	0.48	0.68
CERES-ECHAM4.5	0.46	0.43	0.37
Multi-Model	0.56	0.41	0.57

Table 3.8: ROC scores for the simulated medium season maize yield probabilities.

The ROC curves for medium season maize can be seen in Figure 3.38. The maize yield simulations performed by the CERES-CCAM simulation system (a) show somewhat higher skill for the below-normal category than for the above-normal category and substantially less skill for the near-normal category. The ROC curves of the CERES-ECHAM4.5 simulation system (b) are mainly beneath the no-skill diagonal with ROC scores ranging between 0.37 and 0.46 (see Table 3.8). The Multi-Model simulation system shows some

skill for the below-normal and above-normal categories, but no skill for the near-normal category.

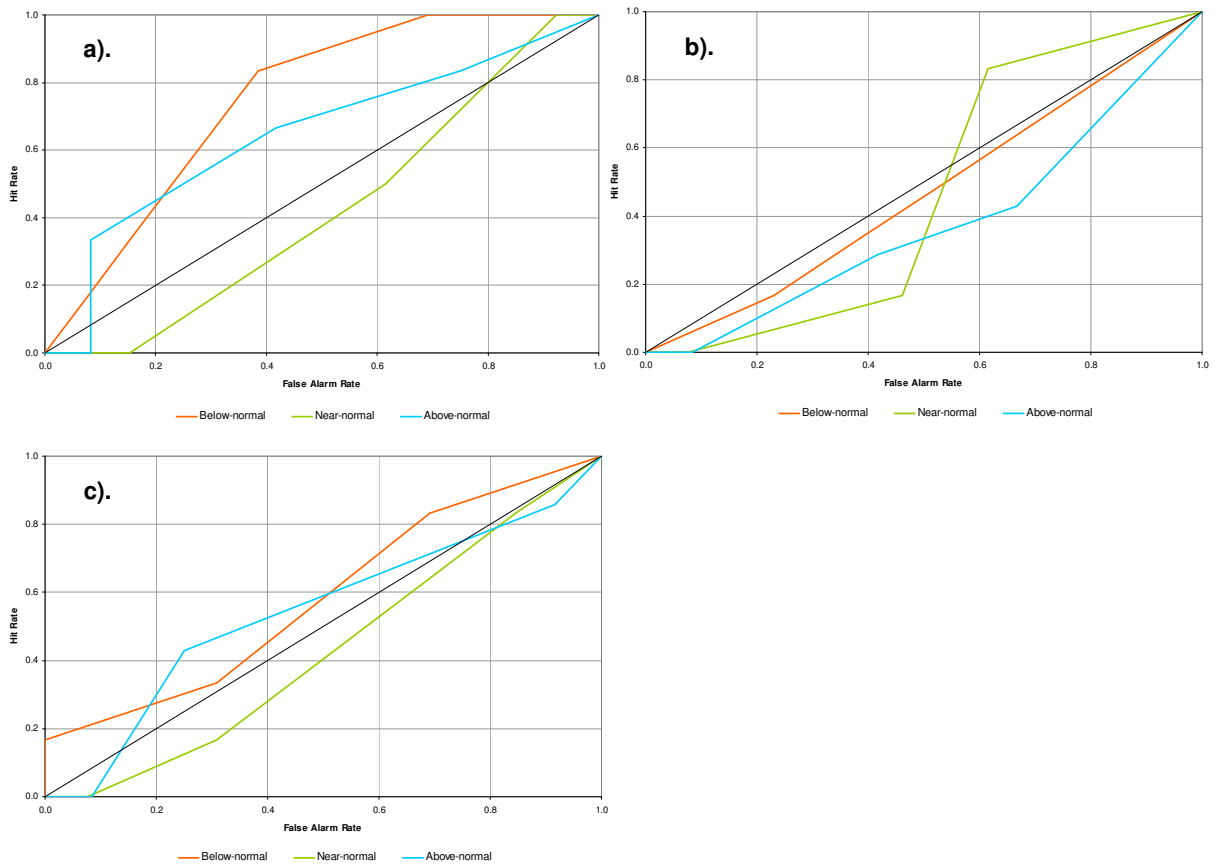

Figure 3.38: ROC curves for above-normal, near-normal and below-normal simulated medium season maize yields. (a) CERES-CCAM maize yield simulation system, (b) CERES-ECHAM4.5 maize yield simulation system and (c) Multi-Model maize yield simulation system.

3.4.2.3.3 Long Season Maize

Figure 3.39 shows the long season maize ROC curves for each of the maize yield simulation systems and Table 3.9 shows the ROC scores. The CERES-CCAM simulation system (a) shows highest skill for above-normal maize yields (ROC score = 0.75), slightly lower skill for below-normal maize yields (ROC score = 0.74) and much reduced skill for near-normal maize yields (ROC score = 0.38). The ROC curves of the CERES-ECHAM4.5 simulation system (b) reveals highest skill for the below-normal category, with the above-normal and near-normal curves falling beneath the no-skill diagonal. It can be seen from the ROC curves of the Multi-Model simulation system that this simulation system is a combination between the CERES-CCAM and CERES-ECHAM4.5 simulation systems. The

ROC scores of the Multi-Model simulation system are 0.70 for the above-normal category, 0.63 for the below-normal category and 0.41 for the near-normal category.

Simulation system	Below-normal	Near-normal	Above-normal
CERES-CCAM	0.74	0.38	0.75
CERES-ECHAM4.5	0.59	0.48	0.40
Multi-Model	0.63	0.41	0.70

Table 3.9: ROC scores for the simulated long season maize yield probabilities.

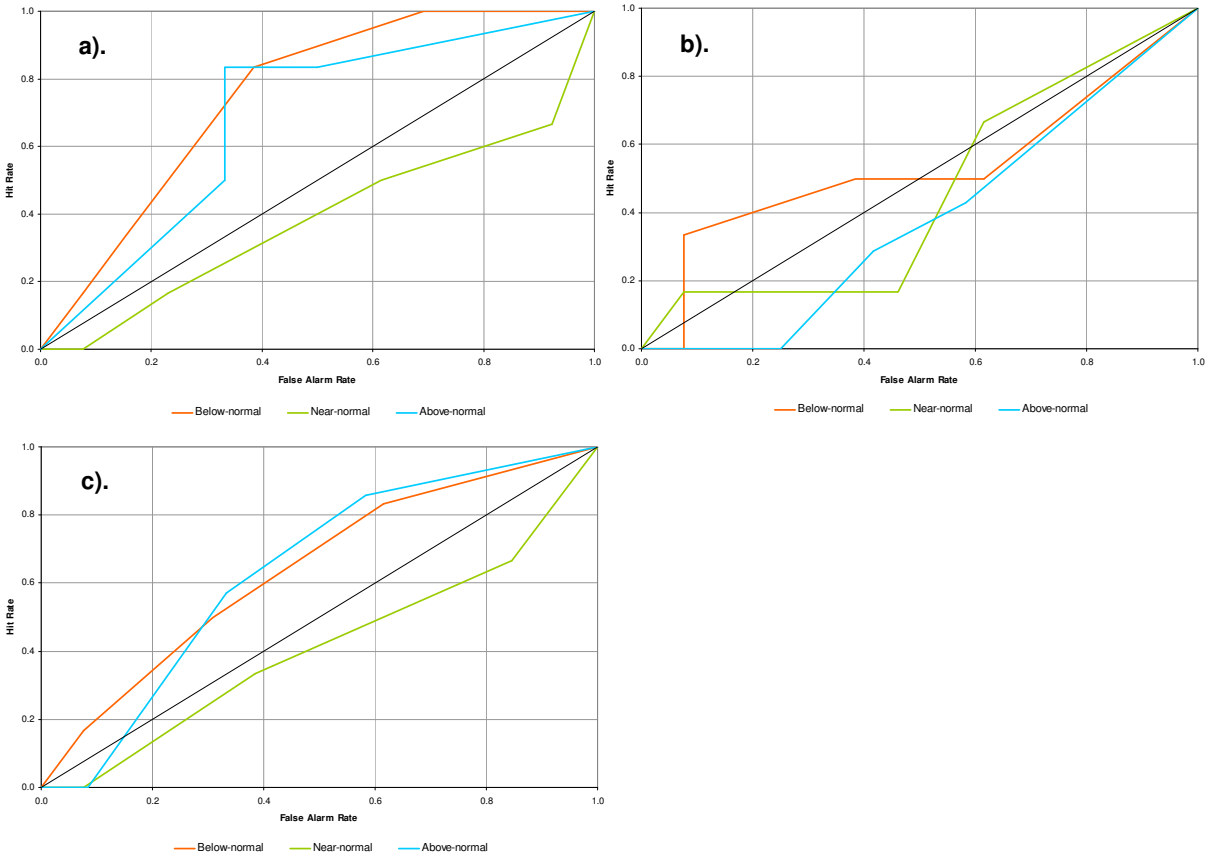

Figure 3.39: ROC curves for above-normal, near-normal and below-normal simulated long season maize yields. (a) CERES-CCAM maize yield simulation system, (b) CERES-ECHAM4.5 maize yield simulation system and (c) Multi-Model maize yield simulation system.

In general, the ROC scores of the below-normal category remain similar in all three scenarios. The above and below-normal categories of all three scenarios show relatively high ROC scores with the highest ROC score (0.83) evident for the short season maize scenario (Table 3.7).

3.5 SUMMARY

The simulated maize yields obtained from the different simulation systems for the primary maize producing region of South Africa have been presented. The simulation systems are tested over 19 seasons from 1980/81 to 1998/99. The simulation systems are constructed by forcing the CERES-Maize model with observed weather data, CCAM-simulated fields and ECHAM4.5 simulated fields. The combination between the CERES-CCAM simulated maize yields and CERES-ECHAM4.5 simulated maize yields forms the Multi-Model system.

In terms of the spatial distribution of the simulated maize yields, the four different maize yield simulation systems capture the east-west gradient in maize yield across the study area. The ability of the different simulation systems in simulating the season-to-season change in maize yield seems to be the lowest for the short season maize scenarios and the highest for the long season maize scenarios. The long season maize planted on plant date 1 scenario stands out as the scenario for which most of the simulation systems show the best results.

The CERES-Maize model shows high skill in simulating South African maize yields, with statistically significant correlations found for several magisterial districts across the study area. The CERES-CCAM simulation system produces skill levels comparable to that of the CERES-Observed weather simulation system. The CERES-ECHAM4.5 simulation system reveals overall poor skill. Since the CERES-Maize model is highly dependant on the weather input data, improved ECHAM4.5-simulated fields will most probably improve the maize yield simulations from the CERES-ECHAM4.5 simulation system. The CERES-ECHAM4.5 simulated maize yields negatively affect the Multi-Model system, as a simple un-weighted averaging approach is used as the combination method to construct the Multi-Model system. The ECHAM4.5-simulated fields can possibly be improved through downscaling and the use of a different combination method which can lead to improved Multi-Model simulations.

CHAPTER 4

SUMMARY AND CONCLUSIONS

South Africa's climate is highly variable and crop production in the country is predominantly rain-fed. Since weather is the primary source of uncertainty in crop management, unexpected climatic extremes can have detrimental effects on South African crop yields. Therefore, weather and climate variations can be seen as the main factors responsible for year-to-year variations in the crop yields. An investigation on ways to reduce the uncertainty in expected weather regime changes of a forthcoming season has therefore become essential. However, farmers can benefit more from information when it is presented in terms of production outcomes rather than from a weather or seasonal forecast that only gives an indication of variations in rainfall and temperature.

Since maize is the primary crop grown in South Africa, this dissertation has investigated the use of seasonal climate forecasts in the prediction of South African maize yields. To do this, a crop model has been run with both observed weather data and GCM-simulated fields. The ability of the crop model to simulate South African maize yields has been established by comparing the maize yield output obtained from forcing the crop model with observed weather data to actual maize yields. The maize yields produced by the crop model-GCM based maize yield simulation systems have been investigated to establish whether these simulation systems can produce skill levels similar to the target skill level set by the crop model forced with observed weather data. Finally, the two crop model-GCM based maize yield simulation systems have been combined through simple un-weighted averaging of the simulated maize yields to form a multi-model maize yield simulation system to establish whether the skill of this multi-model system outscores the skill of the best crop model-GCM based simulation system. The simulation systems have been tested over 19 seasons from 1980/81 to 1998/99.

The findings of the research are summarised as follows:

A. Quantifying the skill of the CERES-Maize model

1. The east to west decrease in maize yield across the study area has been successfully simulated by the CERES-Maize model. The spatial distribution of the

medium season maize (65 – 70 days to flowering) yields seem to show the best agreement with the spatial distribution of the actual maize yields.

2. For all three of the production regions, the CERES-Maize model has performed the best in simulating the inter-seasonal variability of the long season maize (70 – 75 days to flowering) yield scenarios (especially for the first plant date). The CERES-Maize model has performed well in simulating both the relative magnitude and the sign of the anomaly of the maize yields.

3. All 9 scenarios have shown high skill for the western part of the North-West Province (correlations > 0.81). The association between the CERES-Observed weather maize yields and actual maize yields has been found to be stronger for the western parts of the study area than for the eastern parts of the study area. The highest correlations are evident for the long season maize planted on plant date 1 scenario, with the correlations of 39 out of the 44 magisterial districts being statistically significant at the 95% level of confidence and a high level of field significance.

4. In simulating the category of the maize yields (above-normal, near-normal or below-normal) of the dry/warm western production region, the skill of the CERES-Maize model seems to increase from the short season maize (60 – 65 days to flowering) scenario to the long season maize scenario. Highest skill levels have been found for above-normal maize yields. The categorical simulations for the temperate eastern production region have shown high skill levels for the medium season maize scenario and for simulating below-normal maize yields. For the wet/cool eastern production region skill has decreased from the long season maize scenario to the short season maize scenario, and the CERES-Maize model has performed the best in simulating below-normal maize yields.

B. Simulating maize yields with the CERES-CCAM simulation system

1. The CERES-CCAM simulation system has captured the characteristic pattern of high maize yields in the eastern parts and lower maize yields in the western parts of the study area.

2. Overall, the CERES-CCAM simulation system has performed better in simulating the sign of the anomaly of the maize yields than the relative magnitude of the maize

yields. However, this simulation system has failed to correctly simulate the season with the lowest maize yield and the season with the highest maize yield.

3. All 9 scenarios have shown high skill for the western part of the Free State (correlations between 0.61 and 0.8). High skill levels have been found in simulating the maize yields of the first plant dates, thus short season maize planted on plant date 1, medium season maize planted on plant date 1 and long season maize planted on plant date 1. The simulated maize yields for the medium season maize scenarios have shown the most magisterial districts with statistically significant correlations (22 out of the 44) and high levels of field significance.

4. The probabilistic simulations have shown that for the dry/warm western production region the CERES-CCAM simulation system has performed better in simulating the above-normal yield category of the medium season maize scenario than simulating near-normal and below-normal maize yields. For the temperate eastern production region highest skill has been found for the above-normal category of the long season maize scenario and for the wet/cool eastern production region highest skill has been found for the above-normal category of the short season maize scenario.

C. *Simulating maize yields with the CERES-ECHAM4.5 simulation system*

1. The CERES-ECHAM4.5 simulation system has also captured the gradient in maize yield across the study area and in the short season maize scenarios this system has performed well in simulating the distribution in maize yield in the eastern part of the Free State.

2. Possibly due to the low spatial resolution of the ECHAM4.5-simulated fields, the CERES-ECHAM4.5 simulation system has struggled to simulate the sign of the anomaly of the yields over the 19 seasons considered in this study. However, in the long season maize scenarios for the temperate eastern production region this simulation system has produced more realistic maize yields (in terms of the relative magnitude of the yield) for the 1985/86, 1990/91 and 1997/98 seasons than that produced by the, CERES-CCAM and Multi-Model simulation systems. In the long season maize scenarios for the wet/cool eastern production region the CERES-ECHAM4.5 simulation system has performed better than the CERES-CCAM simulation system in simulating the relative magnitude of the maize yields of the 1991/92, 1996/97, and 1997/98 seasons.

3. The probabilistic simulations have shown that for the dry/warm western and wet/cool eastern production regions the CERES-ECHAM4.5 simulation system has no skill in simulating any of the categories for the short and medium season maize scenarios, but show at least some skill in simulating near-normal maize yields and below-normal maize yields for the long season maize scenario in the dry/warm western production region and wet/cool eastern production region respectively. For the temperate eastern production region the CERES-ECHAM4.5 simulation system has shown to have some skill in simulating both below-normal and near-normal maize yields for the short season maize scenario, relatively high skill in simulating near-normal maize yields for the medium season maize scenario and some skill in simulating the near-normal and above-normal categories for the long season maize scenario.

4. Improved GCM-simulated fields should result in more skilful maize yield simulations. It may be possible to improve on the spatial resolution of the ECHAM4.5-simulated fields by nesting a Regional Climate Model (RCM) within the ECHAM4.5 GCM. This process of downscaling will provide more detailed simulated fields, which will represents sub-grid scale features, like precipitation, much better.

D. *Simulating maize yields with the Multi-Model simulation system*

1. Similarly to the two single model simulation systems (CERES-CCAM and CERES-ECHAM4.5) the Multi-Model simulation system has also captured the east to west decrease in the spatial distribution of the maize yield across the study area.

2. Even though this Multi-Model simulation system has performed better than both the CERES-CCAM and CERES-ECHAM4.5 simulation systems in simulating the relative magnitude of the maize yields of 1981/82, 1983/84, 1984/85 and 1996/97 seasons in the temperate eastern production region, overall the inter-seasonal variability in maize yields as simulated by the Multi-Model simulation system was only slightly better than that of the CERES-ECHAM4.5 simulation system and did not outscore the CERES-CCAM simulation system.

3. The Multi-Model simulated maize yields expressed probabilistically have shown that for the dry/warm western production region this simulation system has no skill in simulating any of the categories for the medium and long season maize scenarios, but has some skill in simulating below-normal maize yields for the short season

maize scenario. For the temperate eastern production region the Multi-Model simulation system has shown relatively high skill levels in simulating both above-normal and near-normal maize yields, while for the wet/cool eastern region some skill has been seen for the above-normal and below-normal categories.

4. The combination between the CERES-CCAM simulated maize yields and CERES-ECHAM4.5 simulated maize yields did not improve on the CERES-CCAM simulation system's skill in simulating South African maize yields. Due to the fact that the CERES-ECHAM4.5 simulation system has not performed well, the potential advantage to use an equal-weights multi-model system has not been demonstrated in this study.

The CERES-Maize model has been used to simulate maize yields for each of the magisterial districts in the main maize producing area of South Africa. The crop model has been forced with observed weather data, CCAM-simulated fields and ECHAM4.5-simulated fields. The simulated maize yields from the CERES-CCAM simulation system and CERES-ECHAM4.5 simulation system have been combined, using simple un-weighted averaging, to form a multi-model maize yield system. The simulated maize yields from the different simulation systems have been compared to actual maize yields. From the CERES-Observed weather simulated maize yields it has been found that the CERES-Maize model has significant skill in simulating South African maize yields. This crop model can possibly be used in an operational environment, provided that the forcing fields (e.g. CCAM-simulated fields and ECHAM4.5-simulated fields) are adequately skilful. The CERES-CCAM simulation system has shown comparable skill levels to that of the CERES-Observed weather simulation system, but the CERES-ECHAM4.5 simulation system has shown poor skill. Due to this, the Multi-Model simulation system did not outscore the skill of the best single-model simulation system (CERES-CCAM). Provided that the GCM-simulated fields can be improved, the multi-model simulation system has the potential to improve significantly. This can possibly be achieved by downscaling the raw output from the GCMs.

The most important conclusion of this dissertation is that the potential for seasonal maize yield forecasting in South Africa using a multi-model ensemble system is high. However, before this goal can be realized, it will be necessary to improve the GCM fields that will be used to force the CERES-Maize model.

The maize yield forecast system proposed in this study can provide farmers with usable information on the possible successes of short, medium and long season maize. This study has shown that it is possible to simulate maize yield for South Africa with raw output from high resolution GCMs, which are already being used operationally. Thus, maize yield forecasts with a usable level of skill can be made with the use of an objective maize yield forecast system that incorporates GCMs. Such a system does not currently exist in South Africa.

REFERENCES

Allan, R.J., 2000: ENSO and climate variability in the last 150 years. In: Diaz, H.F. and Markgraf, V. (Eds.), *El Niño and the southern oscillation: multi-scale variability, global and regional impacts*, Cambridge University Press, Cambridge, 3 – 56 pp.

Allan, R., Lindesay, J. and Parker, D., 1996: *El Niño Southern Oscillation and climate variability*. CSIRO Publishing, Victoria, Australia, 405 pp.

ARC-GCI (Agricultural Research Council - Grain Crops Institute), 2008: Maize Information Guide 2008, Agricultural Research Council, Pretoria, 11 – 17 pp.

Arndt, C., Hazell, P. and Robinson, S., 2000: Economic value of climate forecasts for agricultural systems in Africa. In: Sivakumar, M.V.K. (ed), *Climate prediction and agriculture,* International START Secretariat, Washington DC, 157 – 180 pp.

Bannayan, M. and Crout, N.M.J., 1999: A stochastic modelling approach for real-time forecasting of winter wheat yield. *Field Crops Res.*, **62**, 85 – 95.

Barnston, A.G., Mason, S.J., Goddard, L., DeWit, D.G. and Zebiak, S.E., 2003: Multimodel ensembling in seasonal climate forecasting at IRI. *Bull. Amer. Meteor. Soc.*, **84**, 1783 – 1796.

Barnston, A.G., Thiao, W. and Kumar, V., 1996: Long-lead forecasts of seasonal precipitation in Africa using CCA. *J. Climate*, **11**, 506 – 520.

Barnston, A.G., van den Dool, H.M., Zibiak, S.E., Barnett, T.P., Ji, M., Rodenhuis, D.R., Cane, M.A., Leetmaa, A., Graham, N.E., Ropelewski, C.R., Kousky, V.E., O'Lenic, E.A. and Livezey, R.E., 1994: Long-lead seasonal forecasts – Where do we stand? *Bull. Amer. Meteor. Soc.*, **75** (11), 2097 – 2114.

BFAP (Bureau for Food and Agricultural Policy), 2008: The South African Agricultural Baseline. Bureau for Food and Agricultural Policy Report, 22 – 28 pp.

Boote, K.J., Jones, J.W. and Pickering, N.B., 1996: Potential uses and limitations of crop models. *J. Agronomy*, **88**, 704 – 716.

Botha, A.D.P. and Eisenberg, B.E., 1992: Estimation of soil water retention from clay content and cation exchange capacity values of soils. *S.Afr.J.Plant Soil,* **10(3)**, 141 – 143.

Cane, M.A., 2004: The evolution of El Niño, past and future. *Earth. Planet. Sci. Lett.*, **164**, 1 – 10.

Cane, M.A., Eshel, G. and Buckland, R.W., 1994: Forecasting Zimbabwean maize yield using eastern equatorial Pacific sea surface temperature. *Nature*, **370**, 204 – 205.

Cantelaube, P. and Terres, J., 2005: Seasonal weather forecasts for crop yield modelling in Europe. *Tellus*, **57A**, 476 – 487.

Carson, D.J., 1998: Seasonal forecasting. *Ouart. J. Roy. Meteor. Soc.*, **124**, 1 – 26.

Challinor, A.J., Slingo, J.M., Wheeler, T.R. and Doblas-Reyes, F.J., 2005: Probabalistic simulations of crop yield over western Indai using the DEMETER seasonal hindcast ensembles. *Tellus*, **57A**, 498 – 512.

Chen, D., Zebiak, S.E., Busalacchi, A.J. and Cane, M.A., 1995: An improved procedure for El Niño forecasting: Implications for predictability. *Science,* **269**, 1699 – 1702.

Chenje, M. and Johnson, P., 1994: *State of the Environment in Southern Africa.* Southern African Research and Documentation Center, 332 pp.

Chimeli, A.B., Mutter, C.Z. and Ropelewski, C., 2002: Climate fluctuations, demography and development: Insights and opportunities for northeast Brazil. *J. Int. Affairs*, **56**, 213 – 234.

Colberg, F., Reason, C.J.C. and Rodgers, K., 2004: South Atlantic response to ENSO induced climate variability in an OGCM. *J. Geophys. Res.*, **109**, 12 – 15.

Cook, C., Reason, C.J.C. and Hewitson, B.C., 2004: Wet and dry spells within particularly wet and dry summers in the South African summer rainfall region. *Clim. Res.*, **26**, 17 – 31.

Cox, H.G., McLean, G. and King, C., 2004: Natioanl Whopper Cropper – risk management support software. In: Fisher, T., Turner, N., Angus, J., McIntyre, L., Robertson, M., Borrell, A. and Lloyd, D. (Eds.), New directions for a diverse planet. Proc 4th Int Crop Sci Congr, 26 Sep – 1 Oct 2004, Brisbane, Australia.

Crimp, S.J., Lutjeharms, J.R.E. and Mason, S.J., 1998: Sensitivity of a tropical-temperate through to sea-surface temperature anomalies in the Agulhas retroflection region. *Water SA.*, **24**, 93 – 100.

CSIRO (Commonwealth Scientific and Industrial Research Organisation), 1998: Ocean and agriculture changing the odds. Newsletter 9, November. CSIRO Marine Research, Hobart.

D'Abreton, P.C. and Tyson, P.D., 1995: Divergent and non-divergent water vapour transport over southern Africa during wet and dry conditions. *Meteorol. Atmos. Phys.*, **55**, 47 – 59.

Devereux, S., 2000: Famine in the twentieth century. Working Paper, Institute of Development Studies, Sussex.

DoA (Department of Agriculture), 2007: *Strategic plan for the Department of Agriculture.* Department of Agriculture, Pretoria, 12 – 17 pp.

Doblas-Reyes, F.J., Hagedorn, R. and Palmer, T.N., 2006: Developments in dynamical seasonal forecasting relevant to agricultural management. *Climate Res.*, **33**, 19 – 26.

Du Pisani, A.L., 1987: The CERES-Maize model as a potential tool for drought assessment in South Africa. *Water SA*, **13** (3), 159 – 164.

Du Plessis, J., 2003: Maize Production, Department of Agriculture.

Du Toit, W., 1997: *Handleiding vir die verbouing van Mielies in die Somerreënvalgebied*. LNR-Instituut vir Graangewasse, Potchefstroom, 2 – 33 pp.

Du Toit, A.S., Booysen, J. and Human, J.J., 1994: Evaluering en kalibrering van CERES-Maize 2, Groeistadia voorspellings. *S. Afr. J. Plant Soil*, **11(3)**, 121 – 125.

Du Toit, A.S., Prinsloo, M.A., Durand, W. and Kiker, G., 2000: Vulnerability of maize production to climate change and adaptation assessment in South Africa. In: Kikier, G., *Climate Change Impacts in Southern Africa.* Report to the National Climate Change Committee, Department of Environmental Affairs and Tourism, Pretoria, South Africa.

Du Toit, A.S., Prinsloo, M.A., Wafula, B.M. and Thornton, P.K., 2002: Incorporating a water-logging routine into CERES-Maize, and some preliminary evaluations. *Water SA*, **28(3)**, 323 - 328.

Du Toit, D.L., Smallberger, S.A. and Du Toit, A.S., 2001: The use of a weather analogue model to manage seasonal variability. Unpublished paper presented at the Integrated Managemnt for Sustainable Agriculture, Forestry and Fishereis workshop, 28 – 31 August, Cali, Columbia.

Egli, D.B. and Bruening, W., 1992: Planting date and soybean yield: evaluation of environmental effect with a crop simulation model: SOYGRO. *Agric. For. Meteorol.*, **62**, 19 – 29.

Engelbrecht, F.A., McGregor, J.L. and Engelbrecht, C.J., 2009: Dynamics of the Conformal-Cubic Atmospheric Model projected climate-change signal over southern Africa. *Int. J. Climatol.,* **29**, 1013 - 1033.

Engelbrecht F.A., Rautenbach, C.J. deW., McGregor, J.L. and Katzfey, J.J., 2002: January and July climate simulations over the SADC region using the limited-area model DARLAM. *Water SA,* **28**, 361-374.

Fageria, N.K., 1992: Maximizing crop yields. Marcel Dekker, New York.

Fodor, N. and Kovacs, G.J., 2003: Sensitivity of 4M maize model to the inaccuracy of weather and soil input data. *Appl. Ecol. Environ. Res.*, **1**, 75 – 85.

Frost, C., 2006: Using spatial rainfall and products from the MODIS sensor to improve an existing maize yield estimation system. Unpublished MSc. Dissertation, University of Witwatersrand, Johannesburg.

Gebregiorgis, M.F. and Savage, M.J., 2006: Field, laboratory and estimated soil-water content limits. *Water SA*, **32(2)**, 155 – 161.

Goddard, L. and Mason, S.J., 2002: Sensitivity of seasonal climate forecasts to persisted SST anomalies. *Climate Dyn.*, **19**, 619 – 631.

Goddard, L., Mason, S.J., Zebiak, S.E., Ropelewski, C.F., Basher, R. and Cane, M.A., 2001: Current approaches to seasonal to interannual climate predictions. *Int. J. Climatol.*, **21**, 1111 – 1152.

Gong, X., Barnston, A.G. and Ward, M.N., 2003: The effect of spatial aggregation on the skill of seasonal precipitation forecasts. *J. Climate.*, **16**, 3059 – 3071.

Gordon, H.B., Rotstayn, L.D., McGregor, J.L., Dix, M.R., Kowalczyk, E.A., O'Farrell, S.P., Waterman, L.J., Hirst, A.C., Wilson, S.G., Collier, M.A., Watterson, I.G. and Elliott, T.I., 2002: The CSIRO Mk3 Climate System Model. CSIRO Atmospheric Research, Australia. 130 pp.

Hagedorn, R., Doblas-Reyes, F.J. and Palmer, 2005: The rationale behind the success of multi-model ensembles in seasonal forecasting, I, Basic concept. *Tellus*, **A57**, 219 – 233.

Hammer, G.L., Hasen, J.W., Phillips, J.G., Mjelde, J.W., Hill, H. and co-authors, 2001: Advances in application of climate prediction in agriculture. *Agric. Sys.*, **74**, 515 – 553.

Hammer, G.L., Holzworth, D.P. and Stone, R., 1996: The value of skill in seasonal climate forecasting to wheat crop management in a region with high climatic variability. *Aust. J. Agic. Res.*, **47**, 717 – 737.

Hansen, J.W., Challinor, A., Ines, A., Wheeler, T. and Moron, V., 2006: Translating climate forecasts into agricultural terms: advances and challenges. *Climate Res.*, **33**, 27 – 41.

Hansen, J.W. and Indeje, M., 2004: Linking dynamic seasonal climate forecasts with crop simulation for maize yield prediction in semi-arid Kenya. *Agric. For. Meteor.*, **125**, 143 – 157.

Hanway, J.J., 1966: How a corn plant develops. Special Report, Iowa State University, Unite States of America, 48 pp.

Harrison, M.S.J., 1984: A general classification of South African summer rain-bearing synoptic systems. *J. Climatol.*, **4**, 547 – 560.

Harrison, M., 2003: Report to the Commission for Agricultural Meteorology Working Group on the use of seasonal forecasts and climate prediction in operational agriculture. 13th Sess Comm Agric Meteorol World Meteorol Org, October 2002, Ljubjana, Slovenia.

Hattle, J.B., 1968: Polar fronts of the southern hemisphere. Notos: South African Weather Bureau, **17**, 15 – 22 pp.

Hoerling, M.P. and Kumar, A., 1997: Why do North American climate anomalies differ from one El Niño event to another? *Geophys. Re. Lett.*, **24**, 1059 – 1062.

Hoffman, R.N. and Kalnay, E., 1983: Lagged average forecasting, an alternative to Monte Carlo forecasting. *Tellus*, **35A**, 100 – 118.

Hollinger, S.E., 1988: Modeling the effects of weather and management practices on maize yield. *Agric. For. Meteor.*, **44**, 81 – 97.

Holton, J.R., 1979: *Numerical prediction: An introduction to Dynamic Meteorology.* 2nd edition, Academic Press, San Diego, 173 – 213 pp.

Hoogenboom, G., 2000: Contribution of agrometeorology to the simulation pf crop production and its applications. *Agric. For. Meteorol.*, **103**, 137 – 157.

Hoogenboom, G., Jones, J.W. and Boote, K.T., 1992: Modeling growth, development, and yield of grain legumes using SOYCRO, PNUTGRO, and BEANGRO: a review. *Trans. ASAE*, **35**, 2043 – 2056.

Hunt, B.G., Zebiak, S.E. an Cane, M.E., 1994: Experimental predictions of climate variability for lead times of twelve months. *Int. J. Climatol.*, **14**, 507 – 526.

Isard, S.A., Welford, M.R. and Hollinger, S.E., 1995: A simple soil moisture index to forecast crop yields. *Phys. Geog.*, **16(6)**, 524 – 538.

Jinghua, W. and Erda, L., 1996: The impacts of potential climate change and climate variability on simulated maize production in China. *Water, Air and Soil Pollution*, **92**, 75 – 85.

Jones, J.W., Hoogenboom, G., Porter, C.H., Boote, K.J., Batchelor, W.D., Hunt, L.A., Wilkens, P.W., Singh, U., Gijsman, A.J. and Ritchie, J.T., 2003: The DSSAT cropping system model. *Europ. J. Agronomy*, **18**, 245 – 265.

Joubert, A.M. and Hewitson, B.C., 1997: Simulating present and future climate of southern Africa using general circulation models. *Prog. Phys. Geog.*, **21**, 51 – 78.

Jury, M.R., 2002: Economic impacts of climate variability in South Africa and development of resource prediction models. *J. Appl. Meteor.*, **41**, 46 – 55.

Jury, M.R. and Pathack, B., 1991: A study of weather and climate variability over the tropical southwest Indian Ocean. *Meteorol. Atmos. Phys.*, **47**, 37 – 48.

Jury, M.R., Valentine, H.R. and Lutjeharms, J.R.E., 1993: Influence of the Agulhas current on summer rainfall on the southeast coast of South Africa, *J. Appl. Meteorol.*, **32**, 1282 – 1287.

Jury, M.R., White, W.B. and Reason, C.J.C., 2004: Modelling the dominant climate signals around southern Africa. *Climate Dyn.*, **23**, 717 – 726.

Kgatuke, M.M., Landman, W.A., Beraki, A. and Mbedzi, M.P., 2008: The internal variability of the RegCM3 over South Africa. *Int. J. Climatol.*, **28**, 505 – 520.

Kharin, V.V. and Zwiers, F.W., 2003: On the ROC scores of probability forecasts. *J. Climate*, **16**, 4145 – 4150.

Klopper, E., 1999: The use of seasonal forecasts in South Africa during the 1997/98 rainfall season. *Water SA*, **25**, 311 – 316.

Klopper, E. and Landman, W.A., 2003: A simple approach for combining seasonal forecasts for southern Africa. *Meteorol. Appl.*, **10**, 319 – 327.

Krishnamurti, T.N., Kishtawal, C.M., LaRow, T.E., Bachiochi, D.R., Zhang, Z., Willford, C.E., Gadgil, S. and Surendran, S., 1999: Climate forecasts from multimodel superensemble. *Science*, **285**, 1548 – 1550.

Landman, W.A., Engelbrecht, F.A., Beraki, A., Engelbrecht, C.J., Mbedzi, M., Gill, T. and Ntsangwane, L., 2008. Model output statistics applied to multi-model ensemble long-range forecasts over South Africa. Water Research Commission Project Report, in press, Pretoria.

Landman, W.A. and Goddard, L., 2002: Statistical recalibration of GCM forecasts over southern Africa using Model Output Statistics. *J. Climate*, **15**, 2038 – 2055.

Landman, W.A. & Goddard, L., 2003: Model output statistics applied to multi-model ensemble forecasts for southern Africa. Proceedings of the Seventh International Conference on Southern Hemisphere Meteorology and Oceanography. Wellington, New Zealand. 24 – 28 March 2003, 249 – 250 pp.

Landman, W.A. and Mason, S.J., 1999a: Change in association between Indian Ocean sea-surface temperatures and summer rainfall over South Africa and Namibia. *Int. J. Climatol.*, **19**, 1477 – 1492.

Landman, W.A. and Mason, S.J., 1999b: Operational long-lead prediction of South African rainfall using canonical correlation analysis. *Int. J. Climatol.*, **19**, 1073 – 1090.

Landman, W.A. and Mason, S.J., 2001: Forecasts of near-global sea surface temperatures using canonical correlation analysis. J. Climate, 14, 3819 – 3833.

Landman, W.A., Mason, S.J., Tyson, P.D. and Tennant, W.J., 2001: Retro-active skill of multi-tiered forecasts of summer rainfall over southern Africa. *Int. J. Climatol.*, **21**, 1 – 19.

Land Type Survey Staff, 1972 – 2008: Land Types of South Africa: Digital map (1:250 000 scale) and soil inventory databases. ARC-Institute for Soil, Climate and Water, Pretoria.

Lawless, C. and Semenov, M.A., 2005: Assessing lead-time for predicting wheat growth using a crop simulation model. *Agric. For. Meteorol.*, **135**, 302 – 313.

Leith, C.E., 1974: Theoretical skill of Monte Carlo forecasts. *Mon. Wea. Rev.*, **6**, 409 – 418.

Lorenz, E.N., 1963: Deterministic nonperiodic flow. *J. Atmos. Sci.*, **20**, 130 – 141.

Macvicar, C.N., De Villiers, J.M., Loxton, R.F., Verster, E., Lambrechts, J.J.N., Merryweather, F.R., Le Roux, J., Van Rooyen, T.H. and Harmse, H.J.Von.M., 1977: *Soil Classification: A Binomial System for South Africa*. The Soil and Irrigation Research Institute, Department of Agriculture Technical Services, Pretoria, 34 – 115 pp.

Mason, I., 1982: A model for assessment of weather forecasts. *Aust. Wea. Forecasting*, **14**, 713 – 725.

Mason, S.J., 1995: Sea-surface temperature – South African rainfall associations, 1910 - 1989. *Int. J. Climatol.*, **15**, 119 – 135.

Mason, S.J., 1998: Seasonal forecasting of South African rainfall using a non-linear discriminant analysis model. *Int. J. Climatol.*, **18**, 147 – 164.

Mason, S.J., 2001: El Niño, climate change, and Southern African climate. *Environmetrics*, **12**, 327 – 345.

Mason, S.J., 2008: From dynamical model predictions to seasonal climate forecasts. In: Troccoli, A., Harrison, M., Anderson, D.L.T. and Mason, S.J., 2008, *Seasonal Climate: Forecasting and Managing Risk*, Springer, The Netherlands, 205 – 234 pp.

Mason, S.J., Goddard, L., Graham, N.E., Yelaeva, E., Sun, L. and Arkin, P.A., 1999: The IRI seasonal climate prediction system and the 1997/98 El Niño event. *Bull. Amer. Meteor. Soc.*, **80**, 1853 – 1873.

Mason, S.J. and Graham, N.E., 1999: Conditional probabilities, relative operating characteristics, and relative operating levels. *Wea. Forecasting*, **14**, 713 – 725.

Mason, S.J., Joubert, A.M., Cosijn, C. and Crimp, S.J., 1996: Review of seasonal forecasting techniques and their applicability to southern Africa. *Water SA*, **22**, 203 – 209.

Mason, S.J. and Jury, M.R., 1997: Climate variability and change over southern Africa: a reflection on underlying processes. *Prog. Phys. Geog.*, **21**, 23 – 50.

Martin, R.V., Washington, R. and Downing, T.E., 2000: Seasonal maize forecasting for South Africa and Zimbabwe derived from an agroclimatological model. *J. Appl. Meteor.*, **39**, 1473 – 1479.

Matthews, R., 2002: Where to now with crop modelling? In: Matthews, R. and Stephens, W. (Eds.), Crop-soil simulation models, applications in developing countries, CABI publishing, Wallingford, New York, 209 – 229 pp.

Mavromatis, T. and Jones, P.D., 1998: Evaluation of HadCM2 and direct use of daily GCM data in impact assessment studies. *Clim. Change*, **41**, 583 – 614.

McFarlane, N.A., 1887: The effect of orographically excited gravity-wave drag on the general circulation of the lower stratosphere and troposphere. *J. Atm. Sci.*, **44**, 1775 – 1800.

McGregor, J.L., 1996: Semi-Lagrangian advection on conformal-cubic grids. *Mon. Wea. Rev.*, **124**, 1311 – 1322.

McGregor, J.L., 2005a: C-CAM: Geometric aspects and dynamical formulation. CSIRO Atmospheric Research Technical Paper, No 70, 41 pp.

McGregor, J.L., 2005b: Geostrophic adjustment for reversibly staggered grids. *Mon. Wea. Rev.*, **133**, 1119-1128.

McGregor, J.L. and Dix, M.R., 2001: The CSIRO conformal-cubic atmospheric GCM. In: Hodnett, P.F. (Ed.), IUTAM Symposium on Advances in Mathematical Modelling of Atmosphere and Ocean Dynamics, Kluwer: Dordrecht, 197 – 202 pp.

McGregor, J.L. & Nguyen, K.C. 1999: Simulations of the East Asian and Australian monsoons and aspects of the diurnal rainfall behaviour. *Atmospheric Research*, **1**, 1-12.

Neelin, J.D., Battisti, D.S., Hirst, A.C., Jin, F., Wakata, Y. and co-authors, 1998: ENSO theory. *J. Geophys. Res.*, **103**, 14261 – 14290.

Nicholls, N., 1985: Impact of the southern oscillation on Australian crops. *J. Climatol.*, **5**, 553 – 560.

Nicholson, S.E. and Entekhabi, D., 1986: The quasi-periodic behaviour of rainfall variability in Africa and its relationship to the Southern Oscillation. *Arch. Met. Geophys. Bioklim. Ser.*, **34**, 311 – 348.

Nonhebel, S., 1994: Inaccuracies in weather data and their effects on crop growth simulation results II, Water-limited production. *Clim. Res.*, **4**, 61 – 74.

Oram, P.A., 1989: Sensitivity of agricultural production to climatic change, an update. In: *Climate and food security*, International Rice Research Institute (IRRI), Manila, 25 – 44 pp.

Palmer, T.N., Alessandri, A., Andersen, U., Cantelaube, P., Davey, M., Delecluse, P., Deque, M., Diez, E., Doblas-Reyes, F.J., Feddersen, H., Graham, R., Gualdi, S., Gueremy, J.F., Hagedorn, R., Hoshen, M., Keenlyside, N., Latif, M., Lazar, A., Maisonnave, E., Marletto, V., Morse, A.P., Orfila, B., Rogel, P., Terres, J.M. and Thomson, M.C., 2004: Development of a European Multi-Model Ensemble System for Seasonal to Inter-Annual Prediction (DEMETER). Unpublished internal report, Technical Memorandum No. 434, European Centre for Medium-Range Weather Forecasts, England.

Palmer, T.N. and Anderson, D.L.T., 1994: The prospects for seasonal forecasting. *Ouart. J. Roy. Meteor. Soc.*, **120**, 755 – 793.

Palmer, T.N., Shutts, G.J., Hagedorn, R, Doblas-Reyes, F.J., Jung, T. and Leutbecher, M., 2005: Representing model uncertainty in weather and climate prediction. *Annu. Rev. Earth Planet Sci.*, **33**, 163 – 193.

Palmer, T.N., Shutts, G.J. and Swinbank, R., 1986: Alleviation of a systematic westerly bias in general circulation and numerical weather prediction models through an orographic gravity wave drag parameterization. *Quart. J. Roy. Meteor. Soc.*, **112**, 1001 – 1031.

Pathack, B.M.R., Jury, M.R., Shillington, F.A. and Courtney, S., 1993: South African rainfall variability and its association with the marine environment. Water Research Commission Report, 278/1/94.

Petr, J., 1991: Weather and Yield. Elsevier, Amsterdam, Netherlands.

Phillips, J.G., Cane, M.A. and Rosenzweig, C., 1998: ENSO, seasonal rainfall patterns and simulated maize yield variability in Zimbabwe. *Agric. For. Meteorol.*, **90**, 39 – 50.

Podesta, G.P., Messina, C.D., Grondona, M.O. and Magrin, G.O., 1999: Associations between grain crop yields in Central-Eastern Argentina and El Nino – Southern Oscillation. *J. Appl. Meteor.*, **38**, 1488 – 1498.

Porter, J.R. and Semenov, M.A., 1999: Climate variability and crop yields in Europe. *Nature*, **400**, 724.

Potgieter, C.J., 2007: Short-range weather forecasting over southern Africa with the conformal-cubic atmospheric model. Unpublished MSc. Dissertation, University of Pretoria, Pretoria.

Preston-Whyte, R.A. and Tyson, P.D., 1993: *The atmosphere and weather of southern Africa*. Oxford University Press, New York, 207 - 249 pp.

Rautenbach, C.J.deW. and Smith, I.N., 2001: Teleconnections between global sea-surface temperatures and the interannual variability of observed and model simulated rainfall over southern Africa. *J. Hydrol.*, 254, 1-15.

Rawls, W.J., Brakensiek, D.L. and Saxton, K.E., 1982: Estimation of Soil Water Properties. *Trans. ASAE*, 1316 – 1320.

Reason, C.J.C., 2002: Sensitivity of the southern African circulation to dipole SST patterns in the South Indian Ocean. *Int. J. Climatol.*, **22**, 377 – 393.

Reason, C.J.C., Allan, R.J., Lindesay, J.A. and Ansell, T.J., 2000: ENSO and climate signals across the Indian Ocean basin in the global context, part 1: Interannual composite patterns. *Int. J. Climatol.*, **20**, 1285 – 1327.

Reason, C.J.C., Engelbrecht, F., Landman, W.A., Lutjeharms, J.R.E., Piketh, S., Rautenbach, C.J.deW. and Hewitson, B.C., 2006b: A review of South African research in atmospheric science and physical oceanography during 2000-2005. *SA J. Sci.*, **102**, 35 – 45.

Reason, C.J.C. and Jagadheesha, D., 2005: A model investigation of recent ENSO impacts over southern Africa. *Meteorol. Atmos. Phys.*, **89**, 181 – 205.

Reason, C.J.C., Landman, W. and Tennant, W., 2006a: Seasonal to decadal prediction of southern African climate and its links with variability of the Atlantic Ocean. *Bull. Amer. Meteor. Soc.*, **87**, 941 – 955.

Reason, C.J.C. and Mulenga, H., 1999: Relationships between South African rainfall and SST anomalies in the South West Indian Ocean. *Int. J. Climatol.*, **19**, 1651 – 1673.

Reason, C.J.C. and Rouault, M., 2002: ENSO-like decadal patterns and South African rainfall. *Geophys. Res. Lett.*, **29**, 1010 – 1029.

Reddy, V.R. and Pachepsky, Y.A., 2000: Predicting crop yields under climate change conditions from monthly GCM weather projections. *Environmental Modelling and Software*, **15**, 79 – 86.

Ritchie, J.T., 1994: Classification of crop models. In: Uhlir, P.F. and Carter, G.C. (Eds.), *Crop modelling and related environmental data*, 3 – 14 pp.

Ritchie, S.W., Hanway, J.J. and Benson, G.O., 1993: How a corn plant develops. Iowa State Univeristy of Science and Technology, Cooperative Extension Service, Ames, Iowa Special Rep. 48, 21 pp.

Roeckner, E., Arpe, K., Bengtsson, L., Christoph, M., Claussen, M., Dumenil, L., Esch, M., Giorgetta, M., Schlese, U. and Schulzweida, U., 1996: The atmospheric general circulation model ECHAM-4: Model description and simulation of present-day climate. Report 218, Max Planck Institute for Meteorology, Hamburg, Germany.

Ropelewski, C.F. and Halpert, M.S., 1987: Global and regional scale precipitation patterns associated with the El Niño/southern oscillation. *Mon. Wea. Rev.*, **115**, 1606 – 1626.

Rosenthal, W.D., Hammer, G.L. and Butler, D., 1998: Predicting regional grain sorghum production in Australia using spatial data and crop simulation modelling. *Agric. For. Meteorol.*, **91**, 263 – 274.

Rosenzweig, R. and Iglesias, A., 1994: Implication of climate change on international agriculture: Crop Modeling Study. U.S. Environmental Protection Agency, Office of Policy, Planning and Evaluation, Climate Change Division, Adaptation Branch, Washington, DC.

Rotstayn, L.D., 1997: A physically based scheme for the treatment of stratiform clouds and precipitation in large-scale models, I: Description and evaluation of the microphysical processes. *Quart. J. Roy. Meteor. Soc.*, **123**, 1227 – 1282.

Schoeman, J.L., Van der Walt, M., Monnik, A.K., Thachrah, A., Malherbe, J. and Le Roux, R.E., 2000: Development and application of a land capability classification system for South Africa. Agricultural Research Council, Institute for Soil, Climate and Water report, GW/A/2000/57, Pretoria.

Schulze, R.E., 1985: Hydrological characteristics and properties of soils in Southern Africa 1: Runoff response. *Water SA.* **11(3)**, 121 – 128.

Schulze, R.E. and Lynch, S.D., 2007: Annual Precipitation. In: Schulze, R.E. (Ed.) 2007, *South African Atlas of Climatology and Agrohydrology*, Water Research Commission, Pretoria, RSA, WRC Report 1489/1/06, Section 6.2.

Schulze, R.E. and Maharaj, M., 2007: Rainfall Seasonality. In: Schulze, R.E. (Ed). 2007, *South African Atlas of Climatology and Agrohydrology,* Water Research Commission, Pretoria, RSA, WRC Report 1489/1/06, Section 6.5.

Schulze, R.E., Warburton, M., Lumsden, T.G. and Horan, M.J.C., 2005: The Southern African Quaternary Catchment Database: Refinements to, and links with, the *ACRU* System as a Framework fro Modelling of Climate Change on Water Resources. In: Schulze, R.E. (Ed) *Climate Change and Water Resources in Southern Africa: Studies on Scenarios, Impacts, Vulnerability and Adaptation.* Water Research Commission, Pretoria, RSA, WRC Report 1430/1/05. Chapter 8, 111 – 139 pp.

Schwarzkopf, M.D and Fels, S.B., 1991: The simplified exchange method revisited: an accurate, rapid method for computation of infrared cooling rates and fluxes. *Journal of Geophysical Research,* **96**, 9075-9096.

Shannon, L..V., Boyd, A.J., Brundrit, G.B. and Taunton-Clark, J., 1986: On the existence of an El Niño-type phenomenon in the Benguela system. *J. Marine. Res.*, **44**, 495 – 520.

Sivakumar, M.V.K., 2006: Climate prediction and agriculture: current status and future challenges. *Climate Res.*, **33**, 3 – 17.

Soil Classification Working Group, 1991: *Soil Classification: A Taxonomic System for South Africa*. The Soil and Irrigation Research Institute, Department of Agriculture Development, Pretoria, 50 – 190 pp.

Soil Survey Staff, 2008: Soil Profile descriptions and soil analyses data. In: ARC-ISCW Soil Profile Information System. ARC-Institute for Soil, Climate and Water, Pretoria.

Stanski, H.R., Wilson, L.J. and Burrows, W.R., 1989: Survey of common verification methods in meteorology. WMO World Weather Watch Tech. Rep. 8 WMO TD 358, 114 pp.

Stefanova, L. and Krishnamurti, T.N., 2002: Interpretation of seasonal climate forecast using brier skill score, The Florida State University Superensemble, and the AMIP-1 dataset. *J. Climate*, **15**, 537 – 544.

Steyn, A.G.W., Smit, C.F., Du Toit, S.H.C. and Stransheim, C., 1998: Moderne statistiek vir die praktyk. 6th Edition, J.L. van Schaik publishers, Pretoria, 130, 615 pp.

Sun, L., Li, H. and Ward, N.M., 2007: Climate variability and corn yields in semiarid Ceara, Brazil. *J. Appl. Meteor.*, **46**, 226 – 240.

Sun, L., Moncunill, D.F., Li, H., Moura, A.D. and Filho, F.D.A.D.S., 2005: Climate downscaling over Nordeste Brazil ysing NCEP RSM97. *J. Climate*, **18**, 551 – 567.

Tadross, M.A., Gutowski, W.J., Hewitson, B.C., Jack, C. and New, M., 2006: MM5 simulations of interannual change and the diurnal cycle of southern African regional climate. *Theor. Appl. Climatol.*, **86**, 63 – 80.

Tadross, M.A., Hewitson, B.C. and Usman, M.T., 2003: The interannual variability of the onset of the maize growing season over South Africa and Zimbabwe. *J. Climate*, **18**, 3356 – 3372.

Taljaard, J.J., 1986: Change of rainfall distribution and circulation patterns over southern Africa in summer. *J. Climatol.*, **6**, 579 – 592.

Tennant, W.J. and Hewitson, B.C., 2002: Intra-seasonal rainfall characteristics and their importance to the seasonal prediction problem. *Int. J. Climatol.*, 22, 1033 – 1048.

Todd, M. and Washington, R., 1998: Extreme daily rainfall in southern African and southwest Indian Ocean tropical-temperate links. *S. Afr. J. Sci.*, **94**, 64 – 70.

Tsuji, G.Y., 1998: Network management and information dissemination for agrotechnology transfer. In: Tsuji, G.Y., Hoogenboom, G., Thornton, P.K. (Eds.), *Understanding Options for Agricultural Production,* Kluwer Academic Publishers, Dordrecht, The Netherlands, 367 – 381 pp.

Tyson, P.D., 1986: *Climatic change and variability over southern Africa*. Oxford University Press, Cape Town, 220 pp.

Uehara, G. and Tsuji, G.Y., 1998: Overview of IBSNAT. In: Tsuji, G.Y., Hoogenboom, G., Thornton, P.K. (Eds.), *Understanding Options for Agricultural Production*, Kluwer Academic Publishers, Dordrecht, The Netherlands, 1 – 7 pp.

Van Heerden, J., Terblanche, D.E. and Schulze, G.C., 1988: The southern oscillation and South Africa summer rainfall. *J. Climatol.*, **8**, 577 – 597.

Vogel, C. and O'Brien, K., 2006: Who can eat information? Examining the effectiveness of seasonal climate forecasts and regional climate-risk management strategies. *Climate Res.*, **33**, 111 – 122.

Vossen, P., 1995: Early crop production assessment of the European Union, the system implemented by the MARS-STAT Project. Agrometeorological models: theory and application in the MARS project. Publication EUR 16008 EN of the Office for Official Publications of the European Communities, Luxembourge.

Walker, N.D., 1990: Links between South African summer rainfall and temperature variability of the Agulhas and Benguela current systems. *J. Geophys. Res.*, **B 95**, 3297 – 3319.

Walker, N.D. and Lindesay, J.A., 1989: Preliminary observations of oceanic influences on the February-March 1988 floods in central South Africa. *S. Afr. J. Sci.*, **85**, 164 – 169.

Walter, M.W., 1967: Mis(management) of droughts in South Africa: Past, present, future. *South Afr. J. Sci.*, **86**, 382 – 386.

Wang, Y., Leung, L.R., McGregor, J.L., Lee, D.K., Wang, W.C., Ding, Y. and Kimura, F., 2004: Regional climate modeling: Progress, challenges, and prospects. *Journal of the meteorological society of Japan,* **82**, 1599-1628.

Wilks, D., 2006: *Statistical methods in the atmospheric sciences*. 2nd Edition, Elsevier Academic Press, California, Unites States of America.

Williamson, D.L. and Rasch, P.J., 1994: Water vapor transport in the NCAR CCM2. *Tellus*, **46A**, 34 – 51.

Whisler, F.D., Acock, B., Baker, D.N., Fry, R.E., Hodges, H.F., Lamber, J.R., Lemmon, H.E., MacKinnion, J.M. and Reedy, V.R., 1986: Crop simulation models in agronomic systems. *Adv. Agron.*, **40**, 141 – 208.

Ziervolgel, G., Bithell, M., Washington, R. and Downing, T., 2005: Agent-based social simulation: a method for assessing the impact of seasonal climate forecasts applications among smallholder farmers. *Agric. Syst.*, **83**, 1 – 26.